EUROPEAN COMMISSION

Community Research

DOPAS

(Contract Number: FP7 - 323273)

Deliverable n°5.10

WP5 final integrated report

André Rübel (Editor)

M. Åkesson, L. E. F. Bailey, L. Börgesson, J. M. Bosgiraud, D. Buhmann, V. Burlaka, N. Conil, M. Crawford, O. Czaikowski, D. A. Galson, J. Gondolli, M. Hakala, J. Hart, V. Havlová, K. Jantschik, M. Jobmann, J. Kindlein, K. Koskinen, O. Kristensson, T. Lauke, H. C. Moog, X. Pintado, E. Rautioaho, E. Rosca-Bocancea, S. Schirmer, T. J. Schröder, D. Trpkšová, J. Valli, P. Večerník, M. Vuorio, J. Wendling, C.-L. Zhang

Date of issue of this report: **27.09.2016**

Start date of project: 01/09/2012 Duration: 48 Months

Project co-funded by the European Commission under the Euratom Research and Training Programme on Nuclear Energy within the Seventh Framework Programme		
Dissemination Level		
PU	Public	X
PP	Restricted to other programme participants (including the Commission Services)	
RE	Restricted to a group specified by the partners of the DOPAS project	
CO	Confidential, only for partners of the DOPAS project	

EURATOM

Scope	Deliverable n°5.10 (WP5)	Version:	1.0
Type/No.	Report	Total pages	183+4
		Appendixes	
Title	WP5 final integrated report	Articles:	13

ABSTRACT:

This report is the final report of workpackage 5 on "Performance assessment of the plugs and seals systems" of the DOPAS project. The aims of WP5 were to support the experimental work and the construction of the large-scale sealings by predictive process modelling and to understand the implications of the plugs and seal performance on the overall safety for the whole reference period of a final waste repository of one million years. An important element of this work was to develop justification of model simplifications for long-term safety assessment simulations. This includes the objective to improve the state-of-the-art in process modelling and its abstraction in integrated performance assessment. The report summarises the work performed in WP5 and where applicable, links to other reports were the results are given in higher detail.

RESPONSIBLE:

André Rübel (editor)
Authors of individual chapters as indicated.

REVIEW/OTHER COMMENTS:

Internal review by WP5 participants.
External review by expert elicitation process.
See DOPAS Deliverable D6.3.3

APPROVED FOR SUBMISSION:

Approved by DOPAS coordinator 27.9.2016

Executive Summary

This report is the final report of Work package 5 on "Performance assessment of the plugs and seals systems" of the DOPAS project. The Full-Scale Demonstration of Plugs and Seals (DOPAS) Project was a European Commission (EC) programme of work jointly funded by the Euratom Seventh Framework Programme and European nuclear waste management organisations (WMOs). The DOPAS Project was running in the period September 2012 – August 2016. Fourteen European WMOs and research and consultancy institutions from eight European countries were participating in the DOPAS Project. The project was coordinated by Posiva (Finland). A set of full-scale experiments, laboratory tests, and performance assessment studies of plugs and seals for geological repositories were carried out in the course of the project. The purpose of plugs and seals will depend on the disposal concept, the nature of the geological environment and the inventory to be disposed. Plugs and seals e.g. may be required to

- isolate emplaced waste from the rest of the underground excavations during the operating phase to limit radiological exposure to the workers,
- support other EBS components until the repository has evolved to its desired state,
- limit groundwater flow and radionuclide migration,
- prevent inadvertent or unauthorized human access.

The objective of this report is to provide an integrated summary of the work undertaken and the lessons learned in the Work package 5 of the DOPAS project. The role of WP5 within the DOPAS project was mainly twofold: to support the planning, construction and experimental work of the large-scale demonstrators by predictive process modelling and to understand the implications of the plugs and seal performance on the overall safety for the whole reference period of a final waste repository. A variety of modelling tasks has been performed within the WP 5 of the DOPAS project to fulfil this role with the following objectives:

- simulation of processes and their evolution within individual sealing components,
- predictive modelling to support the design and the construction of the large-scale seals,
- modelling of small and mid-scale experiments performed to gain process understanding,
- identification of the main processes that are relevant and thus to be considered for predicting the short and long-term behaviour of the plug and sealing systems,
- identification of remaining uncertainties and their influence on performance assessment,
- development and justification of conceptual models of plugs and seals for the different disposal concepts and geological environments and
- development and application of the PA methodology and integrated PA models to analyse the system behaviour.

The nature of the different modelling approaches presented is unique for each piece of work and cannot be compared to each other directly. Each of the work has a different function for to the related experiment or in the related national program and therefor has to be regarded as independent. The work is presented in eight topical chapters which are representing the views

from the different organisations represented by the authors given and which are solely responsible for the content of the work.

The DOPAS project and Work package 5 contribute significantly to the further development of the safety cases for radioactive waste repositories by bringing forward the plug and sealing concepts in three main host rock types considered in Europe: crystalline rock, clay rock and salt rock. The different aspects of the achievements in WP5 are:

- **Gain in process understanding and improvement of models for safety assessment by evaluation process modelling of laboratory experiments:** Process modelling performed of laboratory experiments was able to predict and interpret the results from laboratory experiments enhancing the confidence in the suitability of the used models to describe the observed processes. The process models were party converted to abstract models that could be included in integrated safety assessment models to achieve a better process representation in future total system performance assessments. Future comparison of the performed predictive modelling on mid-scale experiments with experimental results will contribute in the confidence of the validity of the up-scaling of process modelling results from small scale to metric scale.
- **Advancement of the sealing concept:** The process modelling of laboratory and mid-scale in-situ experiments contributed update of the sealing concept and the choice of sealing materials. The predictive process modelling of the in-situ experiment directly supported and influenced the layout and construction of the experiment.
- **Confidence in concept and models:** Future comparison of the predictive modelling with experimental results will contribute in the confidence of the validity of the up-scaling of process modelling results from small scale to large scale.
- **Proof of constructability:** All aspects given before jointly contribute building the confidence in the fact that the plugging and sealing systems will develop as planned and will be able to meet their designed function in the overall repository concept.

The process modelling work performed in Work package 5 of DOPAS has significantly contributed to the preparation and execution of the experiments and has helped to interpret the obtained results of some of the experiments. Since many of the experiments are not finished at the date of reporting more updated process modelling is expected in the future to investigate the experimental results and to confirm predictive modelling. This also is true for the full analyses of the in-situ large scale experimental data for integrated performance assessment which will mostly be feasible in following programme stage. This work consequently will be reported in company reports of the organisations which per-formed the work presented in this report.

Table of contents

Executive Summary ..... **iii**

1 The DOPAS Project **5**
1.1 Background 5
1.2 Objective of DOPAS 6
1.3 Scope and Link to other DOPAS Deliverables 7
1.4 List of DOPAS Project Partners 8
1.5 List of acronyms 9

2 Context **11**
2.1 The Design Basis of DOPAS Project Plugs and Seals 11
2.2 DOPAS Design Basis Workflow 14

3 Work package 5 as part of the DOPAS project **17**

4 Treatment of Seals and Sealing Systems in Total System Performance Assessment (RWM, GSL) **23**
M. Crawford, D. A. Galson, L. E. F. Bailey
4.1 Introduction 23
4.2 Aims and Objectives 24
4.3 Sweden 25
4.4 Finland 26
4.5 France 27
4.6 Switzerland 29
4.7 Canada 31
4.8 Belgium 33
4.9 USA – Waste Isolation Pilot Plant 34
4.10 Germany 37
4.11 Summary of Review Findings 39

5 Assessment of water tightness and mechanical integrity of POPLU plug (Posiva) **41**
E. Rautioaho, L. Börgesson, M. Åkesson, O. Kristensson, J. Valli, M Hakala, X. Pintado, K. Koskinen, M. Vuorio
5.1 Description of the plug system 42
5.2 Mechanical properties of the system modelled 43
5.3 Prediction of watertightness 46
5.4 Prediction of mechanical integrity 52
5.5 Summary 62
5.6 Conclusions and lessons learned 64

6 Design, implementation, monitoring and simulation of the REM experiment as part of the development program for Performance Assessment (ANDRA) 67

J. Wendling, N. Conil, J.M. Bosgiraud

6.1 Context 67
6.2 Aim of performed work 67
6.3 Summary of actual methodology and phenomenological comprehension of sealing at Andra 68
6.4 The REM experiment 78
6.5 Conclusions 83

7 Process level modelling of compaction processes (DBETEC) 85

V. Burlaka, M. Jobmann, S. Schirmer

7.1 Context 85
7.2 Simulation of compaction 86
7.3 Calibration of impulse compaction model 90
7.4 Summary and conclusions 96

8 Process modelling of seal materials (GRS) 97

O. Czaikowski, K. Jantschik, H. C. Moog, C.-L. Zhang

8.1 Modelling of clay seal materials (THM-Ton) 97
8.2 Modelling of concrete-based sealing materials (LASA) 102
8.3 Modelling of concrete-based sealing materials (LAVA) 109

9 Improvement of plug related processes representation in the integrated performance assessment code LOPOS (GRS) 115

A. Rübel, D. Buhmann, J. Kindlein, T. Lauke

9.1 Context 115
9.2 Aim of performed work 115
9.3 EDZ evolution 116
9.4 Corrosion of salt concrete 116
9.5 Mathematical model 117
9.6 Illustrative calculation 118
9.7 Implementation in and simulations with the LOPOS safety assessment model 122
9.8 Simulations for the ELSA shaft sealing concept 127
9.9 Conclusions 129

10 Process modelling of bentonite saturation in the PHM experiment and testing the influence of bentonite sealing property for safety of deep geological repository (UJV) 131

D. Trpkšová, V. Havlová, P. Večerník, J. Gondolli

10.1 Introduction 131
10.2 Numerical simulation of laboratory physical hydraulic model 131
10.3 Testing the influence of bentonite sealing property for safety of deep geological repository 139

11 Options to link demonstrator activities with performance assessment by the use of indicators (NRG) 147

T.J. Schröder, E. Rosca-Bocancea, and J. Hart

11.1 Introduction 147
11.2 Definition of a generic demonstrator case 152
11.3 Definition of additional PA-related indicators 155
11.4 Establishment of a generic demonstrator case 160
11.5 Synthesis & conclusions 164

12 Conclusions 167

13 References 175

1 The DOPAS Project

1.1 Background

The Full-Scale Demonstration of Plugs and Seals (DOPAS) Project is a European Commission (EC) programme of work jointly funded by the Euratom Seventh Framework Programme and European nuclear waste management organisations (WMOs). The DOPAS Project is running in the period September 2012 – August 2016. Fourteen European WMOs and research and consultancy institutions from eight European countries are participating in the DOPAS Project. The project is coordinated by Posiva (Finland). A set of full-scale experiments, laboratory tests, and performance assessment studies of plugs and seals for geological repositories are being carried out in the course of the project.

The DOPAS Project aims to improve the industrial feasibility of full-scale plugs and seals, the measurement of their characteristics, the control of their behaviour in repository conditions, and their performance with respect to safety objectives. The Project is being carried out in seven Work packages (WPs). WP1 includes project management and coordination and is led by Posiva, Finland. WP2, WP3, WP4 and WP5 address, respectively, the design basis, construction, compliance testing, and performance assessment modelling of five full-scale experiments and laboratory tests. WP2, WP3, WP4 and WP5 are led by SKB (Sweden), Andra (France), RWM (United Kingdom), and GRS (Germany), respectively. WP6 and WP7 address cross-cutting activities common to the whole project through review and integration of results, and their dissemination to other interested organisations in Europe and beyond. WP6 and WP7 are led by Posiva.

The DOPAS Project focuses on tunnel, drift, vault and shaft plugs and seals for clay, crystalline and salt rocks:

- Clay rocks: the Full-scale Seal (FSS) experiment, being undertaken by Andra in a surface facility at Saint Dizier, is an experiment of the construction of a drift and intermediate-level waste (ILW) disposal vault seal.
- Crystalline rocks: experiments related to plugs in horizontal tunnels, including the Experimental Pressure and Sealing Plug (EPSP) experiment being undertaken by SÚRAO and the Czech Technical University (CTU) at the Josef underground research centre (URC) and underground laboratory in the Czech Republic, the Dome Plug (DOMPLU) experiment being undertaken by SKB and Posiva at the Äspö Hard Rock Laboratory (Äspö HRL) in Sweden, and the Posiva Plug (POPLU) experiment being undertaken by Posiva, SKB, VTT and BTECH at the ONKALO Underground Rock Characterisation Facility (URCF) in Finland.
- Salt rocks: tests related to seals in vertical shafts under the banner of the Entwicklung von Schachtverschlusskonzepten (development of shaft closure concepts – ELSA) experiment, being undertaken by DBE TEC together with the Technical University of Freiburg and associated partners, complemented by laboratory testing performed by GRS.

In the DOPAS Project, a distinction has been made between reference and experiment designs:

- The term "reference design" is used to denote the design of a plug/seal within a disposal concept, i.e., the design used to underpin the safety case or licence application.
- The term "experiment design" is used to indicate the design of the plug/seal being tested, e.g., the designs of the plug/seal being tested at full scale in the DOPAS Project.

Experiment designs are typically modified versions of reference designs, with the modifications made to investigate specific aspects of the design during the experiment. In particular, there are differences in the boundary conditions between the experiment designs and reference designs. These include the number of plugs and seals in the actual repository (just one plug/seal for the experiments compared to many tens of plugs/seals for the repository) and the impact on the construction of these plugs and seals (for example cost constraints), and the acceptability, for experiments, to use monitoring instrumentation within the plug/seal structure.

Each experiment represents a different stage of development. The Swedish experiment was started prior to the start of the DOPAS Project. The Finnish, Czech and French experiments were designed and constructed during the Project. The German tests focused on the early stages of design basis development and on demonstration of the suitability of designs through performance assessment studies and laboratory testing, and will feed into a full-scale experiment of prototype shaft seal components to be carried out after DOPAS.

1.2 Objective of DOPAS

The objective of this report is to provide an integrated summary of the work undertaken and the lessons learned in the Work package 5 of the DOPAS project, from the following aspects of the modelling work of the experiments:

- simulation of processes and their evolution within individual sealing components,
- predictive modelling to support the design and the construction of the large-scale seals,
- modelling of small and mid-scale experiments performed in WP3 to gain process understanding,
- identification of the main processes that are relevant and thus to be considered for predicting the short and long-term behaviour of the plug and sealing systems,
- identification of remaining uncertainties and their influence on performance assessment,
- development and justification of conceptual models of plugs and seals for the different disposal concepts and geological environments and
- development and application of the PA methodology and integrated PA models to analyse the system behaviour.

1.3 Scope and Link to other DOPAS Deliverables

This report is part of a series of WP-level summary reports describing the integrated outcomes of the technical work in DOPAS:

- D2.4, the WP2 Final Report (DOPAS 2016a), describes the design basis for the plugs and seals considered in DOPAS, conceptual and basic designs, and the strategy adopted in programmes for demonstrating compliance with the design basis. The design basis is presented for both the repository reference design and the full-scale experiment design.
- D3.30, the WP3 Final Summary Report (DOPAS 2016b), summarises the work undertaken and the lessons learned from the detailed design and construction of the experiments. These include the full-scale demonstrators, laboratory work and its upscaling, and the learning provided by the practical experience in constructing the experiments.
- D4.4, the WP4 Integrated Report (DOPAS 2016c), summarises what has been learnt with respect to the repository reference designs for plugs and seals. The report also considers alternatives to the repository reference designs (e.g. the wedge-type plug investigated by Posiva). It considers what can be concluded from the full-scale experiments conducted in DOPAS with respect to the technical feasibility of installing the reference designs, the performance of the reference designs with respect to the safety functions listed in the design basis, and identifies and summarises achievements of DOPAS WP2, WP3 and WP4 at the time of writing. D4.4 also considers the feedback from the work to the design basis.
- D5.10, the WP5 Final Integrated Report (this report), describes the conceptualisation of plugs and seals in post-closure safety assessments and the expected long-term evolution of plugs and seals. This includes a description of the evidence that the materials used in plugs and seals will maintain their required performance for the period specified in the design basis.

D5.10 is based on information available by the date of a data freeze of 31 December 2015. At this time, all design and installation work had been completed, although some assessment of the work was on-going. Progress in the experiments by this date was as follows:

- DOMPLU: The DOMPLU concrete dome was cast in March 2013 and contact grouting was undertaken in June 2013.
- POPLU: The POPLU concrete wedge was cast in May and September 2015. Contact grouting was undertaken in December 2015.
- EPSP: The EPSP inner plug was cast in November 2014, the bentonite core was emplaced in June 2015 and the outer plug was cast in June 2015.
- FSS: For FSS, the upstream containment wall was cast in June 2013, the clay core was emplaced in August 2014 and the downstream shotcrete plug was emplaced in September 2014. Investigations of FSS were undertaken in the period November 2014 to July 2015, followed by "clever dismantling" between August 2015 and December 2015. The REM experiment has been running since September 2014.
- ELSA: With regard to the long-term sealing element consisting of crushed rock salt and potentially a clay admixture, laboratory and in situ compaction tests had been completed

by December 2015. In parallel, a small-scale in situ test applying MgO-concrete has been performed and a mock-up test of a bentonite shaft seal element is in its final stage. Small-scale in situ tests on the use of bitumen as sealing material were undertaken during the beginning of 2015. In addition, a laboratory programme undertaken within the auspices of the LASA, LAVA and THM-Ton projects addresses sealing materials planned to be utilised in the shaft seals. This laboratory programme provides supporting information to the ELSA Project.

Further description of the achievements in DOPAS, based on additional assessment of the design and construction work undertaken after 31 December 2015, will be included in experiment summary reports (published separately) and in the DOPAS Final Project Summary Report (D6.4) (Hansen et al., 2016).

1.4 List of DOPAS Project Partners

The partners in the DOPAS Project are listed below. In the remainder of this report each partner is referred to as indicated:

Acronym	Company name	Country
Posiva	Posiva Oy	Finland
Andra	Agence nationale pour la gestion des déchets radioactifs	France
DBETEC	DBE TECHNOLOGY GmbH	Germany
GRS	Gesellschaft für Anlagen- und Reaktorsicherheit gGmbH	Germany
Nagra	Die Nationale Genossenschaft für die Lagerung Radioaktiver Abfälle	Switzerland
RWM	Radioactive Waste Management Limited	UK
SURAO	Správa Úložišť Radioaktivních Odpadu (Radioactive Waste Repository Authority – RAWRA)	Czech Republic
SKB	Svensk Kärnbränslehantering AB	Sweden
CTU	Czech Technical University	Czech Republic
NRG	Nuclear Research and Consultancy Group	Netherlands
GSL	Galson Sciences Limited	UK
BTECH	B+ Tech Oy	Finland
VTT	Teknologian Tutkimuskeskus VTT Oy (VTT Technical Research Centre of Finland Ltd)	Finland
UJV	Ustav Jaderneho Vyzkumu (Nuclear Research Institute)	Czech Republic

1.5 List of acronyms

List of acronyms used in the general chapters or in a general way in multiple chapters. Some specific acronyms which are used in the national programs and which are therefore used only in a limited scope are not taken into this list, but are specified when used. Acronyms for the participating organisations of DOPAS are given in section 1.4.

BMU:	Bundesministerium für Umwelt, Naturschutz und Reaktorsicherheit (Federal Ministry for the Environment, Nature Conservation, Building and Nuclear Safety in Germany)
CEA	Commissariat à l'énergie atomique et aux énergies alternatives
Cigéo:	Centre Industriel de Stockage Géologique (Industrial Repository in France)
CMHM	Centre de Meuse/Haute-Marne (Andra's research laboratory including Bure URL)
COX	Callovo-Oxfordian claystone
DGR	Deep Geological Repository
DOMPLU:	Dome Plug
DOPAS:	Full-scale Demonstration of Plugs and Seals
EBS:	Engineered Barrier System
EC:	European Commission
EDZ:	Excavation Damaged Zone **or** Excavation Disturbed Zone
ELSA:	Entwicklung von Schachtverschlusskonzepten (development of shaft closure concepts)
EPSP:	Experimental Pressure and Sealing Plug
FEM	Finite Elements Method
FEP	Features, Events and Processes
FSS:	Full-Scale Seal
GDF	Geologic Disposal Facility
HLW:	High-Level Waste
HRL:	Hard Rock Laboratory
ILW:	Intermediate-Level Waste
LECBA	Laboratoire d'Etude et de Caractérisation des Bétons et des Argiles
LLW	Low-Level Waste
NEA	Nuclear Energy Agency
PA:	Performance Assessment
PDF	Probability Density Function

PHM:	Physical Hydraulic Model
POPLU:	Posiva Plug
R&D:	Research and Development
SA	Safety assessment
THM	Thermal, Hydraulic, Mechanical Processes
TSPA	Total System Performance Assessment
URC:	Underground Research Centre
URL:	Underground Research Laboratory
VSG:	Vorläufige Sicherheitsanalyse Gorleben (Preliminary safety assessment for the Gorleben site)
VTT	VTT Technical Research Centre of Finland LTD
WMO:	Waste Management Organisation
WP:	Work Package

2 Context

This chapter is giving the context of the work presented in this report. The information is taken from the DOPAS WP2 Final Report. The first subchapter very briefly presents the basis of the five different experiments performed in DOPAS. The information of highest relevance for the process modelling work presented in this report are the safety functions each of the plugs and seals is having within the repository concept and the operational period strived for. A second subchapter introduces to the "DOPAS Design Basis Workflow" which describes a generic process for development of the design basis for plugs and seals.

2.1 The Design Basis of DOPAS Project Plugs and Seals

2.1.1 Andra's Drift and ILW Vault Seal

In Andra's Centre Industriel de Stockage Géologique (Cigéo) concept for disposal in a clay host rock, seals are defined as hydraulic components for closure of large diameter (several meters) underground installations and infrastructure components. The safety functions of the drift and ILW vault seals are, following closure, to limit water flow between the underground installation and overlying formations through the access shafts/ramps, and to limit the groundwater velocity within the repository. There are three types of seals envisaged in the French reference disposal concept: shaft seals; ramp seals; and drift and ILW disposal vault seals. Each seal consists of a swelling clay core and two concrete containment walls. The swelling clay core provides the required long-term performance of the seal, whereas the containment walls mechanically contain the clay core.

FSS is a full-scale experiment of the reference drift and ILW disposal vault seal for the Cigéo repository concept. The main objective of the FSS experiment is to develop confidence in, and to demonstrate, the technical feasibility of constructing a full-scale drift or ILW disposal vault seal. As such, the experiment is focused on the construction of the seal, and the materials will not be saturated or otherwise pressurised. Other experiments that investigate saturation phenomena are being undertaken by Andra in parallel with the FSS experiment.

FSS has been implemented in a specially constructed concrete box located in a surface facility. The box can be closed at each end to allow environmental conditions (e.g., temperature and relative humidity) to be representative of those of the underground. The seal itself consists of a cast concrete containment wall, a swelling clay core, and a shotcrete containment plug. The design also includes recesses that represent breakouts that may be generated by the removal of the concrete lining used to support drifts and vaults during operations of the repository; the linings are removed to ensure that the seal meets hydraulic requirements.

The design basis for FSS is derived from a functional analysis of the safety functions specified for the seal. The FSS design and construction is contracted to a consortium, and the design basis is captured in the technical specification produced by Andra in the tendering process for the experiment. The design basis contains requirements on each component of the

experiment, and also on the site, on monitoring, and on procedures to be applied during implementation of the experiment.

2.1.2 SÚRAO's Tunnel Plug

SÚRAO has developed a repository concept for crystalline rock based on the KBS-3H method, in which disposal drifts will be closed by an end plug. The safety functions of the plug are to separate the disposal container and the buffer from the rest of the repository, provide a safe environment for staff, and provide better stability of open tunnels.

The reference design for the tunnel plug in SÚRAO's repository concept is not highly developed. In the current concept, disposal drifts will be closed by a simple steel-concrete end plug, in which the concrete would be of low-pH.

EPSP is an experiment of a tunnel plug, but, unlike DOMPLU and POPLU, the focus of the experiment is on development of fundamental understanding of materials and technology, rather than testing of the reference design. This is because the Czech geological disposal programme is in a generic phase and designs are at the conceptual level. EPSP consists of a pressure chamber, an inner concrete plug, a bentonite zone, a filter, and an outer concrete plug. Concrete walls are used to facilitate emplacement of the experiment. The experiment is pressurised with air, water or slurry, and EPSP is designed so that the pressurisation can occur through the pressurisation chamber or through the filter. The primary sealing component is the inner concrete plug.

The design basis identifies requirements on each component of the experiment (including the host rock), plus general requirements on the experiment, on materials, on technology and on the pressurisation system. Key aspects of the experiment are to evaluate the use of glass fibre-reinforced sprayed concrete for the concrete plugs, and sprayed bentonite pellets composed of Czech bentonite for the bentonite zone.

2.1.3 SKB's Deposition Tunnel Plug

In the KBS-3V method developed by SKB for disposal of spent fuel in crystalline host rock, deposition tunnels are closed with a deposition tunnel end plug. The main functions of the deposition tunnel plugs are to provide a barrier against water flow from the backfilled deposition tunnel and to confine the backfill in it during the operational period of the repository of at least 100 years. As such, they only have a "short-term" function.

The main components of the current SKB reference design for a deposition tunnel plug include a dome-shaped reinforced plug made of low-pH concrete, a bentonite watertight seal, a filter made of sand or gravel, and a backfill end zone (or transition zone) used to manage the swelling pressure loads on the plug. The plug also contains drainage, cooling and grouting pipes, as well as concrete beams to aid construction.

The function of the concrete plug is to resist deformation and to keep the watertight seal, filter and tunnel backfill in place. The function of the watertight seal is to seal water leakage path-

ways and to ensure an even pressure on the concrete. The function of the filter is to collect water draining from the deposition tunnel so that no water pressure is applied on the concrete plug before it has cured and gained full strength. The design basis for the deposition tunnel plugs are separated into requirements on the production (including construction and curing of the concrete), sealing and post-closure phases.

DOMPLU is a full-scale experiment of the reference deposition tunnel plug in SKB's repository design. The DOMPLU experiment is part of an on-going testing and demonstration programme and will help to reduce uncertainties in the performance of deposition tunnel plugs, and to decrease uncertainties in the description of the initial state of the deposition tunnel plugs (i.e., the state of the plug when all components of the plug or seal have been constructed). Specific objectives for the experiment include further development of water tightness requirements on deposition tunnel plugs and plug production requirements. The main difference between DOMPLU and the reference deposition tunnel plug is the use of unreinforced low-pH concrete instead of reinforced low-pH concrete for the dome structure.

2.1.4 Posiva's Deposition Tunnel Plug

The spent fuel disposal concept in Posiva's construction licence application for a repository in crystalline host rock located in Olkiluoto is based on KBS-3V, and, in this concept, deposition tunnel plugs will be placed at the entrance of deposition tunnels following emplacement of the spent fuel, buffer and backfill. In Posiva's reference concept the deposition tunnel plug and backfill are considered together as *"sealing structures of deposition tunnels"*.

The reference design for deposition tunnel plugs in Posiva's concept is the same as SKB's (i.e., the dome-shaped design). The design basis for the reference deposition tunnel plug has been captured in Posiva's requirements management system (VAHA) as a hierarchy of requirements. VAHA concentrates on post-closure requirements and, therefore, the majority of the requirements on deposition tunnel plugs focus on how the deposition tunnel plug contributes to post-closure safety, i.e., by keeping the backfill in place during the operational phase and ensuring that the plug does not significantly affect the post-closure performance of the backfill.

POPLU is a full-scale experiment of an alternative design of the deposition tunnel plug to that of the dome-shaped reference design, which could provide flexibility in Posiva's forward programme. The POPLU design consists of a wedge-shaped reinforced concrete structure cast directly adjacent to a filter layer, which is positioned in front of a concrete tunnel back wall. The plug contains grouting tubes and bentonite circular strips at the rock-concrete interface to ensure water tightness.

The safety functions for POPLU are the same as those defined for the reference deposition tunnel plug in VAHA. An existing conceptual design for a wedge-shaped plug was used to define the requirements on POPLU.

2.1.5 German Shaft Seal Design Basis

The reference concept for disposal of spent fuel, high-level waste (HLW), ILW, graphite and depleted uranium in Germany is based on a repository design for the Gorleben salt dome. The Gorleben repository concept envisages two shaft seals, one in each shaft, and four drift seals. The primary safety function for shaft and drift seals is to provide a sufficiently low hydraulic conductivity to avoid brine paths into the repository and the movement of radionuclides out of it. Work in the DOPAS Project has focused on shaft seals.

At the current stage of the German programme, the design basis for the shaft seal is based on regulatory requirements, mining law, experience from the sealing of mine shafts, previous full-scale testing of shafts, and recent performance assessment studies. The design basis captures this understanding at a high level and groups requirements into those relating to the regulatory safety requirements of the Bundesministerium für Umwelt, Naturschutz and Reaktorsicherheit (BMU), safety and verification concepts (requirements related to the principal safety functions and performance of the seal), technical functional verification (requirements related to the design and demonstration of compliance with safety and verification concepts), site-specific boundary conditions, and other requirements.

The reference conceptual design for a shaft seal at Gorleben includes three sealing elements consisting of different materials to ensure that the performance of the seal system meets requirements. The design of these sealing elements takes into account the different kinds of salt solutions present in the host rock to the need to avoid chemical corrosion. These sealing elements are a seal located at the top of the salt rock and made of bentonite, a second seal made of salt concrete, and a third seal made of sorel concrete which is located directly above the disposal level. The sealing elements are designed to maintain their functionality until the crushed salt backfill in the repository drifts, access ways and emplacement fields have sealed in response to compaction driven by host rock creep.

ELSA is a programme of laboratory tests and performance assessment studies that will be used to further develop the reference shaft seal design for the German reference disposal concepts for repositories in salt and clay host rocks.

2.2 DOPAS Design Basis Workflow

Work on the design basis in the DOPAS Project has allowed assessment of current practice with regard to both the process used to develop and describe the design basis and the content of the design basis of plugs and seals. The design basis is developed in an iterative fashion with inputs from regulations, technology transfer, tests and full-scale demonstrations, and performance and safety assessments. The learning provided by WP2 has been used to describe a generic process for development of the design basis for plugs and seals called the “DOPAS Design Basis Workflow” (Fig. 2.1).

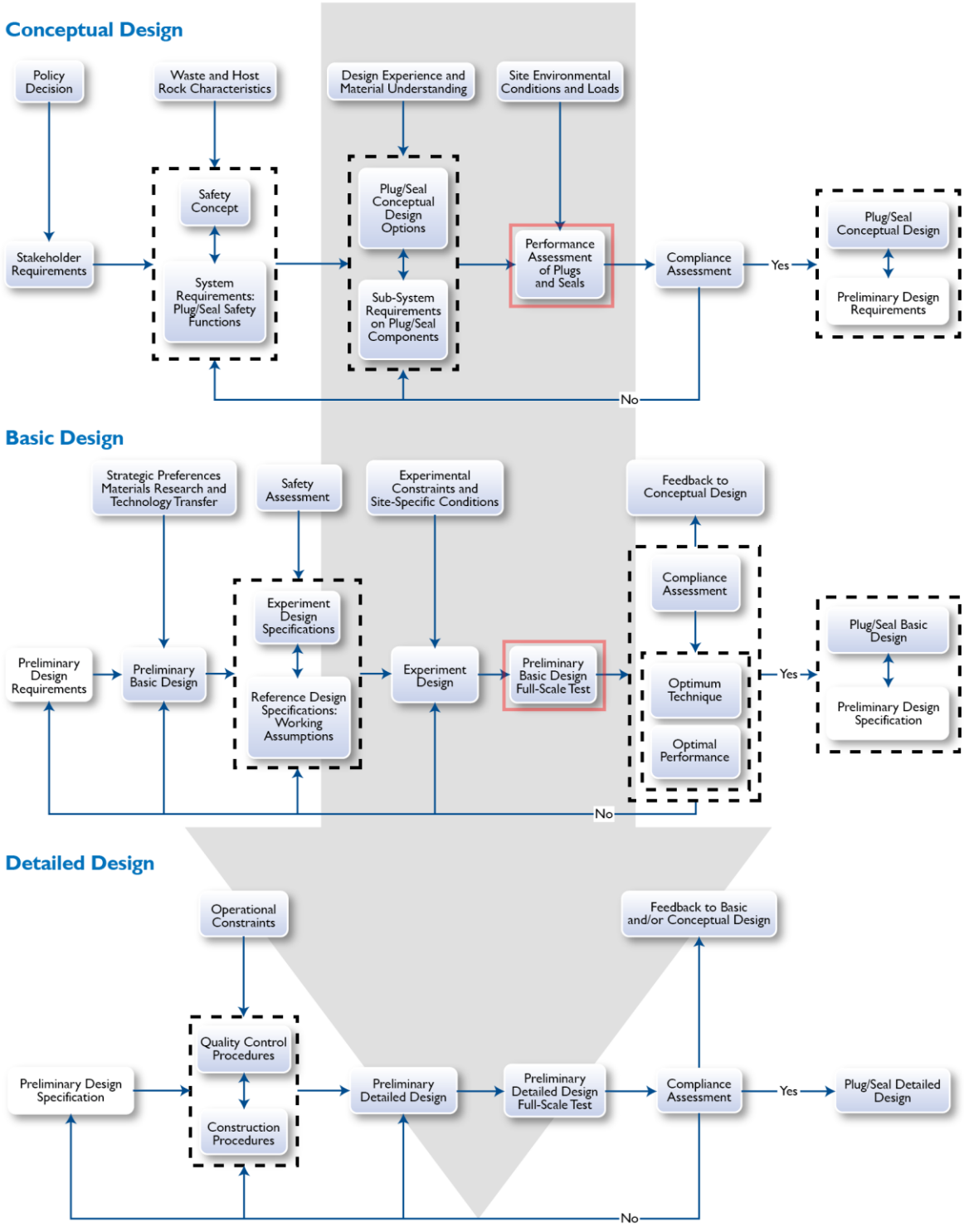

Fig. 2.1: The DOPAS Design Basis Workflow illustrating the iterative development of the design basis. Red boxes show, where the WP5 work falls into.

This workflow is structured to be consistent with three broad design stages:

- **Conceptual Design:** Conceptual designs describe the general layout of a repository structure, including the different repository components and how they are arranged, and the type of material used for each component (e.g., concrete, bentonite, gravel). In a conceptual design, the environmental conditions (including rock characteristics) are presented in generic terms, for example by describing the nature of the processes occurring rather than quantifying the processes. The performance of the components and the overall structure are described qualitatively.
- **Basic Design:** In a basic design, the components in the conceptual design are described in more detail with an approximate quantitative specification of geometry and material parameters. The properties of the environmental conditions are presented in detail, which requires characterisation of the site or elaboration of the assumptions underpinning the design. Performance is described quantitatively.
- **Detailed Design:** In a detailed design, the concept is presented in such detail that it can be constructed, i.e., it provides precise information on all aspects of the structure's components.

The work performed within WP5 falls into the boxes framed in red, which are "*performance assessment of plugs and seals*", shown as central box for the conceptual design and the "*preliminary basic design full scale test*", shown for the basic design. Both are again multi-step processes consisting of the experiments itself and the pre and post work including planning and prediction and evaluation by process modelling (see figure 2.2).

Even for DOPAS, with 48 months of duration being a long running project, this project can only partly represent the iterative process of preparative laboratory work, planning of a large-scale experiment, executing the experiment and finally investigating the results by process modelling. Due to the long duration of the large scale experiments and an early data freeze, the work performed in WP5 does not comprise the last step shown in figure 2.2, the evaluation process modelling of the full scale experiments.

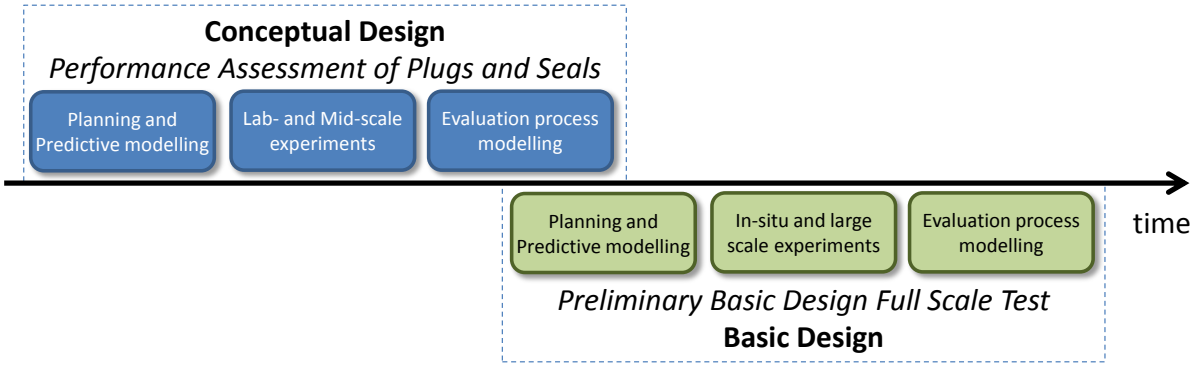

Fig. 2.2: Role of process modelling in the workflow of development of the conceptual design and the basic design

3 Work package 5 as part of the DOPAS project

The report at hand is the final report of Work package 5 on "Performance assessment of the plugs and seals systems". The aim of WP5 was mainly twofold. The first aim was the support the planning, construction and experimental work of the large-scale demonstrators by predictive process modelling. Another aim of WP5 was to understand the implications of the plugs and seal performance on the overall safety for the whole assessment period of a final waste repository of one million years. An important element of this work was to develop justification of model simplifications for long-term safety assessment simulations. This includes the objective to improve the state-of-the-art in process modelling and its abstraction in integrated performance assessment. More specifically the objectives can be defined as follows:

- simulation of processes and their evolution within individual sealing components,
- predictive modelling to support the design and the construction of the large-scale seals,
- modelling of small and mid-scale experiments performed in WP3 to gain process understanding,
- identification of the main processes that are relevant and thus to be considered for predicting the short and long-term behaviour of the plug and sealing systems,
- identification of remaining uncertainties and their influence on performance assessment,
- development and justification of conceptual models of plugs and seals for the different disposal concepts and geological environments and
- development and application of the PA methodology and integrated PA models to analyse the system behaviour.

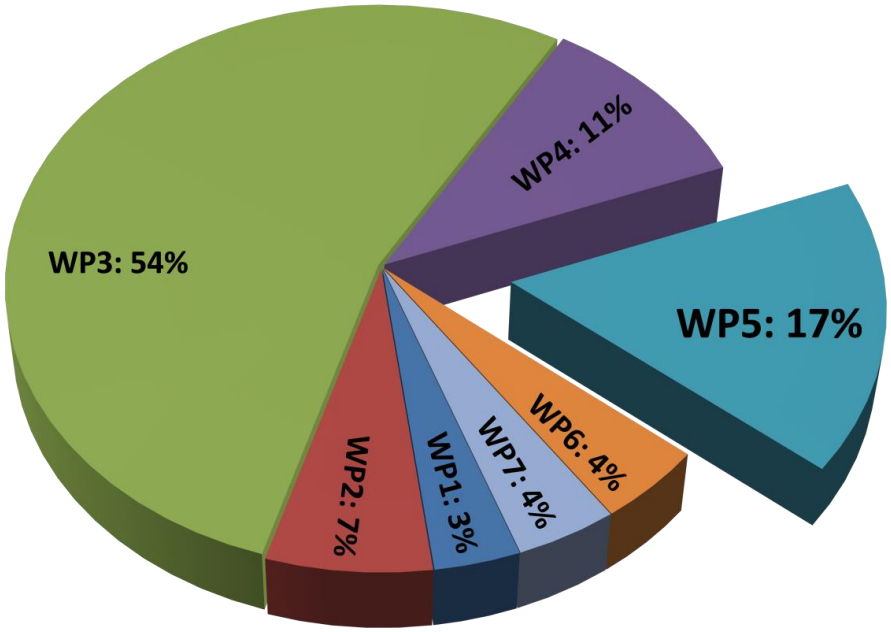

Fig. 3.1: Distribution of efforts within DOPAS project as planned

17 % of the overall DOPAS budget was dedicated to WP5 as shown in figure 3.1. Work-package 5 was divided into the following four different tasks which have a different focus. The task 5.1 is mainly on process understanding and has a very strong link to the experimental work performed in work-package 3 and the other work-packages of the project. The task describes the process on a phenomenological basis and its evolution on different time scales. Suitable process models were identified and improved if necessary to perform process models. The large part of the work performed in this task supported the planning and construction of the experimental work. The first task was the largest part of WP5 regarding work and budget, as can be seen from figure 3.2. In the task 5.2, conceptual models were developed striving for abstraction of the process level-work performed in the first. The second task is therefore the link to the third task which finally focused on integrated long-term performance assessment modelling. Integrated models were finally developed and applied in task 5.3 with regard to demonstrate long-term safety and to determine remaining uncertainties and open questions. The task 5.4was devoted to Work package management and reporting.

Ten out of the 14 organisations participating in DOPAS contributed to the WP5 work. These organisations are: ANDRA, CTU, DBETEC, GSL, GRS, NRG, Posiva, RWM, SURAO and UJV.

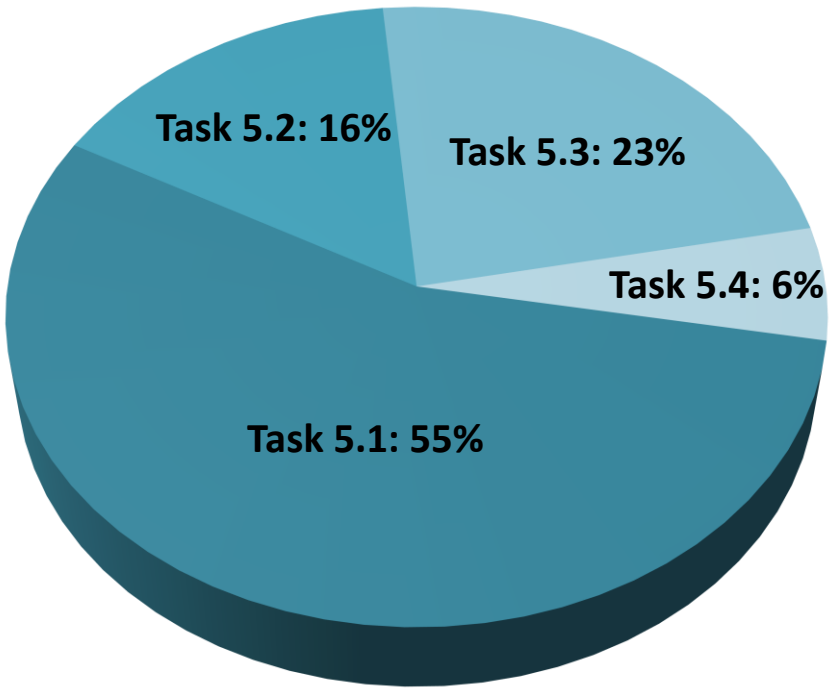

Fig. 3.2: Distribution of efforts within work-package 5

The modelling activities performed in WP5 can be classified and distinguished into the following four categories:

1. **Modelling in support of experimental design** and design optimisation. This type of modelling has to be based on reliable tools and a robust test set-up to be able to predict the

temporal evolution of the experiment and allow for the optimisation thereof. Typical modelling tools and modelling strategies are simple (forward) scoping calculations, sensitivity analyses and scenario assessments, aimed at assessing the experimental procedures for a representative range of initial and boundary conditions.

2. **Model development and model validation.** This type of modelling includes the development of phenomenological or process-level models, often by comparision with experimental results or by code comparison. The model development needs a clear and traceable verification and validation strategy in the framework of prediction-evaluation benchmarks.
3. **Model-based experiment analyses** with verified codes and validated models for model calibration or to analyse the conceptual and parametric uncertainties.
4. **Modelling in support of performance assessment** aims at assessing the expected temporal evolution of the reference (sub-) system on an abstracted or integrated level. Typically this type of modelling includes deterministic simulations, but also stochastic simulations for sensitivity analyses and scenario assessment.

The first four categories fall into the process modelling activities and were performed in the tasks 5.1 and 5.2, while the last category is denoted as integrated performance modelling which was performed in task 5.3. It has to be clearly noted that the process-level modelling work performed in work-package 5 is only partly based on and integrates experimental results of WP3. Actual results of WP3 experiments were only used in the process-modelling for smaller scale laboratory experiments. The main reason for this is the long time needed to execute the full-scale experiments. Most of the experiments were not finished during the time of the DOPAS project and the experimental results were only partially available. Consequently, the large part of the work is not based on the WP3 experiments, but rather contributed to their planning and execution. Process modelling has therefore most effectively helped in design and dimensioning the experiments in advance of the experiments. Additionally, process-level modelling was performed to predict expected results of the large scale experiments. This modelling work will be continued as the experiments progress even after the end of the DOPAS project (see also chapter 12).

This report is to summarise the work performed in WP5 and to links to other reports and DOPAS deliverables were the results are given in higher detail. Not reported here is the work of SKB on predictive modelling for the DOMPLU plug which was performed already prior to DOPAS and is reported in Börgesson et al. (2015). The following eight chapters give an overview of all contributions from the different organisations participating in WP5 and present the following work (numbers of categories for modelling type refer to the preceding list):

– Treatment of Seals and Sealing Systems in Total System Performance Assessment (chapter 4).
  This work is a review performed jointly by Radioactive Waste Management Limited (RWM) and Galson Sciences Limited (GSL) on the state of the art of the treatment of sealing systems in Safety Assessment (SA) or Total System Performance Assessment (TSPA)

in different countries. This work does not include any new modelling and is linked to the DOPAS work by giving the current understanding for organisations working with experiments. The results of the work have not been validated, but are based on the latest safety assessments from the reviewed cases in the regarded countries. Since these safety assessments were partly issued already long time before the start of DOPAS this might not fully be in full agreement with the statements on the repository safety concept and the safety functions of plugs and seals as discussed in WP2 of DOPAS.

- Assessment of water tightness and mechanical integrity of POPLU plug (chapter 5).
  This work of category 1 by Posiva Oy (Posiva) is a predictive process modelling of mechanical and hydraulic processes of the full scale POPLU experiment. The modelling assessed the water tightness and mechanical integrity of the POPLU experiment to serve as input in the experiment construction. The results of this work was directly used in WP3 and the construction of the plug.

- Design, implementation, monitoring and simulation of the REM experiment as part of the development program for Performance Assessment (chapter 6).
  This work of categories 2 and 3 by Agence nationale pour la gestion des déchets radioactifs (Andra) is a predictive process modelling of hydraulic processes performed to estimate the expected resaturation behaviour of the mid-scale REM experiment, which serves as a metric scale demonstrator of the large-scale FSS experiment. This chapter also presents a summary of the actual methodology and phenomenological comprehension of sealing at Andra.

- Process level modelling of compaction processes (chapter 7).
  This work of category 3 by DBE TECHNOLOGY GmbH (DBETEC) is a predictive and evaluation process modelling of mechanical processes for mid-scale in-situ experiments which were performed at the same time, but outside the framework of the DOPAS project. The modelling evaluates the compaction behaviour of crushed salt which is to be used as sealing materials for the long-term sealing in the ELSA experiment.

- Process modelling of seal materials (chapter 8).
  This work of categories 2 and 3 by Gesellschaft für Anlagen und Reaktorsicherheit gGmbh (GRS) is a predictive and evaluation process modelling of mechanical, hydraulical and chemical processes of small-scale laboratory experiments performed in WP3 which are related to the ELSA experiment. This modelling was performed to test the mechanical and chemical behaviour of clay, salt concrete and magnesium concrete materials considered as sealing materials in the ELSA basic design.

- Improvement of plug related processes representation in the integrated performance assessment code LOPOS (chapter 9).
  This work of category 4 by Gesellschaft für Anlagen und Reaktorsicherheit gGmbh (GRS) is a code development and an abstracted integrated performance assessment modelling work on the full scale of the sealing system. The work aims to integrate the processes identified to affect the sealing elements of the ELSA experiment into the integrated performance assessment model LOPOS by GRS.

– Process modelling of bentonite saturation in the PHM experiment and testing the influence of bentonite sealing property for safety of deep geological repository (chapter 10).
  This work of category 2 and 3 by ÚJV Řež, a. s. (UJV) is a predictive and evaluation process modelling of the results from the physical hydraulic model carried out under laboratory conditions as part of the EPSP experiment Predictive and Evaluation process modelling. This work was performed to estimate the hydraulic processes and the resaturation in the bentonite of lab-scale experiments.

– Options to link demonstrator activities with performance assessment by the use of indicators (chapter 11).
  This work of category 4 by Nuclear Research and Consultancy Group (NRG) is an integrated performance modelling work on the full repository system scale. This work aims at using safety and performance indicators to investigate options to link the demonstrator activities with performance assessment.

The nature of the different modelling approaches presented is unique for each piece of work and cannot be compared to each other directly. Each of the work has a different function for to the related experiment or in the related national program and therefore has to be regarded as independent. The eight topical chapters therefore are representing the views from the different organisations represented by the authors given, which are solely responsible for the content of the work.

It has also to be noted that a wide range of definitions and concepts related to nuclear waste disposal exist and the use and meaning of terms differ significantly from country to country. An outcome of the discussion in the PAMINA (Performance Assessment Methodologies in Application to Guide the Development of the Safety Case) project in the 6th EC framework programme (http://www.ip-pamina.eu) was, that there is no need to harmonise the terminology across the different countries, but a common understanding is necessary for communication. Following this conclusions, the following chapters have to be regarded as contributions from the different programs to the DOPAS project, which are based on their national context and use their national terminology.

4 Treatment of Seals and Sealing Systems in Total System Performance Assessment (RWM, GSL)

M. Crawford, D. A. Galson, L. E. F. Bailey

4.1 Introduction

Generally, TSPAs calculations for normal evolution scenarios assume that plugs and seals perform "as expected" and, in turn, the calculations show that the disposal system as a whole provides acceptable post-closure safety. Put another way, any intended post-closure safety function(s) of the plugs and seals – principally hydraulic isolation – is fulfilled by expected performance and contributes to overall safety.

Treatment of uncertainty in seal performance in TSPAs can be categorised using the widely-used three-fold classification of parameter, model and scenario uncertainty:

- **Parameter uncertainty**. Uncertainty analyses or probabilistic calculations may be used to take account of uncertainty in the properties of seals. The parameter values may be based on supporting modelling and/or expert judgement. The properties are either conservatively kept constant over time or changed in a stepwise fashion. Changing properties over time are used to account for known, but often poorly constrained, processes such as concrete degradation, salt compaction, and clay swelling. The potential for sudden change may drive scenario definition rather than be captured as parameter variation within the same scenario.
- **Model uncertainty**. Alternative model configurations or conceptual uncertainty in the modelling of features, events and processes might be captured through sets of analyses specified to address model uncertainty. However, no examples of "top-level" TSPA modelling of actual processes leading to changes of plugs and seal properties during a calculation were found.
- **Scenario uncertainty**. Some TSPAs, particularly those concerned with disposal concepts in low-permeability sedimentary host rock, consider scenarios that explicitly include a situation of poor seal performance. In such scenarios, however, advective migration of radionuclides generally remains limited, since virtually no water enters the disposal areas owing to the low hydraulic conductivity of the host rock. The bounding case of abandonment of a GDF before closure, i.e. before emplacement of final tunnel closures and shaft/access ramp seals, is included in a number of TSPAs. In the case of the Swedish TSPA for disposal of spent fuel in a crystalline rock, the abandonment calculation is considered as a Future Human Action scenario.

4.2 Aims and Objectives

This chapter considered the question "how do existing PAs for long-term safety treat plugs and seals?". The distinction should be made here that the question has considered published PAs for the performance of deep or geologic disposal facilities (GDFs) in their entirety, while DOPAS WP5 is more generally considering PAs for seals only, i.e. at a component scale. Therefore, to be clear on the difference, this report refers to the PAs for GDFs in their entirety as Total System Performance Assessments or TSPAs.

The objective of the review reported here was to evaluate how sealing systems have been considered in published TSPAs undertaken to evaluate the safety of GDFs for radioactive waste. This review is not validated by each organisation handled in this chapter and the content and interpretation represents the general understanding of authors.

Given the objective, it was considered desirable to cover as many examples of TSPAs as possible. It should be noted that the example for each country is the last published TSPA; in a number of cases, the TSPA is quite old and may not therefore represent the current programme position. The countries covered in the review and the associated Waste Management Organisation (WMO) and TSPA are listed below by host geological environment for the GDF:

- Crystalline host rock
    - Sweden; SKB SR-Site 2010, updated 2015 (SKB 2015): Spent Fuel (SF).
    - Finland; Posiva TURVA 2012 (Posiva 2012a): SF.
- Sedimentary non-evaporite host rock
    - France; ANDRA 2005 Argile (Andra 2005, Andra 2005a): SF/high-level waste (HLW)/intermediate-level waste (ILW).
    - Switzerland; NAGRA Entsorgungsnachweis 2002, SGT-E2 (Nagra 2002; Poller *et al.* 2014): SF/HLW/ILW.
    - Canada; OPG DGR (NWMO 2011); Low-Level Waste (LLW) and ILW.
    - Belgium; ONDRAF-NIRAS SAFIR2 (ONDRAF/NIRAS 2001); HLW/ILW.
- Salt
    - United States; USDOE WIPP Compliance Certification Application (USDOE 1996); updated 2004, 2009, and 2014: ILW.
    - Germany; GRS Vorläufige Sicherheitsanalyse für den Standort Gorleben – VSG 2012 (Larue *et al.* 2013): SF/HLW/ILW.

4.3 Sweden

4.3.1 Background

The Swedish WMO, SKB, has submitted an application for a GDF for the disposal of spent nuclear fuel, SR-Site (SKB 2015). The application includes a long-term safety assessment. The disposal concept is the KBS-3V concept involving long-lived copper canisters of spent fuel surrounded by a bentonite buffer placed in vertical boreholes in crystalline rock (Fig 4.1). The boreholes are accessed from deposition tunnels that are backfilled.

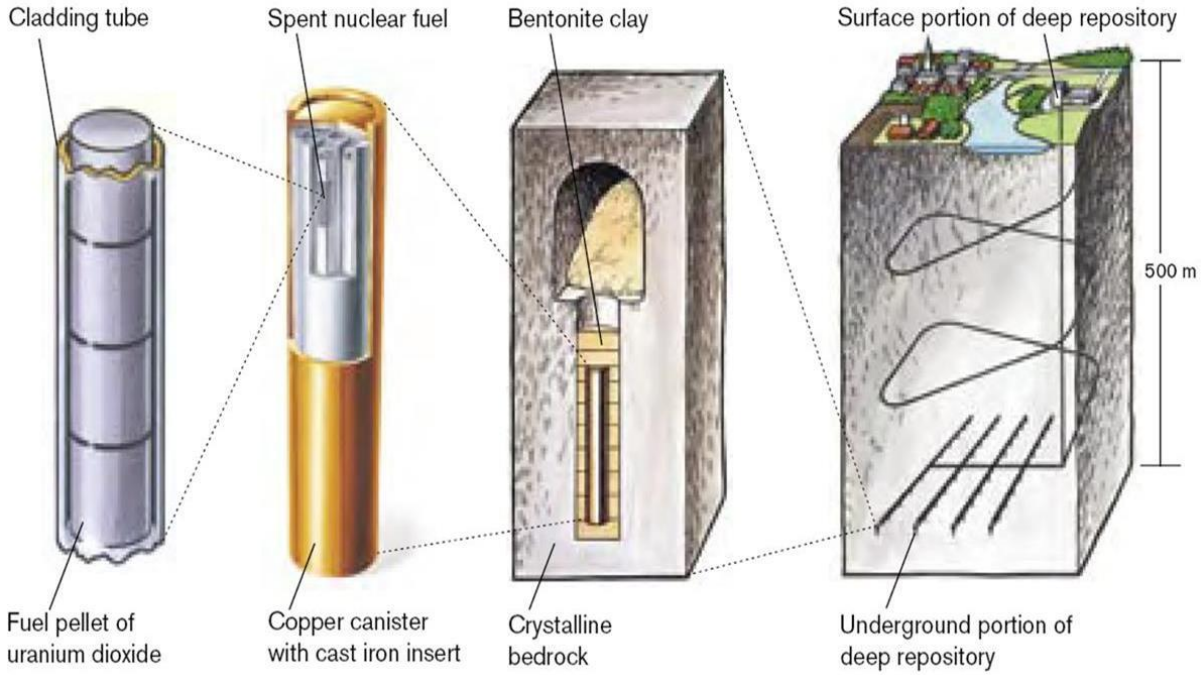

Fig 4.1: Swedish KBS-3V disposal concept for spent fuel (SKB 2015).

The disposal concept makes a distinction between plugs at the ends of the deposition tunnels and seals for the access ramps and shafts. In terms of safety functions, the plugs provide mechanical stability during operations and ensure that the tunnel backfill saturates effectively. The plugs must limit water flow into open tunnels during resaturation and must, therefore, maintain a low hydraulic conductivity during the operational phase of the facility. The sealing system on the ramp leading from the surface to the disposal areas is intended to hinder unintentional intrusion into the GDF, but no restriction is placed on the hydraulic conductivity in the top seal of the ramp. Investigation boreholes drilled during the development of the GDF must be sealed such that they do not unduly impair containment or retention properties of the facility.

4.3.2 Scenarios regarding Sealing

The SR-Site TSPA includes a “Reference Evolution” scenario. The analysis and supporting modelling that consider the development of the reference evolution scenario take account of

uncertainties in the properties of the backfill, tunnel plugs and surrounding Engineered Disturbed Zone (EDZ). These analyses support the expectation that the buffer and backfill will provide the expected performance and the principal radionuclide release pathways will be through the buffer, backfill and fractured host rock, rather than along tunnels and around the plugs. As such, the performance of the plugs is not a significant feature of the scenario development.

Alternative scenarios to the Reference Evolution scenario include the categories of "less probable" and "residual" scenarios, but these are generally concerned with the safety functions of engineered components other than the plugs and seals - principally the waste canister and bentonite buffer.

Regarding the safety function of the ramp seal, a bounding analysis of an unsealed or incompletely sealed facility is conducted as part of a future human action scenario – the "abandonment" scenario. This scenario assumes that the GDF is abandoned when all the spent fuel canisters have been deposited and all deposition tunnels backfilled and sealed, but all other areas and access routes are still open.

4.3.3 Modelling and Results

The modelling of the abandonment scenario considers three principal impacts:

- Analysis of expansion of deposition tunnel backfill into open main tunnels.
- Groundwater flow modelling of open tunnels.
- Simple estimates of oxygen supply and canister corrosion.

The modelling results are intended as an illustration of the possible consequences of abandonment.

The impact of the open tunnels for deposition holes other than those directly affected by the expanding backfill is small.

During the first glacial period (58,000 to 66,000 years from present), corrosion breakthrough of canisters may occur in deposition holes closest to the open tunnels and these would be the first to experience penetrating oxidising groundwater. The annual effective dose from one failed canister would exceed the regulatory risk limit (14 μSv/year). However, if the number of failed canisters is less than c. 20, the effective dose would still be lower than background (1 mSv/year).

4.4 Finland

4.4.1 Background

The Finnish WMO, Posiva, is constructing a GDF for the disposal of spent nuclear fuel in crystalline basement at Olkiluoto. Posiva published a TSPA for Olkiluoto, TURVA-12, in 2012 (Posiva 2012a). The disposal concept is based on the Swedish KBS-3V concept.

4.4.2 Scenarios regarding Sealing

The TURVA-12 PA considers a Base Scenario Reference Case (RC) that accounts for one disposal canister with an initial penetrating defect. Otherwise, modelling and argument show that intact non-defective canisters are not penetrated over the timescale of the safety calculations.

There are no variant scenarios published dealing explicitly with seals and seal performance. Buffer erosion and advective flow scenarios are related to rock shear and/or penetration of dilute water. A calculation case for a scenario accounting for unsealed investigation boreholes is considered in terms of impact in groundwater flow modelling.

4.4.3 Modelling and Results

Seals are not modelled explicitly – transport is through fractures in the host rock, with three transport pathways reflecting different routes to fractures through the deposition hole buffer, disturbed zone around the deposition tunnels, or backfill. The RC groundwater flow modelling includes a calculation that incorporates a 0.1-m thick crown space in disposal tunnels with a high hydraulic conductivity (10^{-3} m/s) (Posiva 2012b). Assuming voids exist in the crown space has a moderate detrimental effect on (i.e. increases) flow in the fractures connected to the deposition tunnels, though not on flow in fractures connected to the deposition holes, and not on flow-related transport resistance.

4.5 France

4.5.1 Background

The French WMO, ANDRA, published an evaluation of the development of a GDF for spent fuel, HLW and ILW in a clay (Argile) and crystalline (Granite) host rock in 2005 (ANDRA 2005). A GDF is now being designed for a clay host rock in the eastern part of the Paris Basin (the Cigéo project). However, no published information is available on the developing TSPA for the Cigéo. Therefore, this review has focused on the 2005 safety evaluation for the GDF in a clay host rock (ANDRA 2005).

The disposal concept envisages a horizontal layout of disposal tunnels of varying diameters at the same depth for all of the waste types (Fig. 4.2). Various components of the horizontal disposal area (the "repository zone" comprising disposal cells, cell access drifts, connecting drifts) will be sealed by plugs of a low permeability. When closure is decided (there may be a period when the facility is kept open for retrievability of the waste), the remaining connecting drifts and access shafts will be sealed. Shaft seals will be constructed in the upper part of the host clay formation by removing the shaft liner over sections of several metres in length, in order to place the swelling clay in the seal in direct contact with the clay host rock.

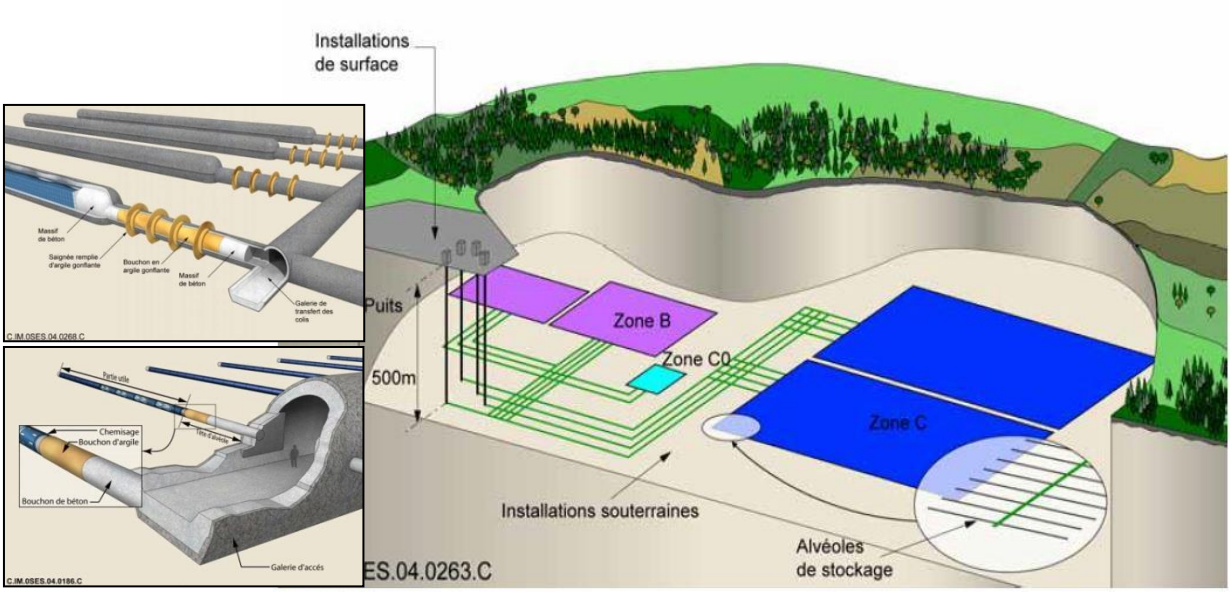

Fig. 4.2: French disposal concept for ILW (Zone B wastes; top insert) and HLW ± SF (Zone C wastes; bottom insert) in clay from Argile 2005 (Andra 2005a). Note that the disposal concept has now developed further under the Cigéo project.

4.5.2 Scenarios regarding Sealing

The Normal Evolution scenario in the safety evaluation includes isolated disposal canister and cell plug failure. This is owing to the consideration that, despite quality control, it is not possible to guarantee the quality of every canister deposition and plug installation.

The safety evaluation also includes an altered evolution scenario that explicitly considers seal failure. The scenario is designed to assess the robustness of the disposal system with respect to various combinations of defects in seal components. The modelling also considers a damaged zone around the engineered structures as a potential radionuclide transfer pathway. Four altered evolution calculation cases are considered in the scenario:

- Failure of shaft seals.
- Failure of seals with hydraulic cutoffs (ILW cell/module seals, repository zone seals and connecting drift seals).
- Failure of all seals.
- Abandonment of GDF without surface to underground access structure seals.

4.5.3 Modelling and Results

For each scenario, two transfer pathways are quantified (Fig. 4.3):

- Transfer through the geological barrier (five calculation compartments - waste packages, disposal cells, repository, geological medium, biosphere).
- Transfer through the engineered structures (additional calculation compartment for repository and access structures).

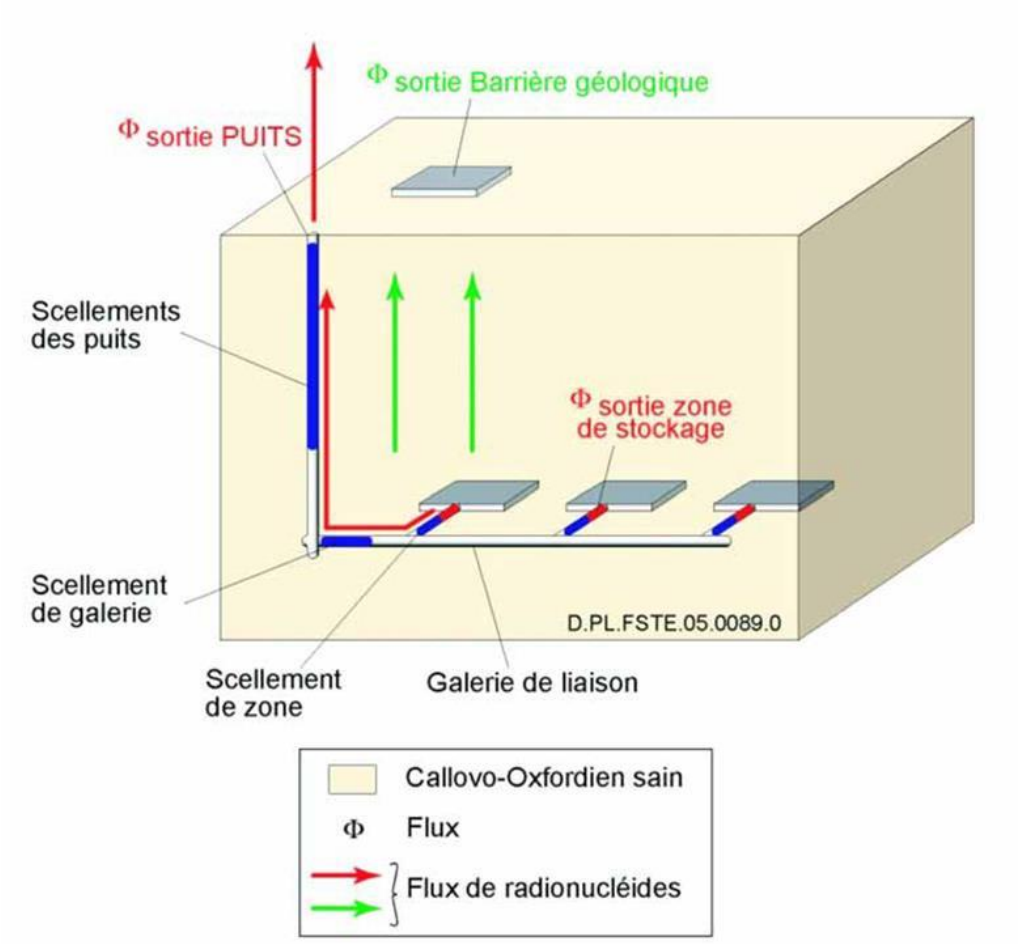

Fig. 4.3: Transfer pathways considered in the Andra Argile 2005 TSPA (Andra 2005a).

The seal failure scenario is represented by introducing a swelling clay to rock interface defect, with the seal core maintaining its hydraulic properties. Seal failure is considered as happening a few centuries (500 years) after GDF closure.

4.6 Switzerland

4.6.1 Background

The Swiss WMO, Nagra, is considering disposal of spent fuel, HLW and long-lived ILW in a GDF in Switzerland. In 2002, Nagra published a safety case for the disposal of waste in the Opalinus Clay host rock (Entsorgungsnachweis). More recently, Nagra has been conducting siting evaluations for a GDF in several areas of Switzerland with a clay host rock. Stage 2 of the work considering six areas was published in 2014 (SGT-E2). This review covers the 2002 Entsorgungsnachweis study (NAGRA 2002) that includes a TSPA with scenario development. At the end of this section, there is also a description of a 2014 modelling study that considered alternative sealing configurations in a GDF in an Opalinus Clay host rock (Poller *et al.* 2014).

The 2002 disposal concept was termed “monitored long-term geological disposal”, with emplacement of waste in horizontal tunnels in the clay host rock. Access to the system of waste emplacement tunnels would be provided, during construction and operation, by a spiral ramp and operations and construction tunnels. A vertical shaft, also used for construction during enlargement of the facility, would provide ventilation. At closure, the operations and construction tunnels, the central area and the access ramp would be backfilled with a bentonite-sand mixture. Seals of highly compacted bentonite between bulkheads would be placed at several locations. The shaft would be sealed with highly compacted bentonite.

4.6.2 Scenarios regarding Sealing

The Reference scenario in the 2002 safety case considered a low groundwater flow rate along the sealed tunnels / ramp / shaft, and through the surrounding EDZs. Uncertainty analyses included consideration of how the release of radionuclides might be affected by the hydraulic properties of the ramp / shaft and their surrounding EDZs.

An alternative scenario was developed specifically to evaluate the release of volatile radionuclides (i.e. C-14) along gas pathways. The analysis considered tight seals, where the transport pathway was through the host rock only, and leaky seals, where the transport pathway was along the access tunnels themselves.

A "What if?" case of gas-induced or gas-driven release of dissolved radionuclides from ILW along the access ramp only was also modelled.

4.6.3 Modelling and Results

Entsorgungsnachweis 2002

The main seals in the access ramp were conceptualised as incorporating a ~40-m-long section of highly compacted bentonite with the concrete tunnel liner and most of the EDZ removed. The long-term hydraulic conductivity of the seals was assumed to be < 1E-13 m/s, approximately the same value as that of undisturbed Opalinus Clay. However, the model also allowed for an EDZ retaining an enhanced hydraulic conductivity (up to ~ 10 times that of undisturbed Opalinus Clay) to represent the case where the swelling pressure of bentonite in the seal and the deformation of the EDZ by convergence do not fully reduce the porosity and permeability of the seal. Few data are available on the large-scale permeability of the EDZ and time-dependent changes in EDZ properties, and the modelling approach was considered to be a pessimistic assumption.

In the alternative scenario considering release of volatile radionuclides (C-14) along gas pathways, the results for tight seals showed reduced doses compared to the Reference Case, while the results for the leaky seals were similar to the Reference Case.

The “What if?” analysis of gas-induced release of dissolved radionuclides from ILW along the access ramp only gave a dose maximum for ILW of 1.1E-5 mSv/y (Base Case analysis) compared to 4.3E-6 mSv/y for the Reference Case (ILW only).

SGT-E2 2014 (Poller* et al. *2014)

PA modelling of sealing of a generic disposal system for HLW and L/ILW in clay considered the impact of alternative arrangements and performance of seals (Fig. 4.4). The overall modelling approach consisted of three broad steps:

1. The network of tunnels and access structures is implemented in a flow model, which serves to calculate water flow rates along the tunnels and through the host rock.

2. All relevant transport paths are implemented in a radionuclide release and transport model, the water flow rates being obtained from the flow model calculations.

3. Individual effective dose rates arising from the radionuclides released from the disposal system are calculated using biosphere dose conversion factors.

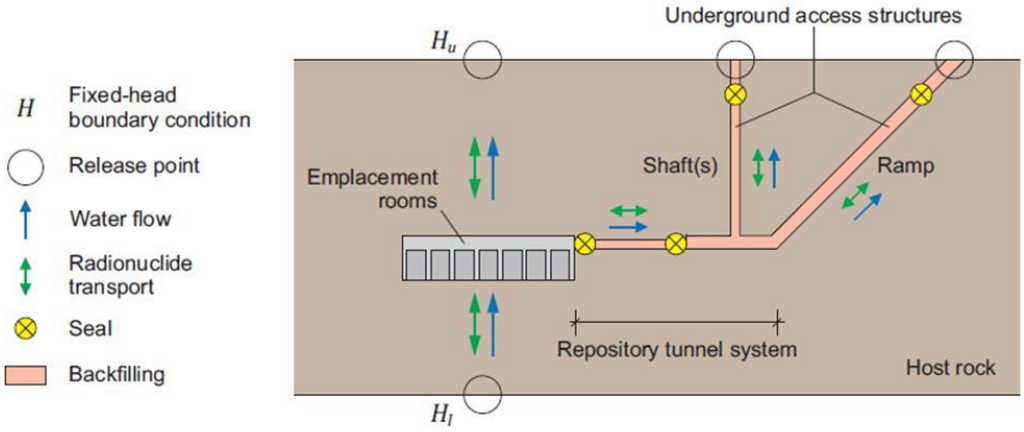

Fig. 4.4: Possible access routes considered in modelling for a GDF for HLW and/or L/ILW in clay in Switzerland (Poller *et al.* 2014).

Using realistic parameter values, radionuclide release along the access structures was shown to be extremely low. The modelling confirmed the reference assumption that radionuclide release occurred predominantly through the host rock rather than along the sealed access structures. Increasing the hydraulic conductivities assumed for the tunnel system and seals (including the EDZ) increased calculated flows along all of the access routes, but the increase in flow levelled off as conductivities were further increased as the flow became controlled by the capacity of the host rock to supply water. Dose rate maxima due to releases via access structures showed the same asymptotic behaviour as flow, and remained low in all cases.

4.7 Canada

4.7.1 Background

Ontario Power Generation (OPG) in Canada is proposing to develop a GDF (or Deep Geologic Repository – DGR) for LLW and ILW in a sedimentary host rock at Kincardine. A post-

closure safety assessment was published in 2011 to support an Environmental Impact Statement (EIS) and Preliminary Safety Report (PSR) for the proposed GDF (NWMO 2011).

4.7.2 Scenarios regarding Sealing

The future evolution of the DGR system is assessed through a Normal Evolution Scenario and four Disruptive Scenarios that consider events that could lead to possible penetration of barriers and abnormal degradation and loss of containment.

One of the Disruptive Scenarios is termed the Severe Shaft Seal Failure Scenario and considers the consequences of rapid and complete seal degradation in the shafts, and the increased degradation of the GDF and shaft EDZs. Otherwise, the evolution of the DGR system is the same as in the Normal Evolution Scenario.

Another of the Disruptive Scenarios concerns a Poorly Sealed Borehole that extends from the surface to the Precambrian basement beneath the DGR The borehole provides a potential additional pathway for contaminants from the host rock to the Shallow Bedrock Groundwater Zone.

4.7.3 Modelling and Results

The conceptual model for the Severe Shaft Seal Failure Scenario is essentially the same as for the Normal Evolution Scenario with gradual degradation of the seals. The modelling is implemented in three software codes: AMBER 5.3, a compartment-model code for assessment-level (system) models; the 3-D finite-element/finite-difference code FRAC3DVS-OPG for detailed groundwater flow and transport calculations (Fig. 4.5); and T2GGM, a code that couples the Gas Generation Model (GGM) and TOUGH2 for detailed gas generation and transport calculations. The calculations for the Severe Shaft Seal Failure Scenario differ from the Normal Evolution Scenario using modifications to parameter values, with significantly degraded physical and chemical characteristics of the seals and increased permeability of the GDF and shaft EDZs (the EDZ properties are simply a multiple of the host rock properties).

The maximum calculated doses for the Severe Shaft Seal Failure Scenario are about 1 mSv/a, based on immediate failure of 500 m of low-permeability shaft seals (to 10^{-9} m/s hydraulic conductivity), reduced sorption in the shafts, increased degradation of shaft and GDF EDZs, and assuming a family is farming directly on top of the shafts (including a house located on the main shaft). The scenario is very unlikely. Therefore, the risk from the severe shaft seal failure scenario is low.

For the Poorly Sealed Borehole scenario, detailed groundwater flow modelling indicates that the borehole has limited influence on hydraulic conditions at the disposal horizon. Results also indicate that the flow of water up the borehole is relatively small, discharging up to 15 m^3/year into the shallow system that is flowing at a rate of about 60,000 m^3/year. Therefore, calculated peak annual doses for the Poorly Sealed Borehole Scenario are much less than the dose criterion.

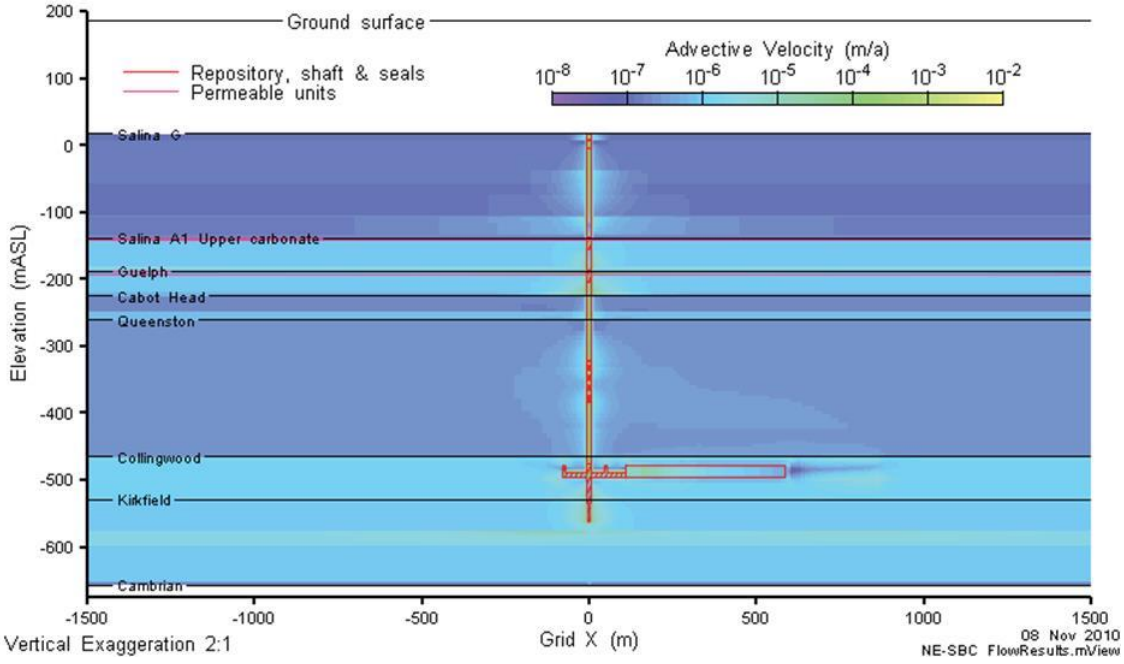

Fig. 4.5: Modelled advective groundwater velocities for the steady state simplified base case for a GDF for LLW and ILW in Canadian basement (NWMO 2011). The figure shows the position of the modelled borehole penetrating the geology directly adjacent to the GDF.

Additional cases were evaluated to determine the conditions necessary for a disruptive scenario to result in larger impacts than those resulting from the base case. For the Severe Shaft Seal Failure Scenario, the hydraulic conductivity of all the shaft seals would have to degrade by 4-5 orders of magnitude beyond the design basis to 10^{-7} m/s, about equivalent to fine silt and sand. In this case, the peak doses to someone living on top of the GDF site could be tens of milliSieverts.

4.8 Belgium

4.8.1 Background

The Belgian WMO, ONDRAF/NIRAS, published a safety case called SAFIR2 for disposal of ILW, HLW and spent fuel in a Boom Clay host rock in 2001. ONDRAF/NIRAS has since revised the disposal concept significantly, but SAFIR2 remains the latest complete published safety case and has been used in this review (ONDRAF/NIRAS 2001).

4.8.2 Scenarios regarding Sealing

A poor-sealing scenario is modelled where the main galleries and access shaft are poorly sealed, with the result that the seal has a much higher hydraulic conductivity than the Boom Clay barrier.

4.8.3 Modelling and Results

Impact of the poor-sealing scenario is limited. Advective migration remains very limited, since virtually no water enters the disposal areas owing to the low hydraulic conductivity of the Boom Clay. Only a small fraction of the radionuclide inventory leaves the near-field.

4.9 USA – Waste Isolation Pilot Plant

4.9.1 Background

The Waste Isolation Pilot Plant (WIPP) is operated by the US Department of Energy (DOE) for the disposal of transuranic (TRU) waste (roughly equivalent to long-lived LLW and ILW) from its defence programs. The WIPP facility is located 42 km east of the town of Carlsbad in southeastern New Mexico. Geologically, the GDF is located in the northern Delaware Basin, and is 655 m underground in the Permian-age Salado bedded salt formation. Drums of contact-handled waste are stacked in "panels", with remote-handled waste drums being emplaced horizontally, either singularly or in pairs, in boreholes in the walls of the panels. Waste panels consist of seven rooms. Each room has approximate dimensions of 90-m long, 10-m wide, and 4-m high. Salt pillars between rooms are 30-m thick. Magnesium oxide is packed in bags around and between the waste drums, to act as a chemical conditioner and to react with carbon dioxide gas after closure. The panels are closed using concrete-based seals when full. The underground is connected to the surface by four vertical shafts, each of which will eventually be sealed.

In October 1996, the DOE submitted its Compliance Certification Application (CCA; USDOE 1996) to demonstrate compliance with radioactive waste disposal standards and criteria that govern post-closure safety. In May 1998, certification was issued. The WIPP has to be periodically recertified, and recertification applications, including an update to the post-closure TSPA, have been prepared in 2004, 2009 and 2014 – however, the PA methodology has remained unchanged since the CCA.

Panel closures use a design based on using salt-saturated mass concrete. Shafts will be closed using a seal that extends throughout the shaft and involves numerous materials intended to control both short-term and long-term fluid flow through the host bedded salt formation. Boreholes are often drilled in the vicinity of the WIPP during resource exploration or exploitation. Any boreholes in the future that inadvertently intersect the GDF are assumed to be sealed according to current practice which will prevent both brine inflow to the disposal rooms from an underlying pressurised brine reservoir and any releases from long-term brine flow to groundwater and the surface.

4.9.2 Scenarios

The WIPP PA is a probabilistic simulation with the results presented in the form of a complementary cumulative distribution function (CCDF) for comparison to the regulatory criteria. The simulation considers an Undisturbed Performance scenario and several Disturbed Per-

formance scenarios involving disruption of the facility and/or its surroundings by some combination of exploration drilling or resource mining.

The panel closures and shaft seals are included in the two-phase water and gas flow calculations and radionuclide transport calculations for all scenarios.

4.9.3 Modelling and Results

Shaft Model

The WIPP TSPA uses a code called BRAGFLO to simulate two-phase water and gas flow through the disposal system. The code was qualified for the 1996 CCA and, therefore, has continued to be used in the later recertifications. In BRAGFLO, the four WIPP shafts are modelled as a single shaft; an analysis was undertaken to justify this assumption. For the 1996 TSPA, each material in the shaft design was represented and analysis indicated no significant flows of brine or gas up the shafts. Therefore, a simplified shaft model was developed for the later TSPAs consisting of three sections (USDOE 2009):

- an upper section (above the Salado – host rock);
- a lower section (within the Salado); and
- a concrete monolith section within the disposal horizon.

The lower section of the shaft is assumed to have a decrease in permeability 200 years after closure to simulate consolidation of seal materials within the Salado; the 200 year timeframe was chosen as conservative overestimate. The concrete monolith is represented as highly permeable throughout the simulation, which means that fluids access the operations area in the model. The permeability is sampled from a probability density function that has been reviewed for each iteration of the TSPA and by the regulators, but has remained unchanged since the 1996 TSPA (Fig. 4.6).

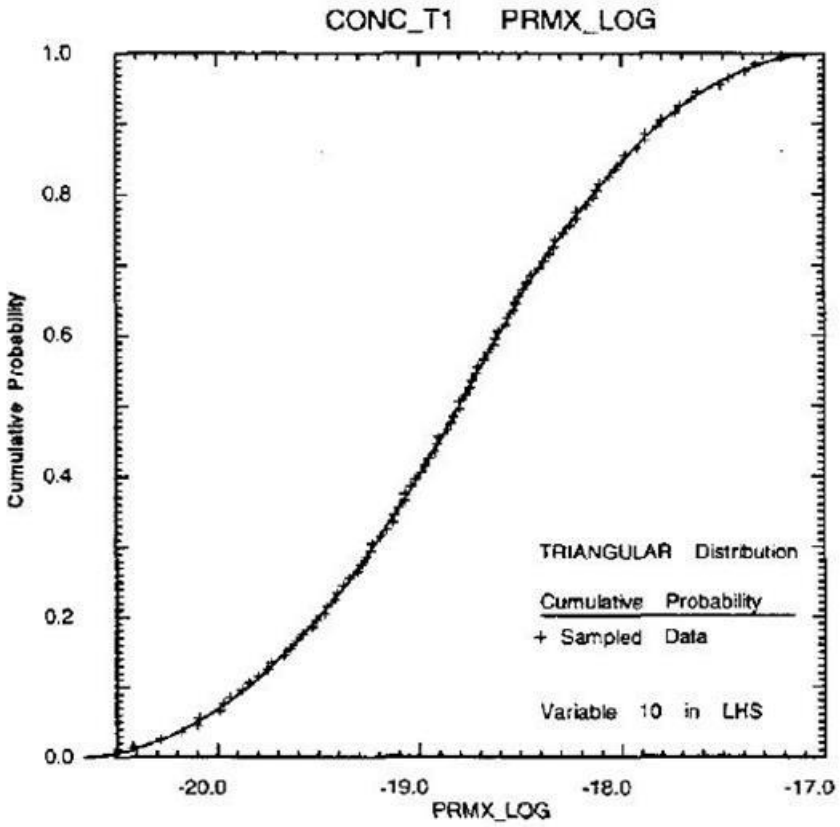

Fig. 4.6: Cumulative probability function for the hydraulic permeability of concrete in a panel closure (seal) at the Waste Isolation Pilot Plant (USDOE 1996).

Panel Closure Model

Disposal rooms are closed off from the access tunnels using panel closures designed to allow minimal fluid flow. The TSPA model in BRAGFLO explicitly represents each set of panel closures in the computational grid for flow modelling using four materials (salt-saturated concrete; anhydrite; an empty drift section; and a block and mortar explosion wall) set out in 13 grid cells (Fig. 4.7).

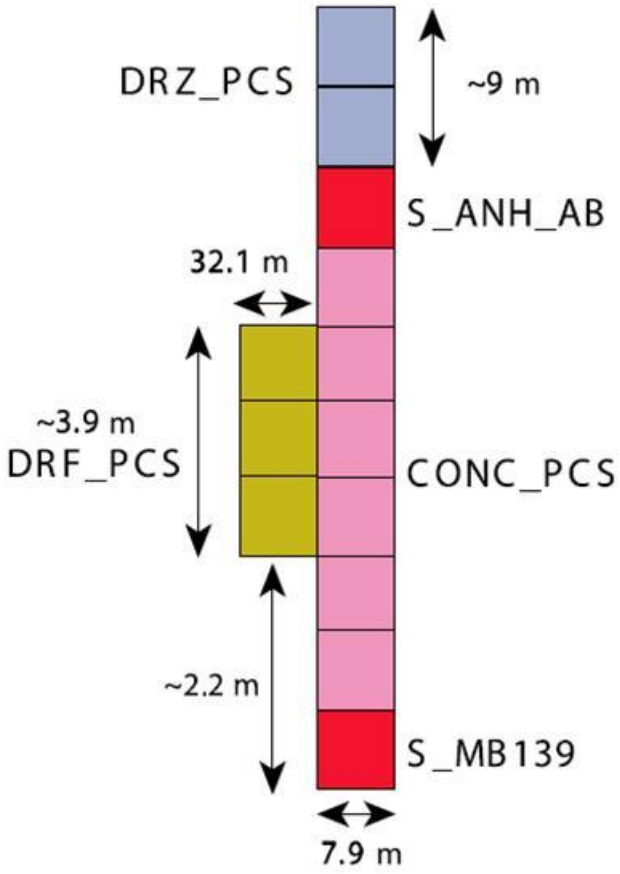

Fig. 4.7: Representation of a WIPP Panel Closure in the BRAGFLO Modelling Grid (USDOE 2009). Key. CONC_PCS = Panel Closure System (PCS) concrete, S_ANH_AB and S_MB139 = Anhydrite marker beds, DRZ_PCS = Disturbed Rock Zone (healed), DRF_PCS = Empty drift and explosion wall.

The permeability of the EDZ is assigned the same probability distributions as used for the closure concrete; this ensures that any fluid flow is equally probable through or around the panel closures, and represents the range of uncertainty that exists in the performance of the panel closure system.

Results

Releases of radionuclides to the accessible environment (surface or surrounding subsurface) from transport in groundwater through the shaft seal systems and the subsurface geology are negligible, with or without human intrusion. No releases at all are predicted to occur at the ground surface in the absence of human intrusion.

4.10 Germany

4.10.1 Background

The Gorleben salt dome in Germany has been investigated as potential site for a GDF for heat-generating waste since the end of the 1970s. A site-specific research project, the Prelimi-

nary Safety Analysis for Gorleben (Vorläufige Sicherheitsanalyse für den Standort Gorleben – VSG) was conducted from July 2010 to March 2013 to sum up the results of the Gorleben investigation achieved so far, to update the concepts for emplacement, layout, sealing and performance assessment, and to compile remaining open questions. The summary here is based on the VSG reports (e.g. Larue *et al.* 2013) as summarised by Rübel *et al.* (2014).

The disposal concept considers emplacement of the waste either vertically in boreholes or horizontally in drifts. During emplacement, seals are installed to isolate each emplacement drift or on top of each emplacement borehole. At closure, four drift seals are installed to isolate the emplacement areas, and the two shafts are sealed. The shaft seals consist of three short-term sealing elements that maintain functionality until the compaction of the backfill in the mine areas is finished, one long-term sealing element (crushed salt), and multiple additional elements like abutments and reservoirs. The position of each element is related to the geologic structure and therefore differs slightly in the two shafts. The long-term crushed salt element compacts and reaches a permeability that is ultimately similar to the permeability of the host rock

4.10.2 Scenarios regarding Sealing

The VSG TSPA includes a probabilistic simulation of the probable evolution scenario. The properties of the shaft seal included in the flow and transport calculations for the probable evolution scenario are changed in steps to cautiously simulate key processes (see Section 4.10.3).

The TSPA also considers a “less probable scenario” simulating failure of the shaft seal.

4.10.3 Modelling and Results

Fluid flow is calculated using an average permeability value over the whole cross-section of the seal including a potential EDZ. The permeability value is constant in set periods and conservative values are used to represent the impact of features or processes like the EDZ or material alterations with time. Any severe changes / events are taken into account by changing the permeability between steps in time.

The crushed salt used in the seal was calculated to become compacted in a relatively short time when applying parameters for modelling of the compaction process based on experimental data. Reasonable but conservative assumptions were used for the final porosity of the salt grit after compaction. Releases were calculated to occur only for the higher assumed final porosities of the crushed salt after compaction, and any release of radionuclides was driven by diffusion only. No transport by advection was calculated to take place. Radionuclides were calculated to be released primarily through the eastern drift seal. The release of radionuclides is higher there than in the western seal since it is closer to the disposal fields. The absolute total value of releases was calculated to be low.

Simulation of the failure of a single seal did not result in advective flow of brine within or into the emplacement areas.

4.11 Summary of Review Findings

Generally, TSPAs calculations for normal evolution scenarios assume that plugs and seals perform "as expected" and, in turn, the calculations show that the disposal system as a whole provides acceptable post-closure safety. Put another way, any intended post-closure safety function(s) of the plugs and seals – principally hydraulic isolation – is fulfilled by expected performance and contributes to overall safety.

Treatment of uncertainty in seal performance in TSPAs can be categorised using the widely-used three-fold classification of parameter, model and scenario uncertainty:

- **Parameter uncertainty**. Uncertainty analyses or probabilistic calculations may be used to take account of uncertainty in the properties of seals. The parameter values may be based on supporting modelling and/or expert judgement. The properties are either conservatively kept constant over time or changed in a stepwise fashion. Changing properties over time are used to account for known, but often poorly constrained, processes such as concrete degradation, salt compaction, clay swelling. The potential for sudden change may drive scenario definition rather than be captured as parameter variation within the same scenario.
- **Model uncertainty**. Alternative model configurations or conceptual uncertainty in the modelling of features, events and processes might be captured through sets of analyses specified to address model uncertainty. One example of examining alternative seal layouts was reviewed. However, no examples of "top-level" TSPA modelling of actual processes leading to changes in plugs and seal properties during a calculation were found.
- **Scenario uncertainty**. Some TSPAs, particularly those concerned with disposal concepts in low-permeability sedimentary host rock, consider scenarios that explicitly include a situation of poor seal performance. In such scenarios, however, advective migration of radionuclides generally remains limited, since virtually no water enters the disposal areas owing to the low hydraulic conductivity of the host rock. The bounding case of abandonment of a GDF before closure, i.e. before emplacement of final tunnel closures and shaft/access ramp seals, is included in a number of TSPAs. In the case of the Swedish TSPA for disposal of spent fuel in a crystalline rock, the abandonment calculation is considered as a Future Human Action scenario.

Two particular challenges for WMOs will be how to translate findings from the DOPAS experiments to representing changes over time in TSPA calculations, particularly given the short timeframes of the experiments, and how to include the results of process-level models developed for the seals in the DOPAS experiments in TSPA.

5 Assessment of water tightness and mechanical integrity of POPLU plug (Posiva)

E. Rautioaho, L. Börgesson, M. Åkesson, O. Kristensson, J. Valli, M Hakala, X. Pintado, K. Koskinen, M. Vuorio

The plug as a structure belongs to the Engineered Barrier Systems (EBS) of Posiva's disposal concept (KBS-3V) as a part of the subsystem consisting of deposition tunnel backfill and of the tunnel end plug. The main function of the plug is to mechanically to keep the swelling backfill material in its intended position as to maintain its sufficient density. Its second function is to hydraulically limit water flows to and from the deposition tunnel to the tunnels near by like central tunnels and adjacent deposition tunnels during the time water contents and hence total pressures differ at the different sides of the plug. Whether the plug can perform the first function is most critical in conditions in which backfill has reached its maximum swelling pressure while there is no closure material emplaced at the downstream side of the plug. To make sure this functional target is met, dimensioning of the plug involves safety factor with respect to tolerated loadings. The structural dimensioning has been carried out using the European standard Eurocode 2: Design of concrete structures – Part 1-1: General rules and rules for buildings (EN 1992-1-1: 2004) and Eurocode - Basis of structural design (EN 1990:2002). The structural dimensioning includes selection of concrete grade and required reinforcement in view of compression and tension forces, crack widths and hydration temperature effects. The plug alone does not have a safety function in the repository system but it supports the backfill in achieving its safety functions.

The design basis for the plug is described in Posiva's VAHA requirements management system, with the focus being on post-closure safety. (Posiva 2012a) The full details about POPLU's Design Basis and Criteria, including the VAHA requirements, are described in detail in DOPAS Deliverable D2.1 (White et al. 2014). POPLU's Conceptual design is described in DOPAS Deliverable D2.2 (White & Doudou 2014). Posiva's requirements for the plug are described within the Structural Design document of DOPAS Deliverable D3.24 (Holt & Dunder 2014). Assessment of monitoring system performance, specifically the sensors, described in DOPAS Experimental Summary Report Deliverable D4.4 (DOPAS 2016c). Evaluation of how POPLU construction showed compliance (or not) with the design requirements is also detailed in the DOPAS Deliverable D4.4 (DOPAS 2016c)

POPLU is commissioned within the DOPAS project (Full Scale Demonstration of Plugs and Seals). The DOPAS project is jointly founded by Euratom's Seventh Framework Programme and is planned to be run in the period September 2012 – August 2016.

This chapter describes the work done for WP5 of DOPAS in Posiva. The work consists of computer simulations committed to assess the water tightness and mechanical integrity of the plug in reference to the POPLU experiment and the impact these simulations had in the POPLU design and the design of monitoring systems of the plug. In this experiment the tunnel space upstream the the concrete plug was originally planned to be pressurised with water up to 10 MPa.

In hydraulic simulations (CODE_BRIGHT) different design options for the potential seal were tested and the flow through the saturated seal at the end of the plug and the gap at the plug/rock interface was assessed. The aim of these computer simulations was to predict the total outflow for the different design options and leakage scenarios in fully saturated, steady-state conditions. The higher level objective of the analytical calculations and computer simulations was to assess the effectiveness and suitability of the different design options for the seal at the end of the plug. Hydraulic assessments were done by B+Tech and Clay Technology.

To assess the mechanical integrity (3DEC v. 5.00) of the plug and mechanical response of the host rock in the expected repository conditions the plug's stress state and host rock's deformation was evaluated in details with computer simulations. These evaluations of the mechanical behaviour of the plug were done by Pöyry Oy as well as proposals for the basis for instrumentation (instrument positions and measuring ranges for monitoring designed by VTT).

At the end of the project these and the hydraulic data will be compared with point wise and other measurements available. In case the resulting comparison error is smaller than the related validation uncertainty and if the safety factor in terms of mechanical integrity in all assessments remains acceptable, the designed plug as it has been built can be judged to perform as targeted. In this connection plug comprises as its main component of a concrete monolith and of a part of near-field host rock in which changes in stress state are induced due to pressurised plug.

5.1 Description of the plug system

The geometries and dimensions of the plug and the potential seal are presented in Figure 5.1. (Holt & Koho 2016).

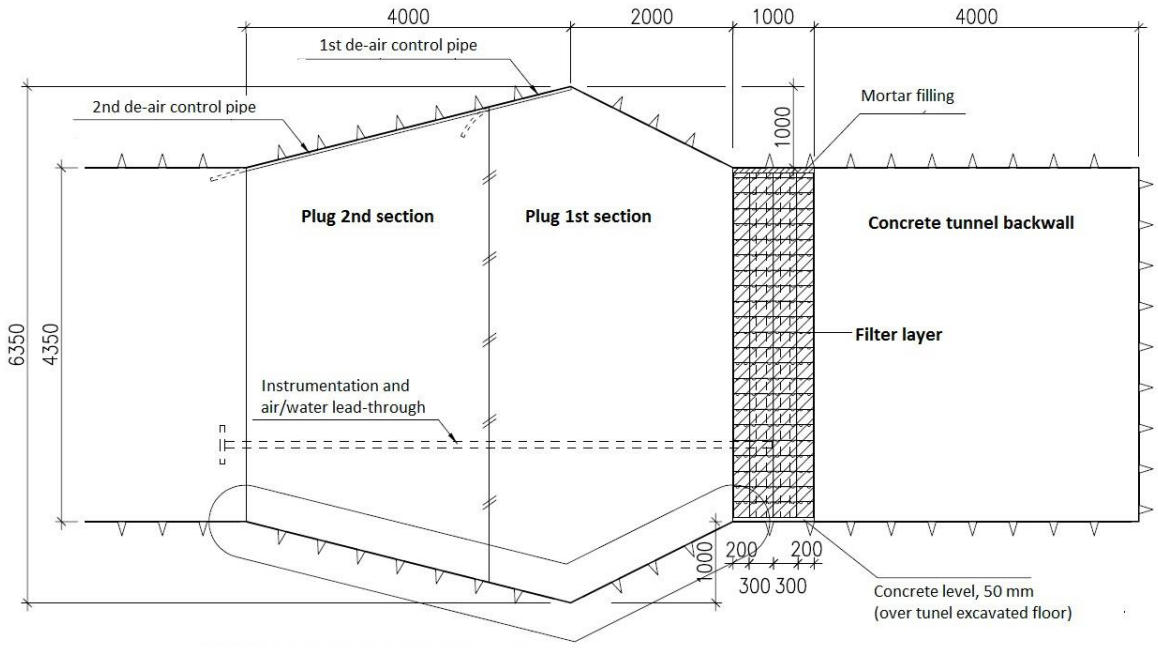

Fig. *5.1*: Dimensions of the Posiva plug and the seal system (DOPAS, 2016b)

5.2 Mechanical properties of the plug-rock system modelled

5.2.1 In situ stress state

The in situ stress state to be used in the simulation was as defined in the 2012 Posiva Site Report with principal stress magnitudes calculated according to a depth level of -423 m (Table 5.1).

Tab. *5.1* In situ stress state in the simulation

	σ_H [MPa]	σ_h [MPa]	σ_v [MPa]	Vertical depth range
Mean [MPa]	**24.9**	**16.7**	**11.2**	HZ20 to BFZ099
Min [MPa]	13.6	9.7	10.2	
Max [MPa]	35.7	23.7	12.3	
Orient. [°N]	112	202		

5.2.2 Rock mass parameters

Measurement results used to define the following parameters (Table 5.2) were obtained from the 2011 Posiva Site Report (Posiva 2012) and Working Report 2005-61 (Hakala et al. 2005). The uniaxial compressive strength (UCS) and tensile strength results for the foliation plane of veined gneiss (VGN) and the VGN matrix were obtained by using their respective means and the mean UCS / TS for VGN, effectively scaling the values to match previously accepted values. Logging results of the core obtained from the pilot hole of Demonstration tunnel 4 were used to define the Young's Modulus of the rock mass. The foliation dip and dip direction were obtained from logging results of ONK-PH26 and ONK-PH27 pilot boreholes.

Tab. *5.2*: Rock mass parameters for different lithologies

Reference / source		VGN Matrix	VGN Foliation plane	PGR
Logging data	DIP/DD	-	45/172	-
Logging data	GSI	93	93	99
Logging data / 2012 Site report	Young's Modulus (GPa)	58	58	59
2012 Site Report	Poisson's ratio	0.25	0.25	0.29
2012 Site Report	Density (kg/m3)	2741	2741	2635
2012 Site Report / WR 2005-61	UCS	120	96	102
2012 Site Report	Crack initiation stress σ_{CI} (MPa)	52	42	57
2012 Site Report / WR 2005-61	Initial Tensile strength (MPa)	14.1	10.1	8.9
2012 Site Report / WR 2005-61	Initial Cohesion (MPa)	19.7	15.6	19.3
2012 Site Report / WR 2005-61	Initial Friction angle (°)	16	16	22
-	Residual Tensile strength (MPa) *	0.1	0.1	0.1
1% of initial	Residual Cohesion (MPa) *	0.2	0.2	0.2
-	Residual Friction angle (°) *	53	52	53
-	Dilatation angle	20	20	20

* full mobilization of residual values requires plastic shear and tensile strain of 3e-3.

5.2.3 Elastic plug parameters

The parameters for a normal fracture representing the contact between the plug and the surrounding rock were obtained from the POSIVA 2012 Site Report as the values for a shotcrete / rock contact were close to parameters for a normal fracture (Table 5.3).

Tab. *5.3*: Plug and rock contact parameters

Cohesion (MPa)	0.14
Tensile strength (MPa)	0.14
Friction (°)	28
Normal stiffness (GPa/m)	254
Shear stiffness (GPa/m)	0.22
Dilatation angle	2

The parameters for the plug were obtained from research carried out by B+ Tech for Posiva and are defined in table 5.4.

Tab. *5.4*: Concrete plug parameters

Young's Modulus (GPa)	34
Poisson's ratio	0.2
Density (kg/m3)	2400

The plug was assumed to be elastic in order to exhibit the maximum stresses imposed on it.

5.2.4 Brittle deformation zone OL-BFZ297 Parameters

Brittle deformation zone OL-BFZ297 intersects the demonstration area of ONKALO from east to west and is observed in Demonstration tunnel 1 and 2 as well as in the central tunnel. It also intersects the pilot hole for Demonstration tunnel 3 as well as pilot hole ONK-PH22, see fig 5.2.

For simulation purposes, data obtained from ONK-PH26, ONK-PH22 and the central tunnel of the demonstration area were deemed best for determining the geometrical properties of OL-BFZ297. These observations result in the following:

- Dip 84°
- Dip direction 185°
- Full width 2.80 m, or:
- Core width 0.30 m, influence zone 1.25 m / 1.25 m

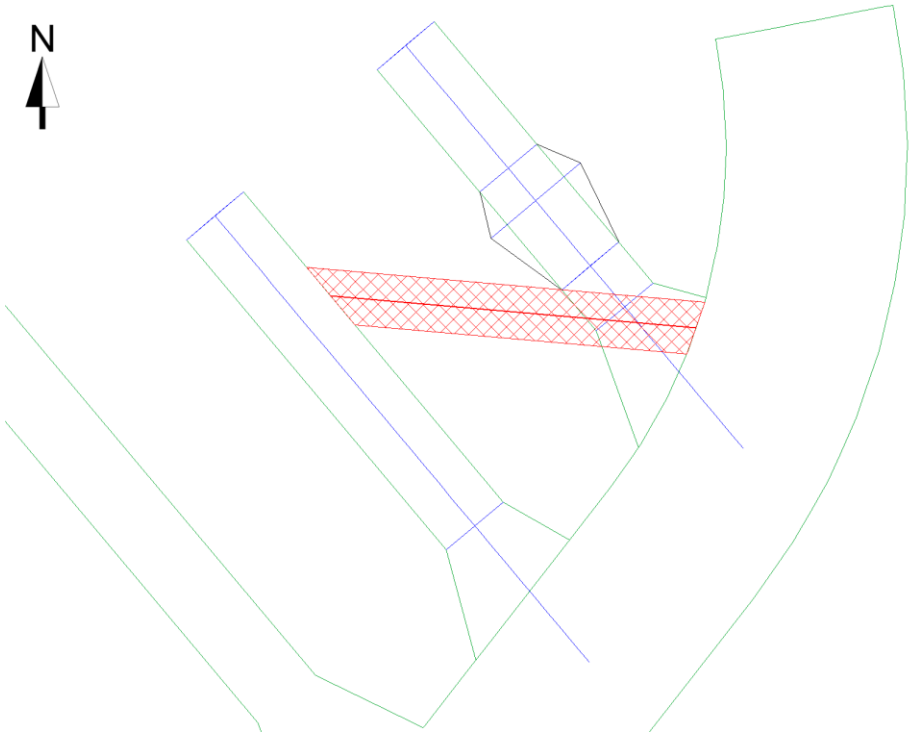

Fig. 5.2: OL-BFZ297 simulation location in red. Demonstration tunnel 4 on the left and Demonstration tunnel 3 on the right

The remaining parameters (Table 5.5) were defined using the Rock Mass Classification method described in WR 2008-67 (Hudson et al.).

Tab. *5.5*: OL-BFZ297 brittle deformation zone parameters. The common parameters were the initial values for the calculation of the core and influence zone parameters. The intact rock modulus Ei and UCS were not included into the calculation. The core was modelled as a fracture, so the Erm modulus was not taken into account either, only the normal and shear stiffness control the stress-strain relationship (Tensile strengt (TS).

	COMMON PARAMETERS	
DIP/DD	84/185	
Density (kg/m3)	2741	
Ei (GPa)	60	
UCS (MPa)	108	
Poisson's ratio	0.25	
	CORE	**INFLUENCE ZONE**
Scale factor determined from Schmidt results	34 %	69 %
Scaled UCS	37	74
Q'	0.2	11.4
GSI	31	66
Erm (GPa)	**5.2**	**39.2**
Thickness (cm)	0.3	250
Tensile strength (MPa)	0.02	0.65
Cohesion (MPa)	0.86	2.59
Friction angle (°)	28	44
Normal stiffness (GPa/m)	17.3	-
Shear stiffness (GPa/m)	6.9	-

5.3 Prediction of watertightness

A three-dimensional hydraulic numerical continuum model was created to simulate the flow through the seal and the gap in contact with the plug. The analyses were performed with the finite-element software CODE_BRIGHT (Olivella et al. 1994, 1996), which was initially developed for modelling the non-isothermal multi-phase flow of brine, heat, liquid and gas through porous deformable saline media.

5.3.1 Simulated cases and scenarios

Three main design options were simulated:

1. Case A containing only the concrete plug and no seal material;
2. Case B containing a seal section made of the current Posiva reference backfill material: Friedland clay blocks, Cebogel pellets and Minelco granules;
3. Case C containing a seal section made of MX-80 bentonite blocks and MX-80 bentonite pellets with a permeable concrete beam placed between the seal and the plug.

Additional design options were also tested to gain a better understanding of the process:

4. Case B2, i.e. case B with a permeable concrete beam placed between the seal section and the plug,

5. Case C2, i.e. case C without a permeable concrete beam placed between the seal and the plug.

Two scenarios for the gap at the plug/rock interface were simulated for each design case:

I. A gap around the entire plug.
II. A gap of 0.1 m width at bottom of the plug.

The simulated cases are presented in Table 5.6.

Tab. 5.6: Simulation case matrix

Case	Seal materials	Concrete beam	Gap width	Gravity
A_I	-	-	Entire plug	-
A_II	-	-	0.1 m	-
Ag_I	-	-	Entire plug	X
Ag_II	-	-	0.1 m	X
B_I	Friedland-Cebogel Minelco backfill	-	Entire plug	-
B_II	Friedland-Cebogel-Minelco backfill	-	0.1 m	-
Bg_I	Friedland-Cebogel-Minelco backfill	-	Entire plug	X
Bg_II	Friedland-Cebogel-Minelco backfill	-	0.1 m	X
B2_I	Friedland-Cebogel-Minelco backfill	X	Entire plug	-
B2_II	Friedland-Cebogel-Minelco backfill	X	0.1 m	-
C_I	MX-80 backfill	X	Entire plug	-
C_II	MX-80 backfill	X	0.1 m	-
Cg_I	MX-80 backfill	X	Entire plug	X
Cg_II	MX-80 backfill	X	0.1 m	X
C2_I	MX-80 backfill	-	Entire plug	-
C2_II	MX-80 backfill	-	0.1 m	-

5.3.2 Simulation geometry

For numerical reasons the actual or potential gap opening was not feasible to be considered explicitly but a gap with similar water transport potential with thickness of 0.1 m was considered in all cases. The dimensions are shown in figure 5.3. The model size was reduced by half, on account of the vertical symmetry plane at the center of the plug and the tunnel.

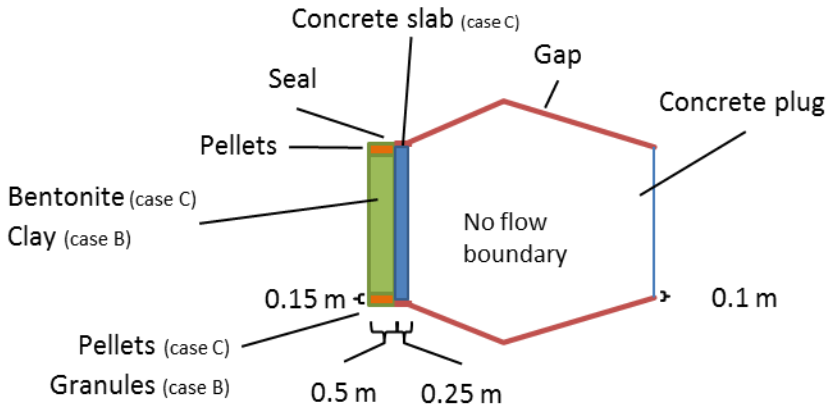

Fig. 5.3: Dimensions of the upstream seal system and assumptions regarding the gap between the concrete and hostrock.

5.3.3 Boundary conditions

A liquid pressure of 10 MPa was applied at the short end of the plug (case A) or on the seal (cases B and C), as illustrated with yellow in Figure 5.4. The surface of the gap facing the central tunnel (green in Figure 5.4) was assigned an atmospheric pressure of 0.1 MPa. No-flow boundary conditions were prescribed on all other boundaries.

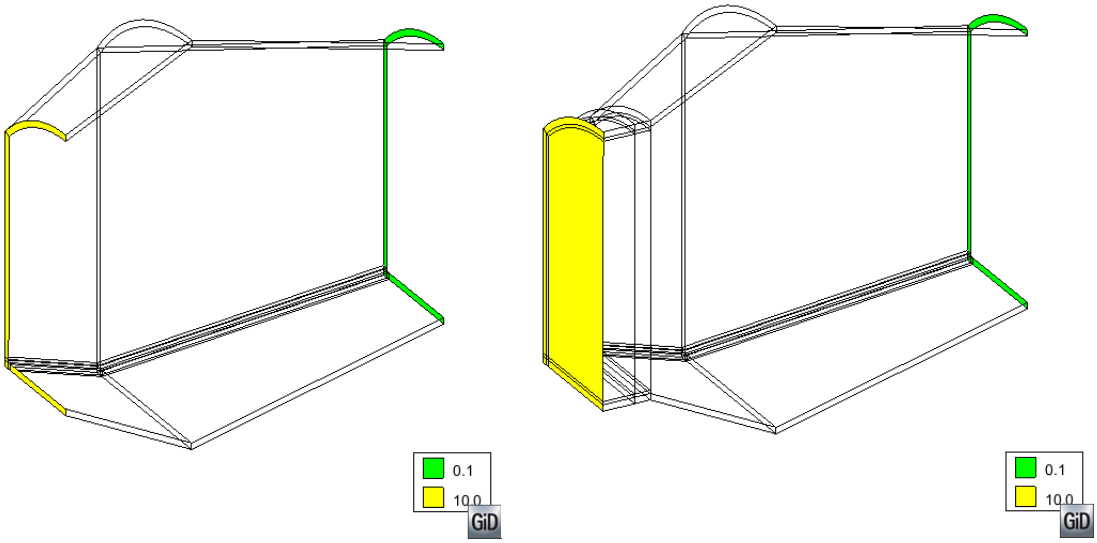

Fig. 5.4: Boundary conditions (MPa) in case A (left) and cases B and C (right). Legend: Green = 0.1 MPa atmospheric pressure; Yellow = 10.0 MPa liquid pressure

5.3.4 Initial conditions and fixed conditions

As the seal is assumed saturated, an initial liquid pressure of 0.1 MPa was assigned to all materials. Gas pressure was fixed at 0.1 MPa (atmospheric pressure) and temperature at 20 °C, as during the operational period the temperature in the tunnels is assumed to be kept at about +20 °C (Haaramo & Lehtonen 2009).

Gravity load was not employed in the base cases in order to study an even flow through the seal and the plug induced by the pressure difference. Incorporating gravity was found, in a few of the cases, to generate inflows at some boundary nodes at the surface of the gap facing the central tunnel (where liquid pressure is maintained at 0.1 MPa), as well as outflows on the seal surface (where liquid pressure is maintained at 10 MPa).

5.3.5 Material properties

The dry density of Friedland clay, Cebogel pellets and Minelco granules was determined based on data from homogenization tests (Johannesson et al. 2008). As the initial dry density of the pellets and the granules in Posiva backfill is likely to be higher than in the homogenization tests, the selected values can be considered conservative. In the end, a dry density of 1290 kg/m^3 was employed for Minelco granules, on account of published saturated hydraulic conductivity data available for this density (Posiva 2013a).

For MX-80, an overall void ratio level of 0.85 was chosen in order to yield a swelling pressure in the order of 3-4 MPa according to the swelling pressure relation presented by Åkesson et al. (2010a). The division in two different void ratio values for blocks and pellets, respectively, was based on the results from the backfill homogenization calculations presented in Åkesson et al. (2010b).

In CODE_BRIGHT, the flow rate in porous media is calculated using Darcy's law:

$$\mathbf{q}_l = -\frac{\mathbf{k}\ k_{rl}}{\mu_l}\left(\nabla P_l - \rho_l \mathbf{g}\right)$$

where k is the intrinsic permeability tensor of the medium, μ_l is the dynamic viscosity of the liquid phase, g is the gravity vector and k_{rl} is the relative permeability of the liquid phase (equal to 1 in saturated material).

The intrinsic permeability value for the gap material was calculated with an analytical solution, aiming for a flow of about 0.1 l/min through the plug (chapter 0, Appendix). The gap permeability therefore changes with gap width, so the two leakage scenarios presented in Section 5.1.2 employ different intrinsic permeability values (e.g. in scenario II the gap width is 0.1 m, which is much smaller than in scenario I, so the intrinsic permeability for the 0.1 m wide gap is higher).

The intrinsic permeability values for the seal materials were selected from reported test data, for estimated homogenized densities of the materials. Sensitivity analysis of this parameter should be undertaken in future calculations.

Groundwater salinity in the repository is expected to be a little above 10 g/l (Pastina & Hellä 2010, Table 6-6). The saturated hydraulic conductivity values were therefore selected from measurements conducted with 10 g/l or higher saline water, depending on the availability of data. Higher salinity implies a slightly higher hydraulic conductivity, so no underestimation of the outflow should be incurred by this consideration.

The material properties in Tab. 5.7 are given in terms of the dry density ρ_d, void ratio e and/or the equivalent porosity ϕ, and the intrinsic permeability k.

Tab. 5.7: Material properties.

Material	ρ_d (kg/m^3)	e/ϕ (-)	k (m^2)	Reference for k
Gap (width: plug circumference, ca. 18 m)	-	-/0.020	5.99E-16	Analytical solution
Gap (width: 0.1 m)	-	-/0.020	1.08E-13	Analytical solution
Friedland clay blocks	1800	0.544/0.353	8.94E-20	Posiva (2013b)
Cebogel pellets	1200	1.36/0.577	1.13E-18	Schatz & Martikainen (2013)
Minelco granules	1290	1.17/0.538	5.65E-18	Posiva (2013a)
MX-80 blocks	1590	0.75/0.429	5.20E-21	Åkesson et al. (2010a)
MX-80 pellets	1430	0.95/0.487	1.80E-20	Åkesson et al. (2010a)
Concrete beam	-	-/0.135	1.00E-15	Åkesson et al. (2010a)

5.3.6 Results

The resulting flow rates through the plug systems as steady-state outflows from the gap surface facing the central tunnel are presented in Table 5.8 for the cases without gravity and in Table 5.9 for cases with gravity.

Incorporating gravity was found, as already said, in a few of the cases, to generate inflows at some boundary nodes at the surface of the gap facing the central tunnel (where the liquid pressure boundary condition is 0.1 MPa), as well as outflows on the seal section surface (where the liquid pressure boundary condition is 10 MPa). The results with and without gravity differ by very little, the most notable difference being the outflows in the two different leakage scenarios of case C (in Tables 5.8 and 5.9).

Tab 5.8: Simulated plug outflows for design cases A, B, B2, C and C2 (no gravity incorporated)

Case	Outflow (l/min)	Case / Case A (%)	Seal section material	Gap width
A_I	0.0917	100	-	Plug circumference
A_II	0.0949	100	-	0.1 m
B_I	0.00544	5.94	Friedland-Cebogel-Minelco backfill	Plug circumference
B_II	0.000468	0.493	Friedland-Cebogel-Minelco backfill	0.1 m
B2_I	0.00643	7.01	Friedland-Cebogel-Minelco backfill + concrete beam	Plug circumference
B2_II	0.00597	6.30	Friedland-Cebogel-Minelco backfill + concrete beam	0.1 m
C_I	0.000128	0.140	MX-80 backfill + concrete beam	Plug circumference
C_II	0.000116	0.122	MX-80 backfill + concrete beam	0.1 m
C2_I	0.0000665	0.0725	MX-80 backfill	Plug circumference
C2_II	0.00000148	0.00156	MX-80 backfill	0.1 m

Tab. 5.9: Simulated plug outflows for design cases A, B and C (gravity incorporated)

Case	Outflow (l/min)	Case / Case A (%)	Seal section material	Gap width
Ag_I	0.0917	100	-	Plug circumference
Ag_II	0.0949	100	-	0.1 m
Bg_I	0.00545	5.95	Friedland-Cebogel-Minelco backfill	Plug circumference
Bg_II	0.000470	0.495	Friedland-Cebogel-Minelco backfill	0.1 m
Cg_I	0.000116	0.126	MX-80 backfill + concrete beam	Plug circumference
Cg_II	0.000121	0.128	MX-80 backfill + concrete beam	0.1 m

5.3.7 Comparison of main design cases (without gravity)

5.3.7.1 Effect of clay material

It can be summarised that when adding a permeable material to face any potential defect in concrete (Cases B), the effect of these defects is that the flow rate through the defect is being reduced at least with an order of magnitude. In the case of less permeable material (Table 5.8) an even further reduction of roughly of two orders of magnitude can be expected. The absolute reduction is not directly comparable to the ratios of permeabilities of concrete part defect to that of backfill material, but of the of the order of an order of magnitude smaller. However, the difference in flow through rates between reference and alternative backfill materials is proportional to their ratio of permeability.

Thus, these simulations suggest that in the case of no backfill material the high hydrostatic pressure will be reduced to atmospheric pressure within potential defects. Should a less permeable material be used to face any potential defect, the reduction in the hydrostatic head over the concrete part of the plug will take place within the less permeable material - the lower the permeability in backfill the bigger the reduction in the hydrostatic head within the backfill. Consequently, in case of introducing a less permeable material a smaller hydrostatic head over the potential defects in the concrete part of the plug can be expected yielding lower flow through rate and better water tightness.

5.3.7.2 Effect of concrete beam

The foreseen effect of concrete beams is that they make the supply of water to the potential defects easier as it can be seen when comparing the concrete beams cases withfull perimeter defect to 0.1 m wide defects: the outflow rates are practically the same in Cases B2_I and B2_II as well as in Cases C_I and C_II (see Table 5.8).

5.3.7.3 Effect of defect width

The effect of a potential defect in the concrete part of the plug is roughly directly comparable to its width in the cases when backfill is in direct contact with the concrete part. However, should there be concrete beams in between clay backfill and the concrete part of the plug, the effect of the defect width is suggested to vanish.

5.4 Prediction of mechanical integrity

5.4.1 Simulated cases and scenarios

The mechanical properties and behaviour of the rock mass together with the concrete part of the plug was simulated with 3DEC 5.00 (Itasca Consulting Group (2012)) that is a jointed polyhedral discrete element software featuring finite-elements for sections considered continuum.

The following three scenarios (cases 1-3) were simulated to assess the impacts of the uncertainties expected to be the most noteworthy.

1. Case 1: (Overly) Homogeneous rock mass: The same fully veined gneiss (VGN) lithology is used as in previous assessments is used as well as the pilot hole observations (i.e. does not include OL-BFZ297).
2. Case 2: (Overly) Heterogeneous rock mass: A change in lithology from VGN to pegmatic granite (PGR) is included but its location is stylised such that its impact would be the worst with respect to the load transferred from the plug to the rock mass. Furthermore, OL-BFZ29 is included but its location is changed to a location that would be as adverse as possible but would still fulfil the rock suitability criteria.
3. Case 3: (Overly) Heterogeneous rock mass with pessimistic parameter values: Case 2 with a decrease of 60% in the respective tensile strengths.

The features included in the model are described in section 5.2 together with the parameter values in Tables 5.1 ... 5.5.

Cases 1 and 2 include results where displacements have been reset prior to implementing water pressure.

5.4.2 Results

The main aim of these calculations was to study the load caused by the fully saturated backfill at the depth of c. 400 m at the upstream side of the plug (assumed to be 10 MPa) which induces a compressive stress field to this face.

Figure 4.5 presents the locations of the horizontal and longitudinal cross-section locations used in presenting the results.

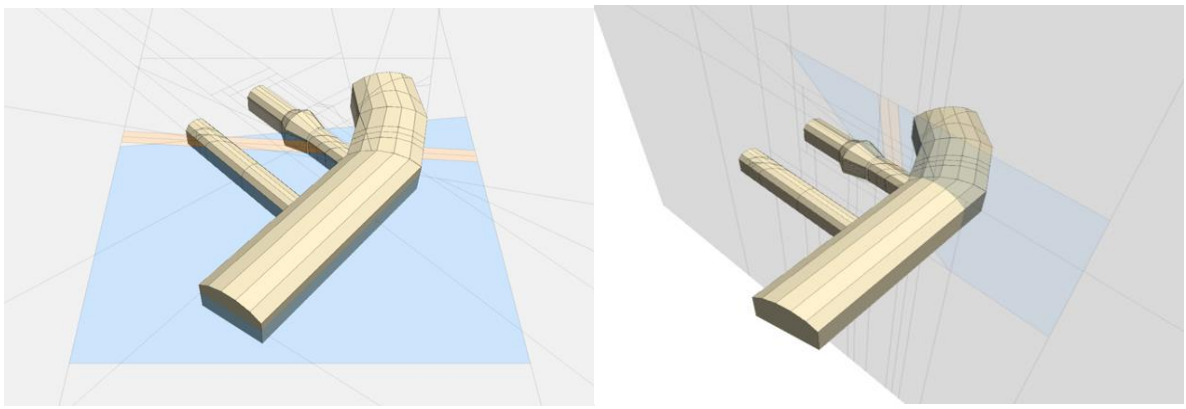

Fig. 5.5: Horizontal and longitudinal section locations © Posiva

5.4.3 Displacements

Figure 5.6 presents simulated displacements. The differences between the scenarios assessed are of the order of a few millimeters in maximum in the rock and less than one millimeter in the concrete part of the plug. The differences in the rock mass are explained by the displacements after the excavation of the demonstration tunnels in cases 2 and 3. This is illustrated in Figure 5.7 that presents displacements for cases 2 and 3 before and after cavity pressurisation.

To follow the changes in displacements more easily, the displacements from which the displacements occurring immediately after cavity excavation are removed are presented in Figure 5.8.

When comparing displacements in the rock mass inside the red circles in case 1 to those of cases 2 & 3 visible in horizontal cross-section Figure 5.8 there appears small differences that are not that clearly visible in Figure 5.6. These differences correlate with the differences in the concrete part of the plug (inside the red circle in Figure 5.8).

The most obvious conclusions that can be done based on simulated displacements are listed in the following.

- The concrete plug was assumed to deform more than the rock mass. This is because Young's modulus for concrete is much lower than that of VGN or PGR rock mass.
- Deformations of the concrete plug are symmetric should the rock mass be homogeneous and asymmetric in case the rock mass is heterogeneous e.g. in terms of lithology or appearance of fractures. The largest deformations in the concrete part that can be expected are 2.5-3 mm located at the side facing the pressurised cavity.
- Heterogeneities in the deformation of the concrete part of the plug correlate with the displacements appearing in the rock mass in the vicinity of a fracture. That is, fractures in the rock mass induce local displacements in the rock mass under load that further induce local deformations in the concrete part of the plug. Should fractures appear in a symmetric manner, the deformations in the concrete part of the plug appear symmetrically.

Regarding the displacements in the rock mass the changes due to upstream cavity pressurisation can be expected to remain in the immediate vicinity of the demonstration tunnel. Some of these changes are due to the increased pressure in the cavity inducing an order of one millimetre backward movement of cavity walls that initially occurred due to relaxation of stresses after cavity excavation. These locations are denoted with red ellipses in Figure 5.9.

Moreover, a deformation of rock mass of similar order of magnitude can be expected in the locations closer to the longer wedge surfaces of the concrete part of the plug once the upstream cavity is pressurised. These locations are indicated with black ellipses in Figure 5.9. This is because of the way the concrete part transfers the mechanical load from the simulated backfill through the longer wedge surfaces to the rock mass. The rock mass is assumed very stiff in this connection so that the deformations are expected to remain small and very local. The asymmetry of both red and black circles coincides with the alignment of the computational grid to such an extent that its influence cannot be excluded.

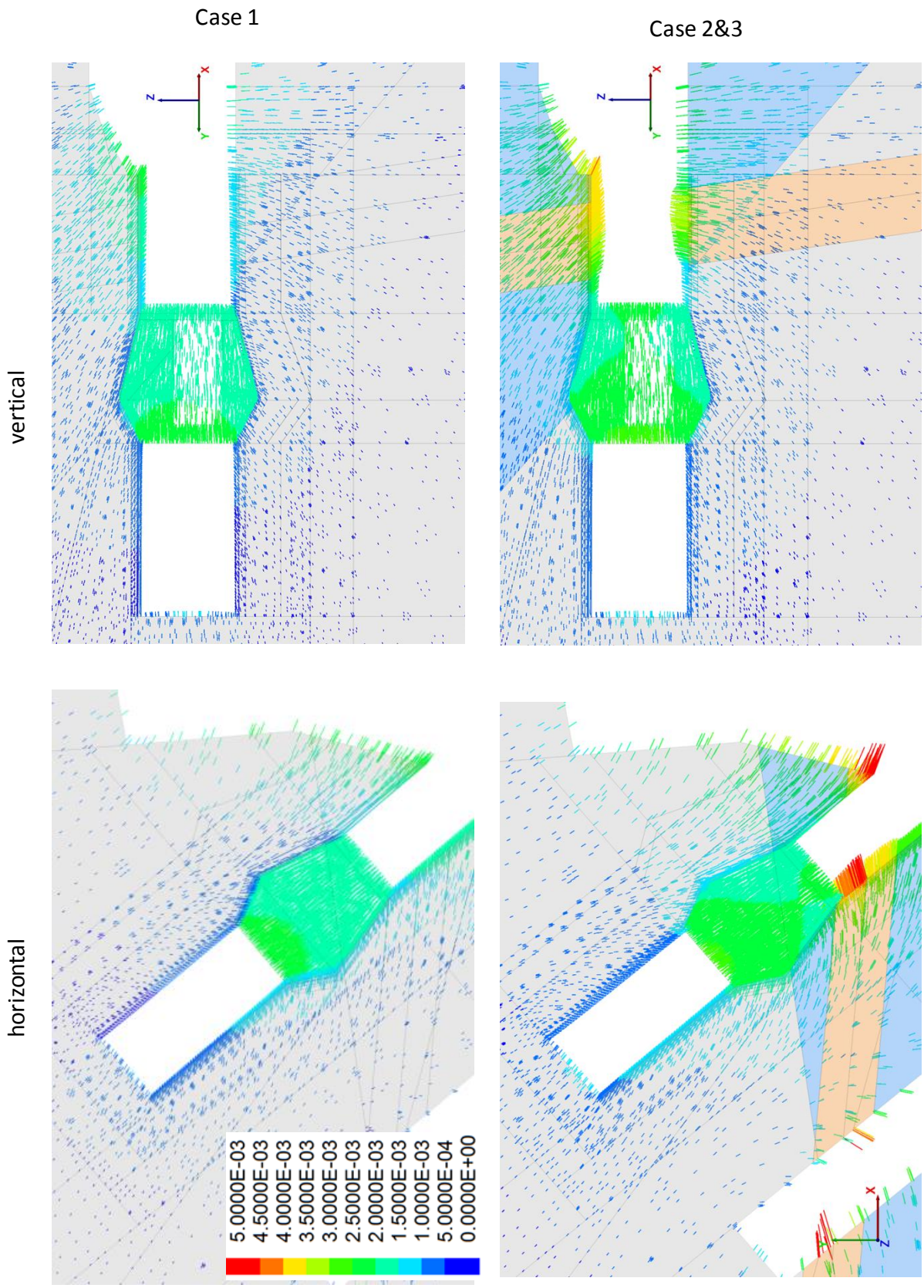

Fig. 5.6: Calculated displacements in [m] after upstream cavity pressurisation (10 MPa) in demonstration tunnel

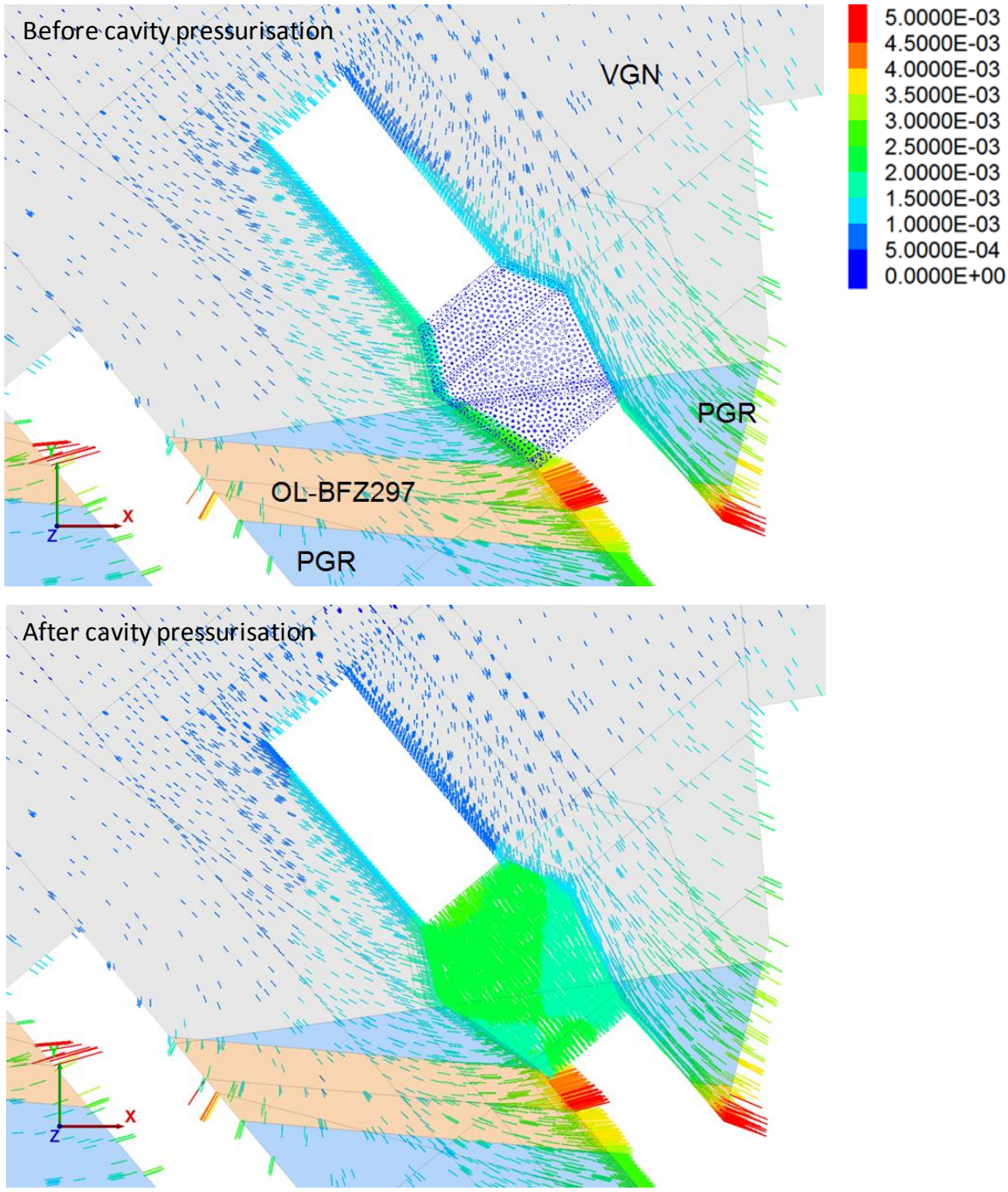

Fig. 5.7: Calculated displacements in [m] for cases 2 and 3 before and after cavity pressurisation. VGN= veined gneiss, PGR = pegmatic granite, OLBFZ297 = brittle deformation zone

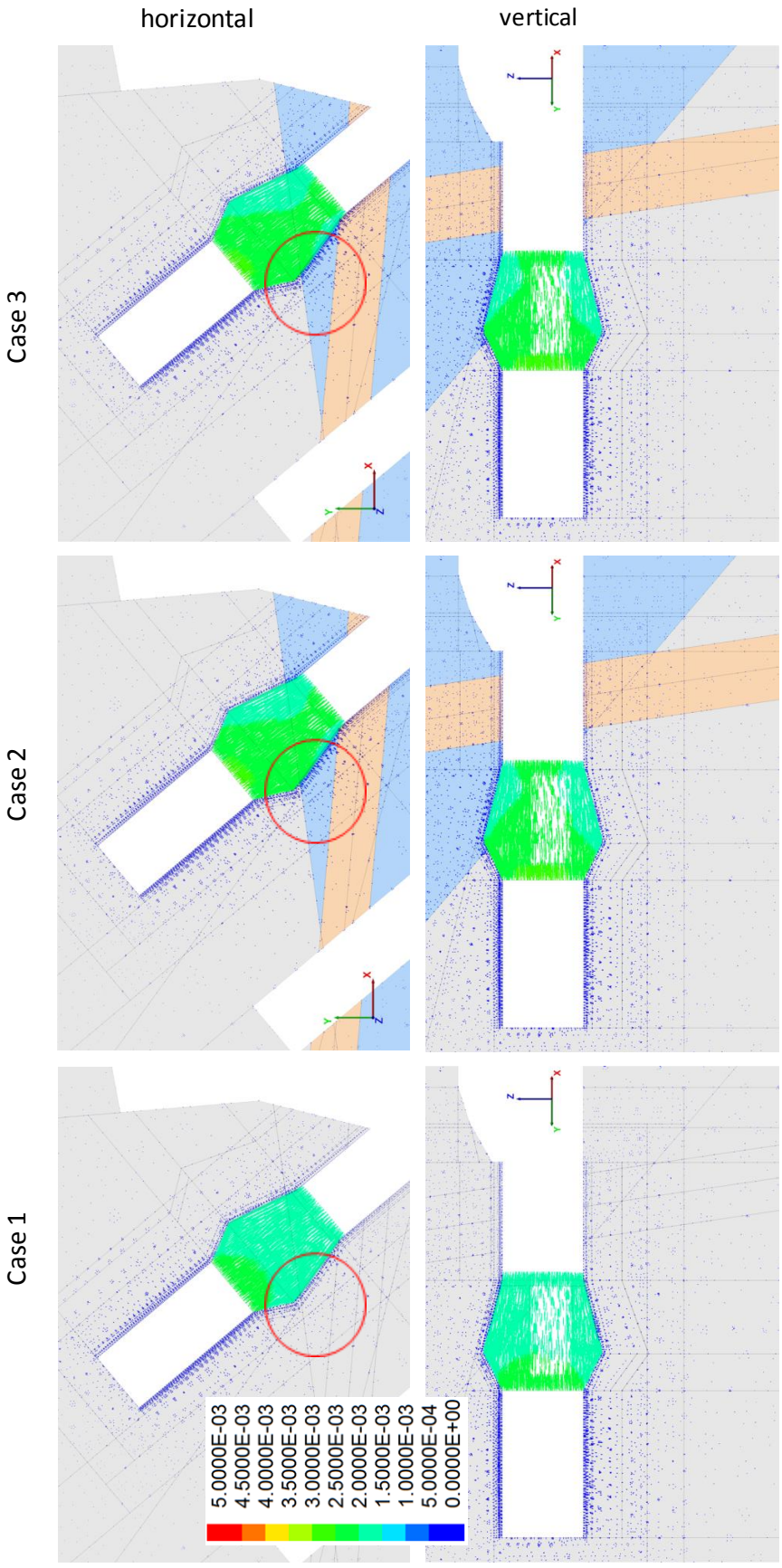

Fig. 5.8: Calculated displacements in [m] after cavity pressurisation. The displacements occurring immediately after excavation are removed. Red circle = displacements.

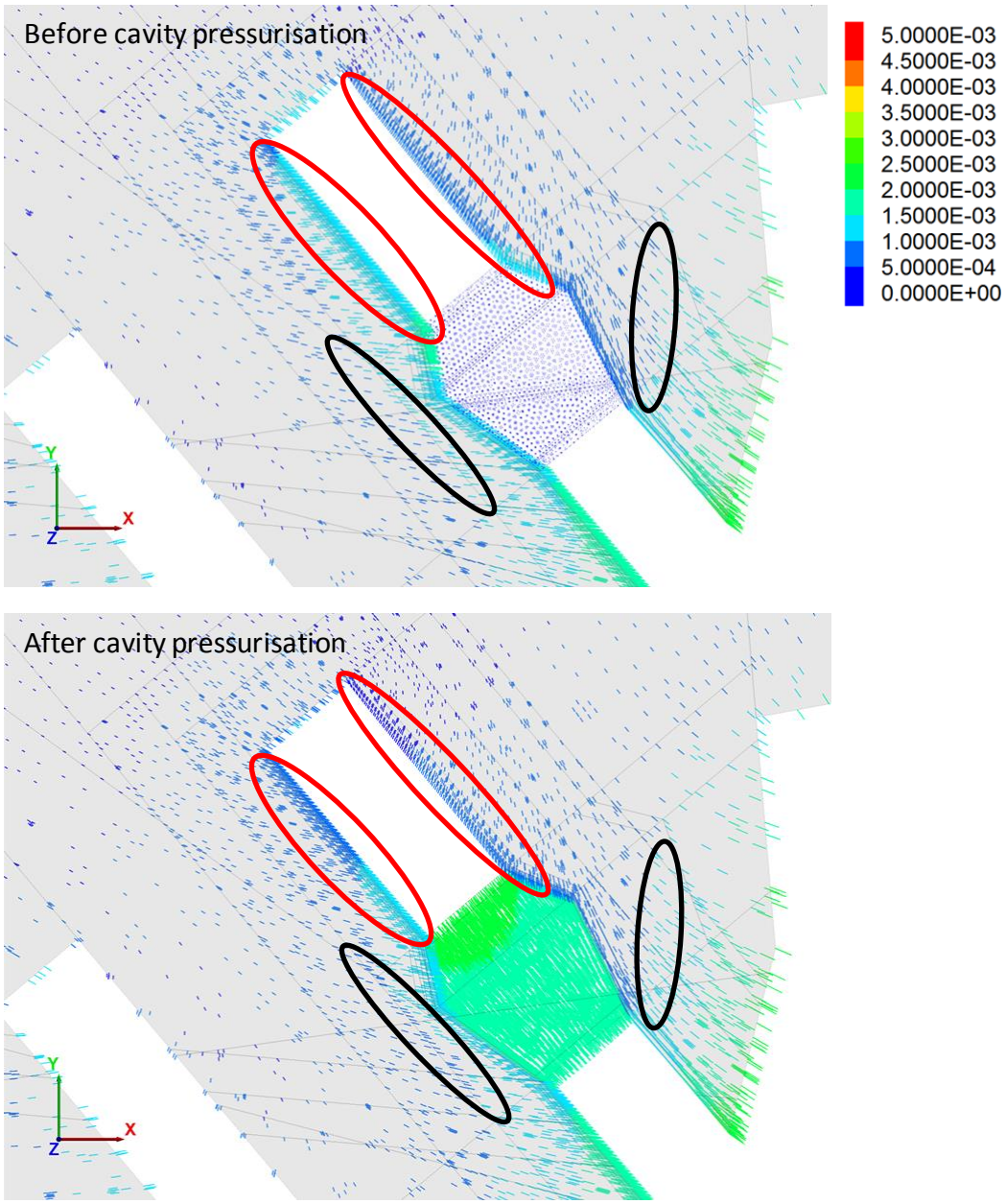

Fig. 5.9: Calculated displacements in [m] for case 1 before and after cavity pressurisation. Red ellipses= movement of cavity walls, Black ellipses = deformation of rock mass.

5.4.4 Maximum and minimum principal stress

Figure 4.10 presents the simulated maximum principal stresses. It can be seen that in the concrete part of the plug there are areas of lower stresses in the more heterogeneous cases with an intersecting fracture highlighted with red circles. These locations coincide with those of larger displacements (see e.g. Figure 5.8). The differences in rock mass are more noticeable. Namely, stresses at the rock-concrete interface appear symmetrical in the homogeneous case and asymmetrical and locally higher in heterogeneous cases as denoted by black ellipses in Figure 5.10. The stresses are lower at more distant locations for the heterogeneous cases since displacements at the fracture can be expected to relax some of stresses around the area denoted with a grey dashed ellipse. Moreover, variation of stresses typically referred to as checkerboard pattern in cases 2 and 3 in location framed with a black dotted line is often related to numerical solution indicating nothing of actual physics. Variation in cases 2 and 3 appears around the value estimated for the case 1.

Minimum principal stresses are presented in Figure 5.11. As a conclusion it can be said that the expected stress fields are more heterogeneous in more heterogeneous conditions as well.

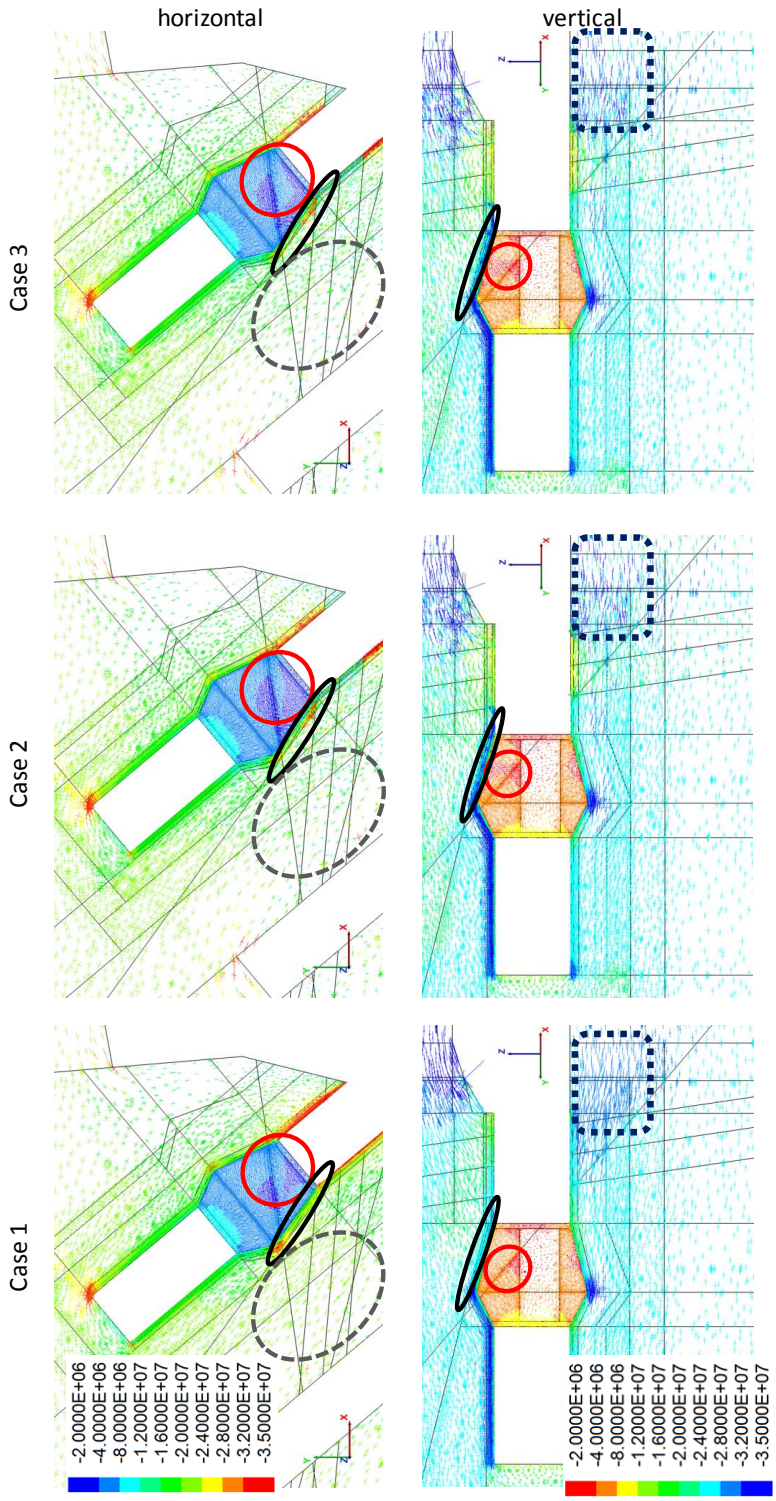

Fig. 5.10: Maximum principal stresses in [Pa] after cavity pressurisation (σ_1 <0 refers to compression). Red circles=areas of lower stresses, Black ellipses=stresses at the rock-concrete interface, Black dotted ellipses=stresses are lower at more distant locations, Black dotted areas=variation of stresses often related to numerical solution indicating nothing of actual physics.

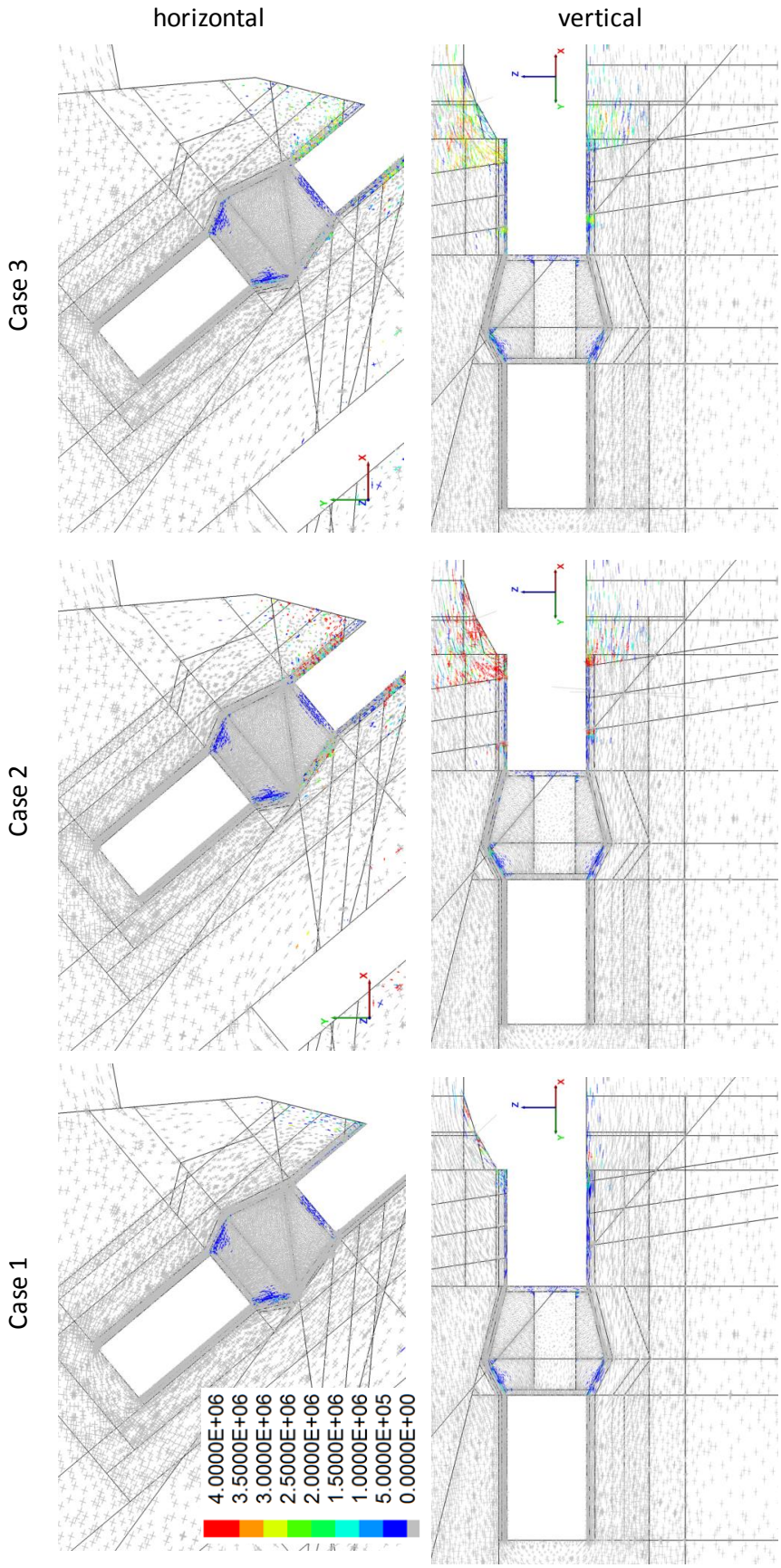

Fig. 5.11: Minimum principal stresses in [Pa] after cavity pressurisation pressurisation (σ_1 <0 refers to compression)

5.5 Summary

5.5.1 Water tightness

In this connection the word plug is used to refer to the concrete part and the rock mass at the distance of a few decimetres from it.

The rate at which water may flow from the pressurised cavity past the plug is directly proportional to

- permeability of the system including potential defects especially at the interface between concrete and rock mass and
- the width of the potential defect that provides a continuous flow path past the plug.

Clay as a low permeability material reduces the potential flow rates past the plug. The lower the clay permeability, the lower the flow rate past the plug. Since clays will be introduced as compacted blocks and pellets filling the gaps into which blocks cannot be placed, the permeability of the outermost parts in contact with the interface between concrete part of the plug and rock mass depends on a) the swelling capacity of blocks to compress the pellets to higher density and b) permeability of the fully water saturated and compressed pellets layer.

The effect of the permeable concrete beams in contact with the plug is to redistribute the water potentially flowing in channels in backfill to the potential defects in the concrete-rock mass interface. This way concrete beams potentially makes the impact of smaller defects larger.

No leakages were expected since grout and bentonite tape will be used to seal potential defects at the concrete-rock mass interface. Ultimately, it is suggested that no clay would be used to get direct evidences of the water tightness of the plug. It was assumed that water saturated clay would reduce the water flows past the plug to a negligible level anyway.

There were two different pressurization actions taken to evaluate the POPLU performance: 1) slow pressurization to evaluation initial leakage; 2) fast filling to evaluate wedging effect of path.

During the slow pressure increase phase the leakage measurement system was collecting all the leakage water from the plug and the adjacent rock mass. Measured total leakage is presented in Figure 5.12. There were leakages via grouting pipes, instrumentation cables and concrete-rock interface. Exact amounts of leakages from different points were not measured, but according to visual estimation quarter of the total leakage came from instrumentation and grouting pipes. There was also small leakage from the concrete lead through in a middle of the plug, but that sealed very quickly (within hours) indicating that the bentonite tape was effective. There was no leakage detected on the rock lead through between Demonstration tunnels 3 and 4. The separate leakage collection system was not utilized due to water tightness of the lead-throughs.

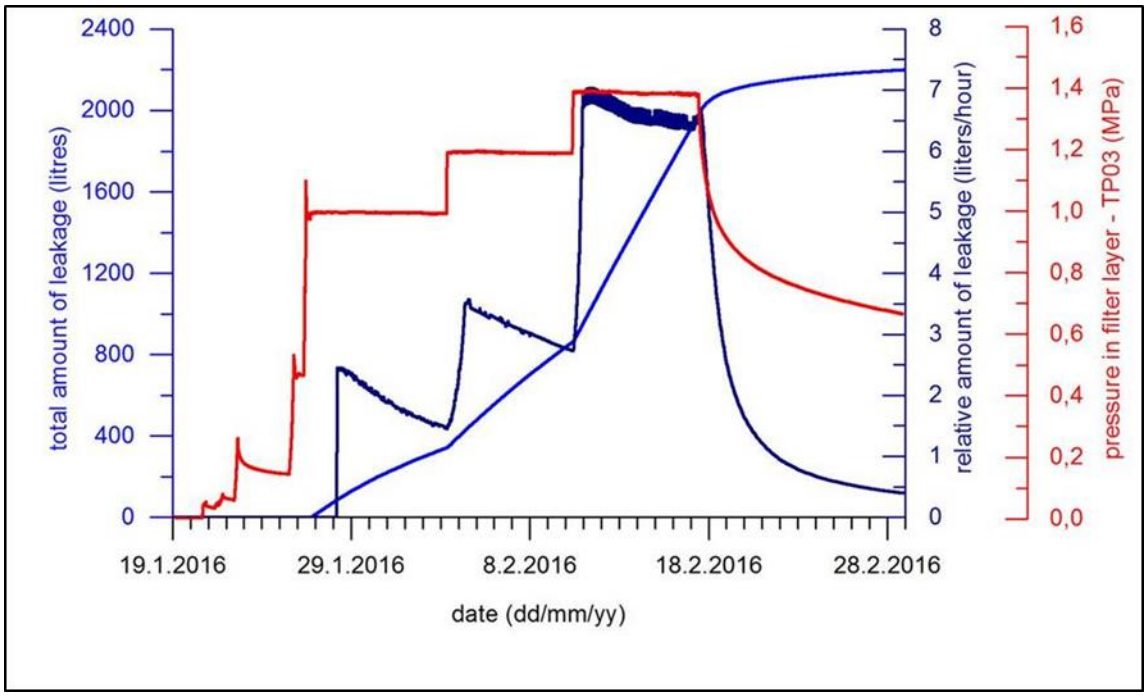

Fig. 5.12: Plot of cumulative leakage, leakage rate and pressure in the filter layer during the slow pressure increase phase of the POPLU experiment (Holt & Koho 2016)

During a fast pressure increase test of the plug wedging effect was observed. Before the test the plug was pressurized to 1 MPa. After this the pressure was increased as fast as possible to 4.2 MPa . This was achieved in the following 24 hours. During pressurization.total leakages increased and in the end were just under 10 l/min. Displacement sensors were indicating possible movement of the plug and to confirm this observation a pressure changes were performed (4.2 MPa – 0.5 MPa – 4.2 MPa). Each pressure change was faster than previous, last one taking less than one hour to reach 4.2 MPa . After this last leakage was about 2 l/min (DOPAS, 2016b).

5.5.2 Mechanical integrity

The expected maximum displacements are roughly 3 mm in the concrete part of the plug whereas the rock mass is expected to have displacements of similar magnitude towards the drift and in the proximity of fractures slightly more.

Water pressure in the cavity is transferred into the rock mass through the longer wedge surfaces of the concrete part of the plug. The more heterogeneous the rock mass (in terms of lithology and fractures), the more uneven the stress field in the vicinity of the drift. In addition, changes in lithology and presence of fractures in the rock mass at the downstream side of the plug in comparison to the pressurised upstream cavity, induce higher displacements to the immediate vicinity of the load transferring surfaces.

To conclude, no material failures are expected even if there would appear undetected features at the most critical locations. Changes due to plug pressurisation were and are being measured in the concrete part of the plug as well as in the rock mass. This way the mechanisms of the

transfer of the mechanical load through the plug to the rock mass can be potentially be validated.

Assumption made in the simulations was that the concrete plug was to deform more than the rock mass, due to Young's modulus for concrete being much lower than that of VGN or PGR rock mass.

During the pressurisation of the plug no mechanical damages were observed. However, displacement sensors were showing movements of the plug during each pressure change, but the data needs to be thoroughly analysed before final conclusions.

5.6 Conclusions and lessons learned

Due to the mechanical modelling VTT designed locations and measurement ranges for monitoring sensors. Aim was to measure the pressure to see if the stress distribution on the upstream face of the plug is even as assumed. Other issues to be monitored were anticipated inward displacement of the brittle deformation zone and excavation damage zone (EDZ) impact at different times.

Due to the hydraulic modelling Case A, no backfill, was selected for the experiment. Initially a targeted 10 MPa backpressure was deemed unfeasible and dropped to 4.2 MPa. This was due to lessons learned from SKB's DOMPLU experiment, the only pressure that the plug needs to resist in the experiment is the hydraulic pressure in contrast to the reference plug design pressure. This is due to the pressurisation done by using an external water source that causes jacking of the rock fractures behind the plug in such a way that would never happen in the system with bentonite backfill behind the plug. However, only the experiment itself will show what is the pressure rock can withstand.

Sensitivity analysis of the intrinsic permeability values for the seal materials should be undertaken in future calculations.

During construction of the plug several holes for brackets and attachments were drilled into the rock on the plug area. These were assessed separately, since they were not considered during the original modelling work, their effect was considered negligible.

Appendix to chapter 4: Analytical solution for gap intrinsic permeability

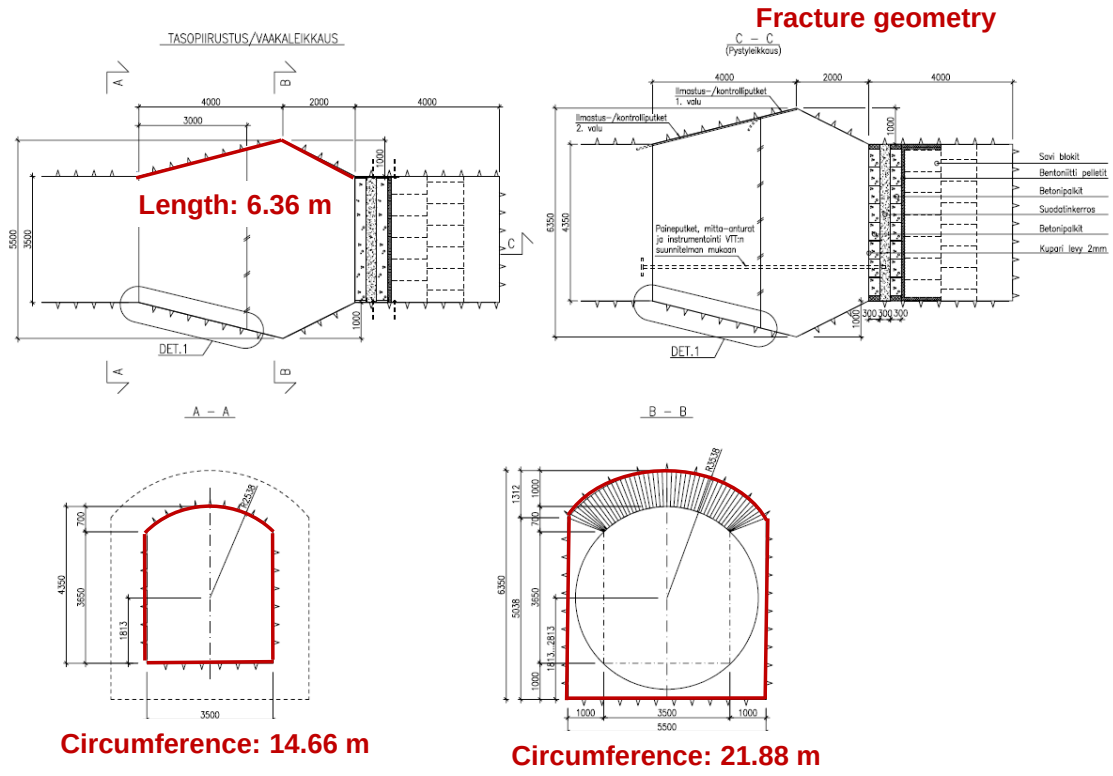

Fig A-1: Simulation geometry used in the analytical solution as applied to Posiva's design (by Mattias Åkesson, Clay Technology AB).

Parameters and constants:

Specific weight of water: $\rho g := 9810$ (Pa/m)

Water viscosity: $\mu := 10^{-3}$ (Pa*s)

Litres/m3 & sec/min: $lpm := 10^{3} \cdot 60$

Geometry:

Length of plug: $L_P := 6.4$ (m) $\quad \sqrt{4^2 + 1^2} + \sqrt{2^2 + 1^2} = 6.36$

Mean circumference: $O_P := 18$ (m) $\quad (14.66 + 21.88) \cdot \frac{1}{2} = 18.27$

Hydraulic relations:

Flow rate: $Q_P := \frac{0.1}{lpm}$

Head (9.9 MPa): $h_H := \frac{9.9 \cdot 10^{6}}{\rho g}$ $\quad h_H = 1009.17$ (m)

		Gap width: 18 m	Gap width: 0.1 m	
Gap transmissivity:	$T_f(B) := \frac{Q_P}{B} \cdot \frac{L_P}{h_H}$	$T_f(18) = 5.87 \times 10^{-10}$	$T_f(0.1) = 1.06 \times 10^{-7}$	(m^2/s)
Thickness of gap material:	$\Delta x := 0.1$ (m)			
Hydraulic conductivity of gap material:	$K_f(B) := \frac{T_f(B)}{\Delta x}$	$K_f(18) = 5.87 \times 10^{-9}$	$K_f(0.1) = 1.06 \times 10^{-6}$	(m/s)
Intrinsic permeability of gap material:	$k_f(B) := \frac{\mu}{\rho g} \cdot K_f(B)$	$k_f(18) = 5.99 \times 10^{-16}$	$k_f(0.1) = 1.08 \times 10^{-13}$	(m^2)

Fig. A.2: Analytical solution and intrinsic permeabilities for cases A-C (by Mattias Åkesson, Clay Technology AB)

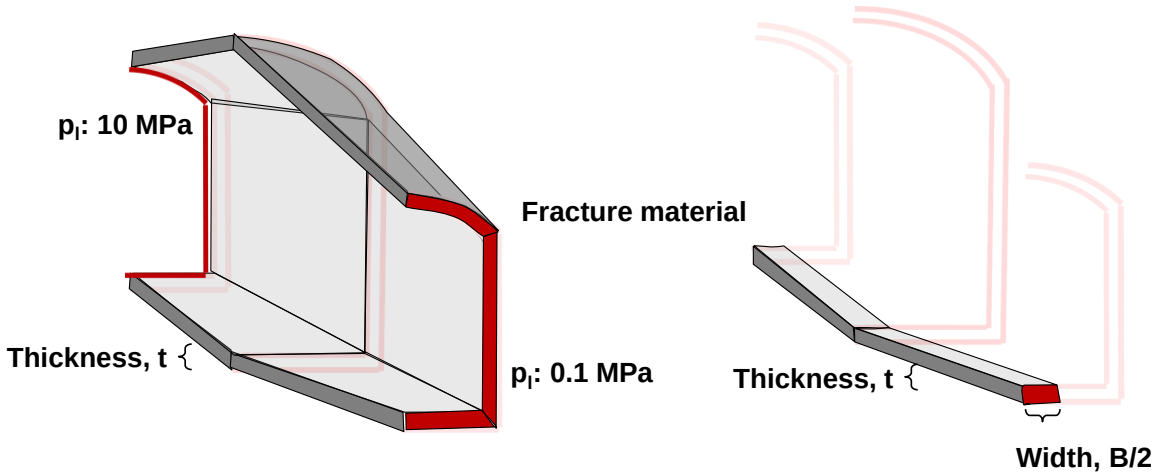

K = T/t
K: Hydraulic conductivity (m/s)
T: Transmissivity (m^2/s)
t: thickness (m), = e.g. 0.1 m

Fig. A.3: Boundary conditions (MPa) in case A (left) and cases B and C (right) (by Mattias Åkesson, Clay Technology AB).

6 Design, implementation, monitoring and simulation of the REM experiment as part of the development program for Performance Assessment (ANDRA)

J. Wendling, N. Conil, J.M. Bosgiraud

The work done by Andra in the framework of the "Performance Assessment" (PA) Work package in DOPAS (WP5) is twofold; first a summary of the past work done at Andra concerning PA under the form of three reports and second the implementation of a metric scale surface demonstrator of a bentonite mixture resaturation process (REM). All this work is related to the French Cigeo deep geological repository in clay rich formation for high level wastes (HLW) and Intermediate level wastes (ILW). The first results available for the REM demonstrator will be used in the next PA process scheduled in 2018 for the Cigeo construction application.

6.1 Context

Since 2005, after the acceptance by the stakeholders of the feasibility dossier presented by Andra, the project of a deep underground repository in clay rich formation has entered its industrial phase. The so called Cigeo project is now in the beginning of the detailed design stage and the construction application is foreseen for the end of 2018.

In this context, improving the knowledge on performance of seals is a major issue for Andra and large scale demonstrators are part of the development program. In the framework of DOPAS, the FSS (Full Scale Seal) surface demonstrator was built at Saint-Dizier in the Noth-East of France. The aim was to test the technical feasibility of the construction of the filling of an about 9 meter in diameter gallery by a bentonite plug maintained in place by two concrete containment walls in as near as possible from underground constraint conditions. To fill this demonstrator in industrial conditions specific machines were developed. More than this, the bentonite core of the FSS seal is made of WH2 (similar to MX80) bentonite pellets and powder mixture specifically developed to comply with Andra's needs in terms of permeability and swelling pressure. This work is detailed in the DOPAS report (Foin et al. 2015).

As the FSS demonstrator is not designed for resaturation, and as upscaling from laboratory experiment (centimetric to decametric scale) is still needed, a specific meter scale resaturation module was designed and implemented in the surface facility of the CMHM (Andra's research laboratory including Bure URL); the so called REM experiment (Conil et al. 2015).

6.2 Aim of performed work

The work done inside DOPAS WP5 by Andra is twofold :

- Presenting in a synthetic way all the work done by Andra during the last ten years in terms of PA in three reports aiming at summarizing the description of the retained sealing methodology (Wendling et al. 2015), of the comprehension of the main phenomenological processes involved (Wendling et al. 2015a) and of the sensitivity analysis strategy applied (Wendling et al. 2015b).

– Design, implementation and monitoring of the REM experiment. Some numerical work concerning estimation of the resaturation process of the REM bentonite core was also initiated and is still ongoing.

6.3 Summary of actual methodology and phenomenological comprehension of sealing at Andra

Since the 2015 feasibility dossier Andra has designed and implemented several seals demonstrators, made a great number of numerical simulations and gained a considerable experience concerning sealing systems in clay rich formations. Part of the work done at Andra in the framework of DOPAS was to produce synthetic reports on the actual position of the agency concerning sealing methodology and phenomenological understanding of seals evolution, including sensitivity analyses strategy to consolidate the reference evolution.

6.3.1 Sealing methodology

The fundamental safety objective assigned after repository closure (protection of human health and of the environment) implies that the repository:

– Can isolate the nuclear waste from surface phenomena and human intrusions, function mainly based on the site geological characteristics (absence of exceptional resources, low permeability, etc.) and the disposal depth;
– Can limit the transfer to the biosphere of radioactive and toxic substances contained in the waste, by gaseous or aqueous channels. The gas transport phenomena are not studied hereafter (in particular the generation and transport of H^2).

To reduce the transfer of radioactive and toxic substances by water, Andra assigns to the repository the three following post-closure safety functions:

– Counteract water flow
– Limit the release of radioactive and toxic substances and immobilize them in the repository
– Delay and reduce the migration of radioactive dns toxic substances that may be released outside the repository cells/vaults

The seals are involved in the fundamental safety objectives after repository closure, mainly by counteracting the flow of water in the repository:

– By limiting the amount of water likely to come from the overlying transmissive formations down through the shafts and ramps during the resaturation phase.
– After saturation of underground structures, by limiting the flow of water in the repository mainly linked to water exchange with the host formation. Hydrogeological characteristics of the site and architecture of the underground facility are mobilized to achieve this function. The aim of seals is to contribute to the flow limitation thanks to their low hydraulic transmissivity.

The main core component of the seals is based on swelling clay (pure bentonite or mixed with natural additives). Andra foresees three types of seals (Fig. 6.12):

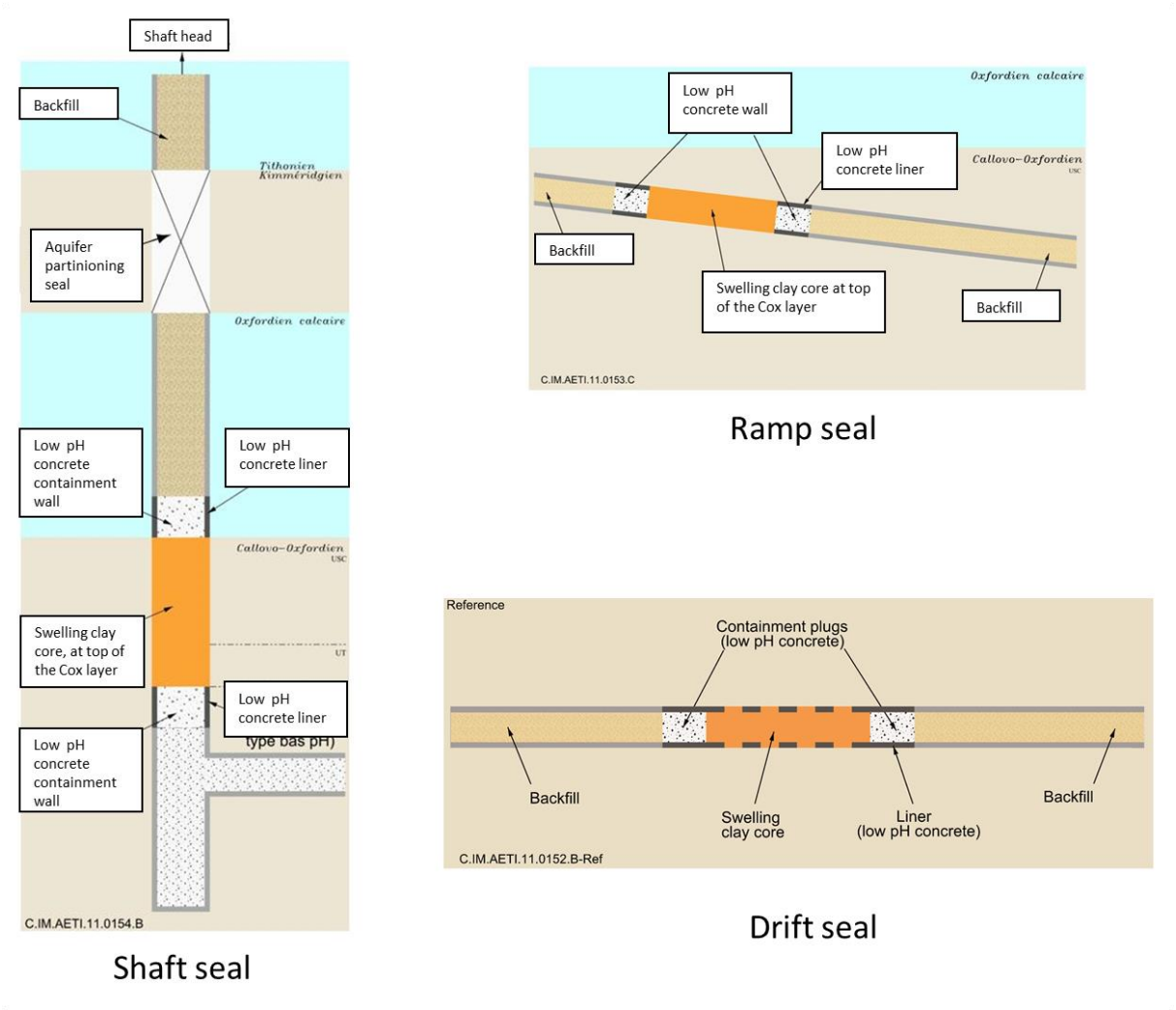

Fig. 6.12 : Schematic view of concepts for all Andra's types of seal

- Vertical shaft and ramp seals, located on top of the Callovo-Oxfordian layer, where carbonate content is higher than in the center involving better mechanical characteristics
- Drift seals at main level in the underground facility, where the clay content of the host rock is maximum
- Seals for IL-LLW disposal vaults, having the same design as the drift seals

The shaft seals make the greatest contribution by participating in the limitation of water flow between the underground facility and the surrounding formations. Seals installed in the drifts connecting each repository zone to the shafts or ramps increase the hydraulic resistance of these drifts. The IL-LLW disposal vault seals, like drift seals, ensure very slow flow conditions in the system and their positions close to the cell, contribute to closer confinement of waste.

6.3.2 Actual comprehension of seals phenomenological evolution

6.3.2.1 Thermal evolution

Excluding local thermal processes that affect seals are very limited in time and space, such as thermal load during hardening of the low pH concrete containment walls or thermal rebalancing in the Callovian-Oxfordian near field, thermal evolution of different seals within the disposal differs primarily according to their position inside the repository, and more specifically according to their position near (or not) exothermic waste packages (mainly HLW). Given the thermal criteria set up for the repository design (maximum host rock temperature not exceeding 90°C) and the different geometrical requirements for repository sub-zones (dead-end sub-zones, exothermic waste stored in specific sub-zones, ...), assessments of the thermal load (considering 2005 and 2009 architectural design) are considered representative of changes in temperature of the various seals, regardless of the architecture finally chosen.

Only seals nearby HLW sub-zones undergo a significant temperature rise of 20°C to 25°C maximum. The temperatures of these seals are therefore between 30°C and 50°C for up to several thousand years. The temperature rise and cooling kinetics are low, of the order of one degree Celsius in a few decades.

All other types of seals in the repository are subject to temperature increases by a few degrees Celsius at a maximum and no thermal coupling is considered.

6.3.2.2 Chemical evolution

Due to the location of seals inside the repository, especially in terms of distance from potential sources of chemical interactions or thermal processes that influence the chemical evolution (cf. heat load above), their chemical phenomenology is generally local and is developed mainly at the interfaces between different materials.

Qualitatively, the experimental data and simulations indicate that the cementitious interactions (coupled with degradation products of the packages for some IL-LLW cells) have a limited extent (in the order of several decimeters for remineralized areas and about a meter for the pH plume front). Given the large dimensions of the seals and the use of low pH concrete for the portions of drift liner maintained and for the containment walls, sources of chemical interactions between those of adjacent structures (to all seals) and those of useful parts of IL-LLW vaults (IL-LLW vault seals only are concerned) are highly buffered on both sides of the seals.

Although chemical modelling of low pH concrete is still incomplete, the results of the reactive transport simulations highlight a slow deterioration of concrete support walls and alkaline disturbance on clay host rock and swelling clay core with limited extension (Fig. 6.13):

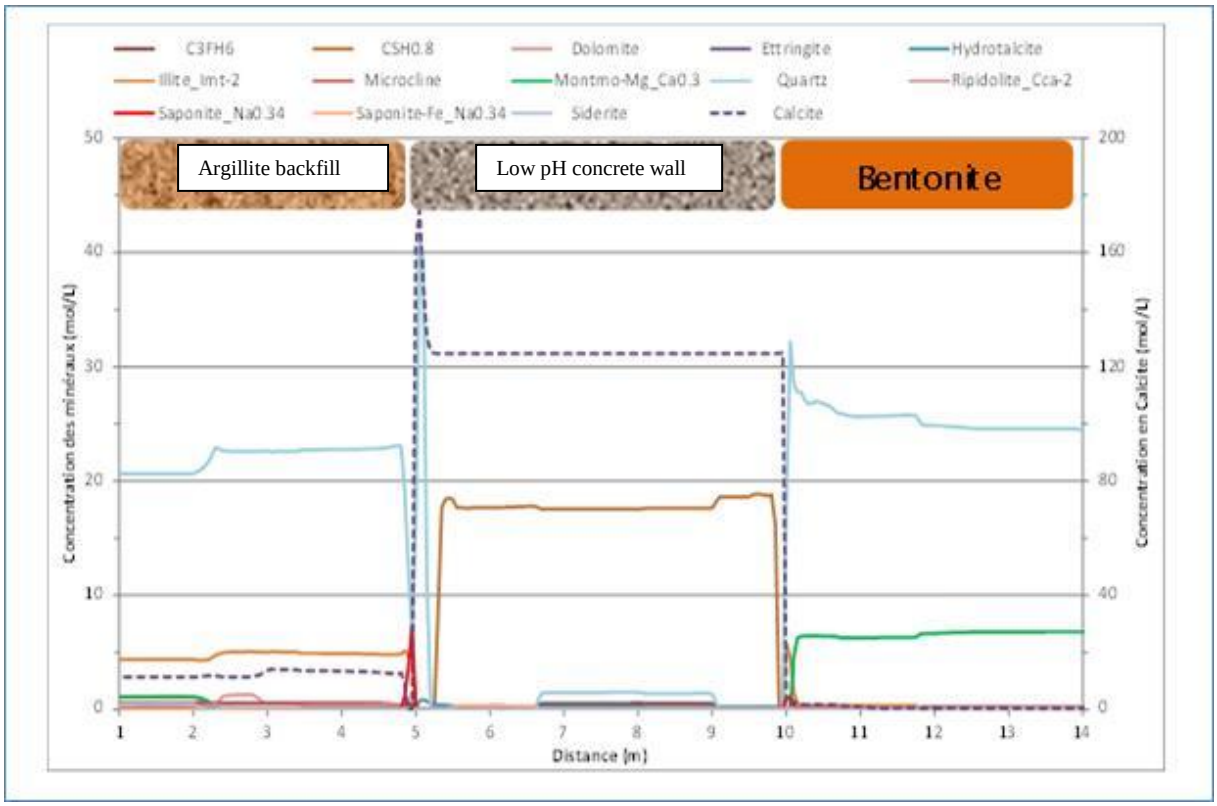

Fig. 6.13: Estimated mineralogical profiles in the low pH concrete containment

6.3.2.3 Hydraulic evolution

Hydraulic behavior of the seals facing a gas flow differs, depending on their state of water saturation and on the different possible paths for gas transfer: through swelling clay core, at the interface between the core and via the damaged zone and also via the host rock itself.

In the unsaturated state, for all of the different pathways described above, there is a continuous escape route for gas transfer. When all the transfer pathways are saturated, there is no continuous gas pathway. Gas must overcome a series of forces to be able to migrate in the gaseous state through the seal (capillary forces, contact visco-plastic forces ...). This set of forces is synthesized in the form of a "gas breakthrough pressure".

Experimental data on retention properties of the seal components show that compact swelling clays, undisturbed host rock clay and low pH concretes have very high capillary pressures, around a few tens of MPa even for weakly desaturated states (95 % to 98 %). This means that only very high gas pressures (beyond ten MPa) may allow penetration of gas in these materials if they are water saturated at the time of gas production, or prevent saturation of these materials if they are not water saturated when gas is produced. This is observed experimentally and reproduced by the simulations.

Conversely fractures in clay host rock (i.e. in the connected fractured zone or EDZ) have low water potential, thus a low gas breakthrough pressure (about 3 MPa) and are likely to let the gas penetrate in the fractures and maintain them highly unsaturated . Therefore, the fractured

connected zone around the horizontal repository level seals will always be a preferred and easy way for gas transfer.

At this stage of knowledge, it appears reasonable to consider that hydraulic-gas transient is not significantly constrained by the saturation state of seals concerning the competition between the transfer of hydrogen (gaseous) and saturation. Therefore, there is no sharp distinction between the behavior of seals in repository zones and those in the central zone (where shafts are located).

Given the above, the global hydraulic-gas transient at repository scale can be summarized as follows for the seals:

– At repository level : hydraulic coupling with the adjacent drifts

  The time needed to reach a full saturation state (in the sense that water flows inside the bentonite core) is affected by the competition between the core and the drift in which it is installed: the core saturates faster than the drift because of a higher water retention curve and of an initial water saturation of the drift backfill implying a void volume by linear meter greater than that of the bentonite core. The time shift is of the order of thousands of years at most. Moreover, resaturation kinetics are slow (several thousand to tens of thousands of years), as they are driven by the (low) transmissivity or the clay host rock combined or not with the presence of gas. There is no “brutal” hydraulic loading of a seal bentonitic core.

  The conditions of water saturation and the presence of hydrogen on either side of a drift seal cannot be perfectly symmetrical. However the characteristics of the bentonite core tend to homogenization with time.

  Thus, simulations carried out in this configuration (assuming a low gas transmissive bentonite core) show a similar to "symmetrical" case behavior and a hydraulic pressure difference between the backfill on both sides of the seal of around 2 to 3 MPa.

– For shafts and ramps seals: hydraulic coupling with the overlying Oxfordizan aquifer.

  The high transmissivity of the overlying Oxfordian aquifer compared to that of the clay host rock leads to a strong hydraulic separation between the upper part (the roof of the Callovian-Oxfordian) and the bottom part of the shafts and ramps seals.

  The rise in the hydraulic head on the upper part of the seal bentonitic core is very fast (a few decades at the most), whereas on the lower part it takes between thousand and several thousand years to reach resaturation.

  The rise of the hydraulic head in the top part of the seals leads to water pressures in the order of some 3 MPa (close to the hydrostatic pressure in Oxfordian aquifer) on the upper part of the bentonite core while they are still far from saturation in their lower part. Thus there is a possibility of a "fast" hydraulic loading on the top. However, in the medium and long terms (beyond a few thousand years), the behavior of shafts and ramps seals will follow that of the repository level seals.

The total resaturation times are variable from one zone to the other, the central zone being potentially the first one to reach the total water saturation (Fig. 6.14). The time shift between total resaturation of the entire storage and hydraulic equilibrium at repository scale is of a few tens of thousands of years at the most.

One can therefore consider that storage is in hydraulic equilibrium after 100 000-150 000 years approximately (i.e. after saturation of the IL-LLW zone and for 2009 architecture design and gas source terms).

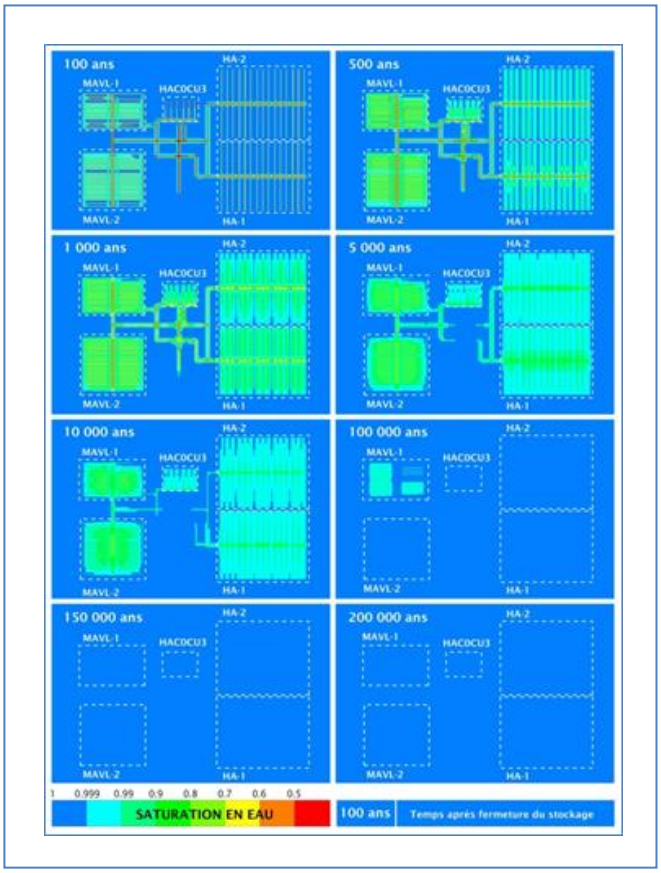

Fig. 6.14: Evolution of water saturation in the repository in connection with the production of hydrogen), 2009 architecture Design and gas source terms

6.3.3 Sensitivity analysis strategy as a consolidation method for the reference evolution

In Andra's loop procedure for safety assessment (Fig. 6.15), uncertainty treatment is present under two different forms in:

– the determination of safety scenarios and especially to define a normal evolution scenario and altered evolution scenarios. This is done in the QSA procedure (Qualitative Safety analysis, AQS in French, see Fig. 6.15). This methodology was developed specifically for the 2005Dossier. It was based on previous attempts and on the comments that these attempts generated, especially from the 2003 NEA peer review of "Dossier 2001 Argile". But since no significant improvement was done. The description below is thus globally the same as the one proposed for the PAMINA European project;

– the analysis of the impact of phenomenological uncertainties on the maintaining of safety functions assigned to certain repository components. This quantitative and scientific uncertainty analysis is done mainly by a mono-parametric deterministic approach and is included in the preparation simulation for scenario definition. But for some processes a probabilistic approach is used. The chapter 6.3.3.2 is summarizing the last of these stochastic studies, done in 2011-2012 and aiming at finding the main parameters uncertainties having an impact on the maximum gas pressure inside the LLW zone of the repository.

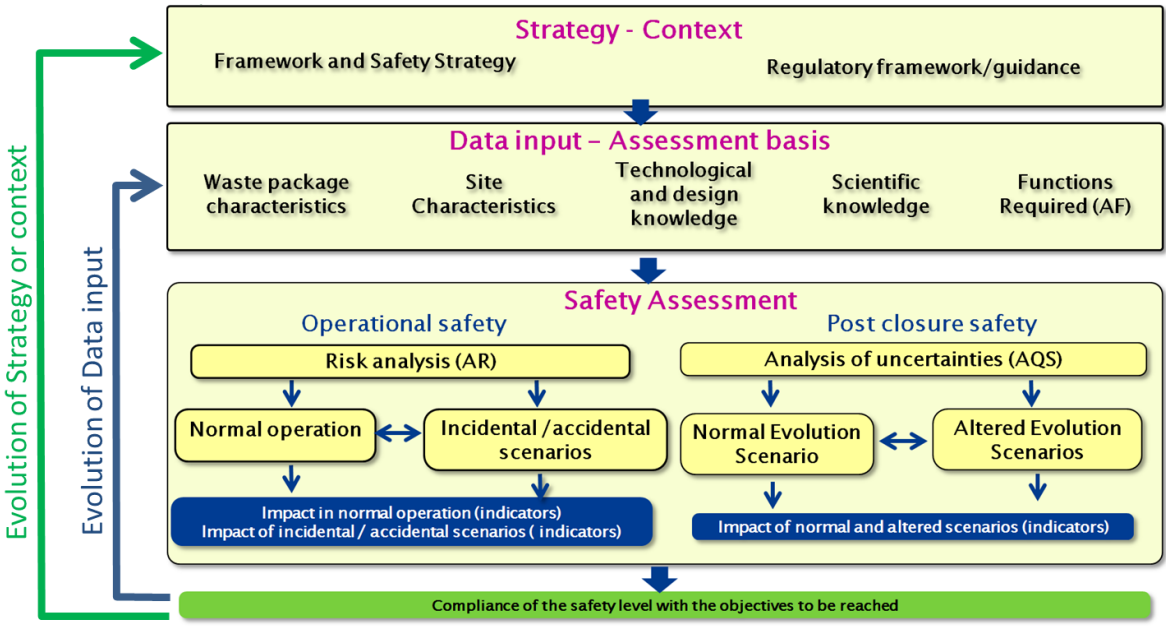

Fig. 6.15 : Safety approach: a global iterative process with key steps

6.3.3.1 Uncertainty analysis in the framework of the safety scenario determination

The management of uncertainties is at the centre of safety analysis of the 2005 Dossier. It directs the design and participates in the definition of the normal evolution scenario (domain) and of the different altered evolution scenarios.

A Qualitative Safety Analysis (QSA) methodology was developed for detailed consideration of FEPs in the Dossier 2005 Argile. The qualitative safety analysis is a method for verifying that all uncertainties in particular in FEPs and design options have been appropriately handled in previous steps of the analysis, thereby justifying *post hoc*, e.g., the selection of altered evolution scenarios. It also led to the identification of a few additional calculation cases and has, in principle, the potential to inform design decisions and the derivation of additional scenarios. Some uncertainties can have a direct influence on the confidence that can be had in a given safety function. For example, if the uncertainty about the permeability of the host formation is too great, this could call into question the performance of the function « prevent water circulation ». Uncertainty is the subject of a systematic study that identifies:

– which component is concerned by this uncertainty, with if relevant the effects caused by one component on another by means of a perturbation ;

- which performance aspects of which safety function can become altered. A qualitative, but argued assessment, including the use of special calculations if relevant, is conducted on the risk of a significant reduction in the expected performances ;
- if applicable, and if such information is useful, the time period involved.

The first objective is to identify whether the uncertainties are correctly covered by the normal evolution scenario (SEN), either in its reference version, or in the sensitivity studies considered. If some of the uncertainties are not, it must be confirmed that they would have little impact on the repository, or that they refer to very unlikely situations.

As a second stage, if the uncertainty is not covered by the SEN, the function(s) and component(s) that could be affected must be identified. A systematic component-by-component analysis is used in particular to identify the shared causes of the loss of several functions: for example, an incorrect assessment of the long-term behaviour of a material can affect all the components that contain it, even though these could have different functions. The qualitative safety analysis provides an assessment of the degree of independence of safety functions, by identifying the possible uncertainties affecting several functions.

The effect of taking each uncertainty into account is described (i.e. the behaviour of the repository if the worst-case value of the parameter in question was the actual value, or if the risk envisaged actually occurred), in terms of the repository's evolution. This is done on the basis of the functions that are likely to be lost. For example, if a series of uncertainties can call into question the function « regulate the pH in the vitrified wastes cells », the corresponding situation is described, i.e. the effects of an uncontrolled increase in pH. If the design can cancel this effect, or if this is taken into account in the SEN or in its sensitivity calculations, the analysis stops at this stage. If a safety function can be affected and the evolution of the repository could start to diverge from normal, with a possible impact on other components, this effect is then specifically identified. If the effect is not covered by any situations in one of the already defined altered evolution scenarios, then a new calculation case is created and quantified. Specific qualitative analyses of external events were also conducted.

The qualitative safety analysis was conducted by Andra engineers who were not involved in writing the scientific documents. In this way, the safety analysis is given a certain degree of independence, since the people in charge of analysing the uncertainties and the possible altered situations (the safety engineers) are not the same as those who established the phenomenological plan for normal evolution.

The comparison between the FEPs databases and Andra's own analyses was an important exercise for the qualitative safety analysis, and provided supplementary information on several aspects, to finally end with consistency between the approaches. It proved to be very useful to safety engineers in ensuring that no fundamental characteristic of the components and no phenomenological process likely to have an influence on the repository had been forgotten.

With regards to the Functional Analysis and to the PARS (Phenomenological Analysis of Repository Situations: specific way to present the scientific knowledge to ease the compre-

hension for its use in the safety analysis), the QSA consisted in a much more systematic identification throughout scientific documentation (PARS, Reference and conceptual notes) of uncertainties, by safety engineers who have not participated in the scientific work. The QSA analyses each uncertainty (on component's characteristics, its evolution, and its interaction with other components) that may either (i) affect its ability to perform a safety function, (ii) or have an influence on another component's ability to perform a safety function, or (iii) modify the component's environment in a way that could affect the way the component fulfils its functions. This analysis permits to check if the uncertainty is taken into account either by design or by the way the normal evolution scenario 'SEN' it represented.

Finally, the QSA offers an integrated vision of all uncertainties by taking into account the various types of treatment (qualitative, calculation results, and scenarios). In that context, for the 2005 Dossier, a set of four "Altered evolution scenarios" (SEA) were developed to provide an understanding of the potential impact of unlikely future evolutions related to specific system failures : (i) partial or overall deterioration of seal performance, (ii) waste disposal packages failure (WPD), (iii) human intrusion and (iv) strongly degraded safety functions. As an end calculation, results (radionuclides flows through barriers & endof pipe impact) based on these SEAs and sensitivity cases within the SEN and SEAs make it possible to evaluate overall repository feasibility and robustness, with information on the contribution of each component/barrier to safety.

6.3.3.2 Stochastic uncertainties analysis: example of the maximum gas pressure in the ILW zone

Questions related to the performance of the repository integrate concerns regarding the impact of the (mainly) hydrogen gas generated by anoxic corrosion of metallic components and radioactive waste. One particular interest is assessment of overpressure in the near field of the repository, whose level could affect the mechanical integrity of geotechnical and geologic barriers.

Achieving a good understanding of the hydraulic-gas system behavior of the repository requires numerical, non-isothermal, two-phase flow and transport simulations. Most of the parameters governing the main phenomenologies (two phase flow and diffusion migration of dissolved gas) have remaining uncertainties linked to various origins (horizontal variability, vertical variability, measurement method uncertainty, …). The number of these parameters is quite high (around ten per material including host rock, EDZ, seals bentonite core, concrete liner and backfill of the galleries) but after analysis of some previous mono-parametric sensitivity analysis it was possible to reduce this number to ten. Having a more complete analysis implies now to do at least a multi-parametric sensitivity analysis and to be sure to cover the entire variation domain it requires in fact a stochastic uncertainty analysis.

Another point is that a priori the coupling between phenomenologies (mainly thermal, two-phase flow and diffusion of solute gases) is neither linear nor monotonic. This implies that stochastic uncertainty analysis needs at least an ANOVA (ANalysis Of VAriance) approach to be performant and thus several tens of thousands os simulations.

Last point is that the gas generation process lasts several tens of thousands of years and that the gas phase spreads throughout the whole repository. This implies a two phase flow numerical simulation of the whole gallery network and of whole the storage cells over at least one hundred thousand years. Even using highly parallel codes this means several days of calculation per simulation.

It is thus impossible to use a simple Monte Carlo method to generate the results to be analysed: the number of numerical simulation should be reduced to a minimum and used to construct a response surface that will at his turn be used to generate the several tens of thousands of results to compute a SOBOL analysis (specific way to deal with an ANOVA analysis).

Having shown that the surface is valid, we applied the "Brute-Force Sobol" first-order variance Method, on the 90,000 data sample. The Fig. 6.16 shows the computed Sobol index for all the ten parameters (not representative if less than 0.1).

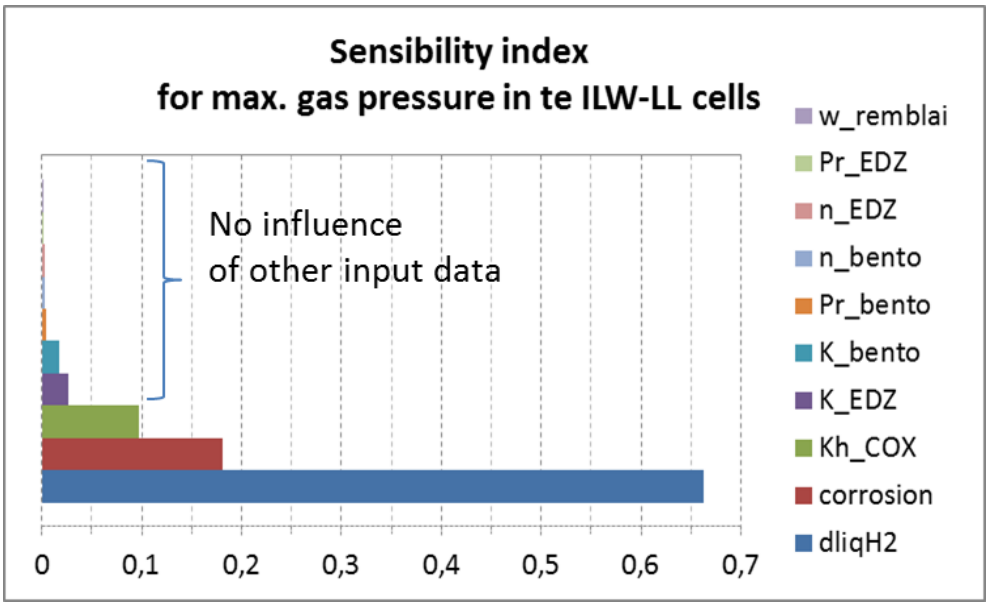

Fig. 6.16: Brute Force Sobol index sensitivity analysis results

The most influencing parameter is the dissolved diffusion coefficient (on average, more than 50% of the gas dissolves inside the ILLW vaults, and more than 90% during the transfer toward the shafts and ramps ; the higher the dissolved diffusion coefficient, the smaller the gas pressure); the second-most decisive parameter is the corrosion rate (the bigger the corrosion rate, the higher the gas pressure in direct relation with the gas flux generated) and the third most decisive parameter is host-rock (COX) permeability (the higher the permeability, the higher the pressure in relation with the resaturation leaving less place for the gas to expand).

These results have been used to optimize the research program on characterization of the host rock and on engineered components.

Concerning determination of most influencing parameters on certain specific criteria, during 2016 a new program on high parallel computation for transient two-phase flow at repository

scale will be issued on (i) a new architecture, (ii) with new phenomenology (mainly more representative solute diffusion processes taking into account the effect of desaturation which was not the case in the previous attempts) and (iii) on different criteria (maximum gas pressure in the ILW zone, resaturation time, …).

6.4 The REM experiment

In the design phase of the CIGEO Deep Geological Repository project, Andra plans to progressively build horizontal drift seals to re-establish site integrity and safety on closure. Various technical solutions have been considered, involving a swelling clay core inserted between two concrete support structures (aka "containment walls"). In order to check the industrial feasibility of this facility, a Full-Scale Seal (FSS) technological demonstrator was built in Saint-Dizier within the frame of the European DOPAS project. This demonstrator tested industrial construction equipment by using existing and specifically developed technologies to set up and perform a full scale sealing operation. The seal core was made from a material formed of an admixture of bentonite pellets and crushed pellets (aka "powder"). The core support structures (also called "containment walls") are made of low PH concrete, with self-compacting concrete for the "upstream wall" and shotcrete for the "downstream wall".

Given the size of the construction facility, a phenomenological test could not be envisaged. In fact, the saturation of a **decametric**-sized core would take hundreds or thousands of years and would generate very high levels of mechanical stress on the drift model structure (concrete liner) due to bentonite swelling. A series of experiments are therefore being implemented in addition to the FSS construction demonstration in order to test the phenomenological aspects and the seal hydro-mechanical behaviour under real operating conditions.

The REM saturation experiment is thus complementary to the FSS construction experiment and will demonstrate the feasibility of resaturating the bentonite admixture used in FSS and analyse the pellets/powder mixture behaviour during resaturation at a **metric** scale that is difficult to achieve with standard laboratory equipment (**decimetric** scale cells at most).

6.4.1 Design of the REM experiment

In order to get as close as possible to *in situ* conditions, several criteria were defined for experiment design. The pellet/powder admixture emplacement should be representative of the technique used in FSS (use of screw type conveyors to transport materials), particularly in terms of compacting rates. To ensure comparable properties (permeability, swelling pressure) between the REM model and the FSS demonstrator, equivalent dry density must be similar in both systems. Equivalent dry density primarily depends on the compacting rate, residual void level and initial water content. The technique for pellet/powder admixture emplacement, although manual, should draw on the technique used in FSS. The reduced dimensions of REM prevent the use of the backfilling devices used in FSS.

The experimental strategy used in the REM experiment is as follows:

- Monitoring of water saturation;
- Monitoring of injected water volumes;
- Monitoring of removed air volume;
- Measurement of pore and total pressure;
- Occasional permeability measurements (water and gas);
- Measurement of swelling pressure;
- Measurement of gas entry pressure.

It is also necessary to know the system's initial hydraulic state and the exact volume available for bentonite emplacement (excluding the volume of sensors and other instruments).

Measurements must give a three-dimensional view of the hydraulic and mechanical behaviour within the test, throughout the entire resaturation phase. They must also determine when saturation is achieved from a hydraulic and mechanical standpoint (swelling pressure).

Because hydration of the granular mixture is "one-dimensional", the vessel installed is inspired by the large-diameter swelling cells used at LECBA (Laboratoire d'Etude et de Caractérisation des Bétons et des Argiles, part of CEA). In order to facilitate filling and avoid creating "arching" effects that prevent the material from reaching uniform density, sensors had to be spread out with intervals of at least the size of the pellets, and for the experiment as a whole, the vessel diameter had to be at least equal to its height (slenderness ratio of 1/1 to minimise edge effects).

The vessel environment comprises the vessel hydration or injection circuit and the air outflow circuit. The injection system must supply water to the sample inside surface and regulate and/or quantify the volume of water provided.

The hydration water (host formation water) is taken from the "Bure site borehole FTP1101". This borehole was drilled in October 2010 along the underground "GMR drift" wall. It is subhorizontal and 100 m long with a 10 cm diameter. Since April 2012, water has been collected from the borehole and its composition is monitored by sampling and laboratory analysis.

The injection pressure is slightly higher than atmospheric pressure, typically 1 to 2 meters head of water (10 to 20 kPa).

The output circuit collects air ejected from the vessel. A very precise flowmeter must measure the flowrate and a Relative Humidity (RH) measurement sensor is placed on a branch of the circuit. Fig. 6.17 is a diagram of the vessel with its 2 systems.

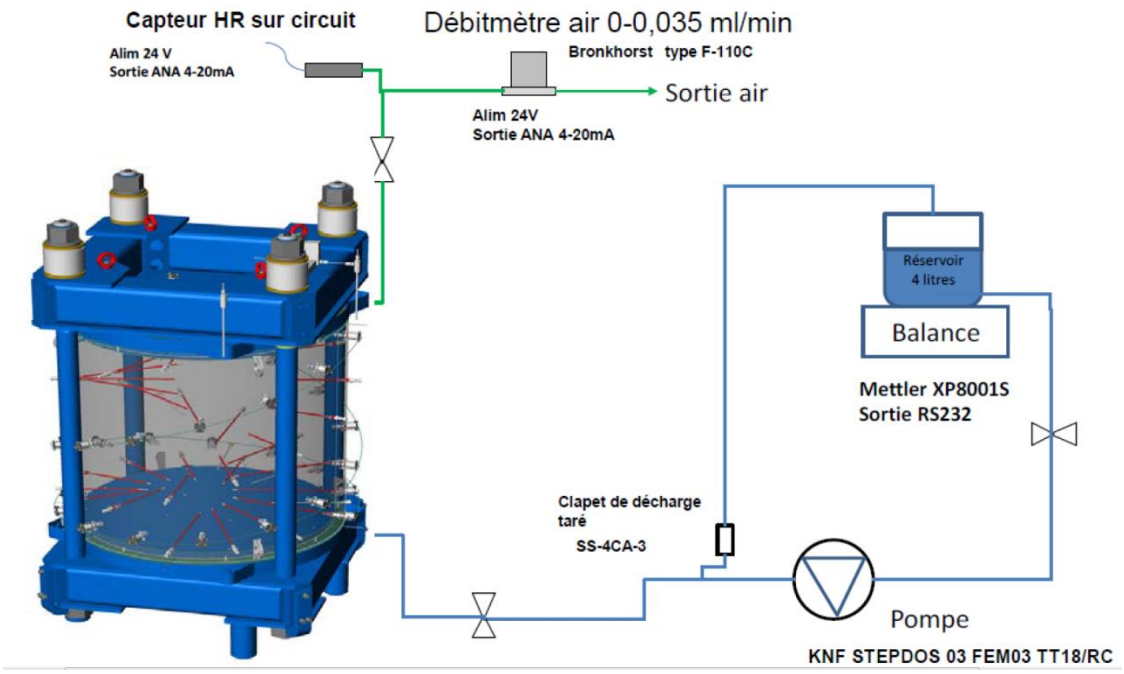

Fig. 6.17: Schematic representation of the REM vessel and its environment

6.4.2 Implementation of the REM experiment

The vessel was delivered to the CMHM technical area on 27 May 2014 in 2 packages. The first package related to the factory-mounted bottom part of the vessel. This part of the vessel included the lower frame, legs and the 4 tie rods installed, and the bottom lid placed on the frame to support the confinement cylinder. A rubber plate was in place to protect the rim of the confinement cylinder during transport. A plywood panel was used to space the tie rods apart and rested against the top part of the cylinder. This panel was held in place by four M 72 nuts via four spacers.

This assembly constitutes the receptacle for the swelling clay material. It was unloaded from the lorry using a bridge crane, with M16 lifting rings screwed onto the bottom panel for this reason. The first package had a mass of 3,100 kg.

The second package contained the top frame placed on the transport pallet, which supported the top lid's two discs. The stainless steel panel including the porous disc and air collection nozzle was on top of this, and the steel force absorption panel was underneath. It was unloaded using the same tools as for package no. 1. This second package had a mass of 1,550 kg.

The bentonite core, inside part of the REM vessel, has a filling volume of 785 litres, which represents approximately 1 300 kg of material, comprising 900 kg of pellets and 400 kg of crushed bentonite (powder). These materials were taken from the FSS test manufactured stock.

The REM test was installed by filling the vessel during the third week of September 2014 (Fig. 6.18), which was finished late morning on 25 September 2014 when the final sensor was connected to the SAGD (Steam-Assisted Gravity Drainage) measurement system.

Fig. 6.18: Principal REM installation phases

6.4.3 Main results available

As the total resaturation period is of several tens of years (see section 6.4.4), for the moment, after only a bit more than one year of measurement, the only sensors reacting significantly are the relative humidity ones.

30 humidity/temperature sensors were installed in the vessel. A diagram showing sensor location is given in Fig. 6.19. To facilitate comprehension of the results, measurements are broken down by section and relative humidity measurements for the two sections are presented in Fig. 6.20.

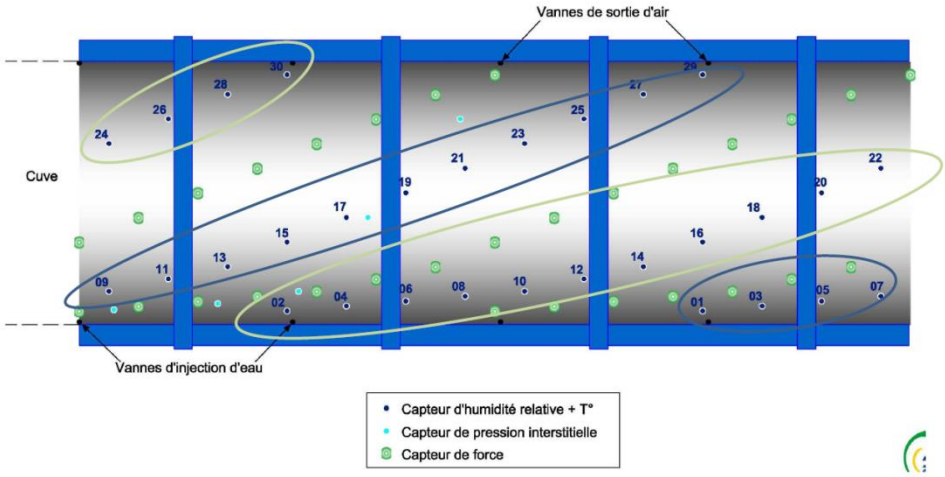

Fig. 6.19: Emplacement of the relative humidity sensors in the two sections (1 in blue, 2 in green)

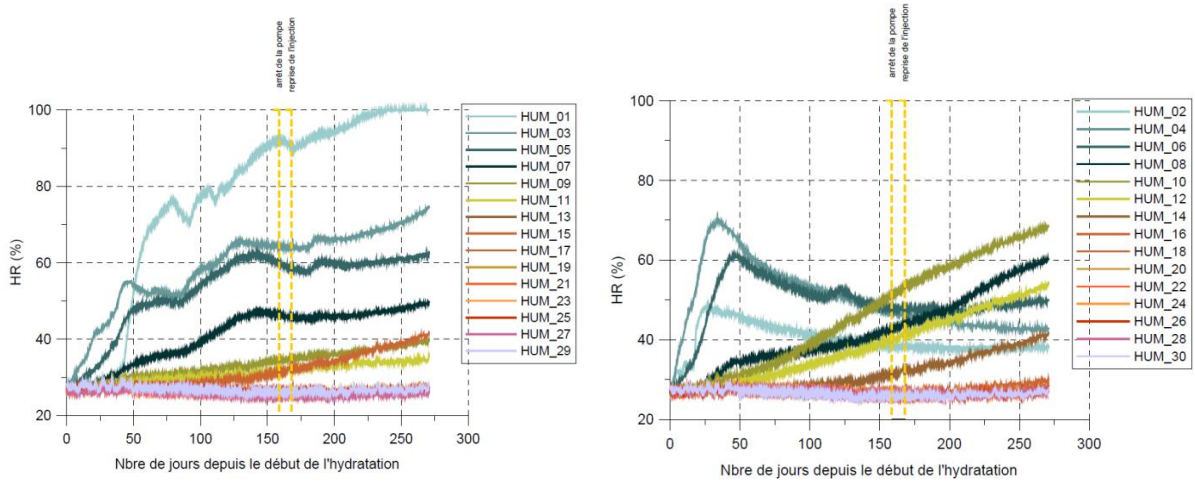

Fig. 6.20: Relative humidity measurement in section 1 and 2 during the first 270 days

On average, RH was at 27% at the start of hydration. The most reactive sensors were sensors 01/03/05/07 in section 1. Recently, sensor 01 has even reached 100%. This is due to their proximity to the injection system and they were also the only sensors to react to when injection was stopped following pump failure. Sensor 01 will be removed and its position resealed in order to avoid backflow and leaks along this sensor.

The other sensors that react, both in section 1 and section 2 are also located at bottom of the vessel and close to the point where water enters the sintered metal. *Above 300 mm, the sensors react very little or not at all.* Analysis of the curves shows that hydration in the vessel is not uniform. If the sensors located at the same depth are compared, not only is the hydration kinetics different, but also the amplitudes. To illustrate this observation, the values measured by sensors 01 and 02, 03 and 04 and 05 and 06 can be compared. They are located around the vessel at respectively 20 mm, 40 mm and 60 mm from the bottom of the vessel. Sensors 02, 04 and 06 show comparable kinetics, with a fairly significant increase during the first 40 days (up to 70% for sensor 04), followed by a drop of up to over 20% for the same sensor. The

sensors in section 1 react differently; the initial phase is more gradual and then RH increases very rapidly up to values of over 60% for all three sensors. In light of these results, it is clear that the homogenization process will probably be long, as suggested by the estimation of total resaturation time (around 30 years, see next section).

6.4.4 Simulation of the REM experiment resaturation

Some preliminary simulations of the resaturation time of the REM experiment are already available. These simulations are based on simple Hydraulic models, with no mechanical coupling. This assumption was made following the results of some small scale experimental tests showing that the powder/pellets mixture water uptake was not significantly different than the one measured with powder only.

Under this assumption, and using other small scale experimental results, one was able to determine two-phase flow parameters for the bentonite mixture. Using than Darcy flow approximation model, the resaturation time was estimated around 30 years (Fig. 6.21).

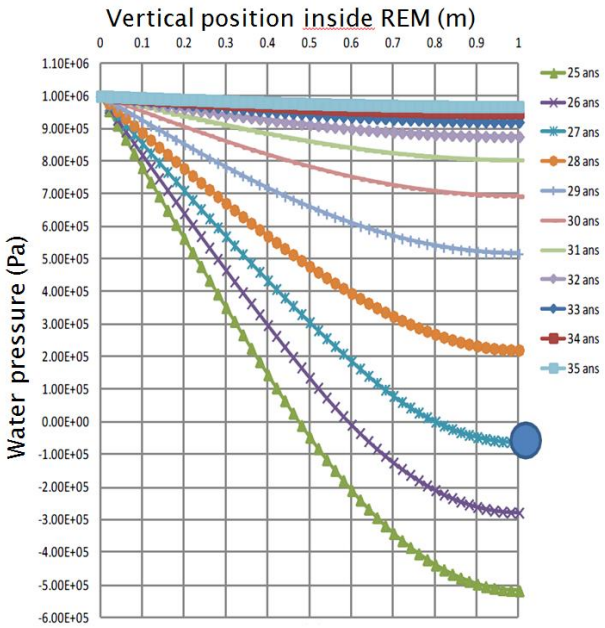

Fig. 6.21: Two-phase flow simulation results of water pressure inside REM showing that total resaturation time can be estimated around 30 years

Based on return of experience on previous comparison between experimental data and simulation results, this estimated time can be seen as a minimum value.

Some HM simulations using specific hydromechanical bentonite model developed by the UPC are ongoing and their results should be available around mid 2016.

6.5 Conclusions

The work done by Andra in DOPAS WP5 is twofold and in accordance with the initial program:

– Summarizing today's view on seal concepts, seals phenomenological evolution and sensitivity analysis strategy;
– Design, implement and monitor a meter scale resaturation test (REM) which results will help consolidate the arguments on seal phenomenological evolution. Numerical simulations of the resaturation time are still ongoing using actual partial data to calibrate specific HM models and refine the predictions.

Concerning the future, REM monitoring is planned to last for several decades and numerical simulation exercises will be planned periodically to actualise the models during this whole time length.

7 Process level modelling of compaction processes (DBETEC)

V. Burlaka, M. Jobmann, S. Schirmer

The modelling work performed by DBETEC in DOPAS is mainly related to the R&D on Plugging & Sealing for repositories in salt. The work presented here, is accompanying the laboratory and in-situ experiments regarding the compaction of granular materials used for sealing purposes, also presented in more detail in the DOPAS deliverable D3.30 (DOPAS 2016b).

7.1 Context

The current reference concept for shaft sealing (Fig. 7.1) developed during the "preliminary safety assessment for the Gorleben site" (VSG), contains different elements for sealing and supporting functions (Müller-Hoeppe et al. 2012). One element in the middle is called "long-term sealing element" which is a column made of crushed salt. Constructing a column of the same material as the host rock would have the benefit that the long-term sealing effect of this material could be taken into account. Due to the convergence of the rock mass, the crushed salt is compacted further and its permeability is continuously reduced. Low permeabilities can be obtained if the compactibility of the material is as high as possible.

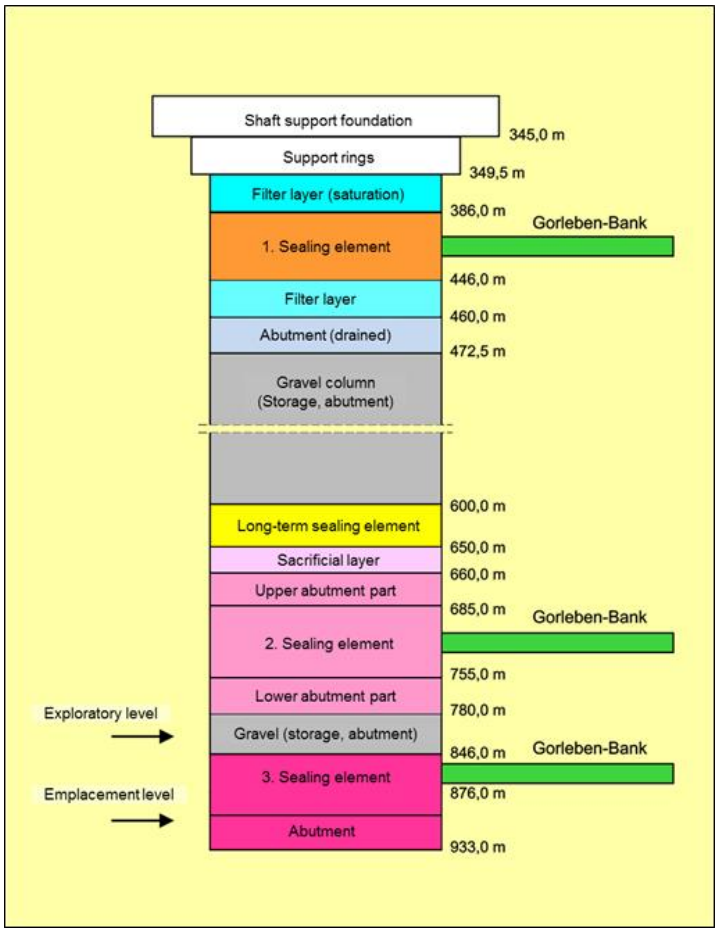

Fig. 7.1: Current shaft sealing concept for the Gorleben site (Müller-Hoeppe et al. 2012).

During laboratory and in-situ experiments improvements of individual elements of the concept have been investigated (see DOPAS 2016a). Great effort has been spent to investigate the compactibility of the crushed salt. A low initial porosity right after installation is crucial to achieve good sealing properties as early as possible. To further improve the sealing abilities of crushed salt an admixture of granular clay has been used and tested during different experiments (Glaubach et al. 2016).

To investigate the system behaviour especially of the crushed salt, numerical model calculations have been performed. On the one hand these model calculations were intended to increase the understanding of the crushed salt compaction process. On the other hand these calculations should serve as a first approach to develop a modelling tool which, after its final qualification, can be used to predict the compaction behaviour of crushed granular material to be applied as sealing material.

The current safety requirements in Germany (BMU 2010) state that prior to any installation of an engineered barrier or its components the proper functioning and the integrity of the barrier components have to be proven to the authorities. That means that the structural design of the barrier system has to be submitted to the authorities together with a calculational proof which demonstrates that if the barrier is built as planned, the integrity of the barrier and thus it's proper functioning is assured. Details of the calculations proof can be found in (Herold & Müller-Hoeppe 2013), (Kudla et al. 2013), and (White & Doudou 2015). The calculational proof has to consider all THMCB processes that have an impact on the designed barrier and it has to show that none of the processes will jeopardize the proper functioning of the barrier. The authorities will check the submitted documents and will provide the results of their evaluation to the implementer.

The modelling work in DOPAS will be used to improve the corresponding modelling capabilities with regard to specific constitutive laws for describing sealing material compaction. The results of the laboratory and in-situ investigations are a fundamental basis for the constitutive material laws which can be used within the calculational proofs for this specific purpose.

7.2 Simulation of compaction

Model calculations were performed not only to identify suitable grain size distributions but also to get information about compaction procedures which lead to a suitable in-situ compactibility and thus a suitable initial porosity after installation. For this purpose, a particle model was developed that can be used to generate different grain size or grain distributions and which is able to simulate different compaction processes (Fig. 7.2). The computer code PFC2D of Itasca® (Cundall & Strack 1979), (Itasca 2008) which employs the Discrete Element Method (DEM) was used for this purpose.

In a first step, the compactibility of crushed salt as a function of grain size or grain size distribution and particle shape of the material was studied by simple pressure compaction. The control parameter is the mean value of the porosity measured in four different areas of circular shape as illustrated in (Fig. 7.2). At first, round particles with different grain sizes were

studied. In order to approach the best distribution curve possible, the first simulation runs were carried out with samples that consisted of particles with two different sizes. The best compaction could be achieved using particles with a size ratio between 20 and 10. Using a size ratio of 15, various size distribution curves were generated. The best compaction could be achieved using a normal size distribution.

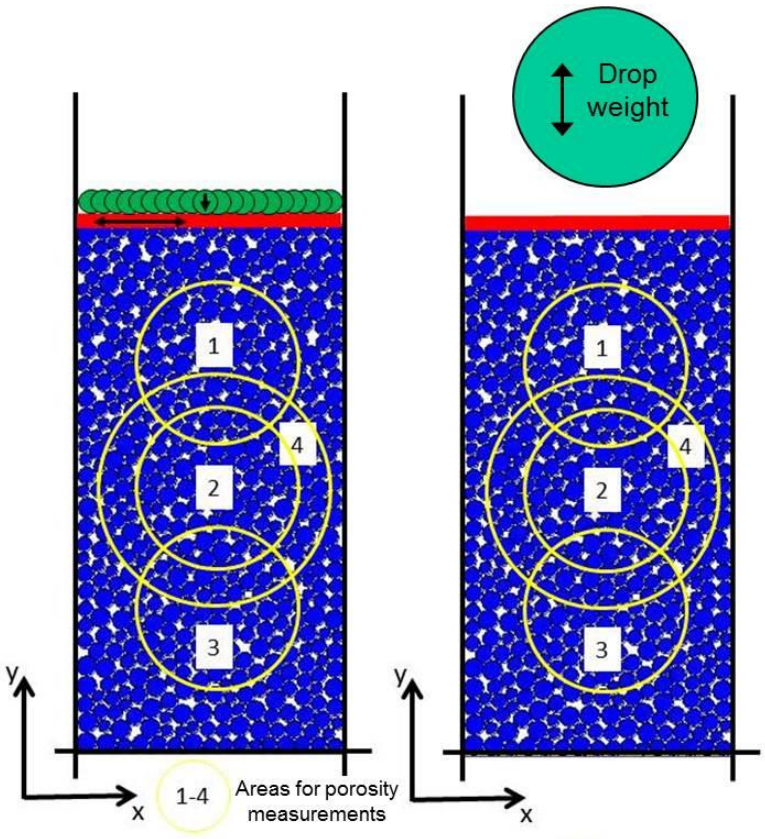

Fig. 7.2: Discrete element model used to simulate simple pressure compaction, compaction due to a vibrating load and impulse compaction.

Following the grain size spectrum analysis, the influence of the particle shape was studied. The particles were divided into 3 categories depending on their axial ratios (from shortest to longest axis): plate-like, flat-stemmed, and columnar. The residual porosity increases with increasing ratio of the axes' lengths. If the axial ratio increases, more and more particles interlock so that higher pressures would be necessary to break individual grains and to further compact the material. The best compaction could be achieved with a uniformly plate-like, round particle shape.

In a second step the model has been further developed to simulate two different types of compaction processes, compaction by a vibrating plate and impulse compaction. To simulate a vibrating plate a horizontal plate was put on top of the granular material which is able to move in horizontal directions with different frequencies (Fig. 7.2 left). The amplitude of the movement is set to be no larger than 2/3 of the minimum particle diameter to ensure that no particles can escape via the gaps at the boundaries. On top of the plate a clump of particles act as a weight to simulate the weight of an industrial vibrating plate. To simulate impulse com-

paction a circular shaped clump was created to bounce on top of the plate with different weights and velocities (Fig. 7.2 right). The drop height and drop frequency are kept constant.

The modelling results show that impulse compaction is much more efficient. Using the vibrating plate model a mean porosity reduction of about 10% could be achieved depending on material composition and vibrating frequency. The impulse compaction models deliver a mean porosity reduction of about 23%.

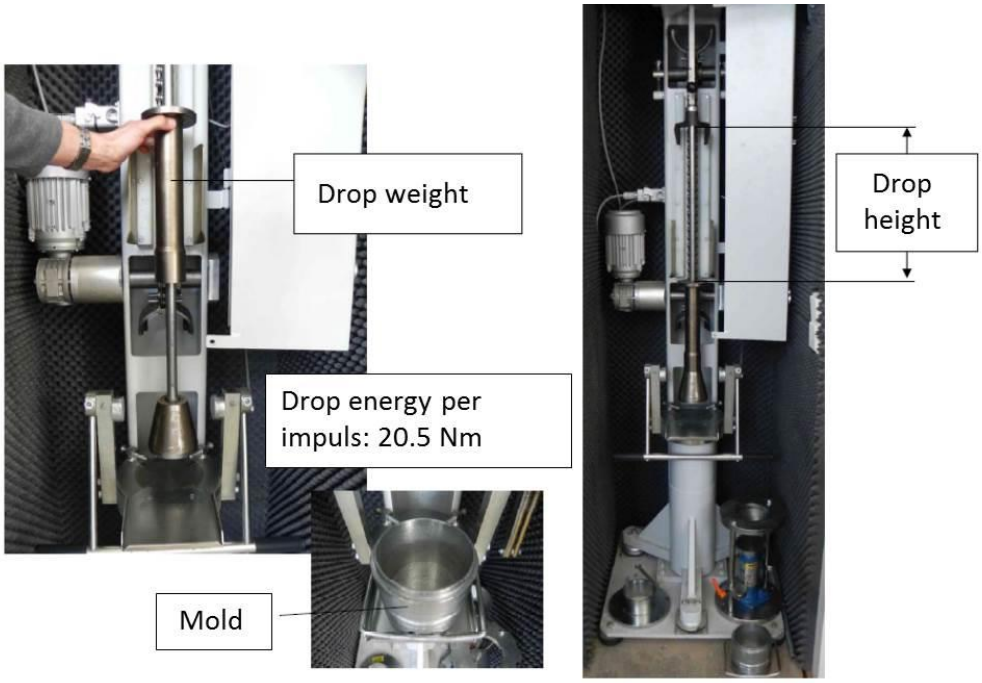

Fig. 7.3: Experimental design of the laboratory tests (Glaubach et al. 2016)

Laboratory and in-situ compaction tests (White et al 2016b) lead to a similar evaluation. Using impulse compaction higher compaction energy can be applied leading to a more efficient compaction. For a first model calibration the impulse compaction procedure was preferred. The laboratory test of pulse compaction represents a repeated sequence of drops of the weight from the certain height onto the surface of material placed in the mold (Fig. 7.3). Even and efficient transfer of energy into material is ensured during the remaining of the drop weight for a while on the surface of material after each drop. The specific compaction energy is defined by the total volume of the compacted sample. The laboratory test parameters are listed in Table 7.1.

Tab. 7.1: Laboratory test parameters

Property	Value
Mold height, *h*	0.0771 m
Mold diameter, *d*	0.1015 m
Drop weight, *m*	4.55 kg
Drop height, *H*	0.465 m
Energy per drop, *E*	20.5 Nm

Various mixtures of salt grains and clay particles have been taken into account in laboratory tests (Table 7.2). The grain size range of each fraction is presented in Table 7.3. The total pore content consists of the volume of added-water and air pores. However, compaction energy is defined only by the total volume of the solid material. Grain size distributions for each grain fraction are shown in Figure 7.4 (Grain density is 2200 kg/m^3).

Tab. 7.2: Investigated mixtures of salt grains and clay particles used in laboratory tests. Results provided by Uwe Glaubach, TU Bergakademie Freiberg.

Mixture	Volume fraction (M%)				
	Without clay	With 10% clay	With 15% clay	With 20% clay	With 30% clay
Clay	-	7.8	11.3	14.5	20.2
Band 8	44.0	40.6	39.0	37.6	35.1
Band 6	27.0	24.9	24.0	23.1	21.5
Überkorn	29.0	26.7	25.7	24.8	23.1
Added-water [M%]	4.0 w/clay -.--	4.0 w/clay 0.44	4.0 w/clay 0.31	4.0 w/clay 0.24	4.0 w/clay 0.17
Total pore content [Vol%]	17.4	10.9	10.4	10.2	10.5
Air pore content [Vol%]	10.2	2.9	2.4	2.1	2.3

Tab. 7.3: Grain size range of grain fractions

Fraction	Grain size range
Überkorn	3 mm - 10 mm
Band 6	0.4 mm - 4 mm
Band 8	0.1 mm - 1 mm
Clay particles	0.03 mm – 0.3 mm

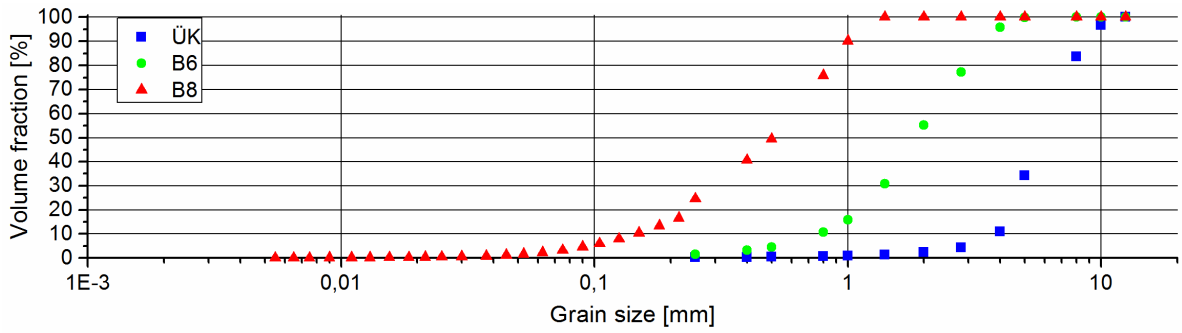

Fig. 7.4: Grain size distributions for different grain fractions. Überkorn, Band 6, Band 8 denoted as ÜK, B6 and B8, respectively.

The results of laboratory tests are shown in Figure 7.5. The lowest porosity by pulse compaction was achieved using a mixture of 85% of salt grains and 15 % of clay and equals to 2.37%.

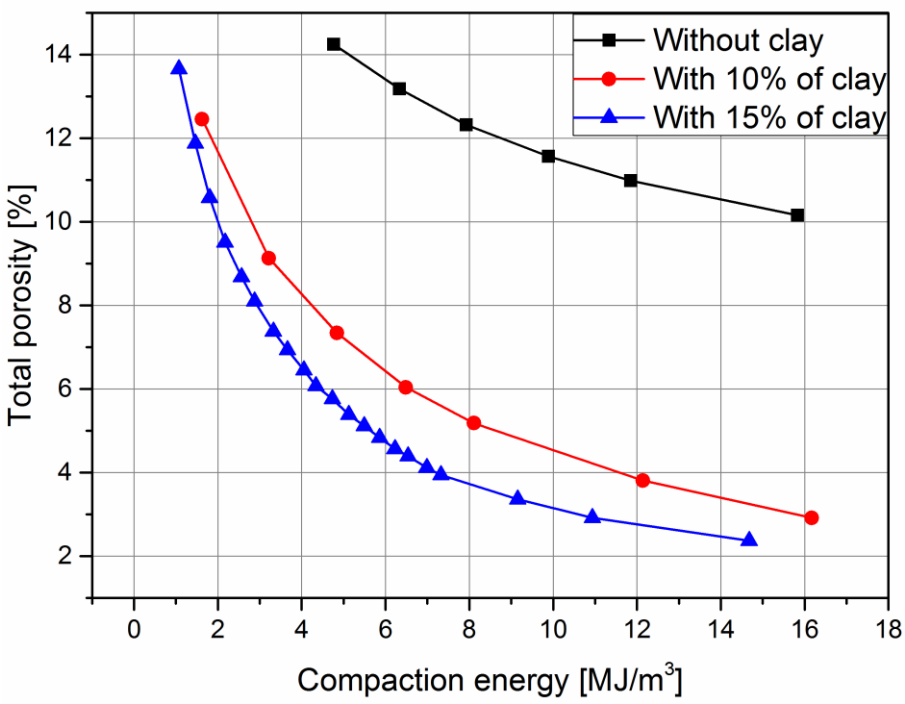

Fig. 7.5: Total porosity as a function of compaction energy for different crushed salt and clay mixtures. The results were provided by Uwe Glaubach, TU Bergakademie Freiberg.

7.3 Calibration of impulse compaction model

Two-dimensional numerical modelling has been performed for study a pulse compaction using a discrete element method. The interaction of particles is based on a force-displacement law and Newton's second law of motion. The model components like clumps (collection of circular pebbles), balls and wall elements, are assumed to be rigid and interact with each other at contacts or interfaces between the entities. The linear contact model was used here, which is defined by normal and shear contact stiffness, friction angles and damping ratios between two entities. The parameters used in simulations are presented in Table 7.4.

Tab. 7.4 Parameters used in simulations

Entities	Parameters			
	k_n, normal contact stiffness	k_s, shear contact stiffness	friction coefficient	damping ratio
Pebble-pebble	1e8	1e8	0.47	0.1
Pebble-wall	5.5e8	5.5e8	0.38	0.8
Pebble-ball	1e8	1e8	0.47	0.1
Ball-wall	5.5e8	5.5e8	0.38	0.8
Ball-ball	1e8	1e8	0.47	0.1

To reproduce the shape of salt grains used in laboratory tests, a microscopic analysis on thin sections has been carried out (Fig. 7.6). Seven representative shapes were selected and clumps with the proper shape were created (Fig. 7.7).

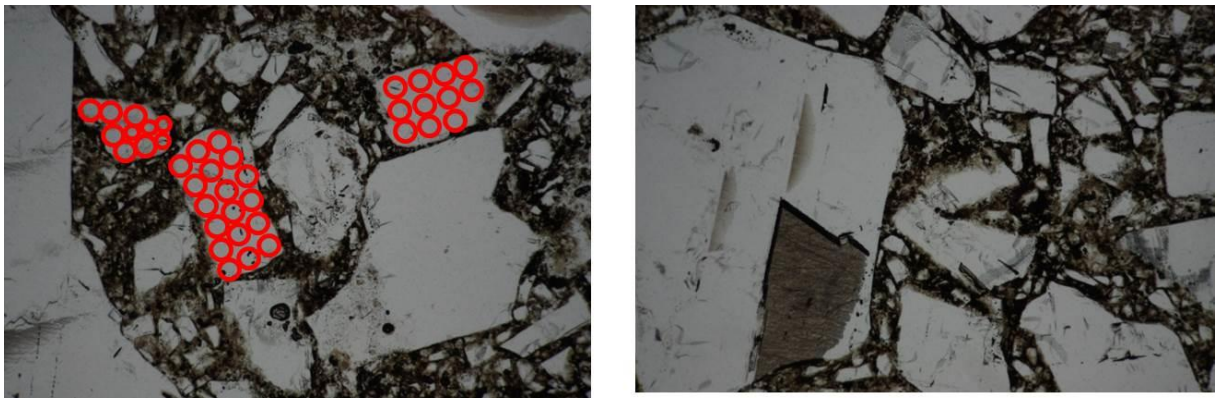

Fig. 7.6: Representative thin section images of salt grains and adaptation to model clumps (red circles).

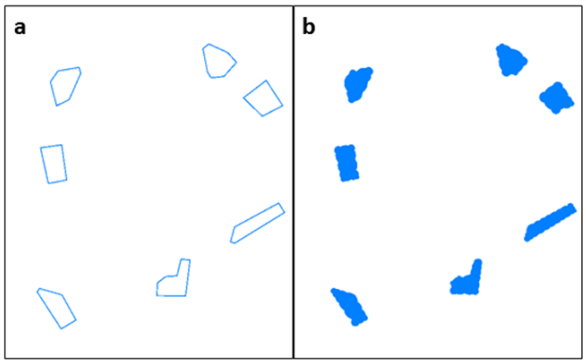

Fig. 7.7: Seven representative shapes of grains (a), seven shapes of clumps used in simulations (b)

To simulate the laboratory tests in a proper way, the grain size distribution functions of clumps were fitted with the grain size distribution functions of salt grains for each fraction: Band 6, Band 8 and Überkorn (see Fig. 7.4). To simulate clay particles, fine balls were created with the radius in the range of 0.03-0.3 mm.

Firstly, the model without clay particles was generated with a specific grain composition compiled from different grain size distributions (44 % of Band 8, 27% of Band 6 and 29% of Überkorn), a description of which can be found in Glaubach et. (2016). Within the mold, which consists of three fixed walls and has diameter of 101.5 mm (as diameter of the mold in laboratory tests), clumps were generated with the representative shapes and settled down under gravitation. The filling height was measured at the y-position of the highest particle.

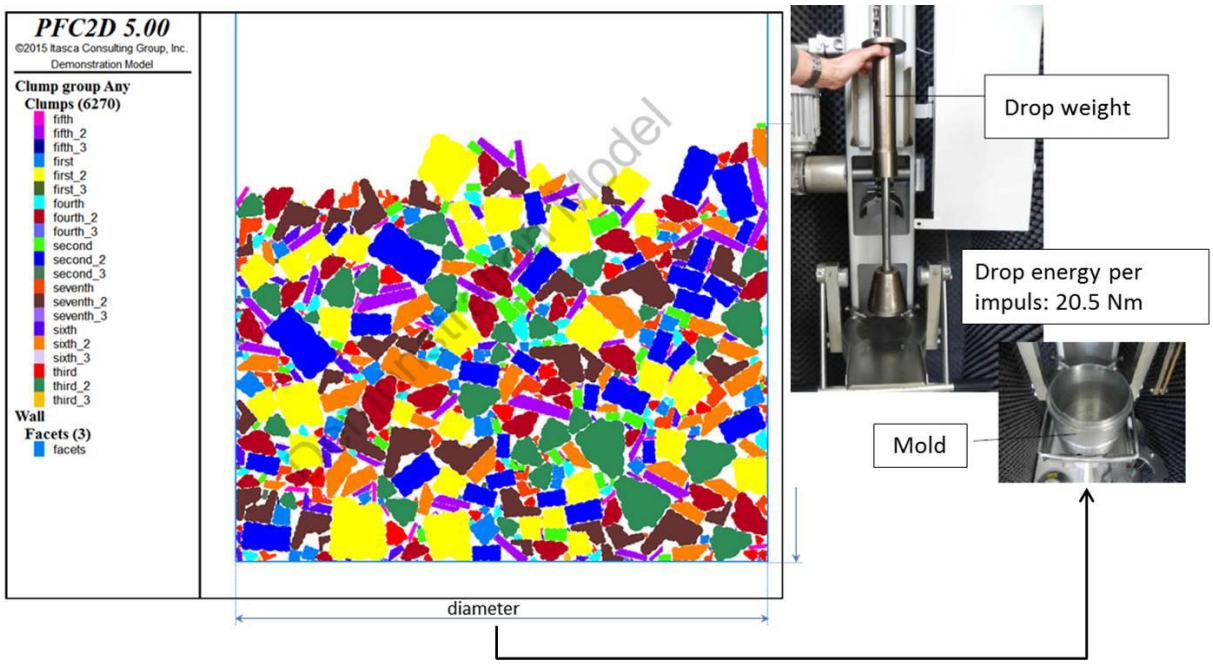

Fig. 7.8: Initial state of the particle model. The mixture consists of 44 % of Band 8, 27% of Band 6 and 29% of Überkorn salt grains.

To simulate pulse compaction, the fourth wall was created above the particles (0.1 mm higher than the y-position of the highest particle) and moved down with the constant velocity until it touched first particles, after that the wall continued to move with the same velocity for 3 seconds simulating a specific pressure on the particles. Afterwards, the wall was moved up again to start the next blow on the particles. The same procedure has been repeated 480 times, simulating 480 drops. The states of the particle model after 30 and after 480 drops are presented in Figure 7.9.

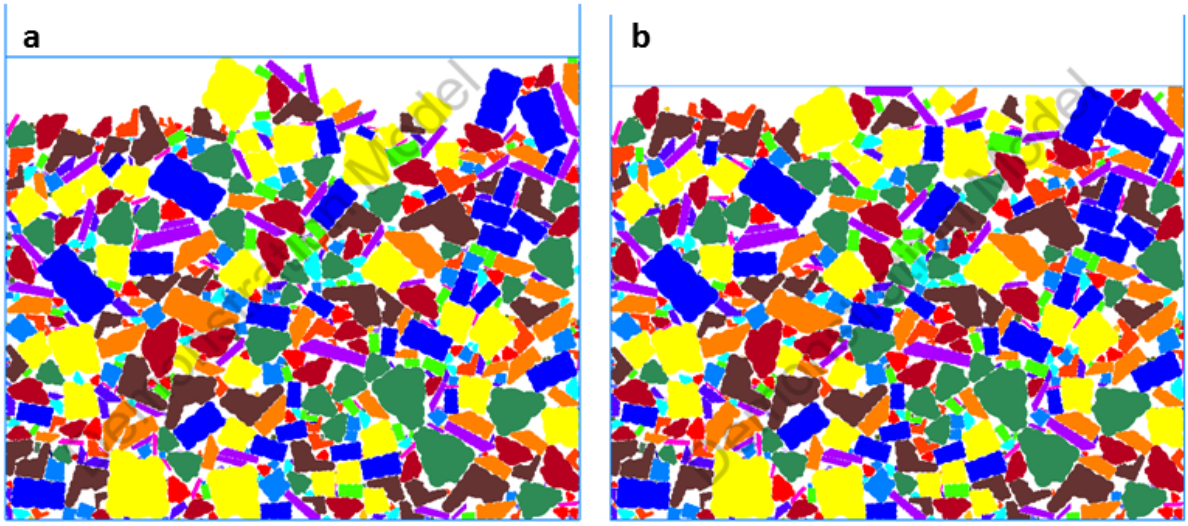

Fig. 7.9: Compaction state of the particle model after 30 drops (a) and after 480 drops (b).

As the next, the model with a mixture of 15 % of clay particles, 39 % of Band 8, 24 % of Band 6 and 25.7 % of Überkorn was created. In order to simulate the content of added-water, friction angle between particles was set smaller than friction angle between salt grains.

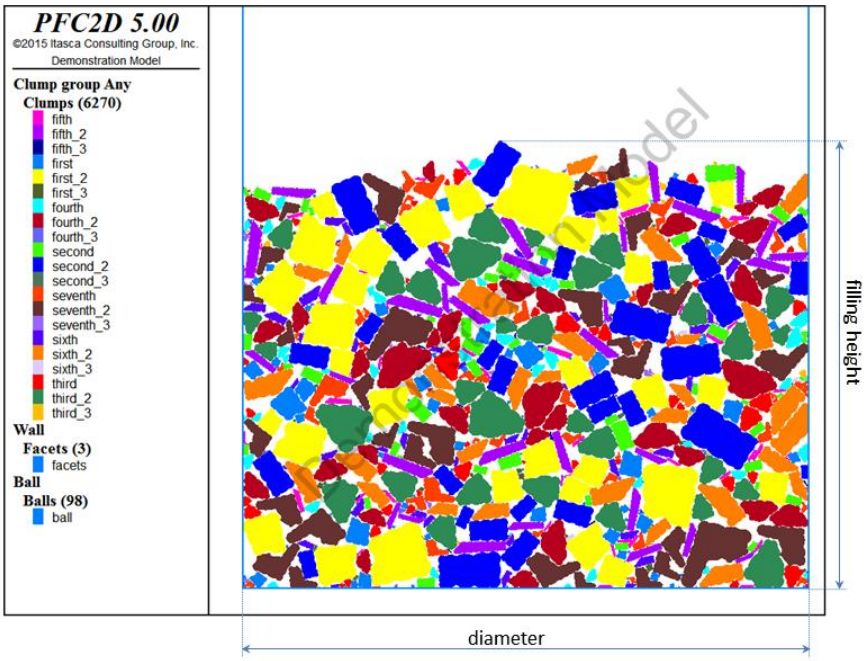

Fig. 7.10: Initial state of the particle model including a clay fraction. The mixture consists of 15 % of clay particles, 39 % of Band 8, 24 % of Band 6 and 25.7 % of Überkorn salt grains.

The same procedure of a pulse compaction has been repeated for this particle model. The states of the model after 45 and after 480 drops are presented in Fig. 7.11

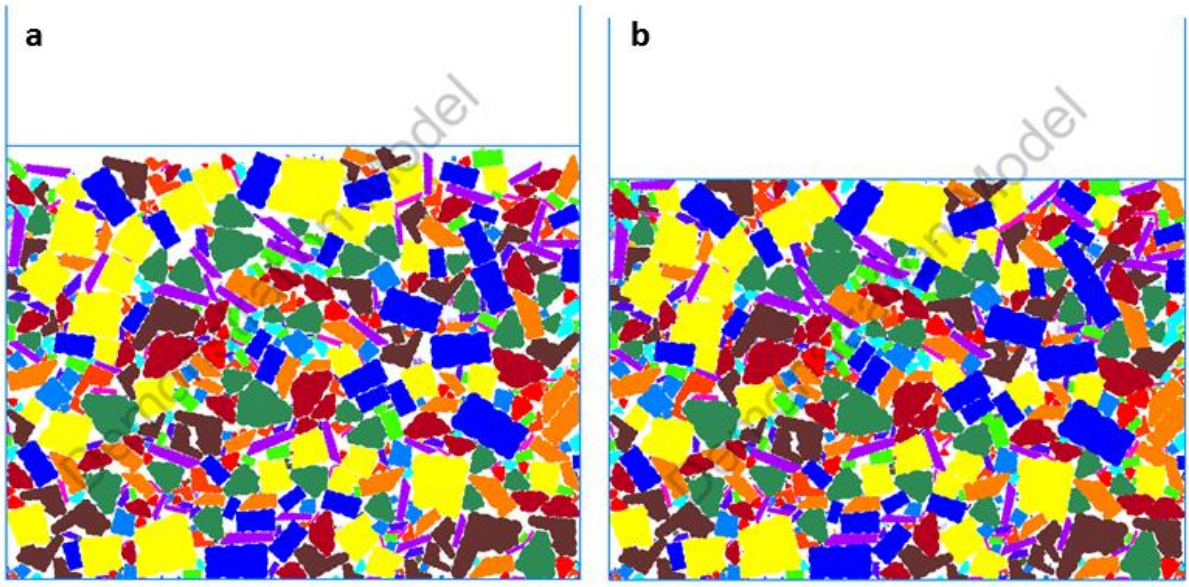

Fig. 7.11: Compaction state of the particle model after 45 drops (a) and after 480 drops (b).

To calibrate the results of modelling, the compaction energy applied on the samples was calculated as follows:

$$W = (Number\ of\ drops) \cdot \frac{m \cdot g \cdot H}{V} 10^{-6}\ [\mathrm{MJ/m^3}] \quad (1)$$

where m is the mass of the drop weight, H is the drop height and V is the volume of the mold, g is the gravity acceleration constant. Considering the volume of the mold

$$V = \pi \cdot \left(\frac{d}{2}\right)^2 \cdot h \quad (2)$$

(See Table 7.1) used in the laboratory tests, the compaction energy as a function of the number of drops results in:

$$W = (Number\ of\ drops) \cdot 0.03327\ [\mathrm{MJ/m^3}] \quad (3)$$

After each drop the total porosity in the particle model was calculated as follows:

$$Total\ porosity = 1 - \frac{V_{particles}}{V_{mold\_model}} \quad (4)$$

where V_{mold_model} was calculated as the multiplication of filling height which is changed after each drop, with the diameter of the mold, which equals to d. Since this is 2D modelling, the width of the mold equals to 1.

Examples of the simulation results achieved for pure crushed salt are plotted in Figure 7.12. Using a friction angle of 23.5°, which is a plausible value, a good fitting of the simulation results with the experimental results could be achieved.

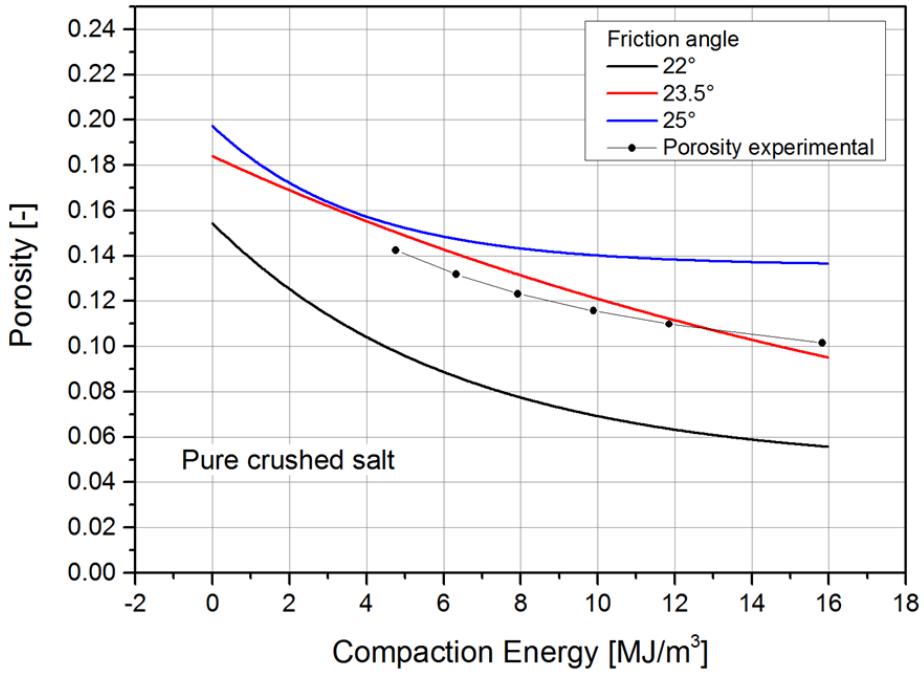

Fig. 7.12: Simulation results for pure crushed salt. Total porosity plotted as a function of compaction energy.

Examples of the simulation results achieved for mixtures of crushed salt and fine clay (10% and 15%) are plotted in Figure 7.13. The fitting is good but not as good as for pure crushed salt. Nevertheless, the fitting process was stopped here since the necessary calculation times are very high and thus very time consuming. It was assumed that after an additional fine tuning a better fit would be possible. It was agreed that for a further development emphasis should but put on a model that allows much reduced calculation times. To develop a tool for predicting the compaction behavior of these materials an extension to a 3D model, at least for a reference calculation, is necessary.

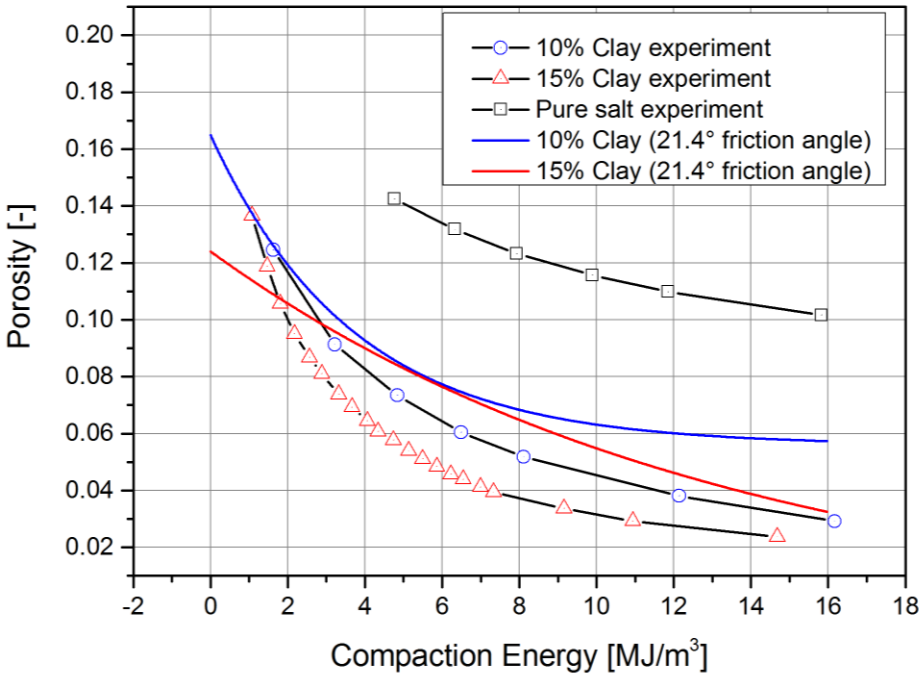

Fig. 7.13: Simulation results for pure crushed salt. Total porosity plotted as a function of compaction energy.

7.4 Summary and conclusions

The laboratory and in-situ investigations regarding the compaction of granular material to be used as sealing elements within shaft sealing concepts were accompanied by numerical simulations. Prior to any installation of an engineered barrier or its components the proper functioning and the integrity of the barrier components have to be proven to the authorities by means of a calculational proof which demonstrates that if the barrier is built as planned, the integrity of the barrier and thus it's proper functioning is assured. During DOPAS a 2D discrete element numerical model could be developed that allows the simulation of a compaction process of granular sealing materials. The modelling results are in sufficient agreement with laboratory data. A more fine-tuned fitting was not performed due to long calculation times. Further work will focus on the development of a model with reduced calculation times to allow for a 3D modelling.

The results of the modelling work performed during DOPAS will be used to improve the corresponding modelling capabilities with regard to specific constitutive laws for describing sealing material compaction. The results of the laboratory and in-situ investigations are a fundamental basis for the constitutive material laws which can be used within the calculational proofs for this specific purpose.

Finally, the developed model will be used to predict the compaction of the crushed salt and clay mixture planned to be performed during the large scale in-situ test during ELSA phase 3. The results of the 3D model and the large scale in-situ test will allow a determination of the uncertainties to be dealt with when performing the calculational proof for the authorities.

8 Process modelling of seal materials (GRS)

O. Czaikowski, K. Jantschik, H. C. Moog, C.-L. Zhang

For the last decade, GRS has used the FEM code CODE_BRIGHT (UPC 2015) for analysis of coupled thermo-hydro-mechanical (THM) processes in repositories in clay formations. This code was developed by the Technical University of Catalonia in Barcelona. The theories of the THM modelling are presented by the code developer (Olivella et al. 1994), (Gens et al. 1998), (Gens & Olivella 2006) and (UPC 2015). There are a large number of constitutive models implemented in the code for description of the THM behaviours of the geo-materials. For modelling and process analysis of a seal system, one has to identify which constitutive models are adequate for the individual elements of the seal system such as host rock, EDZ, clay-based seal, concrete plug, and others. The associated model parameters for the materials have to be determined from laboratory experiments. In order to enhance the predictive capability for the long-term performance of the seal system, it may be necessary to develop new constitutive equations for some specific aspects, for instance, long-term deformation of clay rock, permeability changes due to damage and reconsolidation, and so on. GRS defined main objectives of the modelling work in task 5.1 of the DOPAS project as follows:

- Identification of constitutive models and parameters for the studied seal materials
- Simulation of typical laboratory experiments for verification of the constitutive models currently available from the code;
- Scoping calculation of the long-term performance of a seal.

The process modelling work that has been done within the DOPAS WP5.1 is summarized in the following chapters. The sealing properties of the investigated clay seal materials are reported in chapter 8.1. Chapter 8.2 highlights the concrete sealing materials from a hydro-mechanical point of view and chapter 8.3 gives inside in the chemical corrosion processes.

8.1 Modelling of clay seal materials (THM-Ton)

8.1.1 THM coupling phenomena

Geological and geotechnical porous materials are composed of three species: mineral, water and air; and distributed as three phases: solid (*s*), liquid (*l*) and gas (*g*). The liquid phase contains liquid water and dissolved air, while the gas phase is a mixture of dry air and water vapour. In the porous media simultaneously subjected to thermal, hydraulic and mechanical conditions, complex THM processes and interactions take place as for instance,

- Thermal loading inducing deformation and stress variations (T → M) and expansion of porewater as well as pore pressure changes (T → H);
- Mechanical loading leading to changes in porosity / cracks and hydraulic conductivity (M → H) as well as thermal conductivity (M → T);

– Pore pressure changes being directly related with the effective stress (H → M), and water saturation as well as water/gas flow influencing the heat transfer and the temperature field (H → T).

According to (Gens & Olivella 2006), the important aspects of THM coupling are illustrated in Fig. 8.1.

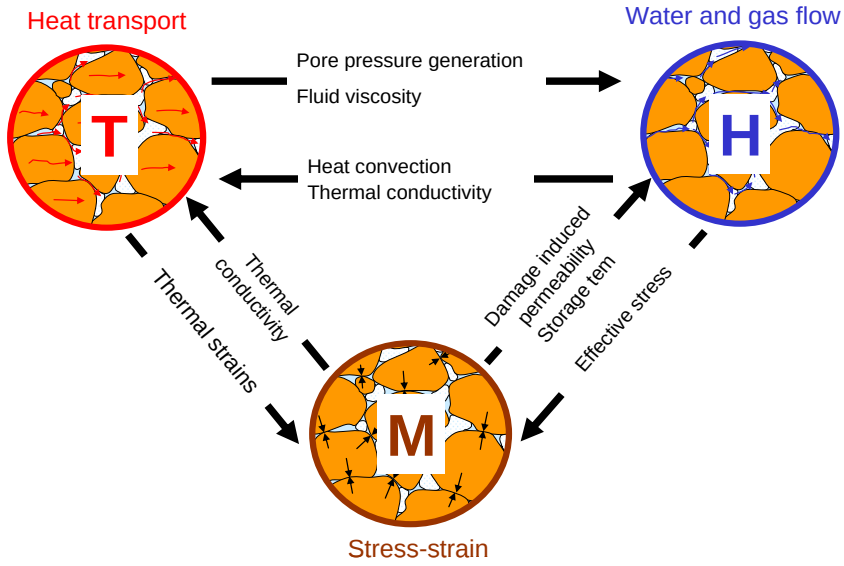

Fig. 8.1 Main relations between THM processes in porous media (Gens & Olivella 2006)

8.1.2 Water saturation

Three seal materials are selected for modelling and analysing the long-term performance of a drift seal (Zhang 2016): (1) the compacted bentonite (MX80) that has been extensively characterised as buffer/seal in HLW repositories in crystalline and clay rocks, for instance, by SKB / Clay Technology (Åkesson et al. 2010b), (Åkesson & Andersson 2013) with determined material parameters, (2) the compacted bentonite-sand mixture with a ratio of MX80/Sand = 70/30 that has being investigated by ANDRA for drift sealing in the COX (Callovo-Oxfordian) clay rock (de La Vaissiere et al. 2015) and (3) the compacted claystone-bentonite mixture with a ratio of COX/MX80 = 60/40 as a favourable alternative material for drift sealing in clay rock;

The water saturation tests on the compacted 70MX80+30Sand and 60COX+40MX80 mixtures as well as the COX claystone have been described in (Zhang 2016). Selected tests for compacted claystone-bentonite mixture are shown in this section. The initially unsaturated samples were placed in steel cylinders of 50 mm diameter and 100 mm length and wetted from an end face with the synthetic clay water at atmospheric pressure. The tests are modelled using CODE_BRIGHT (v3ß) as a coupled HM problem by an axisymmetric geometry with 100 elements as shown in Fig. 8.2.

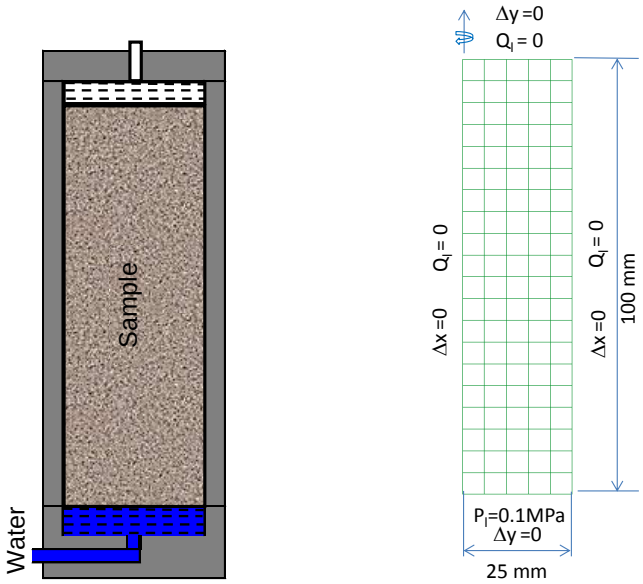

Fig. 8.2 Model geometry and boundary conditions for modelling the water saturation of the seal materials

The liquid pressure at the entre face is kept at atmospheric level, $P_l = 0.1$ MPa, and the atmospheric gas pressure is kept for the whole sample, $P_g = 0.1$ MPa. The other boundaries are isolated with zero fluid flow, $Q_l = 0$. The initial suction s_o is obtained from the water retention curve and the initial water saturation S_{lo} for each sample. The initial stresses are nearly zero: $\sigma_1 = \sigma_2 = \sigma_3 = 0.15$ MPa. A constant temperature maintains at 20 °C. As a result, the distribution of water saturation in the sample at the end of each saturation period is predicted.

Three water saturation tests on the 60COX+40MX80 mixture are simulated using the van Genuchten retention curve b and the modified model b for a dry density of 1.81 g/cm^3. The associated retention parameters, the other hydraulic parameters, and the initial properties of the tested samples are summarized in Table 8.1. The modelling results are illustrated in Fig. 8.3 with the measured distributions of water saturation in the samples at different time periods. The predictions using the van Genuchten retention curve (solid line) and the modified retention curve (dash line) are close to the measured data for sample 1 but slightly overestimate for the other two samples. The measured low degrees of water saturation in the water entre sides are probably caused by measurement errors.

Tab. 8.1 Hydraulic parameters of the claystone-bentonite mixture

Hydraulic parameters	ϕ_o = 0.304, k_o = 6x10^{-20} m^2, $k_{rl} = S_l^5$
van Genuchten model (1)	P_o = 0.1 MPa, β = 0.16
Modified model (2)	P_o = 0.03 MPa, β = 0.1, P_1 = 350 MPa, $\lambda = 1$
Sample-1 initial properties	ϕ_o = 0.345, S_{lo} = 30.0 %, $s_{o\text{-}1}$ = 400 MPa, $s_{o\text{-}2}$ = 87 MPa
Sample-2 initial properties	ϕ_o = 0.31, S_{lo} = 41.6 %, $s_{o\text{-}1}$ = 75 MPa, $s_{o\text{-}2}$ = 35 MPa
Sample-3 initial properties	ϕ_o = 0.30, S_{lo} = 44.4 %, $s_{o\text{-}1}$ = 50 MPa, $s_{o\text{-}2}$ = 22 MPa

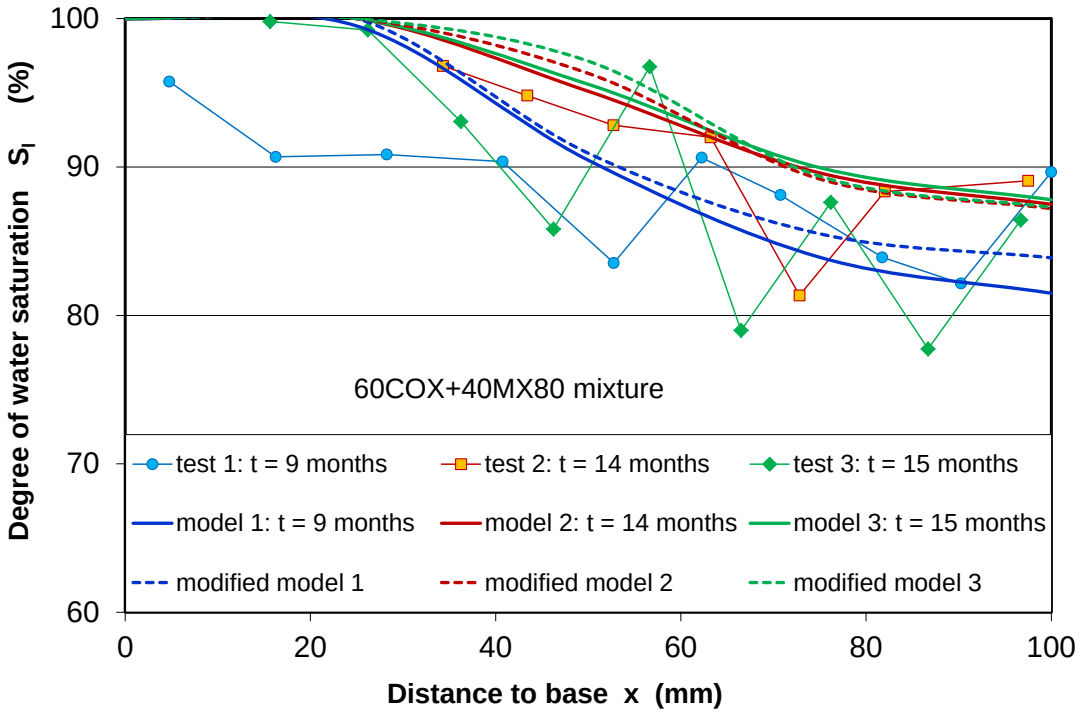

Fig. 8.3 Predictions of the water saturation in the claystone-bentonite mixture using the van Genuchten model (solid line) and the modified model (dash line)

8.1.3 Swelling pressure

The swelling pressure tests on the compacted bentonite-sand (70MX80+30Sand) and claystone-bentonite (60COX+40MX80) mixtures have been described in (Zhang 2016) and selected for modelling. The initial unsaturated samples in steel cells of 50 mm diameter and 30 mm height are modelled by an axisymmetric geometry with 50 elements, see Fig. 8.4. The initial properties of the mixtures are

– 70MX80+30Sand: ρ_d = 1.82 g/cm^3, ϕ = 34.0 %, w_o = 11.0 %, S_{lo} = 59.0 % g/cm^3
– 60COX+40MX80: ρ_d = 1.86 g/cm^3, ϕ = 32.0 %, w_o = 10.0 %, S_{lo} = 58.0 % g/cm^3

The samples are confined with the fixed boundaries. The liquid pressure at the bottom is kept at atmospheric level, $P_l = 0.1$ MPa, and the gas pressure is atmospheric, $P_g = 0.1$ MPa. The other boundaries are isolated with zero fluid flow, $Q_l = 0$. The low initial stresses are applied with $\sigma_1 = \sigma_2 = \sigma_3 = 0.11$ MPa. A constant temperature is kept at 20 °C.

The BBM model is adopted for the mechanical behaviour of the seal materials. The hydraulic models and parameters are adopted. The water retention curve and the curve b are adopted for 70MX80+30Sand and 60COX+40MX80 mixture, respectively. Both have been already used for modelling the water saturation tests. The initial suctions are obtained to be $s_o = 1.4$ MPa for 70MX80+ 30Sand and $s_o = 2$ MPa for 60COX+40MX80.

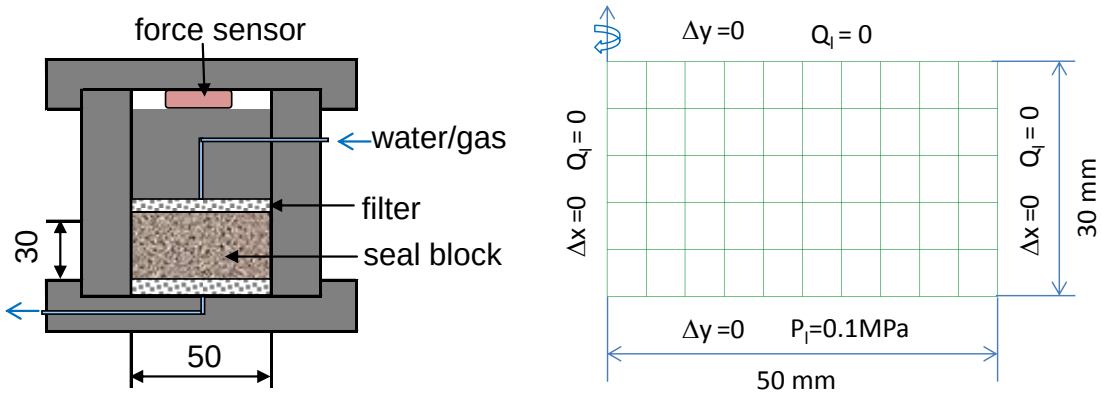

Fig. 8.4 Model geometry and boundary conditions for modelling the swelling pressure of the seal materials

Fig. 8.5 compares the modelled and measured evolution of swelling pressure for 70MX80+30Sand (a) and 60COX+40MX80 (b) mixture respectively. The sensitivity of the relative permeability parameter λ is examined using two values of λ = 5 for model A and λ = 3 for model B.

The calculated development of swelling pressure with λ = 3 (model B) is faster than using λ = 5. But the increased rates are still lower than the observations during the first stage. Obviously, the evolution of swelling pressure is directly related to the hydration process.

Even though the fluctuations of the swelling pressure could not be reflected, the maximum values are provided by the model: p_s = 5.6 MPa for the bentonite-sand mixture and p_s = 3.7 MPa for the claystone-bentonite mixture. Since the swelling pressures are much lower than those pre-consolidation pressures of 14 to 18 MPa, the seal materials remain in the elastic domain during hydration and the plastic parameters the plastic parameters do not play any role in the computation (Gens et al. 1998).

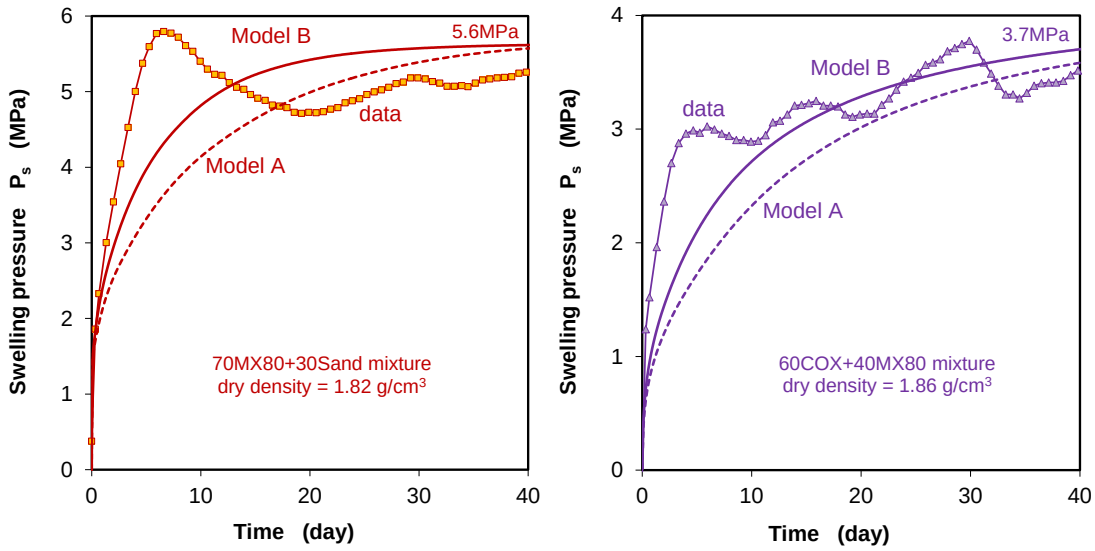

Fig. 8.5 Predictions of the swelling pressure developed in the compacted bentonite-sand (a) and claystone-bentonite (b) mixture during hydration

8.1.4 Conclusions

In order to enhance the predictive capability of numerical models for the long-term performance of the sealing systems in a repository, the existing constitutive models describing the hydro-mechanical behaviour of the sealing materials were verified and improved. New constitutive equations were formulated and the related parameters fitted to the laboratory observations. Based on the experimental results, the key parameters were determined for each sealing material. They were applied for numerical simulations of various laboratory experiments using the THM code CODE_BRIGHT.

First of all, adequate hydro-mechanical material models were established for the studied sealing materials, i.e. the compacted bentonite, bentonite-sand and claystone-bentonite mixtures. Model parameters were determined from the test data, including the porosity, permeability, water retention curve, the nonlinear elastic modulus, and others. Based on these parameters, the development of water saturation and swelling pressure in the seal materials was calculated.

The modelling provides a satisfactory agreement with the measured data. However, some uncertainty in the models and the parameters remains and has to be minimized through further investigations.

8.2 Modelling of concrete-based sealing materials (LASA)

The deformation behaviour of salt concrete was investigated by laboratory testing and numerical modelling (Czaikowski et al. 2016). In the laboratory different types of tests were carried out: Triaxial compression tests, uniaxial and triaxial creep tests. The tests were simulated using CODE_BRIGHT and the calculation results were compared to the laboratory results. The simulation of the triaxial tests aimed at the investigation of material changes between the sec-

ond and third stress level in the uniaxial tests. The results were useful because the onset of dilatancy could be pinpointed.

8.2.1 Long-term deformation behaviour

The result of the modelling of the uniaxial creep test by using different constitutive laws is shown in Fig. 8.6. Its development corresponds well to the development of stains of the laboratory test. Additional the individual deformation components are also shown in Fig. 8.6. If the calculation was executed only by HOOKE, there are only elastic deformations at the moment of increasing axial stress and no further deformations until the next increase of axial stress followed. Below HOOKE was combined with transient creep by using the viscoplasticity law with parameters analogue to phase 1. Now there are transient creep deformations in all stress levels. Strains increase fast in the beginning after increasing axial stress. Strain rates decrease gradually and consequently strains increase less with further interval to load increase. This phenomenon is clearly to see in phase 2.

In the next step dislocation creep law was used additionally to HOOKE and viscoplasticity law. The development in phase 1 is nearly identical to the calculation before. Stationary creep is of less importance in stress levels up to 10 MPa. In third stress level stationary creep becomes relevant. The curve increases and strains increase constant. This corresponds to the assumptions from laboratory results. The development of strain rates is shown in Fig. 8.7 versus axial strain. The figure shows the development of strain rates resulting from the individual deformations components correspondent to Fig. 8.6. If linear elastic and transient creep deformations were combined (using HOOKE and viscoplasticity law with parameters from phase 1), strain rates are high in the beginning after increasing axial stress and become smaller gradually.

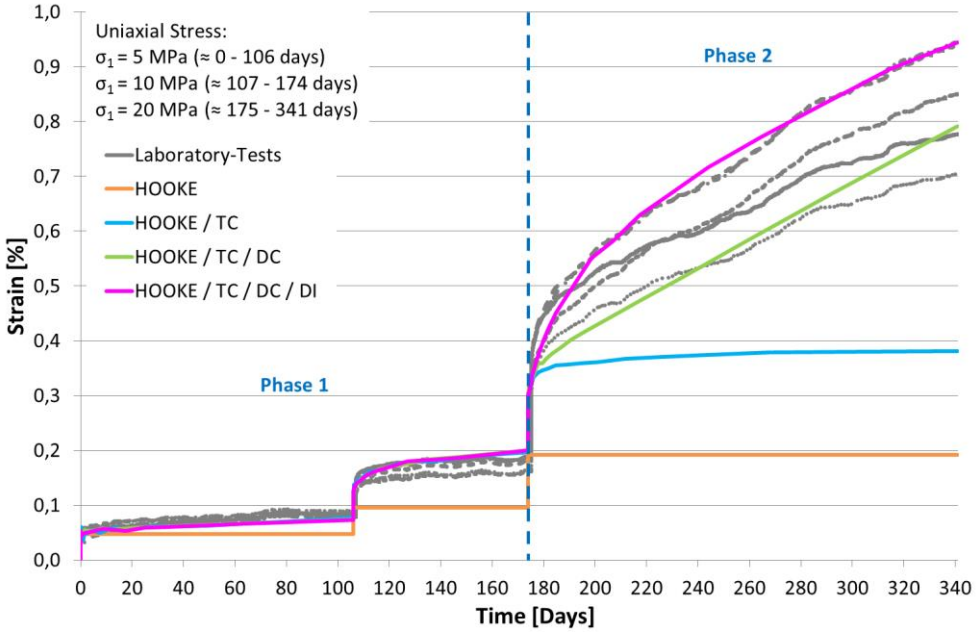

Fig. 8.6 Depiction of the deformation components, which results of the parameter variations before and the combination of adaptation in phase 1 and phase 2. Deformations consist of elastic deformations (HOOKE), transient creep (TC), dislocation creep (DC) and dilatancy (DI)

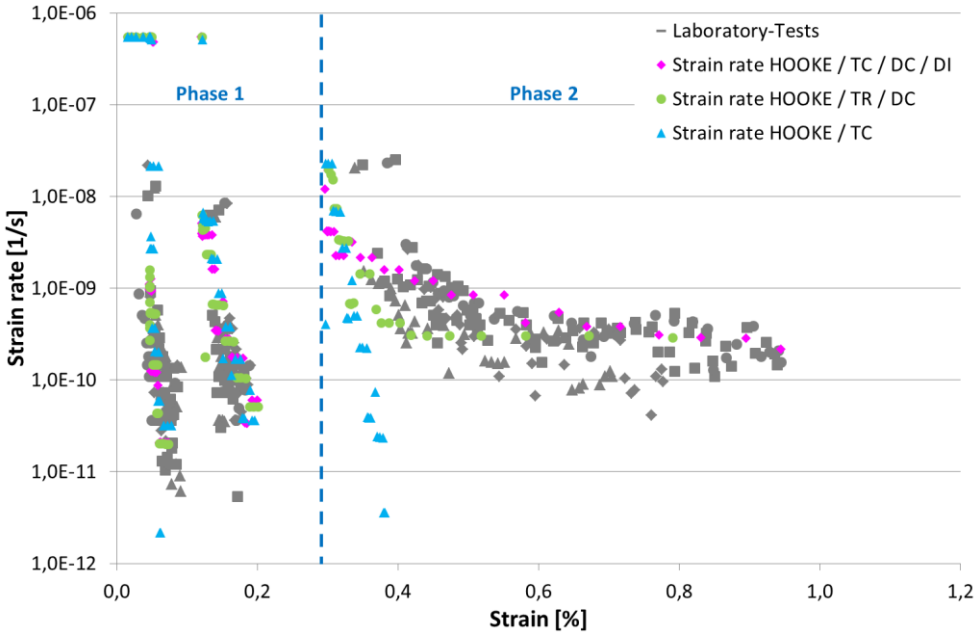

Fig. 8.7 Exercise UCc 5 - Comparison between strain rates versus axial strain of laboratory tests and calculation results

Two values of strain rate are clearly too small in the first stress level. Probably this might be a problem of iteration, because the curve in Fig. 8.6 has a small break at this moment. This deviation dissolves in further calculations by using more constitutive models. Generally strain rates are in the right range for phase 1.

In phase 2 strain rates are too small, because stationary creep and dilatancy were not considered yet. If dislocation creep law was used additionally to HOOKE and viscoplasticity law (with parameters for phase 1), the development of strain rates is similar as before in phase 1 in Fig. 8.7. The different steps of iteration can explain the small differences between the calculated strain rates. The deviation of strain rates in the first stress level from calculation before was extinct, which supports the assumption, that the process of iteration can explain the aberrations. Hence, stationary creep has less influence to phase 1. In phase 2 strain rates show a different development versus the calculation without dislocation creep law. Figure 8.7 shows that strain rates are higher than before. They adapted much better to the laboratory results. Only in the beginning they decrease to fast, probably.

Finally strain rates by using dislocation creep law, HOOKE and viscoplasticity law with combined parameters for phase 1 and phase 2 were considered. Strain rates are in a good range for second and third stress level in both figures. Strain rates decrease more slowly in phase 2 because of the shear thickening material behavior. In the first stress level strains are a little bit too small in the second part (Fig. 8.7) as expected from consideration of Fig. 8.6. The depiction of strain rates versus strains shows, that strains develop rarely at a stress level of 5 MPa and become higher in the second stress level. A clear development of strains is shown in third stress level. This development corresponds to the laboratory results. So the consideration of the development of strain rates supports, that the time dependent deformation behavior of salt concrete is well simulated by using HOOKE, dislocation creep law and viscoplasticity law with individual parameters for phase 1 and phase 2.

8.2.2 Modelling of concrete-based sealing materials – porosity-permeability relationship

The porosity-permeability relationships examined in the present study are the same as examined in (Wieczorek et al. 2010) for rock salt. As there is no relationship which has been developed specifically for salt concrete, basic porosity-permeability relationships and models considering fracture development were used here. During laboratory measurement, the development of porosity could not be tracked, so volumetric strain is used as a proxy for porosity here. This is applicable in so far, as volumetric extension represents the increase in porosity and there is no other extending mechanism present. The porosity-permeability relations examined here are:

1. A Kozeny-type function:

$$k = k_0 \left(\frac{V}{V_0}\right)^n \tag{8.1}$$

with

$k_0 = 5e^{-19}$ and $V_0 = 0.07697\ m^2$ and $n = 8$.

2. A micro fracture model after Olivella & Alonso (2008) with spacing of fractures and variable aperture as a function of volumetric strain:

$$k = k_{matrix} + \frac{b^3}{12s} \qquad b = b_0 + \Delta b \qquad \Delta b = s(\varepsilon - \varepsilon_0) \tag{8.2}$$

with $k_{matrix} = 1e^{-20}$; $b_0 = 3e^{-13} - 1e^{-10}$; $s = 5e^{-8} - 1e^{-7}$;

ε_0 = volumetric strain at onset of gas flow

The threshold parameter ε_0 is associated with failure of the sample, which in this case is defined as the point, when microcracks connect to enable gas flow.

3. A percolation model for rock salt in the EDZ, modified from Alkan (2009):

$$k = k_f \cdot A \cdot \left[\left(1 - e^{\left(\frac{V}{V_p}\right)}\right) - 0.63\right]^2 \qquad V_p = V_0 \cdot (1 + \varepsilon_p) \tag{8.1}$$

k_f = maximum measured permeability $\qquad A = 35 \qquad V_0 = 0.07697\ m^2$

The parameter V_p (percolation threshold) defines at which volumetric increase, flow starts. The k_f value is inserted for each sample individually.

Permeabilities for these relationships were calculated from volumetric deformations measured in triaxial compression tests and compared with permeabilities obtained from those tests. Fig. 8.8 shows the results for different permeability-relationships, compared with laboratory data. With the exception of B4KK3 P2, samples follow a trend, that with increasing confining stress, the onset of gas flux is at higher volumetric strains, while initial permeability is lower. This coincides well with the assumption, that increasing confining stress inhibits evolution of micro cracks and delays gas flow. As already delineated in (Wieczorek et al. 2010), the Kozeny-type function yields poor results and is not able to describe the development of permeability. This is confirmed by the results of the Kozeny-Carman equation for sample B4KK4 P13.

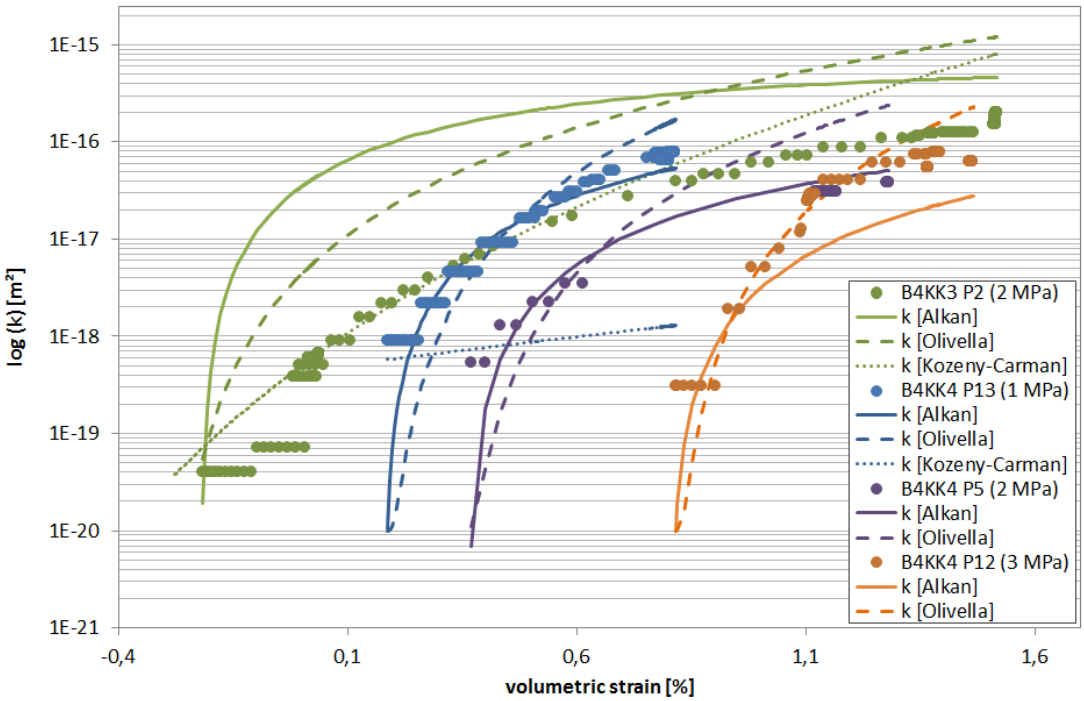

Fig. 8.8 Permeability as a function of volumetric strain. Laboratory data for confining pressures of 1-3 MPa are compared with calculated permeabilities

At first sight, both the percolation model after (Alkan 2009) and the micro fracture model after (Olivella & Alonso 2008) appear as a good approximation. However it was not possible to describe the porosity-permeability relation with one parameter set, using Olivella's model. Instead, parameters for obtaining the curves in Fig. 8.8 have to be varied several orders of magnitude. On the other hand, describing the porosity-permeability relation with the Alkan model is possible without changing the parameters. For samples B4KK4 P13 and B4KK4 P12, Alkan's percolation model underestimates permeability at high volumetric strains. This is due to Alkan's model strongly depending on the maximum measured permeability. If deformation of those samples continued, the maximum measured permeability would be higher and hence, permeability at high volumetric strains would not be underestimated.

Figure 8.9 shows the development of permeability for the multi-stage triaxial test. Parameters for the percolation model after Alkan are unchanged from the previous TC-tests, whereas parameters for fitting the Olivella model had to be significantly changed ($b_0 = 2e^{-6}$; $a = 3e^{-4}$).

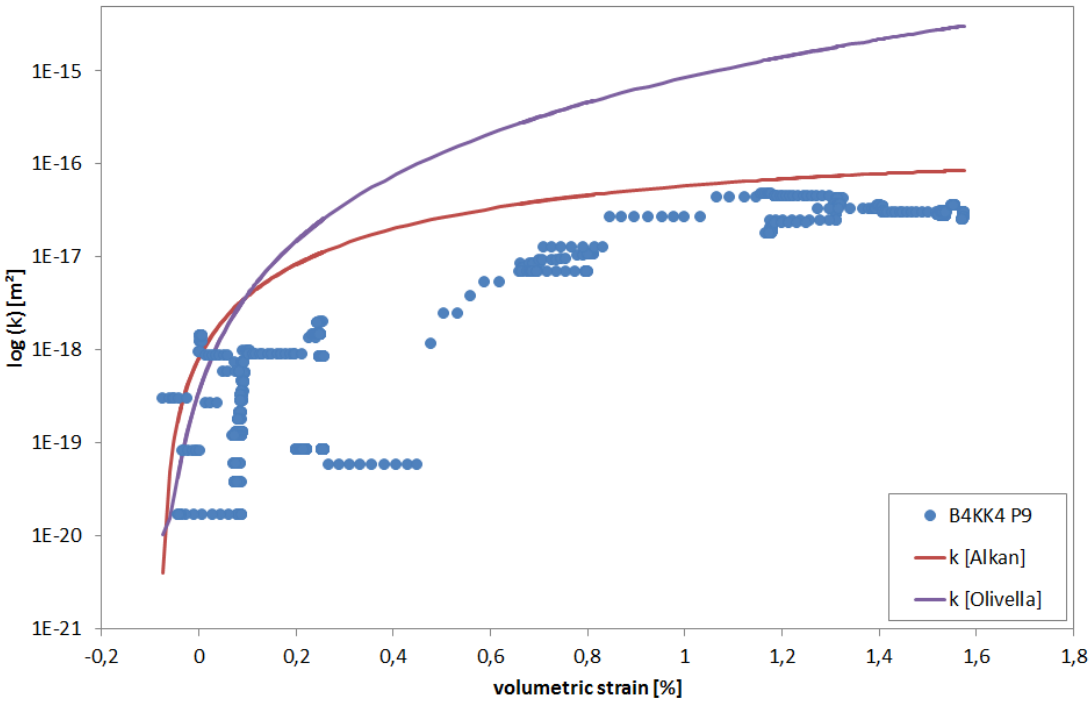

Fig. 8.9 Development of permeability for the multi-stage triaxial test

Inhomogeneity in permeability increase of laboratory data is due to the un- and reloading between each increase in confining pressure. Olivella's model clearly overestimates permeability at high volumetric strain. The percolation model after Alkan slightly overestimates permeability at low volumetric strain but nicely fits with laboratory data at higher volumetric strain. The fact, that Alkan's model was able to predict the evolution of permeability of the multi stage triaxial test from the parameter set obtained on triaxial tests creates confidence in its applicability. Although Olivella's model is more conservative, the parameter combination has to be calibrated for each test individually, which makes prediction of permeability impossible. Therefore, Alkan's model, which also more accurately describes the relationship between permeability and volumetric extension, is chosen here for further investigation of salt concrete (Czaikowski et al. 2016).

8.2.3 Conclusions

In all the simulations, the onset of dilatancy occurred before the load limit was reached. The perceptions of the uniaxial tests in combination with the results of the triaxial tests showed that the material behaviour of salt concrete at an axial stress up to 10 MPa is different from the material behaviour at 20 MPa. Strains and strain rates clearly increase at higher stresses. The simulations showed that an adaptation to laboratory results was only possible if two different sets of parameters were used at the lower stress level (phase 1) and the higher stress level (phase 2). The main problem of simulating the deformation behaviour of salt concrete is the description of the viscoplastic (transient creep) material behaviour. Elastic deformations and stationary creep can be adapted by the available material properties. For a better description of transient material behaviour a constitutive model should be adapted or developed.

It has been shown, that Alkan's model fits very well with laboratory data. However the major drawbacks are: (1) that the maximum measured permeability (ultimate connectivity) has to be inserted individually for each sample and (2) that the onset of gas flow has to be defined for each sample individually. In the present study, it was not possible to define a percolation threshold or ultimate conductivity for a specific state of confining stress due to the limited amount of measurements. As a consequence of the heterogeneity of salt concrete, it remains questionable, if a specific percolation threshold can be defined at all.

The constitutive models used here allowed only mathematical adaptation. Salt concrete consists of the cement matrix and the grains of salt concrete. This structure and its changes could not really be considered yet. If the structure of salt concrete could be considered in detail, the description of the deformation behaviour at different stress levels would become easier and clearer (Czaikowski et al. 2016). Further investigations and developments in this direction are necessary.

8.3 Modelling of concrete-based sealing materials (LAVA)

8.3.1 Chemical corrosion mechanisms

In general, the chemical corrosion mechanisms in salt concrete are the same for the diffusive and advective reactive transport process (Jantschik et al. 2016). A model for the diffusive and advective corrosion processes of salt concrete in contact with the corrosive Mg-, SO_4- and Cl-rich brine are shown schematically in Fig. 8.10. The left part of the figure shows the diffusion controlled corrosion process in the undisturbed concrete matrix. On the right the corrosion on cracks is illustrated.

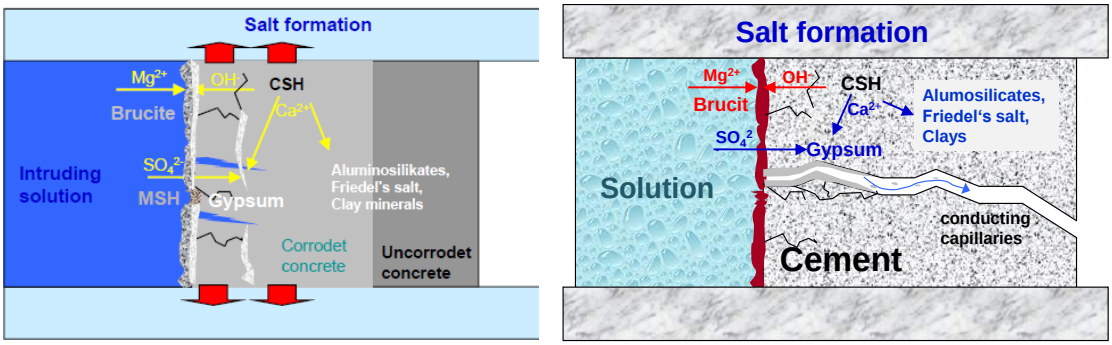

Fig. 8.10 Schematic representation of the chemical corrosion processes in salt concrete due to the interaction with Mg-, SO4- and Cl-rich salt solutions (left) diffusive matrix corrosion, (right) advective matrix corrosion on cracks (in (Hagemann & Meyer 2003) modified after (Bonen 1992))

If a Mg- and SO_4-rich salt solution attacks salt concrete first brucite ($Mg(OH)_2$) will be formed at the surface of the cement structure. This leads to a mass flux of OH^- from the matrix towards the exterior of the structure and to a SO_4^{2-} flux from the intruding solution into the matrix. Due to the depletion of OH^- ions in the concrete CSH phases will be dissolved. The released Ca^{2+} reacts with the SO_4^{2-} to precipitate as gypsum (Fig. 8.10). The crystalliza-

tion pressure of the newly built phases can lead to the formation of cracks in the material structure.

After the portlandite ($Ca(OH)_2$) from the concrete matrix is exhausted the pore fluids are not buffered anymore and the pH decreases from about 13 to 9. The CSH (Calcium-Silikate-Hydrate) phases in the concrete matrix become instable and will gradually disappear (Fig. 8.10 corroded part).

If the diffusion velocity of the OH^- from the concrete body towards the surface of the structure is lower than the formation of brucite, Mg enters into the matrix and can lead there to the formation of high amounts of MSH phases. If the fluid pressure at the exterior of the sealing structure is high enough and if the pores in the concrete are interlinked and conductible the corrosive brine can enter far into the structure and lead to an accelerated corrosion. The Mg content in solution decreases continuously until Mg is consumed. The chemical processes have been observed in many experiments with cemented materials (Skalny et al. 2002) and could be reproduced by geochemical modelling for the system salt concrete in contact to different brines (Meyer & Herbert 1999), (Meyer et al. 2002), (Meyer et al. 2003), (Meyer et al. 2003a), (Meyer & Herbert 2003), (Meyer 2004).

8.3.2 Batch experiments

In this section calculation results and results of batch-experiments are compared. Therefore batch-experiments in the system salt concrete / Mg-rich solution is considered. The batch-experiments were executed with a solid-solution-ratio of 0,3. Hence results are compared on basis of this proportion.

Fig. 8.11 and Fig. 8.12 show comparison of calculation and experimental results in the system salt concrete/Mg-rich-solution. The Mg-content in solution decreases continuously which correspondents to observations in batch-experiments. Certainly Mg-concentrations in batch-experiments are clearly smaller than of calculations at a solid-solutions ratio of 0,3. Calculated and experimental determined values of Ca- and K-concentrations fit much better although K-concentration is a little small and Ca-concentration a little too big. Against laboratory results Ca-concentration first increases if a solid-solution-ratio greater than 0,3 has been reached. Laboratory tests show an increase of Ca-concentrations nearly direct.

Development of sulfate-concentrations (concentration reduces) corresponds to laboratory results although concentration of calculated sulfate content is nearly three times higher than in batch-experiments.

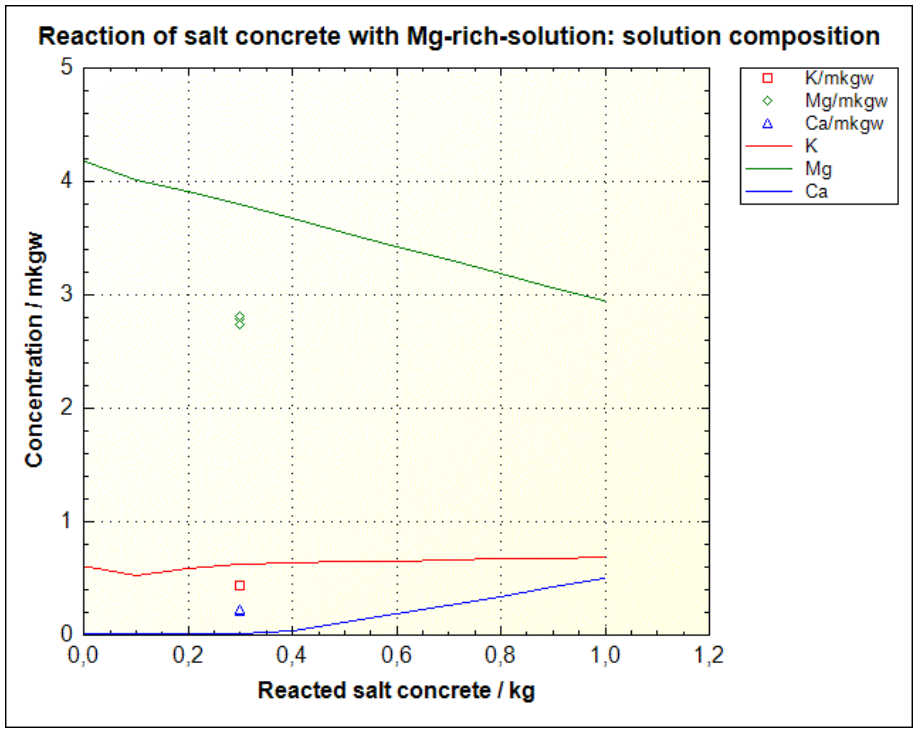

Fig. 8.11 Comparison of calculated K-, Mg- and Ca-concentrations in the system salt concrete/ Mg-rich-solution with experimental data of batch-experiments

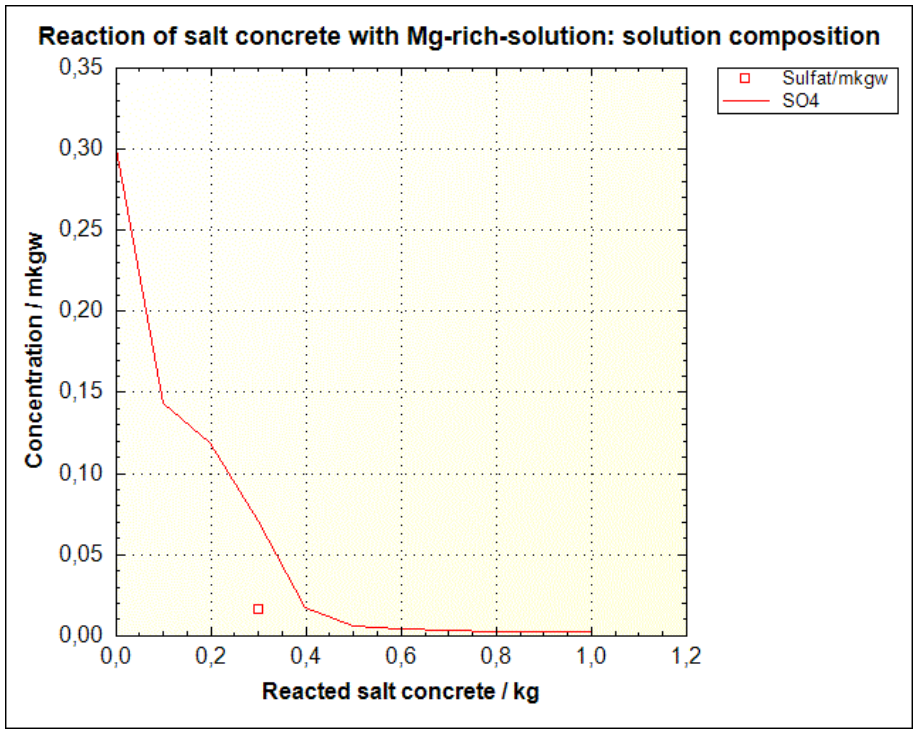

Fig. 8.12 Comparison of calculated sulfate-concentration in the system salt concrete/ Mg-rich-solution with experimental data of batch-experiments

8.3.3 Velocity of the degradation of concrete barrier

Salt concrete or sorel concrete is conceptualized as consisting of two domains: one domain represents fissures or cracks – pores essentially – featuring higher porosity, thus higher permeability. The second domain represents intact regions within the concrete matrix. Aqueous solution can still penetrate these regions, but the exchange of matter between both domains is retarded. The rate of exchange of matter between both domains is governed by the diffusional velocity within the second domain and its active surface with the first domain.

In the second domain solid phases may dissolve and precipitate. These processes may be (and probably are in reality) subject to kinetic restrictions. They lead to a net-volume change which lets the second domain in relation on the first domain swell or shrink. If the overall volume of solid phases in the second domain increases, the volume of the first one decreases accordingly, thus the overall permeability of the concrete.

Still lacking reliable kinetic data, a prototype model has been designed. As a first approximation granules representing the second domain may be visualized of spherical in shape with a radius of r = 0.01m. The diffusion coefficient within the granules is estimated at $D_e = 3 \cdot 10^{-10}$ m^2/s. The overall porosity of the first domain is approximated to be 0.3, the second 0.1 (Parkhurst & Appelo 1999). As a further simplification the net volume change in the second domain does not exert yet an influence on the total volume of the first domain.

This conceptual model should hold for both salt concrete and sorel concrete. It has been run for the more complicated case where IP21-solution reacts with salt concrete. The result is shown in the following fig. 8.13.

After altogether 20 pore volumes degradation of the concrete is most pronounced within the first 10 cm (at the very left of the diagram. Al- and Si concentration is controlled by Gibbsite, Hydrotalcite, and Kerolite. The precipitation of Halite and Polyhalite is also indicated, adding to the overall volume of the second domain. On the right hand side we still see largely unreacted concrete, Si- and Al-concentrations still featuring those values which representing thermodynamic equilibrium between salt concrete and NaCl-solution.

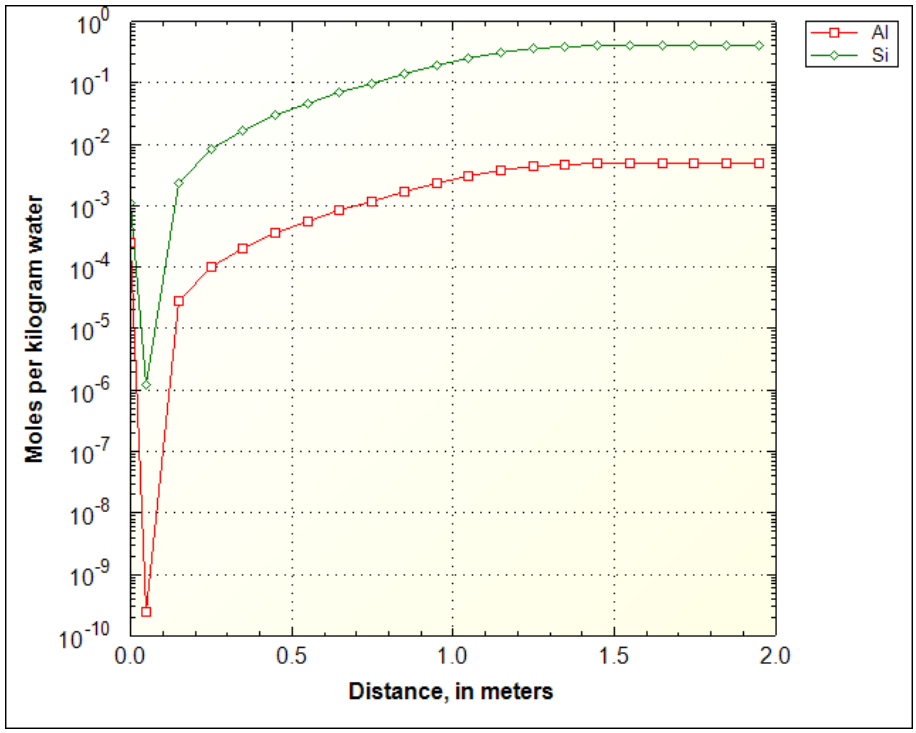

Fig. 8.13 Si- and Al-concentrations in an idealized dual-pore column of salt concrete of 2 m length

This concept thus seems promising but still needs refinement. For example, mineral densities must be included in the calculation. The effective volume of low-permeable granules need to be supported, using e. g. microscopic methods.

8.3.4 Conclusions

In general calculations correspond in development of concentrations with laboratory results. Indeed calculations show development of concentrations versus mass of reacted concrete while batch-experiments investigate development of solution composition versus time. Hence a comparison could only be given up to solid-solution-ratio of 0.3 and calculation does not consider development of solution composition versus time. Results from cascade-experiments need to be awaited for a better comparison between calculation and laboratory results. On basis of cascade-experiments the chemical reaction path between concrete and solution until equilibrium between powdered concrete and solution is reached can be determined similar to executed calculations.

Further aspect to be considered is the adaption of thermodynamic database to calculations with saline solutions. In doing this a better agreement of modelling results with laboratory data probably could be achieved.

9 Improvement of plug related processes representation in the integrated performance assessment code LOPOS (GRS)

A. Rübel, D. Buhmann, J. Kindlein, T. Lauke

The work performed by GRS in DOPAS is mainly related to the R&D on Plugging & Sealing for repositories in salt. The work is of fundamental importance for the salt option which represents one of the three European repository options in addition to the clay and the crystalline options. The concepts used for development and testing in the following are based on results obtained in the German research project Preliminary Safety Analysis for Gorleben (VSG) and precedent research projects. The work presented here, is related to the long-term safety assessment work performed by GRS in DOPAS, also presented in more detail in the DOPAS deliverable D5.8 (Rübel et al. 2016).

9.1 Context

In rock salt, the long-time separation of the radioactive waste from the biosphere is done by the salt. This is on the one hand the undisturbed part of the salt host rock formation and on the other hand the crushed salt, which is used to backfill the mine openings in the emplacement areas and galleries. The crushed salt backfill is compacted over time and achieves a sufficiently high hydraulic resistance to avoid entries of brines into the emplacement areas of the repository. Plugs and seals must provide their sealing function during the early post closure phase, until the compaction of the backfill is adequate and the permeability of the backfill is sufficiently low. At a certain stage, backfill and host rock both have a permeability in the same order of magnitude. The research during the VSG shows that in this case the process is finished after a few thousands of years, at most. The functionality of the shaft seal is designed to last until the next ice age, which is expected to occur in 50,000 years. After the ice age, hydro-geologic and topographic conditions change dramatically and a prediction of the chemical composition of inflowing waters is of high uncertainty, which makes it impossible to design robust seals against those chemical conditions. During the late post closure phase, after the ice age, the main sealing function is achieved by the host rock and the compacted backfill.

9.2 Aim of performed work

As part of the work presented, it was aimed to further develop the integrated model for safety assessments LOPOS (Loop structures in repositories) to better simulate the brine inflow through the shaft sealing. The development should include the effects studied in the experimental and related process level modelling work that was performed in WP3 and also WP5 of DOPAS.

Two effects are to be considered in more detail in DOPAS, making the permeability a function of time *t*. The first one is the existence of an excavation disturbed zone (EDZ). The EDZ develops around excavations during the construction of the mine due to stress release. Most of the EDZ around sealing locations is removed by means of mining technique before sealing construction. However, part of the EDZ often cannot be removed or is quickly redeveloping

during the time between EDZ removal and sealing construction. This disturbed zone around the drift section where the sealing is constructed has an increased permeability and extends up to several tens of centimetres into the rock.

The second process to be considered is the degradation of the sealing material by corroding fluids flowing through the sealing. In most cases, the sealing material is not in chemical equilibrium with the inflowing brine. This is the case, for instance, when using MgCl-based concrete material for a sealing which is flown through by a sodium chlorine brine (or a NaCl-based concrete material which is flown through by a magnesium chlorine solution) resulting in a dissolution of minerals and precipitation of others. The permeability of the corroded material is typically higher than the initially used material. Due to the low permeability of the sealing, the corrosion process occurs within a sharp corrosion front slowly progressing through the sealing.

9.3 EDZ evolution

Excavation disturbed zones (EDZs) in rock salt develop in the vicinity of cavities during and after excavation. The highly inhomogeneous stress state around a cavity leads to dilatancy, i.e., an inelastic increase in volume (and thus pore space) by microfracturing, and thus to a potential increase in permeability.

The temporal evolution of the EDZ-permeability during the progression towards a homogenous stress state and the healing of the EDZ can be described by a function derived from existing experimental or process level modelling work. Since no admitted function is currently available describing the actual process, empirical parameter functions are used that are fitted to process level model results which are again using experimental data.

9.4 Corrosion of salt concrete

Salt concretes are considered as material for sealing elements like sealing element two and three of the concept regarded in the preliminary safety analysis for Gorleben (see also figure 7.1). Crushed salt replaces sand and gravel as additive in salt concretes, which are used only in a salt environment. These materials consist mainly of cement, crushed salt and fly ash. In case of brine intrusion into the repository, the sealing elements made of salt concrete may be affected by significant changes regarding their mineralogy, their chemical composition as well as their hydraulic and mechanical properties. The changes are due to dissolution and precipitation reactions, inducing changes in brine composition and pH-value.

The extent of the concrete corrosion due to the reaction with saline solutions can be estimated by experiments and geochemical modelling and is to be considered in long-term safety assessment. The corrosion capacity $\kappa_{L,M}$ of a brine solution is defined by the mass of concrete M_c which is affected by corrosion by the volume V_B of brine.

9.5 Mathematical model

The detail of the representation of sealings in integrated performance assessments differs in the different national programmes. The long-term safety assessments for high-level waste in salt in Germany so far used approaches regarding the sealings as quasi homogenous elements. In this approach, the fluid flow through sealings is calculated by using an averaged permeability value over the whole cross-section of the sealing including a potential EDZ. The permeability value is constant in time and conservative values are used to regard for special process like the EDZ or material alterations with time. More severe changes in permeability are taken into account by changing the permeability stepwise in time. This approach has also been used in the simulations for the VSG (Larue et al. 2013). This chapter describes a mathematical model to overcome the limitations of the use of averaged permeabilities in integrated safety assessment and by this reduce conservatisms in the simulations.

The total resistance of the sealing can be calculated at each point in time from the fractional resistances of the individual compartments. It has to be noted, however, that due to the dependence of the resistance from the viscosity of the fluid, the resistance of a compartment might change over time just due to changes in fluid composition.

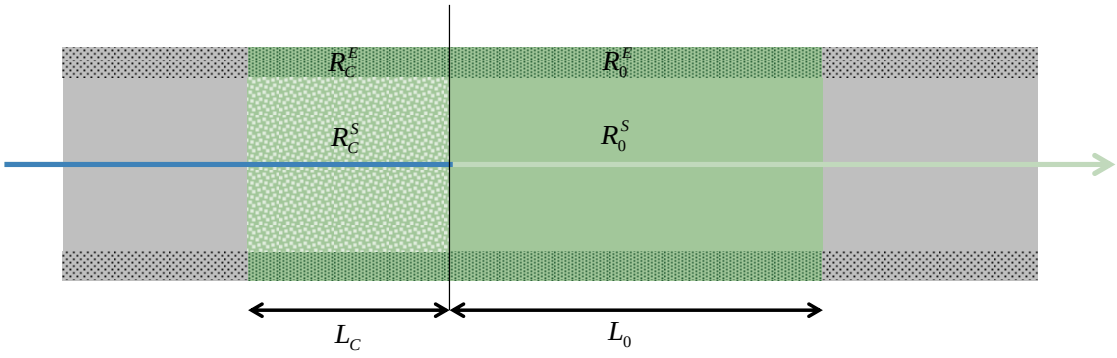

Fig. 9.1: Resistances of the sealing compartments

For each point in time, each of the compartments is characterized by a porosity ϕ, a density ρ, a brine viscosity μ and a permeability k. A lower index C denotes for the corroded region, while the lower index 0 denotes for the region still unaffected by corrosion. The upper index S refers to the sealing material, while the upper index E refers to the EDZ properties.

The total resistance of the entire sealing can be calculated from

$$R = R_C + R_0 = \frac{R_C^E R_C^S}{R_C^E + R_C^S} + \frac{R_0^E R_0^S}{R_0^E + R_0^S} = \frac{R_C^E R_C^S \left(R_0^E + R_0^S\right) + R_0^E R_0^S \left(R_C^E + R_C^S\right)}{\left(R_C^E + R_C^S\right) \cdot \left(R_0^E + R_0^S\right)}$$

with

$$R_0^S = \frac{\mu_C L_0}{A^S k_0^S},\ R_0^E = \frac{\mu_C L_0}{A^E k_0^E},\ R_C^S = \frac{\mu_0 L_C}{A^S k_C^S},\ R_C^E = \frac{\mu_0 L_C}{A^E k_C^E}.$$

9.6 Illustrative calculation

The influences on a sealing element of the two processes EDZ-closure and cement corrosion are illustrated by an exemplary calculation in the following. The time dependent fluid flow is explicitly calculated by spreadsheet analysis according to the Darcy Law under the assumption of a constant pressure head at the sealing front face.

A sealing of 30 m in length is regarded with an initial permeability of the sealing core made from salt concrete material of $5 \cdot 10^{-19}$ m^2. The EDZ around the sealing extends 1 m into the rock and has an initial permeability of $4.5 \cdot 10^{-17}$ m^2. The EDZ behaviour with time and the cement behaviour under brine corrosion are considered in the way as discussed in the preceding chapters. The inflowing brine has a hydraulic pressure of 10 Pa, which is close to the fluid pressure expected on the emplacement level of the Gorleben mine. To simplify this example, a constant depth was assumed for the whole sealing length, what corresponds to a drift sealing rather than a shaft sealing. All parameters used for the example calculation are given in table 9.1.

Tab. 9.1: Example calculation parameters

Parameter	Value
Length of the sealing [m]	30
Diameter of the sealing [m]	7
Hydraulic pressure at sealing [MPa]	10
Viscosity of brine μ [Pa s]	$5.3 \cdot 10^{-3}$
Porosity of salt concrete material ϕ [-]	0.2
Initial permeability of salt concrete material k_0^S [m^2]	$5 \cdot 10^{-19}$
Factor of permeability increase of corroded material [-]	1 000
Corrosion capacity of the brine $\kappa_{L,V}$ [l/l]	1
Extension of the EDZ [m]	1
EDZ initial permability k_0 [m^2]	$4.5 \cdot 10^{-17}$
EDZ long-term permeability k_∞ [m^2]	$1.6 \cdot 10^{-19}$
EDZ fitting parameter a [-]	0.4
EDZ fitting parameter b [-]	0.35

The results of the simulation are shown in figure 9.2 which shows the hydraulic resistance of the sealing. The black solid line denotes the resulting effective resistance across the entire cross section of the sealing, while the dashed lines distinguish between the concrete core of the sealing and the EDZ in the host rock around the sealing. At the beginning, the hydraulic resistance of the sealing is dominated by the comparatively low resistance of the EDZ. The EDZ is than recompacting with time and the resistance of the EDZ is increasing during the

first 300 to 400 years by one order of magnitude. After about 500 years, the hydraulic resistance of the EDZ exceeds those of the sealing core, which dominates the resistance of the sealing thereafter. The hydraulic resistance of the sealing concrete core is nearly constant for nearly one thousand years. After one thousand years, the resistance is slowly decreasing due to the progressing corrosion process, but does not change more than a factor of two until about ten thousand years. After about 13 000 years, the hydraulic resistance is rapidly decreasing and reaches its minimum value after about 15 300 years. After this time, the cement sealing material is fully corroded.

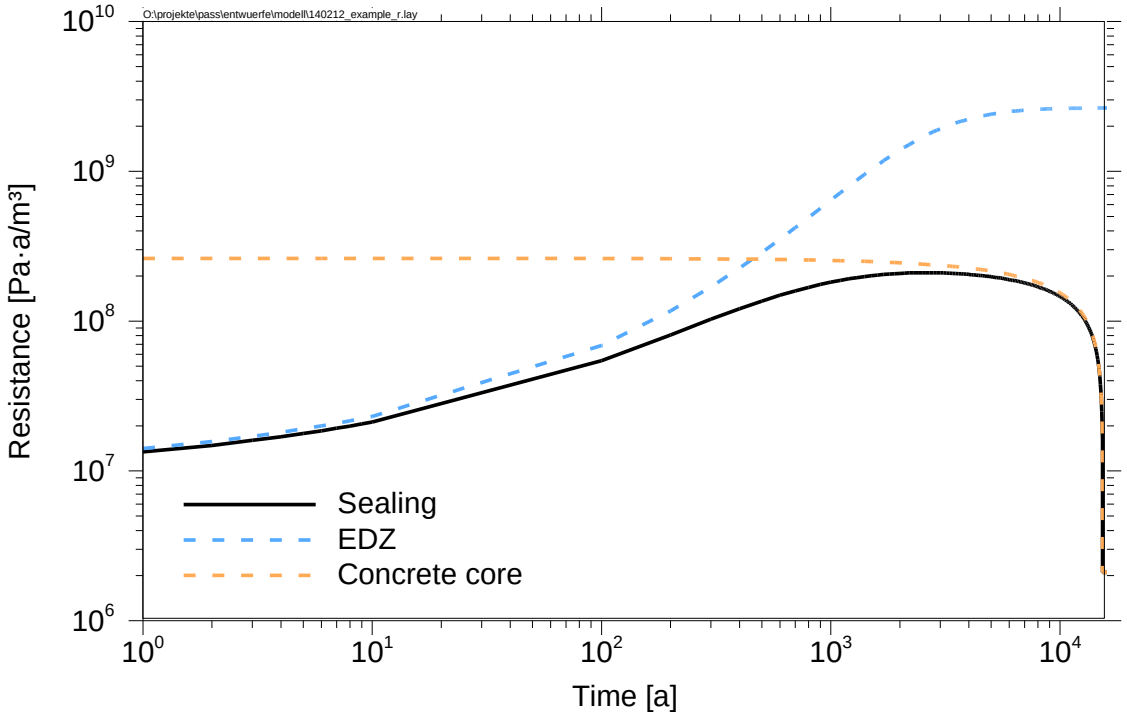

Fig. 9.2: Hydraulic resistance of a sealing, its concrete core and the EDZ around the sealing versus time

The integrated amount of brine inflow until the point in time of a sufficient high compaction of the crushed salt in the access drifts of the repository is the main quantitative performance requirement of the permeability of the shaft sealing. The permeability of the shaft seal is sufficiently low, if the amount of inflow does not completely fill the void spaces in the infrastructure area for the conditions expected in the reference scenario. The integrated amount of brine inflow is plotted in figure 9.3. The amount of brine until the complete corrosion of the seal is about 1 500 m^3. After this point in time, the amount of brine increases rather quickly to one million cubic meters of brine.

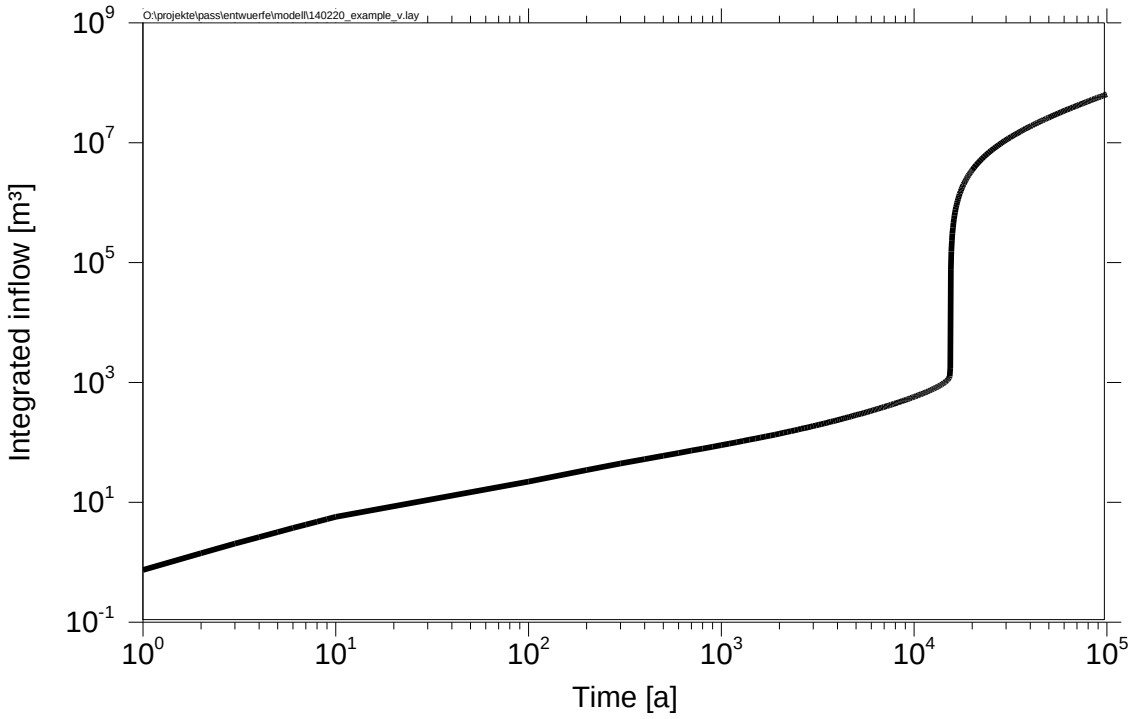

Fig. 9.3: Integrated inflow through sealing versus time

It has to be clearly noted that this is only an exemplary result which is highly sensitive to the input parameters listed above. Figure 9.4 shows some deterministic parameter variation where one parameter has been changed compared to the reference parameters in each calculation. The largest deviation compared to the reference case comes from the change of the sealing length. An increased sealing length by a factor of two results in a time needed to fully corrode the sealing which is increased by a factor of four.

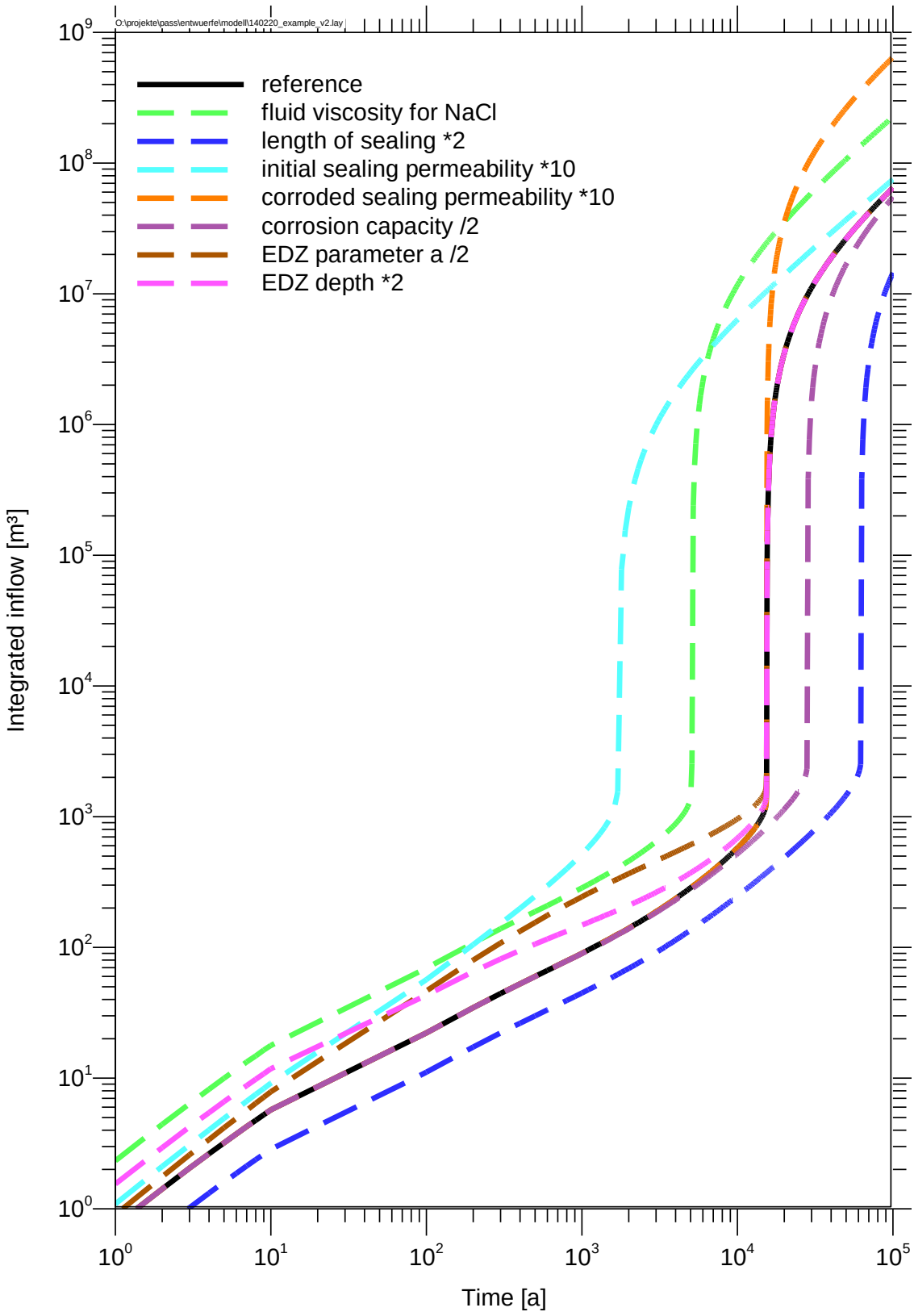

Fig. 9.4: Integrated inflow through sealing versus time for different parameter variations

9.7 Implementation in and simulations with the LOPOS safety assessment model

After successfully testing the mathematical model, it was implemented as a segment model in the LOPOS code. The integrated safety assessment code LOPOS (Loop structures in repositories) has been developed by GRS to simulate the one-dimensional, single-phase transport processes in the repository mine of a nuclear waste repository in salt (Hirsekorn et al. 1999). A simulation includes the calculation of the inflow of brine from the overburden, through the mine to the emplaced waste, the mobilisation of the radionuclides from the waste matrix and the transport of the radionuclides through the repository mine up to the shaft top. For modelling the transport in the repository mine, the mine is broken down into segments, each representing parts of the mine.

To reflect the changing hydraulic behaviour of the EDZ, which is induced by dilatancy reduction and healing of micro-fractures due to increasing rock pressure, the EDZ-permeability had to be no longer treated as constant but to develop in time. The temporal evolution of the EDZ is described as a function of time using the empirical fitting function:

$$k^E = k_\infty + k_0 e^{\left(-a \cdot t^b\right)}$$

with

t time in years,
k_0 initial permeability value at $t = t_0$,
k_∞ permeability value converging against after long times and
a, b curve shape fitting parameters.

The numerical implementation of the corroding concrete core is, however, considerable more complicated. This is owing to the fact, that the progression of the corrosion front is implicitly controlled by the amount of brine flowing through the sealing, which is on the other hand controlled by the changing permeability due to corrosion. In order to solve the problem, an incremental approach has been chosen. A separate subroutine calculates the incremental change of permeability dependent of the currant flow rate through the sealing, which is calculated within the segment model itself beforehand, for each time step. Subsequently the hydraulic resistance for the entire sealing is again calculated from the permeabilities as described above in another subroutine, herein before mentioned.

The corrosion model described below is based on the following assumptions:

- The geometry of the sealing is square and straight,
- The sealing may be surrounded by a temporally constant or variant, but homogeneous EDZ,
- The corrosion proceeds one-dimensionally,
- The reaction zone is narrow enough to be considered as a sharp front,
- The viscosity μ of the brine and the porosity ϕ of the material remain constant,
- The permeability k changes abruptly at the corrosion front (by ε powers of ten).

For the illustrative case presented above, the results from the LOPOS simulations using the enhanced code are in good agreement for the presented deterministic case. The influence of the parameter uncertainty was studied by a probabilistic Monte-Carlo simulation with 1.000 runs. The bandwidth of the variation of the input parameters and the according probability density functions (PDF) are given in table 9.2. Those variables where an explicit function is given in the table instead of a PDF were varied dependent on another variable. The variation of the EDZ fitting parameter *a* was chosen in a way that the time needed for the resealing of the EDZ varies between 2.000 years and 80.000 years. Examples for the random parameter samples are shown in figure 9.5.

As result of the probabilistic uncertainty analysis, figure 9.6 shows the cumulative brine flow through the sealing in the deterministic case together with the maximum, minimum, mean, median and the 5 and 95 percentiles of the probabilistic simulations. The result shows that the uncertainty of the result characterized by the bandwidth between the 5 and 95 percentiles is about two orders of magnitudes over most of the time. The uncertainty is even much higher during the phase of corrosion of the sealing material between some thousands and some tens of thousands years.

A bit astonishing on the first glimpse might be that the deterministic case is lying at the lower end of the considered bandwidth. The reason for this is mainly that the EDZ permeability of the is at the lower end of the bandwidth of a log-normal PDF and therefore a rather unrealistic value from the view of the uncertainty analysis.

A sensitivity analysis on the cumulative flow was performed on the probabilistic Monte Carlo simulation to determine the most important parameters influencing the simulation result. The following methods have been used for the evaluation: Standardised Regression Coefficients (SRC) Standardised Rank Regression Coefficients (SRRC), and Effective Algorithm for Computing Global Sensitivity Indices (EASI) (for the methods, see e.g. (Rübel et al. 2010)). The result is shown in table 9.3 which shows the ranks of those parameters with a correlation coefficient greater 0.1 to the cumulative inflow at the end of the simulation run. The three parameters which are identified as sensitive for the cumulative flow at simulation end are all related to the corrosion process of the sealing material. The most sensitive parameter is more or less the permeability of the corroded material. This parameter is still ill defined and only known from process modelling due to the long experimental time needed to achieve the final state of the material in an experiment. Additional research might be needed to better define that parameter. However, additional parameters are sensitive if other times are regarded. For early times, the initial EDZ permeability is the most sensitive parameter (see figure 9.7).

Tab. 9.2: Probabilistic varied parameters

Parameter	lower limt	upper limit	probability density function
Length of the sealing [m]	25	35	equal
Brine characteristic ξ	0	1	equal
Viscosity μ [Pa s]	$2 \cdot 10^{-3}$	$6 \cdot 10^{-3}$	$\mu = (4\ \xi + 2)\ 10^{-3}$
Porosity ϕ [-]	0.1	0.3	equal
Initial permeability k_0^S [m^2]	$5 \cdot 10^{-20}$	$5 \cdot 10^{-18}$	log normal
Permeability increase factor [-]	10^3	10^5	equal
Corrosion capacity $\kappa_{L,V}$ [l/l]	0.5	1.5	$\xi + 0.5$
EDZ initial permability k_0 [m^2]	10^{-17}	10^{-14}	log normal
EDZ long-term perm. k_∞ [m^2]	10^{-20}	10^{-17}	k_0 / 1 000
EDZ fitting parameter a [-]	0.15	0.6	normal

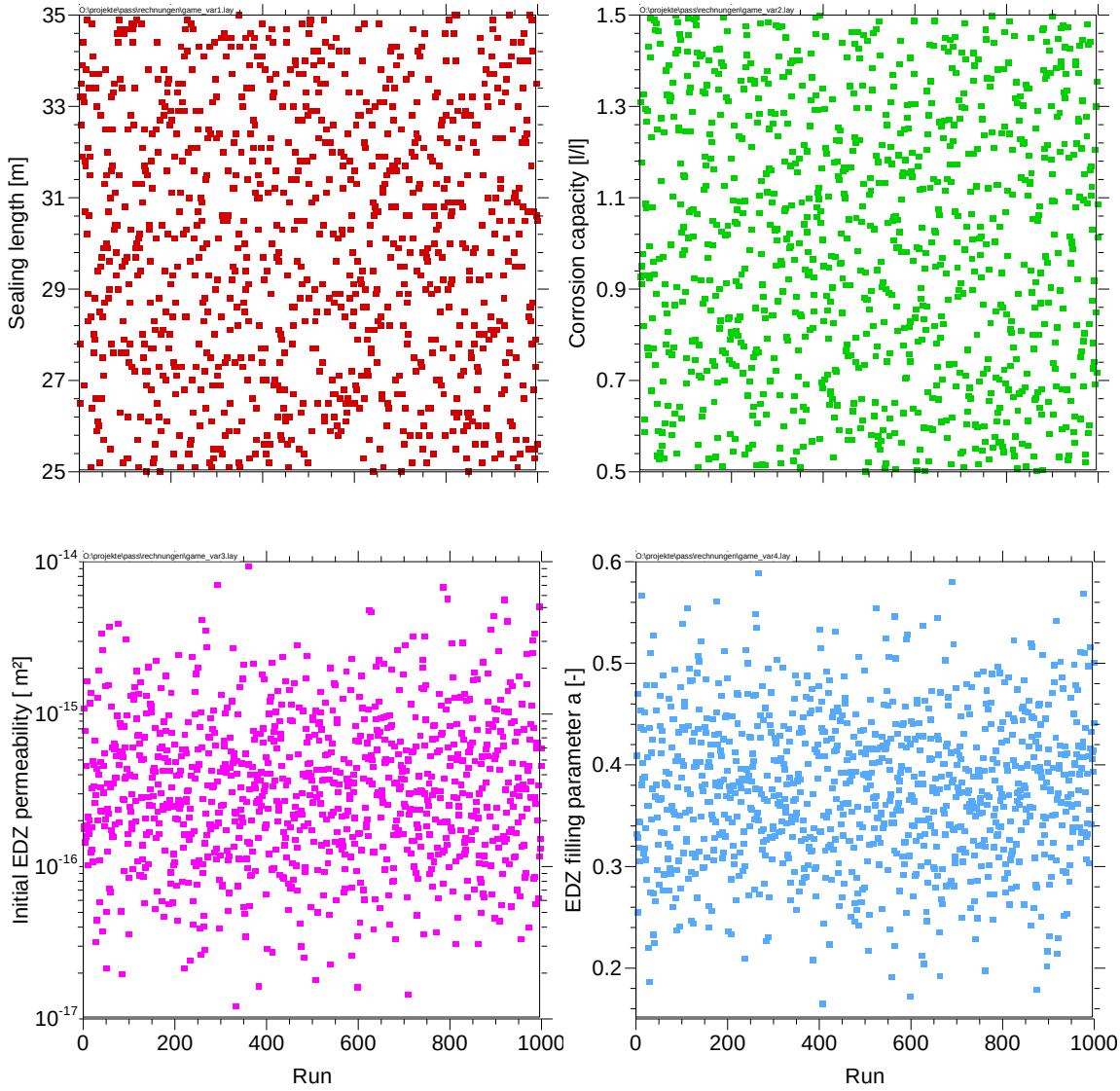

Fig. 9.5: Examples for the parameter distributions

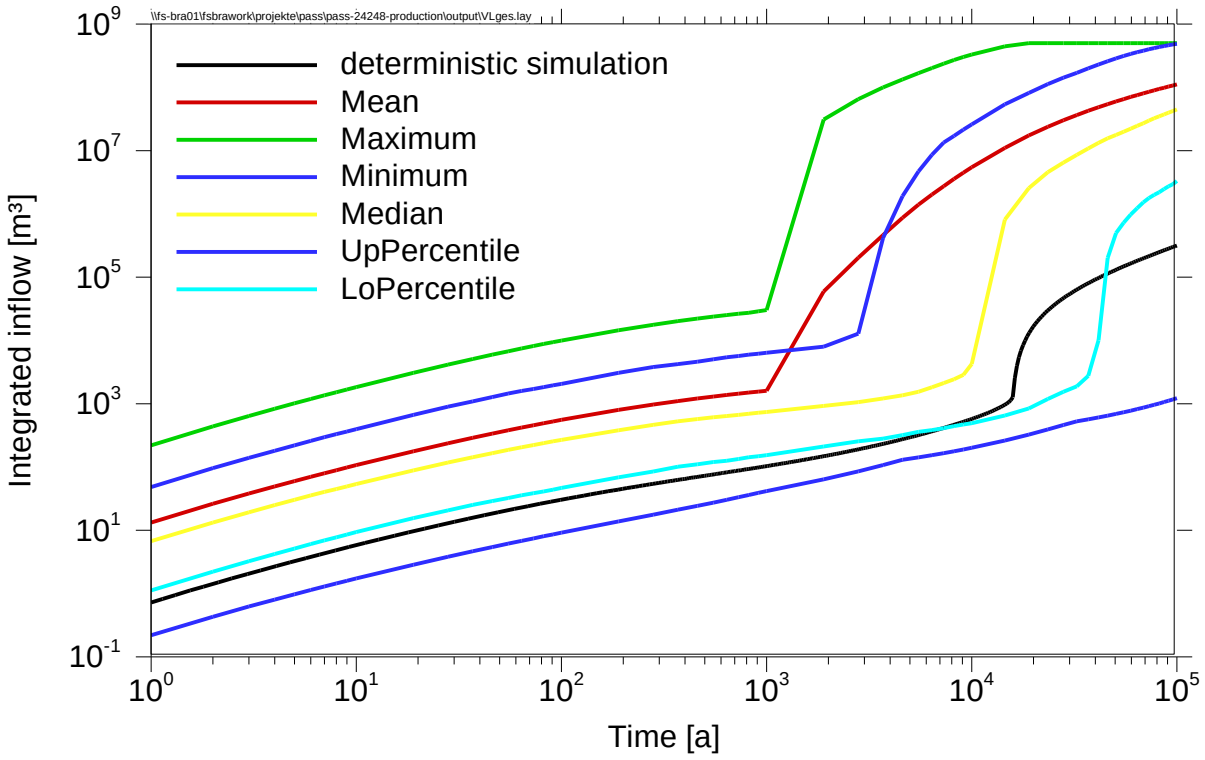

Fig. 9.6: Result of the probabilistic simulation compared to the deterministic simulation

Tab. 9.3: Ranks of the parameters in the sensitivity analysis

	SRC	SRRC	EASI
Length of the sealing			
Brine characteristic	3	3	
Porosity			
Permeability increase factor	1	1	1
EDZ fitting parameter			
Initial permeability	2	2	2
EDZ initial permability			

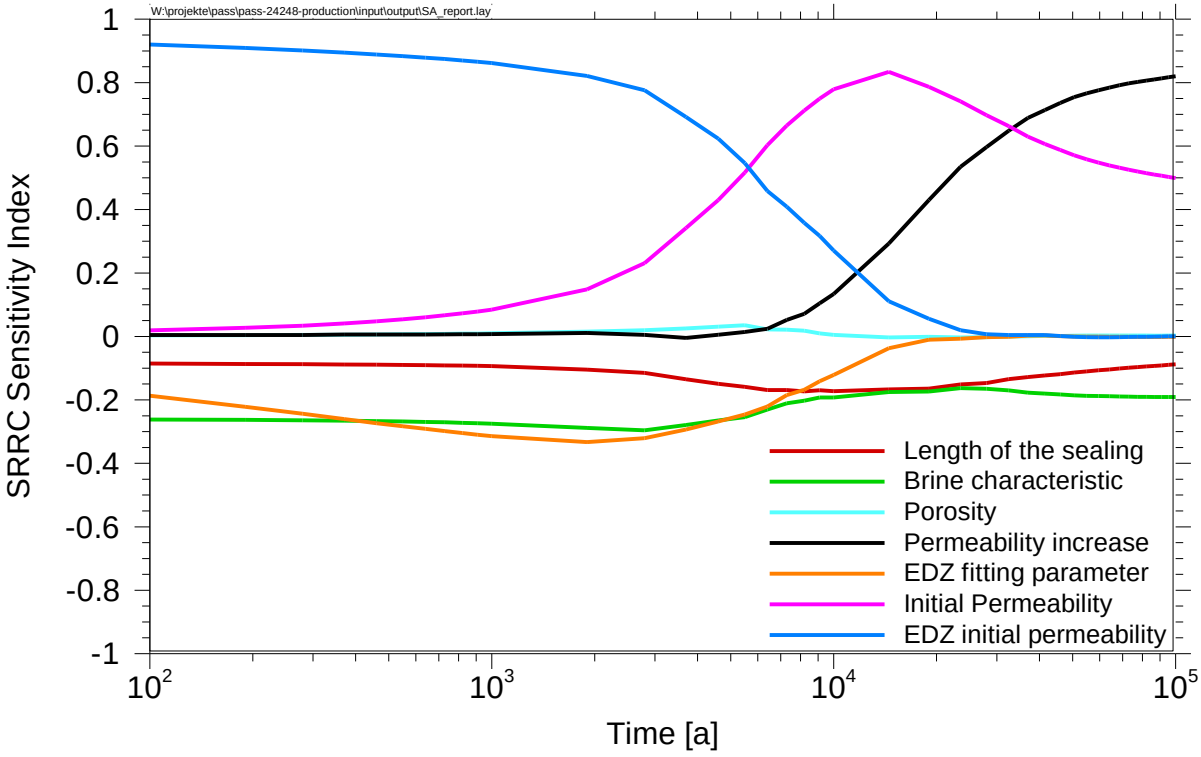

Fig. 9.7: Temporal evolution of the sensitivity indices for the SRRC method

9.8 Simulations for the ELSA shaft sealing concept

The following integrated performance assessment modelling refers to the ELSA shaft sealing concept developed within the scope of the Preliminary Safety Analysis for Gorleben (VSG). For this sealing concept, integrated performance assessment model calculations were performed for several scenarios. Previous model calculations yielded good results although neglecting effects of time dependent hydraulic properties as investigated within the DOPAS project (Müller-Hoeppe et al. 2012). The aim of the new model calculations presented here is to compare previous model results with new results obtained with the extended LOPOS segment model described above.

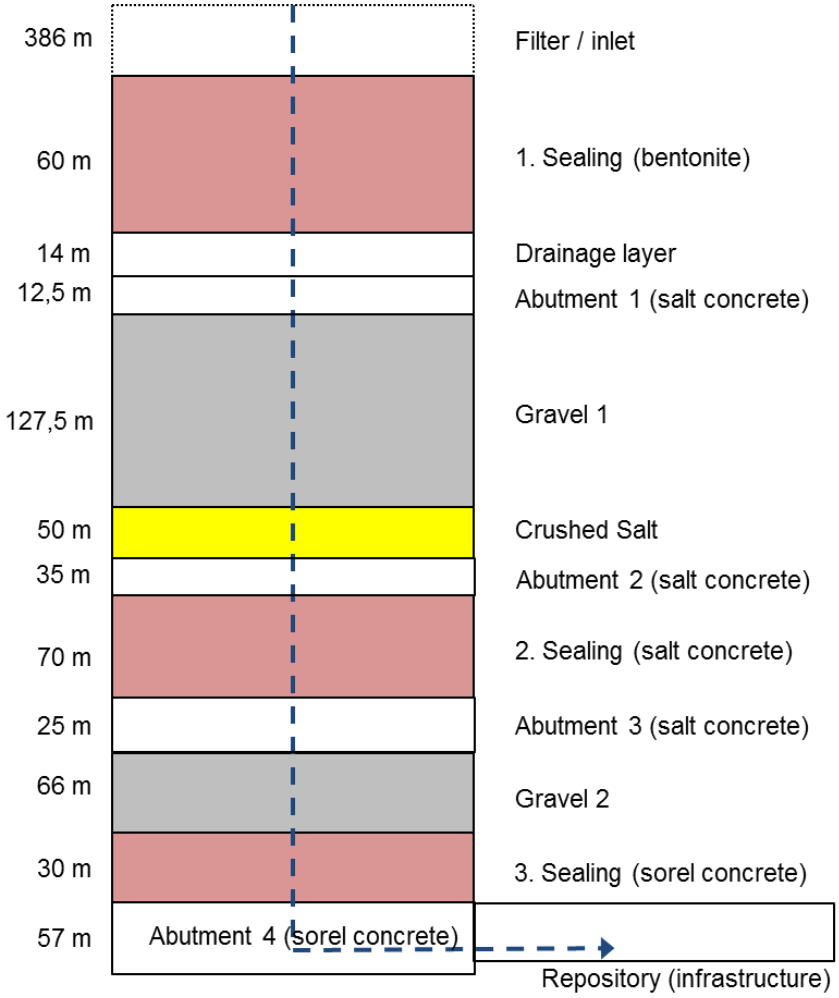

Fig. 9.8: Sketch of model segment structure for the shaft sealing concept including values for segment lengths (compare also figure 5.1)

The pressure at the top of the uppermost sealing element (bentonite) is constant and amounts to 5.1 MPa accordingly 436 m water column. After the date of full saturation of the pore space in the drainage layer and the gravel column (1600 years) the pressure in the bentonite increases to 5.35 MPa. There and in every other component above the salt concrete sealing the maximum values are reached in the period after 1740 years, when the sealing element of salt concrete is saturated with inflowing brine. In all components underneath the salt concrete

sealing element the pressures remain near atmospheric pressure and below 0.2 MPa throughout the whole model time.

These new test cases refer to the ELSA shaft sealing concept presented above with the extension of time dependent EDZ and/or concrete corrosion for the second and third sealing element, namely the salt concrete and MgO-based concrete sealings. Accordingly, the newly developed LOPOS segment model is applied to represent the 2nd and 3rd sealing elements. The parameters for EDZ evolution and concrete corrosion were selected consistent with the exemplary values given above and represent an Mg-content of the brine of about 10 % of that of an IP-21 solution. Remaining parameters were left unchanged compared to the LOPOS simulations performed in the VSG (Müller-Hoeppe et al. 2012).

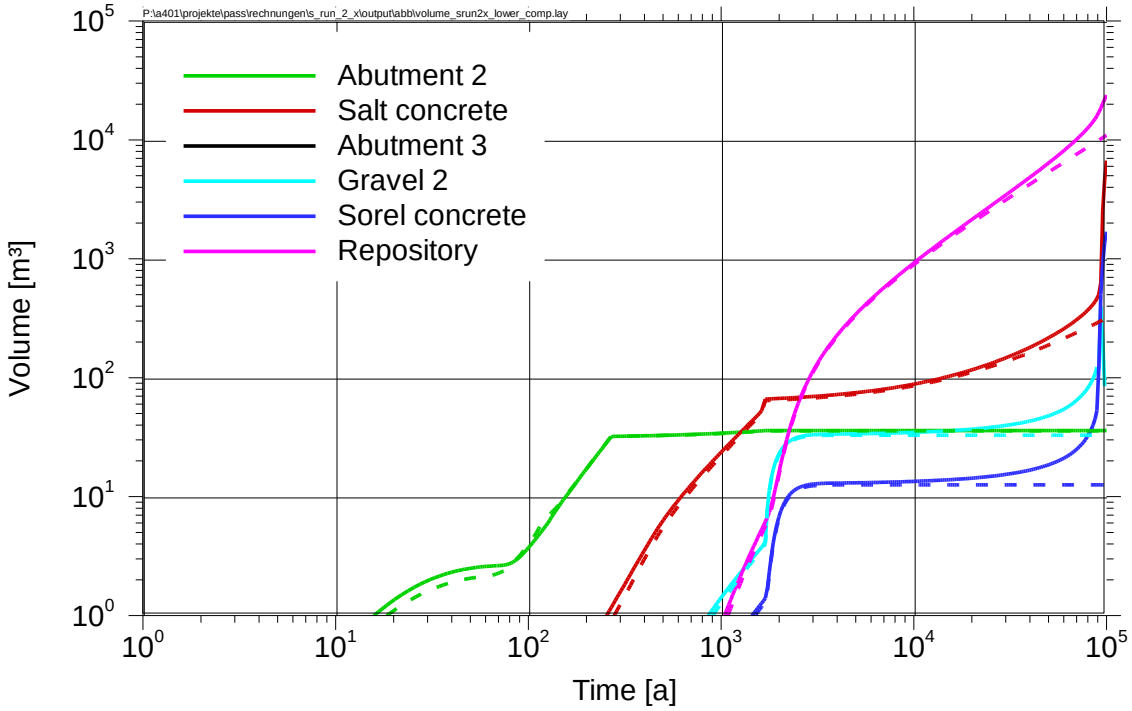

Fig. 9.9: Brine volumes of lower sealing elements over time; new results vs. VSG results (dashed)

It can be noticed, that the consideration of EDZ-closure is having only slight effects at early times, almost completely vanishing in the long term (cp. srun2a vs. srun2). In contrast, the effects of concrete corrosion are negligible for long periods of time but exuberantly grow in importance in the long run. Beyond that it can be observed that for long periods – from beginning till about 30 000 to 40 000 years – the brine outflow from the entire sealing system in the example presented here is virtually unaffected by EDZ-development and concrete corrosion. This result supports the design of the sealing system, as it was designed accordingly from the beginning to not be largely affected by those effects.

9.9 Conclusions

The safety assessment code LOPOS which is used by GRS for the integrated long-term safety assessments of repositories in salt has been further developed by the work presented to account for the excavation disturbed zone around sealings and for the corrosion of the concrete sealing material. The models used for abstraction of those two processes were developed to well describe experimental and process level findings achieved before and during the early phase of the DOPAS project. Not all experimental results could be included due to the parallel timing of the work, but the newer experimental findings do not contradict to the work performed. The new model was successfully tested on a simplified test case with deterministic and probabilistic simulations and applied to the ELSA shaft sealing concept. Additional processes might be considered in the future cracks in the sealing material which allow for an advancing non-homogeneous corrosion of the sealing material along these pathways.

10 Process modelling of bentonite saturation in the PHM experiment and testing the influence of bentonite sealing property for safety of deep geological repository (UJV)

D. Trpkšová, V. Havlová, P. Večerník, J. Gondolli

10.1 Introduction

Work done by ÚJV Řež, a. s. in the DOPAS WP 5 consisted mainly of simulating the physical hydraulic model (PHM) carried out under laboratory conditions in WP 3 (Vašíček at al., 2016) by means of numerical modeling and further integration of different state of bentonite layer into a complex model used for safety assessment of deep geological repository (DGR).

10.2 Numerical simulation of laboratory physical hydraulic model

As the simulation of unsaturated swelling materials is somewhat complicated and the EPSP underground laboratory experiment will not be dismantled during the course of the project, the construction of plug physical models at the laboratory scale (physical hydraulic model – PHM) was proposed in the laboratory work plan. The aim of these experiments is to gain data for of numerical model calibration of bentonite saturation. Geometry, boundary conditions and monitored parameters are described in detail in the report D3.21 (Vašíček at al., 2016). Two PHM tests were constructed; the first one using bentonite powder and the other one using bentonite pellets.

10.2.1 Conceptual model

The core task addresses the HM (hydro-mechanic) response of a highly compacted bentonite barrier. The HM coupled analyses have been performed using 2-D axi-symmetric longitudinal section. The model area has a rectangular shape with dimensions of 0.04 x 0.45 m, the area being covered with a uniformly structured grid. The grid step is 0.5 cm, it means 8 points in the *x* direction and 90 points in the *y* direction.

The program Code_Bright was used for the numerical modeling.

The main process being addressed in the PHM in pressurized saturation under controlled conditions. The testing procedures involved:

- An initial hydration phase, in which the bentonite was flooded with water under zero pressure in order to allow the closure of the joints between bentonite blocks. The duration of this initial phase was 1 day in both PHM with bentonite powder and in PHM with bentonite pellets.
- Once the initial hydration phase was completed, the process of pressurized saturation was started (about one year).

Initial parameters have been taken from FEBEX (Full-scale Engineered Barriers Experiment) reports (UPC 2015a). The HM version of the Barcelona Basic Model (BBM) is adopted in the analysis for the mechanical behaviour.

10.2.2 Initial and boundary condition

Solving HM problem, the following conditions have to be defined:

Mechanical boundary condition:

In order to take into account that the main body of the cylinder is made from stainless steel cell, an assumption of null displacements has been prescribed at the outer boundaries, as follow:

- Restriction of vertical displacement along the horizontal boundaries (perpendicular to the wall of the cell)
- Restriction of horizontal displacement along the vertical boundaries

Hydraulic boundary condition:

At the lower horizontal boundary a 2 MPa water pressure is prescribed, to simulate the bentonite saturation. At the upper horizontal boundary a condition of seepage face is prescribed.

Initial conditions:

A constant hydrostatic value of 0.11 MPa has been adopted as an initial stress value in the bentonite material. The initial porosity for the bentonite is considered equal to 0.5 (measured in laboratory). The main initial unknown is the water pressure in the model area before starting the saturation. An initial value of suction of -192 MPa has been adopted for the PHM with bentonite powder and -80 MPa for PHM with bentonite pellets. These values were taken from RH sensors and were converted to pore water pressure using the Kelvin equation

$$s = -10^{-6}\frac{R \times T}{V_w} ln\left(\frac{RH}{100}\right),$$

where R is universal gas constant, T is absolute temperature, V_w is molar volume of water and RH is relative humidity.

Time interval:

The duration of computed task is depending on the duration of a laboratory experiment. In the case of bentonite powders the simulated period is 450 days, in the case of the model with bentonite pellets then 380 days.

10.2.3 Calibration of numerical model

10.2.3.1 Numerical model of PHM with bentonite powder

The data measured in laboratory (namely volume of infiltrated water and development of relative humidity recalculated to the pore water pressure) formed the basis for the model calibration. Furthermore, the model retention curve and the curve measured in the laboratory were compared. Prescribing more calibration criteria should reduce the degree of freedom of numerical solution, when the model is able to receive the same result when different combinations of model parameters.

Due to large number of model parameters the only parameters describing saturation, i.e. the parameters of retention curve and the hydraulic conductivity, were considered in the calibration. Thus, it took into account the change of model results depending on change of three model parameters.

The resulting parameters for task with bentonite powder are listed in Tab. 10.1, the comparison between measured and modelled values of the development of infiltrated water volume is shown in Fig. 10.1; comparison water pressure development in the individual observation points is shown in Fig. 10.2 - Fig. 10.4 and the conformity between the model and measured retention curve is shown in Fig. 10.5.

Tab. 10.1 The resulting model parameters describing hydraulic data in the model using bentonite powder. Retention curve parameters P1, P2 and P3 describe the parameters necessary for expression of its shape by using van Genuchten equation, intrinsic permeability parameters P1, P2 and P3 represent anisotropy of hydraulic conductivity. Individual values and their units are explained in detail in UPC (2015b).

Parameters	ITYCL	P1	P2	P3	P4	P5
Retention curve	1	20	0.072	0.27	0.001	1
Intrinsic Permeability	1	5.E-21	5.E-21	5.E-21	5.E-01	0

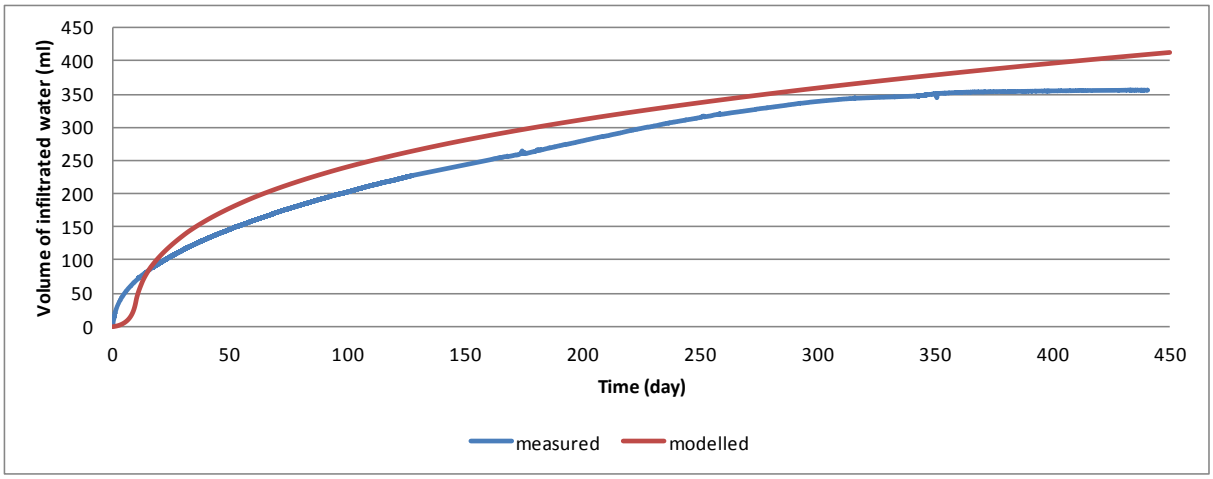

Fig. 10.1 Comparison between the model and measured values of infiltrated water volume to the bentonite powder sample

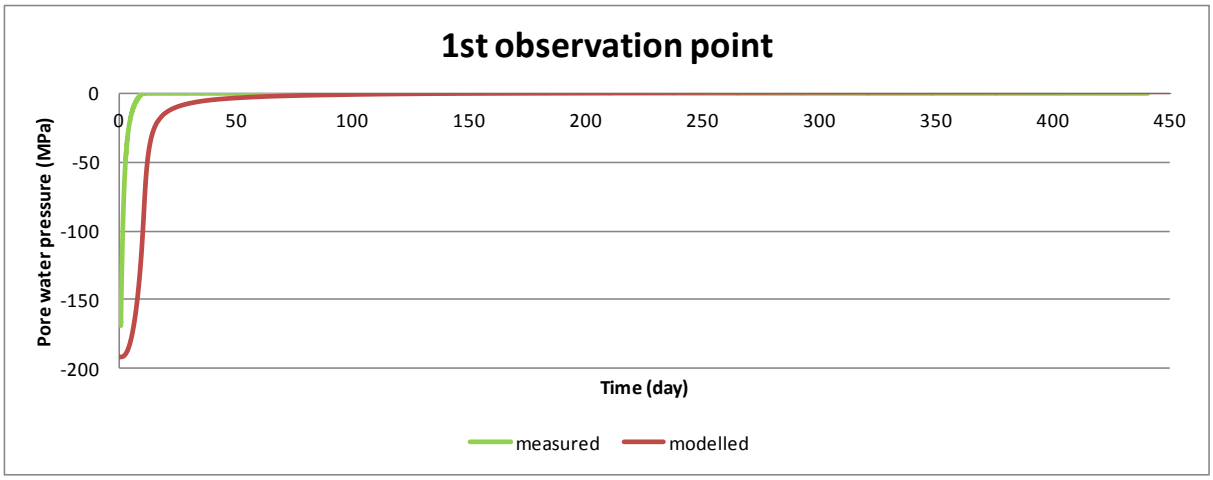

Fig. 10.2 Comparison between the model and measured values of water pressure in 1st observation point

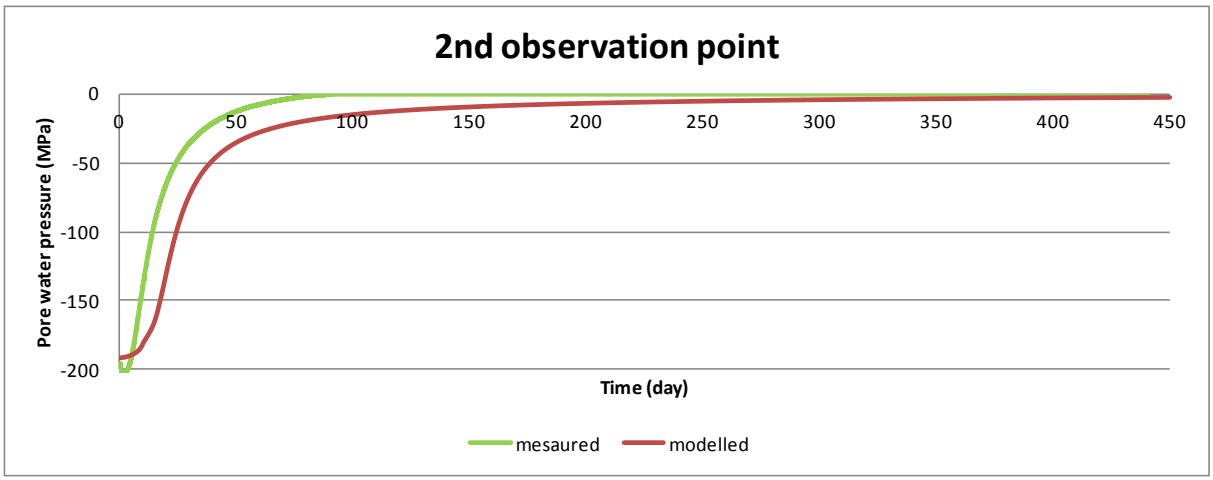

Fig. 10.3 Comparison between the model and measured values of water pressure in 2nd observation point

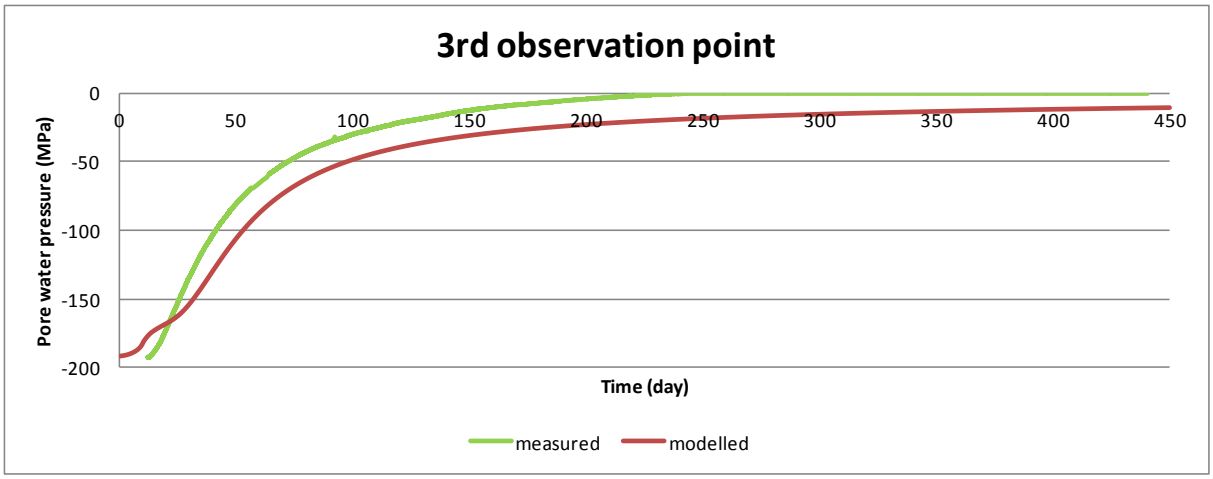

Fig. 10.4 Comparison between the model and measured values of water pressure in 3rd observation point

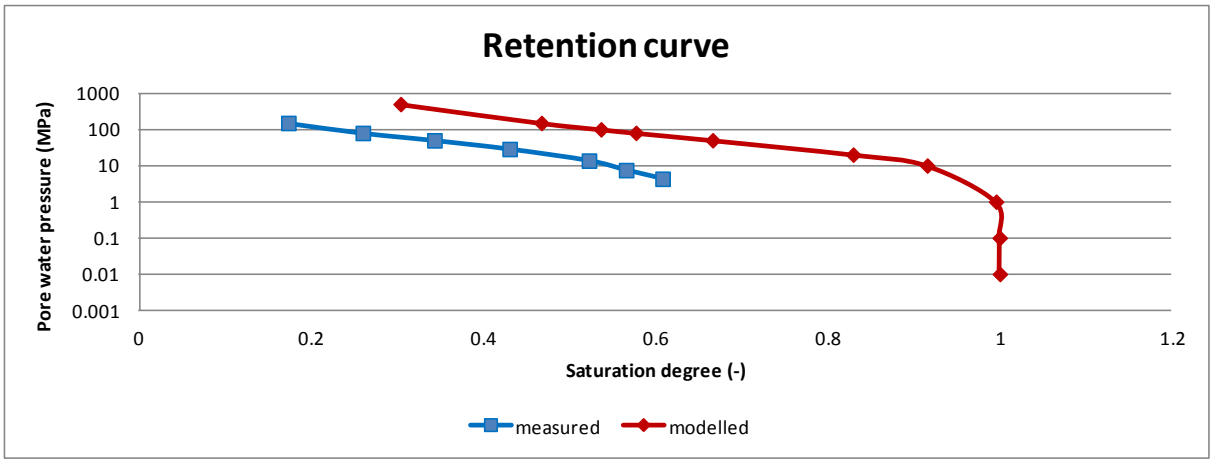

Fig. 10.5 Comparison between the model and measured retention curve

A comparison of water pressure development in the individual observation points shows that the agreement in modelled and measured values decreases with the distance from the saturation point, especially at the beginning (from the time of view) of the experiment. It was possible to achieve a better match for each calibration criteria separately during calibration, but with the better agreement in one criterion agreement in other two criteria decreased. In case we require compliance at all three calibration criteria, it was necessary to disregard the perfect agreement between measured and modelled values.

The calibrated parameters were used for predictive modelling, when the most important question was to predict the expected time necessary for whole saturation for 45 cm long bentonite sample. This is shown on Fig. 10.6, where the outlet from the second end of the model occurred at 2992.4 days.

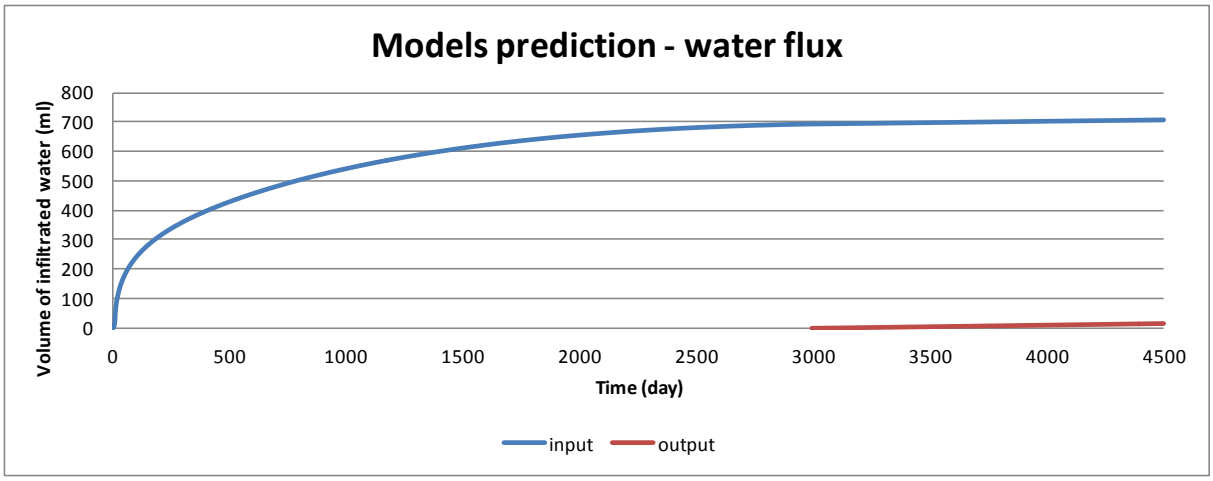

Fig. 10.6 Model prediction of water balance development at the beginning and at the end of the bentonite sample

10.2.3.2 Numerical model of PHM with bentonite pellets

The same criteria as for the calibration of the model with bentonite powder were used for model calibration with bentonite pellets

- Volume of infiltrated water
- Water pressure in each observation point
- Retention curve

The structure of the pellets was not taken into account during simulation model. The material is considered as a homogeneous and is presumed presence of pellets throughout the whole model area.

The resulting parameters for the task with bentonite pellets are listed in Tab. 10.2. The comparison between measured and modelled values of the development of volume of infiltrated water is shown in Fig. 10.7. Comparison the development of water pressure in the individual observation points is shown in Fig. 10.8 - Fig. 10.10 and the conformity between the model and measured retention curve is shown in Fig. 10.11.

Tab. 10.2 The resulting model parameters describing hydraulic data in model with bentonite pellets. Retention curve parameters P1, P2 and P3 describe the parameters necessary for expression of its shape by using van Genuchten equation, intrinsic permeability parameters P1, P2 and P3 represent anisotropy of hydraulic conductivity. Individual values and their units are explained in detail in UPC (2015b).

Parameters	ITYCL	P1	P2	P3	P4	P5
Retention curve	1	10	0.072	0.22	0.001	1
Instrinsic Permeability	1	1.E-20	1.E-20	1.E-20	5.E-01	0

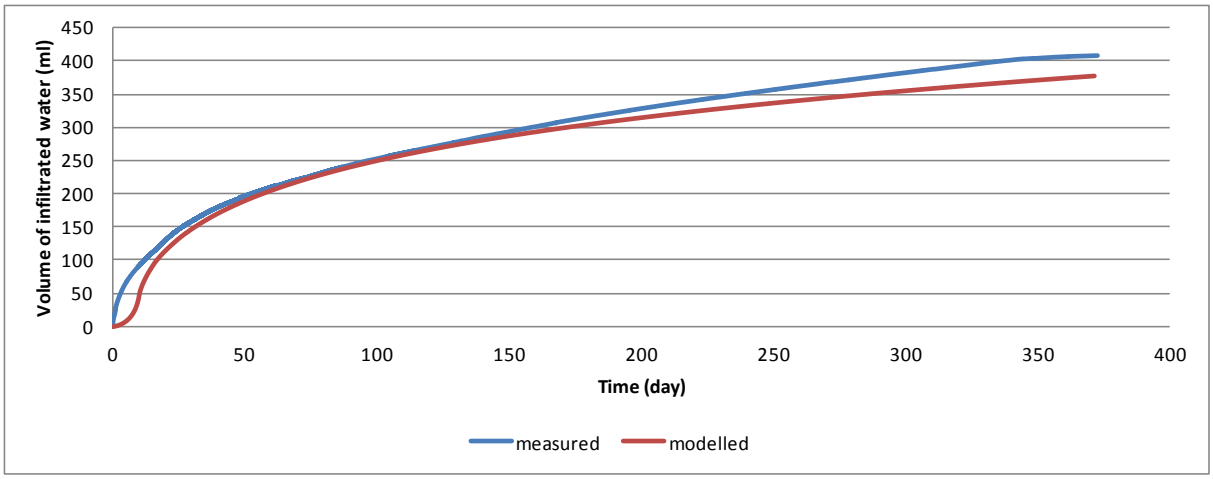

Fig. 10.7 Comparison between the model and measured values of infiltrated water volume to the sample of bentonite pellets

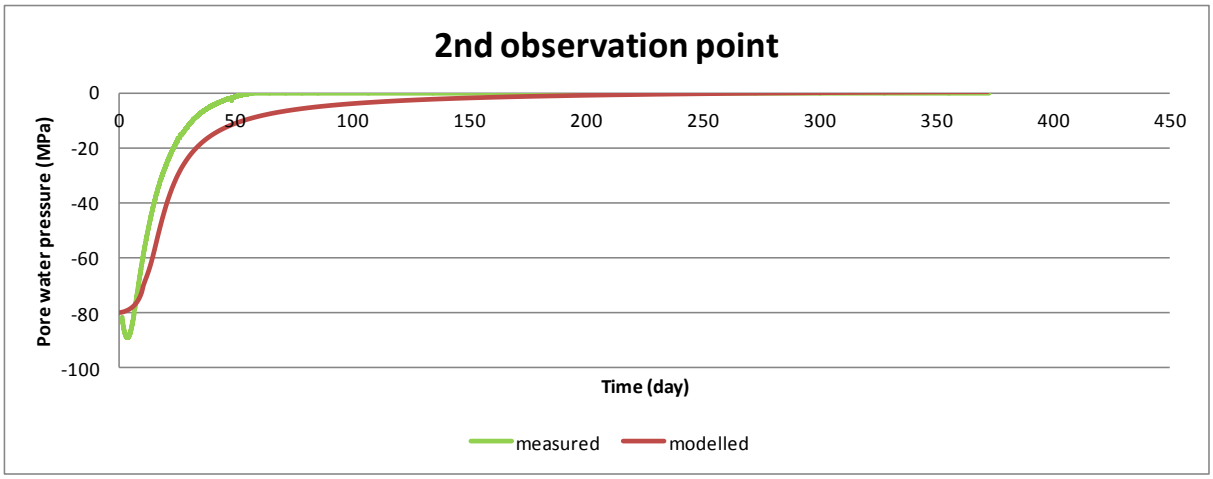

Fig. 10.8 Comparison between the model and measured values of water pressure in 2nd observation point

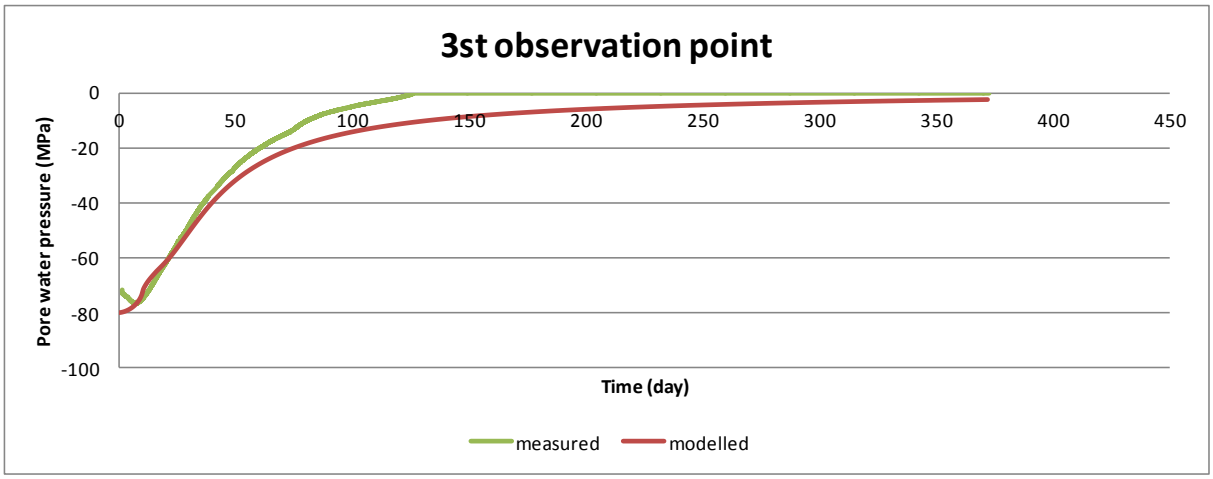

Fig. 10.9 Comparison between the model and measured values of water pressure in 3rd observation point

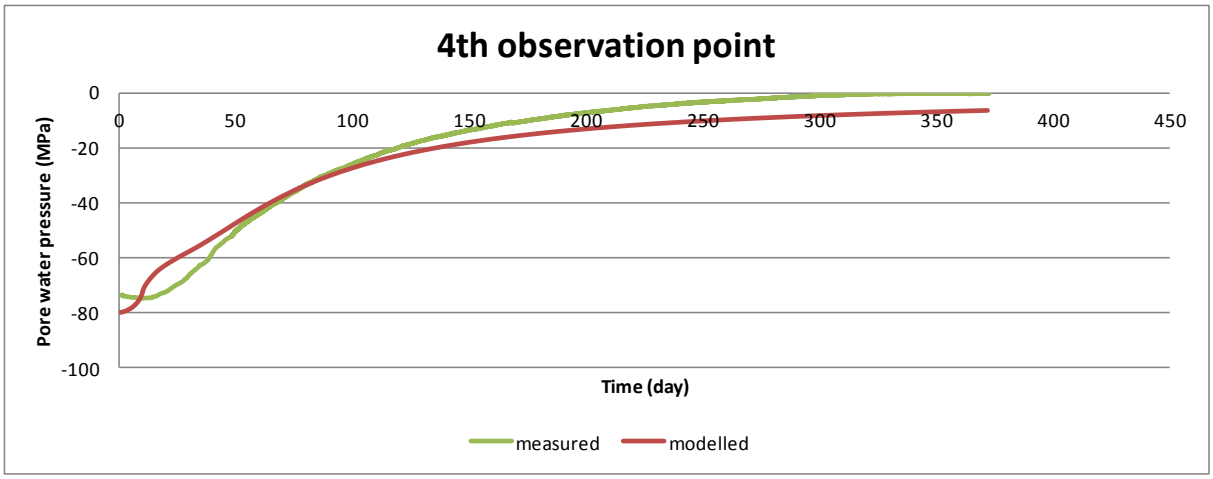

Fig. 10.10 Comparison between the model and measured values of water pressure in 4th observation point

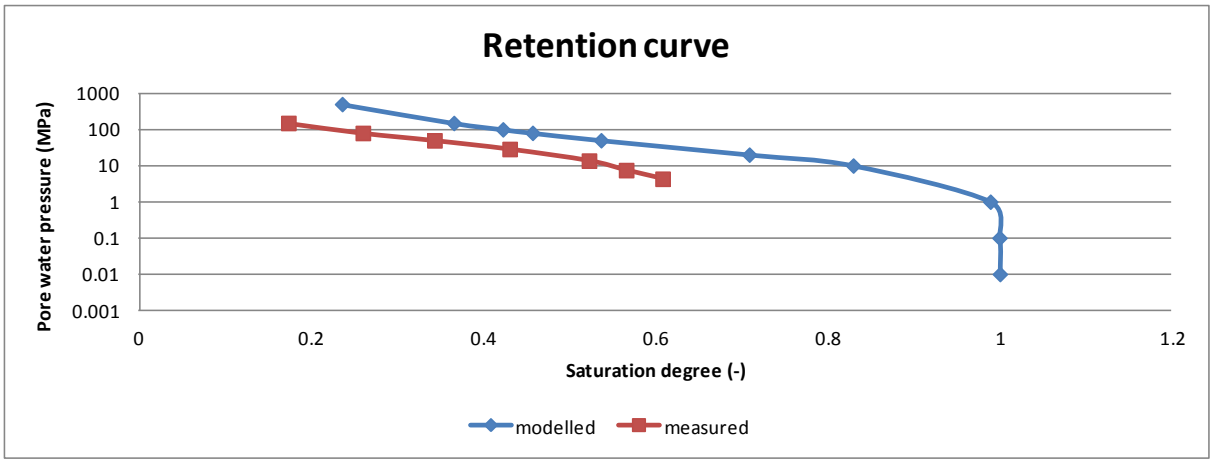

Fig. 10.11 Comparison between the model and measured retention curve

Better agreement between measured and model results than when calibrating the model with bentonite powder has been achieved in model calibration with bentonite pellets.

The calibrated parameters were used for predictive modelling, when the most important question was again the expected time necessary for the whole saturation of 45 cm long bentonite sample. This is seen on Fig. 10.12, where the outlet from the second end of the model occurred at 1833.8 days, which is about a third time shorter than time necessary to saturation of bentonite powder. But it is necessary to take into account, that initial degree of saturation of bentonite pellets was higher than initial degree of saturation of bentonite powder (initial water pressure of bentonite powder was -192 MPa, initial water pressure of bentonite pellets was -80 MPa).

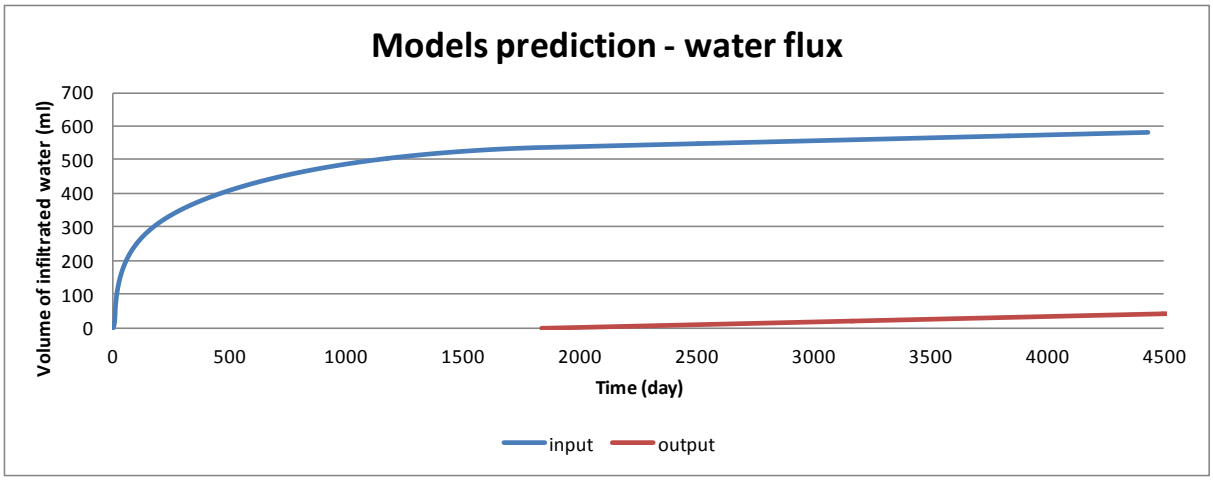

Fig. 10.12 Model prediction of development of water balance at the beginning and at the end of the bentonite sample

10.3 Testing the influence of bentonite sealing property for safety of deep geological repository

Although the plug itself does not fulfil a safety function sensus stricto, it contributes to the safety function of bentonite sealing layers via keeping the bentonite material in a defined place and preserves it as much as possible in the predefined form (mainly in terms of bulk density). The requirement for a minimum lifetime of SNF (spent nuclear fuel) container in Czech deep geological disposal concept is 10 000 years. During this time, it is assumed that there is no damage of SF container. Therefore the time can be considered as the starting time point in simulations, concerning safety of deep geological repository. However, during this time the bentonite material will be saturated and could be exposed to an increased inflow of groundwater from structures with increased hydraulic conductivity. That might affect the structure of bentonite material around the SNF container. Especially therefore it is necessary to consider the formation of erosion channel in bentonite layer, being caused by washing out the bentonite material. Therefore, the setting of complex model, used for DGR safety assessment using GoldSim program, was varied in order to consider such a damage of bentonite layer. The following four variants states of bentonite layer were considered (Fig. 10.13a):

1. Bentonite material behind plug remain intact; the erosion channel was not created
2. The erosion channel was created in bentonite material: the channel was filled by material with lower bulk density due to swelling properties of bentonite material
3. The erosion channel was created in bentonite material: the channel remained empty
4. All bentonite was washed out, the space between the plug and SF canister remained empty

Concerning the second and the third variant, several values of the erosion channel opening were simulated. The degree of bentonite layer disturbance is given by multiplication of the SNF containers circumference and percentage of damage (Fig. 10.13b).

From the Fig. 10.13 it is clear that 100% damage in a third variant (empty piping channel) corresponds to the fourth variant, namely the state where the bentonite material was completely washed out from the area between the borehole wall and the SNF canister. It is obvious that this case is very unrealistic. Furthermore, the Czech concept of DGR does not consider damage of the bentonite layer to such an extent. Therefore, the variants 3 and 4 were simulated just to highlight the impact of f the bentonite layer state to the effective dose rate.

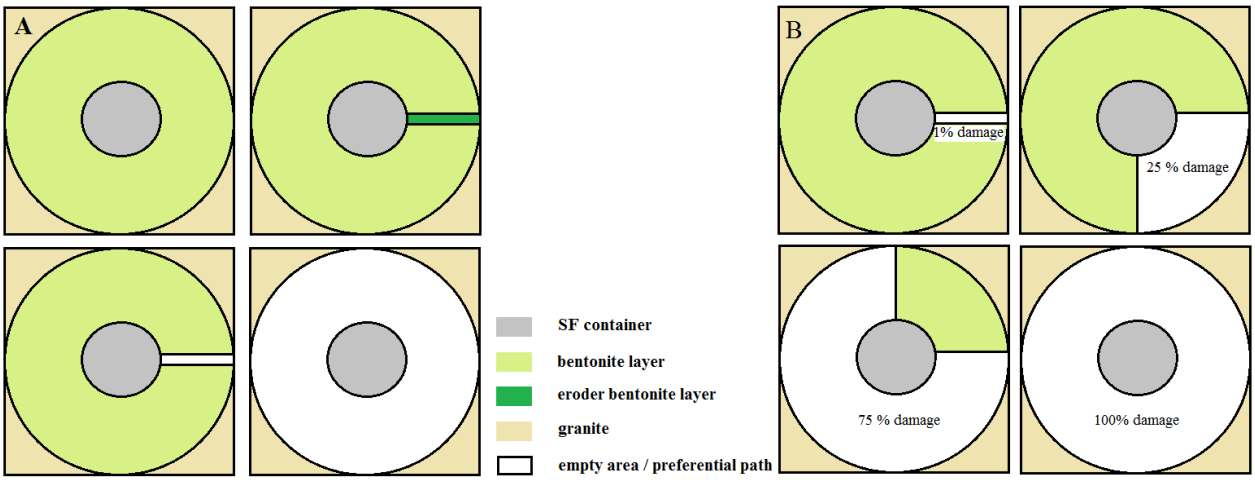

Fig. 10.13 Four variants of the bentonite layer simulated states (A) and the rate to the bentonite layer damage (B), contemplated in the various simulations.

10.3.1 Conceptual model

Czech concept of SNF and HLW (high level waste) disposal generally assumes emplacing the SNF into the metal containers, that are stored in disposal boreholes in the rock massive at the depth of about 500 m below the surface. The SNF container will be surrounded by bentonite buffer layer. It is assumed that leakage from SNF containers can occur only after the corrosion the container material or after mechanical damage of the container. Contamination (activity) spreads from the container by diffusion through the bentonite buffering and sealing layer into the rock environment where it is transported by the groundwater flow toward the interface with the biosphere.

The model assumes disposal of 6000 SNF container made of carbon steel. Activity release occurs after degradation of SNF container. The main transport process considered is diffusion. The SNF container degradation is described by distribution curve obtained by applying the Weibull distribution. Minimum container life-time is 10,000 years, and the median is 110,000 years. When damage occurs in SNF container, there is immediate release of a part of inventory (IRF - instant release fraction). Since this point the waste matrix degrades, (meaning UO_2, MO_X, construction materials). The basic rate of SNF degradation (UO_X matrix) is $1e^{-8}$ $year^{-1}$ and for activated materials is $1e^{-5}$ $years^{-1}$.

Bentonite layer is modelled by fifteen concentric layers in order to gain better accuracy. The outer layer represents the interface with the repository surrounding (rock compartment). The

rock diffusion layer is modelled at the interface bentonite/ rock compartment in order to eliminate the influence of advection in bentonite layer.

The radionuclides are transported by diffusion through the bentonite layer toward a rock compartment (model view only). Rock massive is modelled as compartments with 3km × 1km × 10 m size. At each time step, the concentration balance is set in this area, is meaning that the same conditions are valid in the whole area. Radionuclides from the disposal environment are transported by the groundwater flow (advection is considered as a transport process) to a preferential path in the geosphere.

Geosphere is modelled using the components "Pipe" (more than one), considering the model transport processes as advection, diffusion into the rock matrix and sorption. From the last "Pipe" groundwater flows into the compartment which model processes in biosphere.

The biosphere is modelled using four compartments representing the land (cultivable and forest), pond and river, and represents a universal model that corresponds to the current lifestyle of the Czech Republic. The output of the biosphere model is the effective dose rate to humans living in the area affected by DGR.

The Parametric model settings will be described in report D5.7, which will be available in next months.

10.3.2 Results and discussion

The development of the effective dose rate in the case with empty piping channel (variant 3) for various degrees of bentonite layer failure of the is shown in Fig. 10.14; for the case with filled piping channel (variant 2) in Fig. 10.15. The contributions of individual radionuclides to the total effective dose rate in case of empty and filled piping channel for different degrees of damage is shown in Fig. 10.16 - Fig. 10.20.

The figures Fig. 10.14 and Fig. 10.15 show that the effective dose rate grows with an increase rate of damage of the bentonite layer. The explanation for this phenomenon is based on the loss of material available for radionuclide sorption. In case of a sorption decrease more radionuclides are released directly into the water (increases their concentration in water).

Significant increase of effective dose rate due to contribution of ^{126}Sn is seen in the case of empty piping channel with damage (Fig. 10.16 and Fig. 10.17). This contribution of ^{126}Sn is evident also in the case of a filled piping channel too, although it exhibit different trends over time and the effect of ^{126}Sn appears only in the case of higher damage rate of the bentonite layer (Fig. 10.18 and Fig. 10.19).

In case of empty piping channel the contribution radionuclides of ^{126}Sn, ^{229}Th, ^{230}Th and ^{242}Pu to the total effective dose increases with the degree of damage to the bentonite layers.

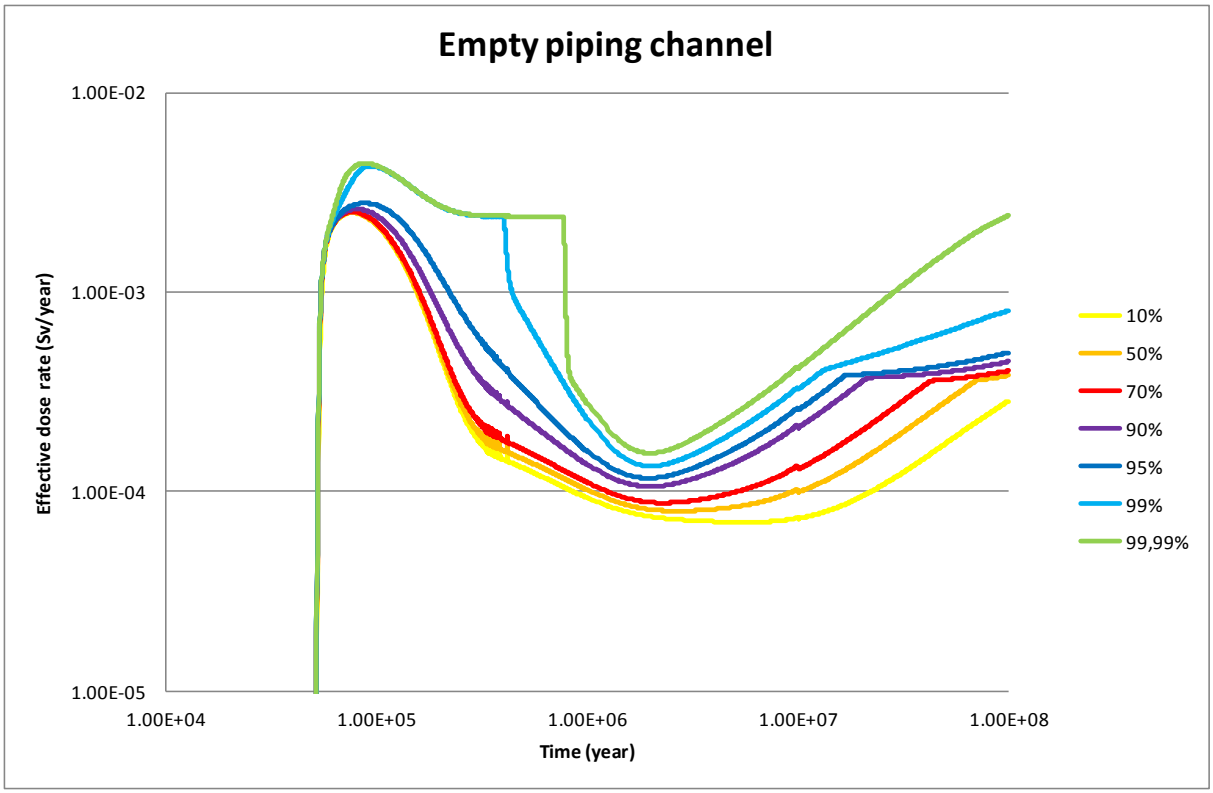

Fig. 10.14 Development of effective dose rate in the case of empty piping channel considering different degrees of damage to the bentonite layer.

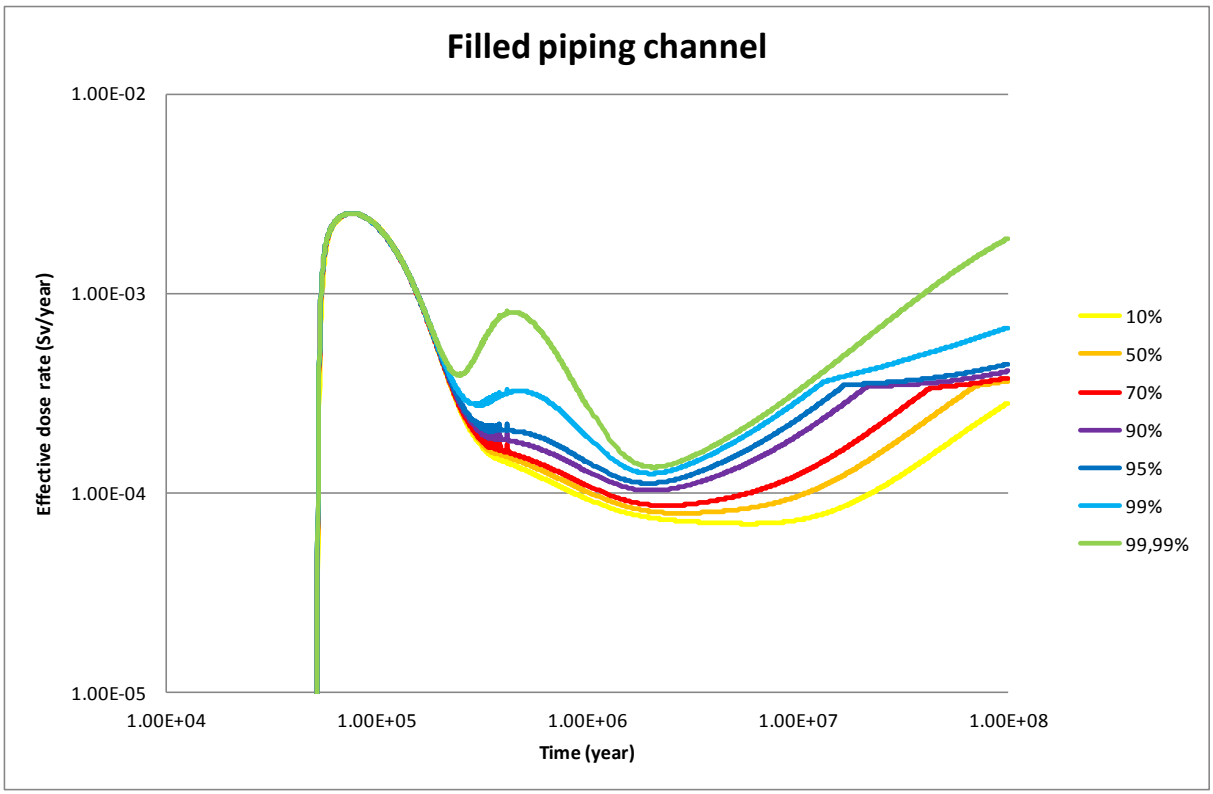

Fig. 10.15 Development of effective dose rate in the case of filled piping channel, considering different degrees of damage to the bentonite layer.

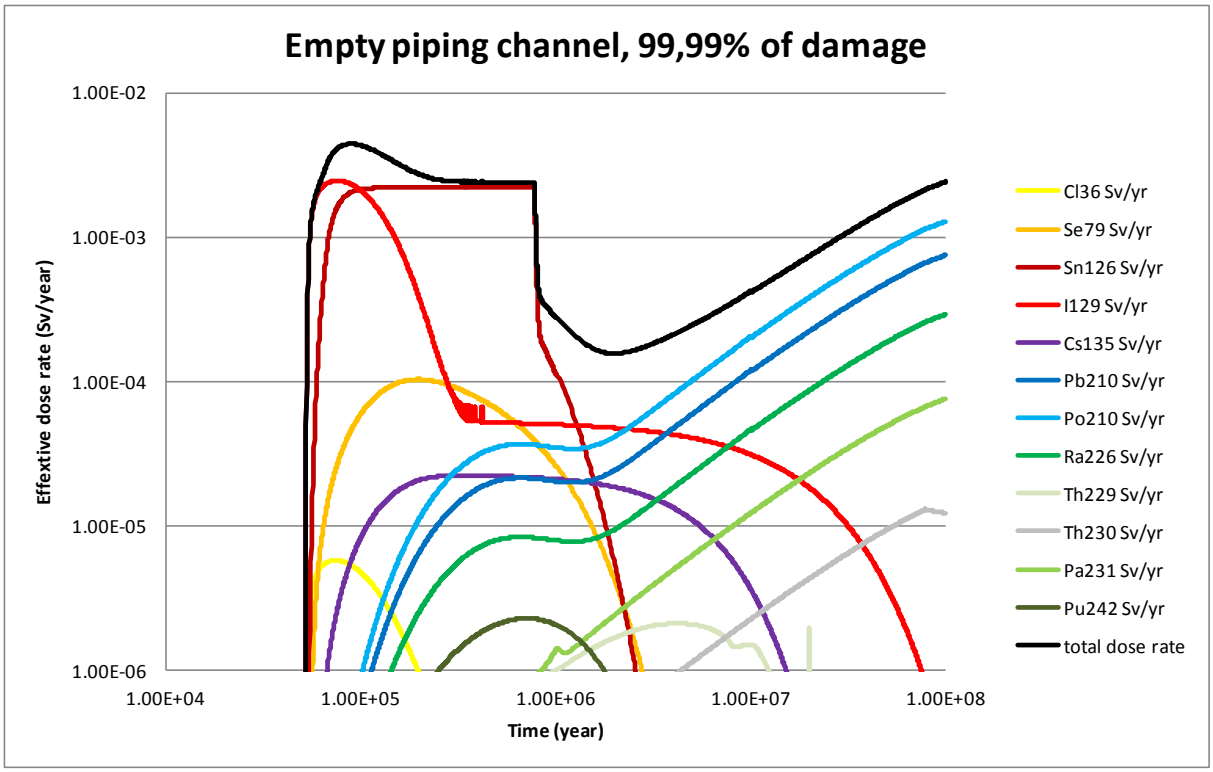

Fig. 10.16 The contributions of individual radionuclides to the total effective dose rate in the case of empty erosion channel simulating 99.99% damage bentonite layer.

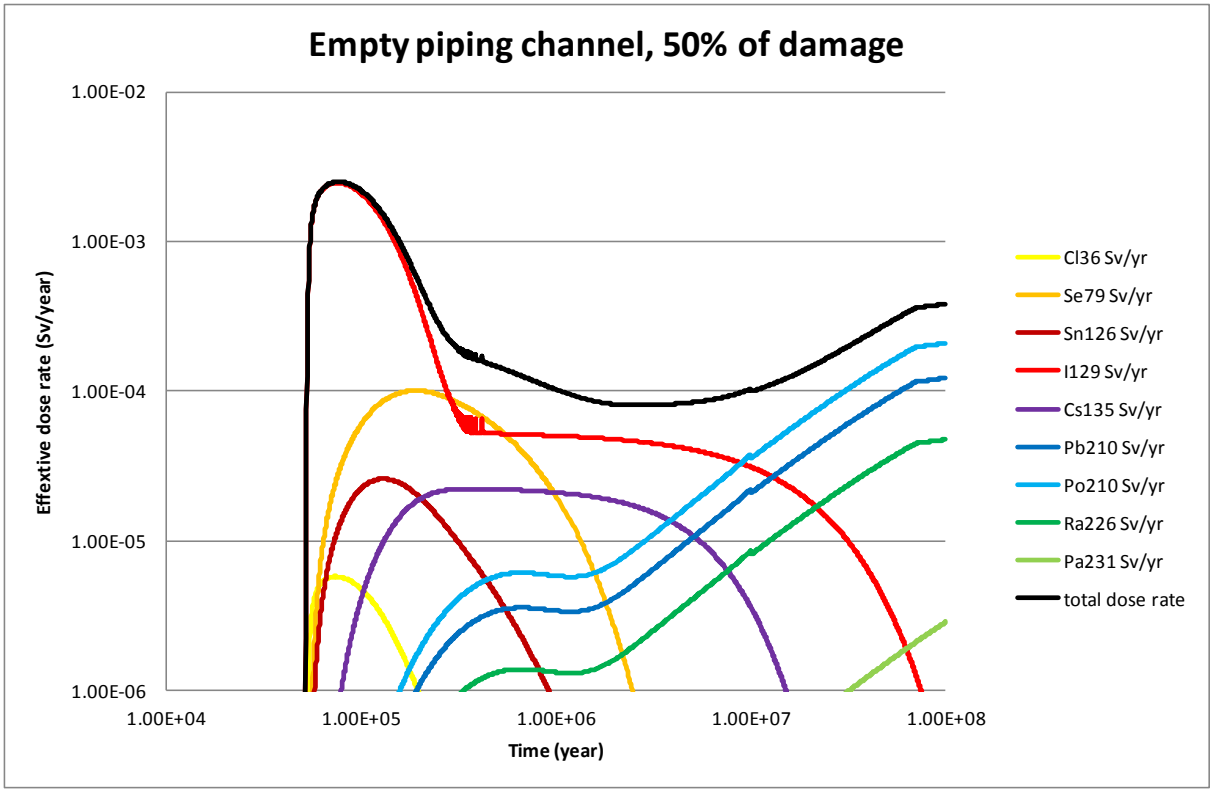

Fig. 10.17 The contributions of individual radionuclides to the total effective dose rate in the case of empty erosion channel simulating 50% damage bentonite layer.

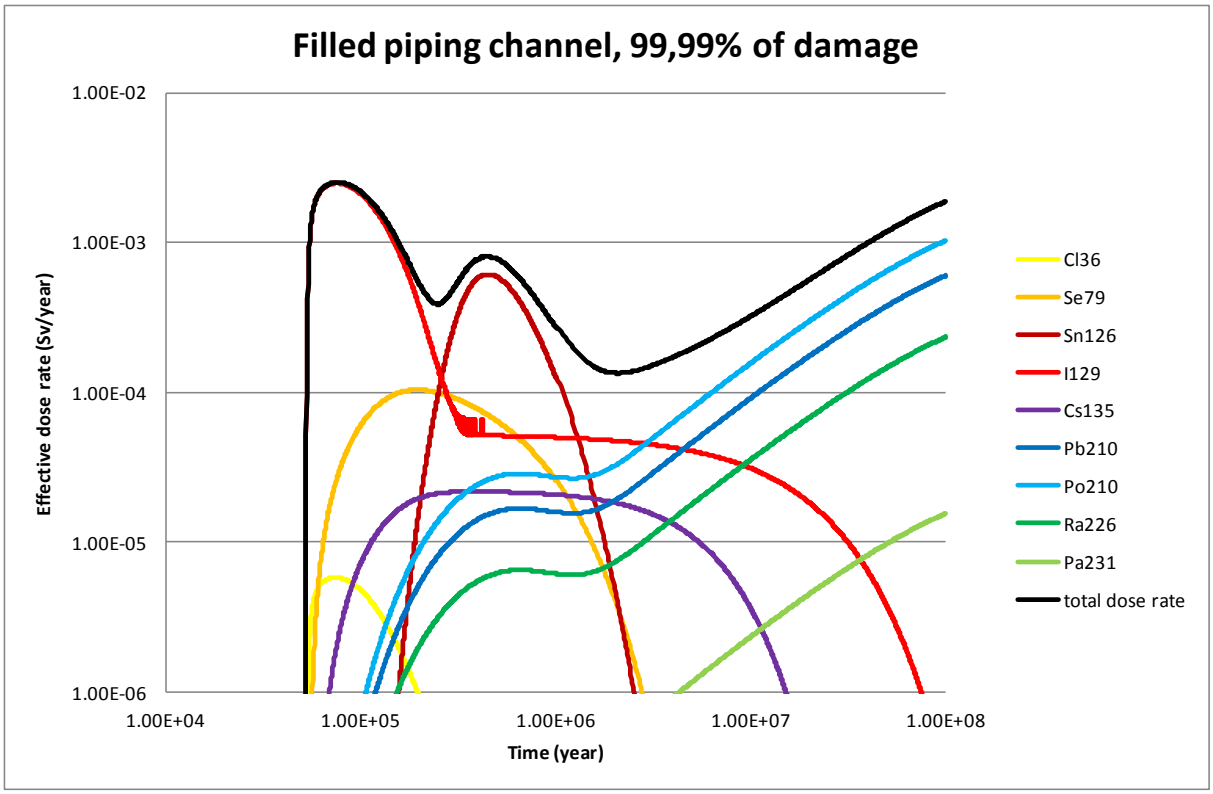

Fig. 10.18 The contributions of individual radionuclides to the total effective dose rate in the case of filled erosion channel simulating 99.99% damage bentonite layer.

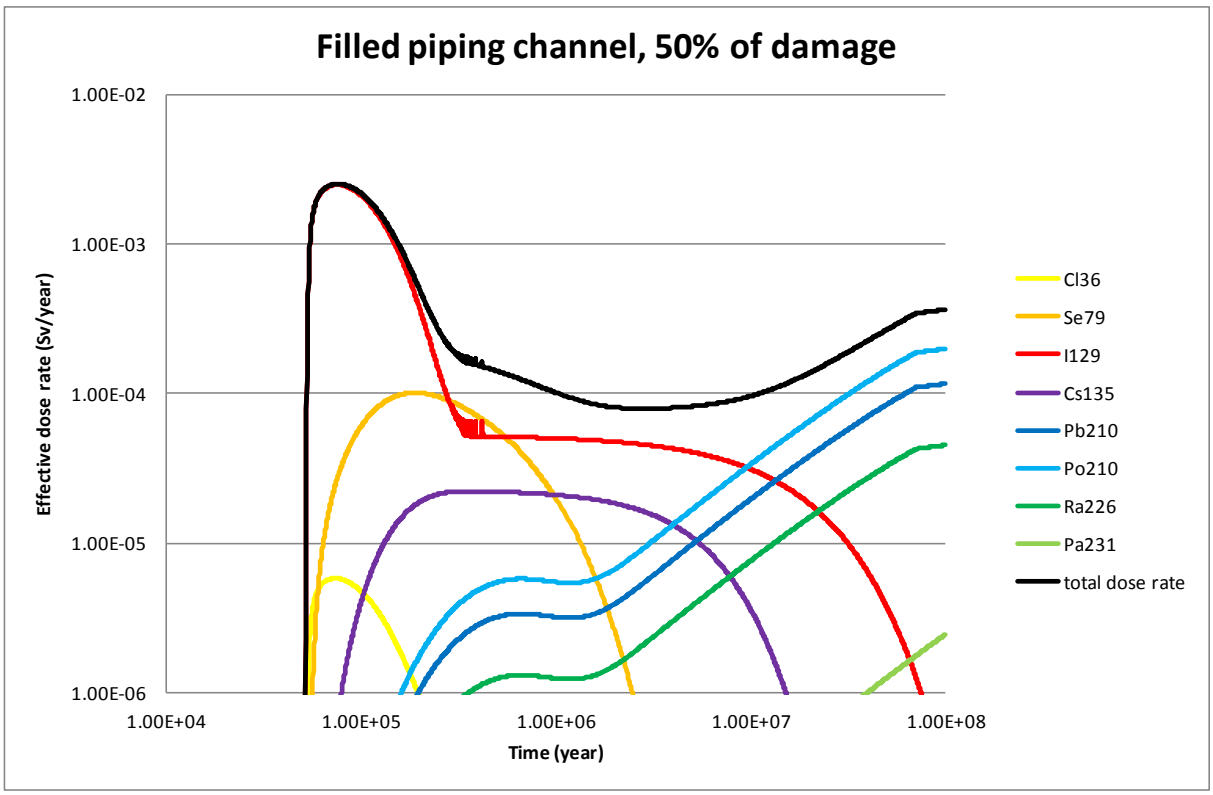

Fig. 10.19 The contributions of individual radionuclides to the total effective dose rate in the case of filled erosion channel simulating 50% damage bentonite layer.

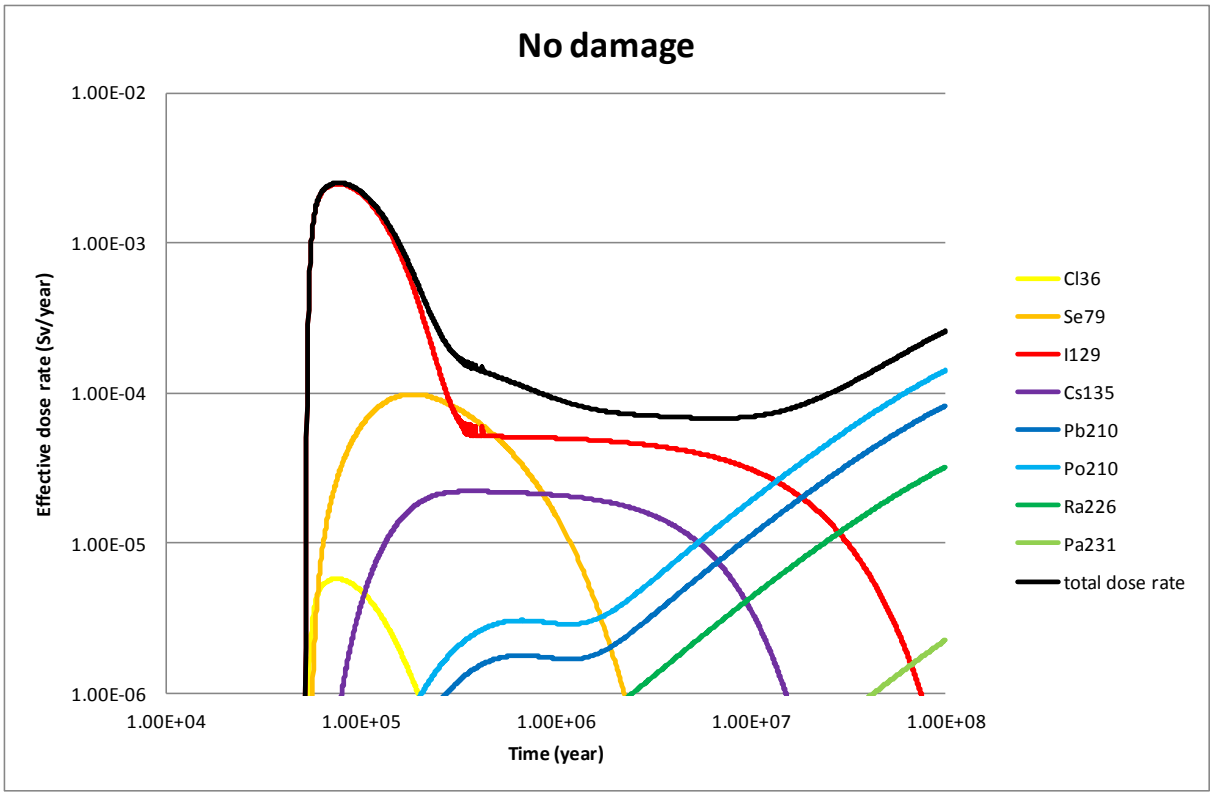

Fig. 10.20 The contributions of individual radionuclides to the total effective dose rate considering intact bentonite layer.

The results showed that the state of the bentonite layer has an influence not only on the effective dose rate, but also on contribution of dominant critical radionuclides. On the other hand, it should be noted that cases with a larger radius of erosion channels are almost unrealistic, being taken into account only for parametric study. None of the scenarios for DGR development in the Czech Republic considered the washing out of bentonite to such an extent.

11 Options to link demonstrator activities with performance assessment by the use of indicators (NRG)

T.J. Schröder, E. Rosca-Bocancea, and J. Hart

11.1 Introduction

Plugs and seals as part of the engineered barrier system (EBS) have essential roles in the design of radioactive waste disposal facilities, with the design basis and related criteria and requirements extensively reviewed in (White & Doudou, 2014 & DOPAS 2016a). Performance and safety assessments have been identified as important step in the iterative process for developing the design basis (White & Doudou, 2014, Fig. 8-1).

NRG investigated how demonstrator monitoring activities can be coupled more closely to performance assessment (PA) calculations as part of the safety case, and developed, tested and discussed options to allow the integration of the results of technical demonstrators in a PA. Performance assessment is related to the assessment of the performance of a system or subsystem and its implications for protection and safety, and can be applied to parts of a facility. Unlike in a safety assessment, it does not necessarily require the assessment of radiological impacts (IAEA, 2007). Presently the results of PA calculations are communicated in a safety case by so-called *safety and performance indicators* (e.g. Becker et al., 2009). The definition of suitable indicators allows the analysis, understanding and communication of the outcomes of PA calculations. They can have a relevant role in supporting system understanding and providing evidence for safety, and thus are expected to contribute to the overall objective of confidence building. *Monitoring* of relevant processes *in-situ*, either in experimental or demonstrator systems, on real scale in URLs or in disposal facilities, can provide valuable evidence for safety. Therefore NRG aims to develop a strategy for integration of monitoring results in PA calculations by identifying meaningful indicators that have two characteristics:

- the indicator is directly or indirectly measurable in demonstrators, and
- the indicator allows assessing the complete system behaviour.

This chapter summarizes the work performed by NRG in DOPAS Work package 5 - *Performance assessment of plugs and seals system* that is reported in (Schröder & Rosca-Bocancea, 2016).

11.1.1 Objectives

The main objective of DOPAS WP5 is to understand the implications of the plugs and seal performance on the overall safety on the long term. An important element of this work is to develop a justification of model simplifications for long-term safety assessment simulations. More specific objectives for the NRG contribution were defined as follows:

- Development and description of the overall methodology, in particular of the extensions needed to include demonstrators in existing methodologies.

- Identification of (new) indicators that can potentially be measured and analysis of their technical feasibility.
- Qualification of the potential weight (or relevance) of the indicator in respect to the (seal's) performance status by discussing its potential impact on the overall safety.
- Establishment of a generic demonstrator case, and development and application of a suitable PA model representation to derive potential evolutions of the selected indicators in time.
- Analysis and discussion of the results of the actual demonstrator's projects performed in DOPAS.

11.1.2 Safety functions

A *safety function* defines the role of a repository component in terms of its contributions to the overall safety of the disposal system, and complements the multi-barriers principle. The concept of safety function is expected to make the role of various components of a disposal concept more transparent (NEA, 2008). Slight differences in definition between different countries were noted in (Marivoet et al., 2008), and for the purpose of work in DOPAS the definition of (SKB, 2006a) is found suitable:

"A safety function is a role through which a repository component contributes to safety."

Three key safety functions of a multi-barrier disposal concept can be distinguished (Chapman et al., 2011):

- the *isolation* of the wastes by safely removing them from direct interaction with people and environment;
- the *containment* of the radionuclides by preventing for as long as required the release from the waste container;
- the *retardation* of the radionuclides associated with the waste by retaining them within various parts of the multi-barrier system until their potential hazard decreases considerable by decay.

Similar descriptions for these high-level safety functions are given in e.g. the "*PAMINA Handbook*" (Bailey et al. 2011, Section 5.4.1).

11.1.3 Scenarios and scenario analysis

Scenarios represent specific descriptions of potential evolutions of the repository system from a given initial state. They are used to identify and define assessment cases and are based on a compilation of safety relevant features, events and processes (FEPs) that are part of the safety case methodology (IAEA, 2012). Typically, five different types of scenarios can be distinguished (Röhlig et al., 2012, p.10)[1]:

[1] note that not all types of scenarios are necessarily part of a safety case or license application

1. a *normal evolution scenario*, the central scenario aimed at representing the expected evolution of the repository,
2. *plausible alternative scenarios* representing less likely but still plausible repository evolutions,
3. extreme *natural events* that are very unlikely,
4. possible *future human actions*, which may significantly impair the performance of the disposal system,
5. *'what-if' scenarios*, conceptual scenarios in which implausible or physically impossible assumptions are adopted in order to help test the repository robustness.

In the context of this chapter two aspects are of particular interest:

– The set-up of a demonstrator reflects boundary conditions that represent one or several, but not all scenarios considered in a safety case. This limits the usability of the demonstrator monitoring results for PA purposes for two reasons:

  - Because of the multi-barrier principle, it is likely that the PA calculation of the normal evolution scenario show no relevant increase of the risk, even in case of a total failure of the barrier examined in a demonstrator. The performance of a demonstrator under conditions of the normal evolution scenario is thus expected to render incomplete information on the role of the barrier for the long-term safety.
  - The environmental conditions under normal evolution are expected not to lead to any relevant impairment of the safety function of a properly designed barrier. A demonstrator reflecting normal evolution conditions may not allow drawing conclusions on the behaviour of the barrier's safety function under altered, more critical conditions.

– If the temporal evolution of each parameter of interest is computed for all scenarios considered in a safety case, this results in a group of parameter evolutions that altogether cover all potential evolutions of that particular parameter. However, it may happen that during a demonstrator parameter values or evolutions are observed that are not covered by any of the considered scenarios.

11.1.4 Safety and Performance indicators

Geological disposal of radioactive waste in deep geological formations is based on the multi-barrier concept and implies a redundant set of safety functions for each of the individual barriers. Main purpose of safety assessments is the quantification of post-closure radiological impacts of the disposal concept. This requires an analysis of the long-term evolution of a disposal system and its individual components, the quantification of the performance of the engineered barriers, and the evaluation of radiological exposure or other endpoints of the assessment. The results of PA calculations for a safety case are expressed by so-called *Safety and Performance Indicators*. These indicators provide means to assess and communicate the overall safety of the system and allow analysing and understanding the behaviour of the repository at a sub-system- or component-level.

A number of systematic schemes and formal definitions proposed for indicators have been discussed in (NEA, 2012) and shortly presented in the next sections. For DOPAS, a classification scheme is used that is adopted from (NEA, 2012) and summarized in Fig. 11.1:

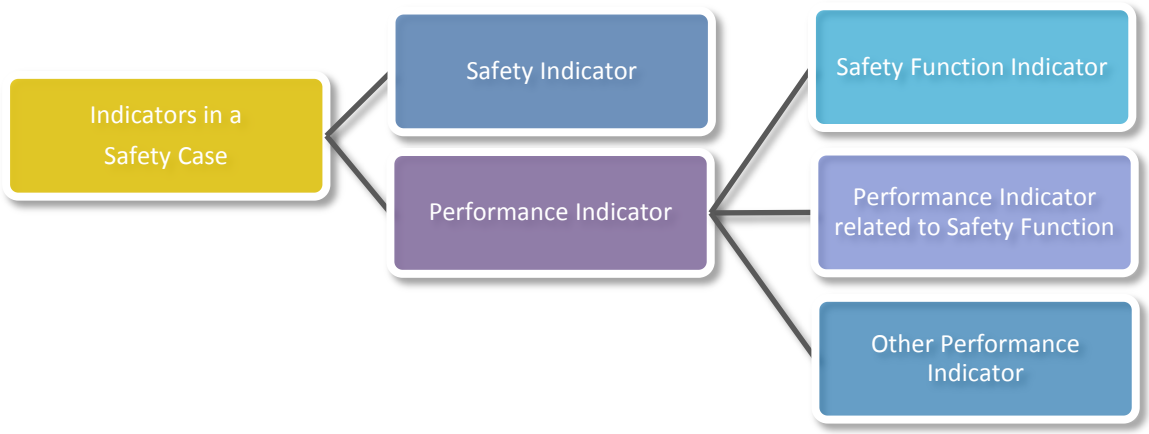

Fig. 11.1: Classification of indicators

Safety indicator

The *PAMINA* project (Becker *et al.*, 2009) provided a definition of the term *safety indicator* and the related *reference value*:

> *" A safety indicator is a quantity, calculable by means of suitable models, that provides a measure for the total system performance with respect to a specific safety aspect, in comparison with a reference value quantifying a global or local level that can be proven, or is at least commonly considered, to be safe."*

Primary safety indicators are related to a legally or regulatory defined radiological constraint. They can be accompanied by *complementary safety indicators* that provide alternative and independent means to assess the overall safety of the repository system (NEA, 2012). Primary and complementary safety indicators are results of PA calculation and cannot be directly or indirectly measured in demonstrators.

Performance indicator

A *performance indicator* provides measures of performance to support the development of system understanding and to assess the quality, reliability or effectiveness of particular aspects of components of a disposal system or the disposal system as a whole (IAEA, 2003). Several performance indicators were tested in the EC projects *SPIN* and *PAMINA* (Becker *et al.*, 2002 & 2009). While performance indicator found to be useful for PA, most indicators considered are not directly or indirectly measurable in a demonstrator.

Safety function indicator

Some programmes distinguish a subset of the performance indicators as *safety function indicators* (SFI). (SKB, 2006a) defines a SFI and the SFI criterion as:

"a measurable or calculable property of a repository component that indicates the extent to which a safety function is fulfilled. A safety function indicator criterion is a quantitative limit such that if the safety function indicator to which it relates fulfils the criterion, the corresponding safety function is maintained."

SFIs can be identified by considering the basic safety functions of the repository's multi-barriers system and can be used to demonstrate how these safety functions are fulfilled. Comparable to safety indicators, *criteria* can be developed for most SFIs to define quantitative limits. SBK develops this conceptual approach further and provides safety functions indicators and accompanying criteria for their *KBS-3* Safety Case (SKB, 2006a). They found the approach very useful in helping focus on the critical issues in safety assessment and suggested to use SFIs as instruments to discuss and prioritise FEPs once a project is mature. SKB emphasises that unlike for reference values related to safety indicators, SFIs criteria that are not met do not necessarily imply an unsafe repository. The different facets related to a safe evolution of the repository cannot be easily captured by a simple comparison to a SFI criterion (NEA, 2008).

Performance indicator related to safety functions

Performance indicator related to safety functions represents another subset of performance indicators of interest. This type of indicator was tested during *PAMINA* (Becker et al. 2009), (Schröder et al., 2009a) and is applied in the Dutch and Belgian research programme (Marivoet et al., 2009 & 2010; Weetjens et al., 2010; Rosca-Bocancea & Schröder, 2013; Schröder & Rosca-Bocancea, 2013). *Performance indicators related to safety functions* quantify the contribution of each safety function to the overall safety, and of the safety provided by the overall set of safety functions of a disposal concept. Examples of performance indicators related to safety functions defined as part of the Dutch research programme *OPERA* (Rosca-Bocancea & Schröder, 2013; Schröder & Rosca-Bocancea, 2013) are:

- *Containment* (C-RT);
- *Limitation of release* (R1-RT);
- *Retardation due to migration through buffer and host formation* (R3 - RT);
- *Retardation due to migration through geosphere* (R4 - RT);
- *Performance of the integrated repository system* (PI-RT).

11.1.5 Monitoring of indicators

The *monitoring* of various parameters and processes related to the geological disposal of radioactive waste is generally expected to have an important role in providing evidence for safety and contribute to the general objective of increasing confidence. In 2001, the IAEA defined monitoring in relation to radioactive waste disposal (IAEA, 2001) as:

"continuous or periodic observations and measurements of engineering, environmental or radiological parameters, to help evaluate the behaviour of components of the repository system, or the impacts of the repository and its operation on the environment."

Looking into the subject in more detail shows that the topic of monitoring is a complex socio-technical question, already extensively discussed in the EU-FP7 project *MoDeRn* (MoDeRn, 2012 & 2013c). Despite the progress made during *MoDeRn*, a general need was expressed to understand better what monitoring can contribute to safety, how it should be integrated in a safety case and how it can be implemented in the decision-making. These questions are topic of the ongoing European Horizon2020-project *Modern2020* (European Commission, 2015).

A number of aspects of interest with respect to demonstrator monitoring are:

- Availability of suitable technology: not all parameters or processes that are identified as useful to be monitored are directly or indirectly "monitorable". Some parameters or processes might not be measurable at the desired location and with the necessary accuracy, precision, or are only measurable during a (too) limited time interval. Careful screening of potential technologies must be performed in order to evaluate the performance of a monitoring technology in a specific setting.
- Reliability & failures: in case of deviating, "unexpected" results, it is important to be able to exclude failures of the monitoring system. This is essential for the usability of monitoring results for decision-making and is a main challenge for repository monitoring. Systematic approaches to failure detection were identified (MoDeRn, 2013b).
- Technical limitations for repository monitoring and the potential role of demonstrators: requirements for repository monitoring and available technical options present a limiting factor with respect to the kind of deviating evolutions or events that can be identified by monitoring. The discussion in the EU-FP7 project *MoDeRn* (MoDeRn, 2011, 2013a, 2013b, 2013c) shows that long-term monitoring under harsh environmental conditions as prevail in a geological disposal facility is currently technically challenging. More clarity is needed on the technical ability to detect events or evolutions that may impair the long-term safety by monitoring in the operational and post-closure phase, in order to get a realistic picture of what contribution repository monitoring actually can provide for decision-making. Demonstrator monitoring allows accessing sensors or other components of the monitoring equipment for testing, recalibration or replacement more easily than in case of repository monitoring, and thus potentially can overcome technical limitations as discussed above.

11.2 Definition of a generic demonstrator case

11.2.1 Temporal aspects of safety functions

Safety function(s) attributed to an EBS component can change with time, and in case of the plugs and seals investigated in the DOPAS project, two main periods can be distinguished:

- period of full containment
- period after container failure

Period of full containment

The first period covers the interval from waste placement until the waste container fails. The main function of barriers during this period is related to the support of the containment function of the waste container, e.g. by keeping the backfill in place or by establishing favourable chemical and mechanical conditions for the waste container. For some designs it makes sense to distinguish two other sub-phases during this period:

- **Period until full barrier performance is reached:** until the plug or seal has reached its final performance, e.g. full saturation of a bentonite seal or sufficient compaction of a salt plug, additional functions of the barrier may be of relevance, e.g. related to operational safety aspects or related to specific scenarios (e.g. early failure of container, flooding), or additional safety functions may apply.
- **Period after which the barrier function is taken over by other components:** at a certain moment in time, other barriers may take over the function of a plug or seal. For example after closure of the facility, the upstream backfill may provide additional mechanical support to keep the backfill in place and may fully substitute the plugs function on the long term, when degradation and corrosion processes may lead to an impairment of the initial performance of a plug.

Period after container failure

The second period starts from the moment the waste containment has failed, and radionuclides can migrate outside the container. The main function of the barrier in this period is related to delay the migration of radionuclides from the waste containers outside the disposal facility. e.g. by limiting the access of solutions to the waste or by avoiding advective or convective solution movements. This could also include functions complementary to the previous period, e.g. keeping the backfill in place or providing suitable environmental condition to limit radionuclide solubility.

11.2.2 Generic functional abstraction of plugs and seals during the period of full containment

In the most generic case, a plug or a seal consists of a constructional element (abutment) that keeps the downstream backfill in place. After closure, also upstream of the plug or seal a backfill is present that may take over the abutment function of the plug or seal on the long term. As part of the multi-barrier concept, several sequential abutments can be present, e.g. a plug for each disposal cell, seals or dams to close access drifts, and shaft seals to isolate the overall disposal. Fig. 11.2 provides a graphical representation of the simplified system.

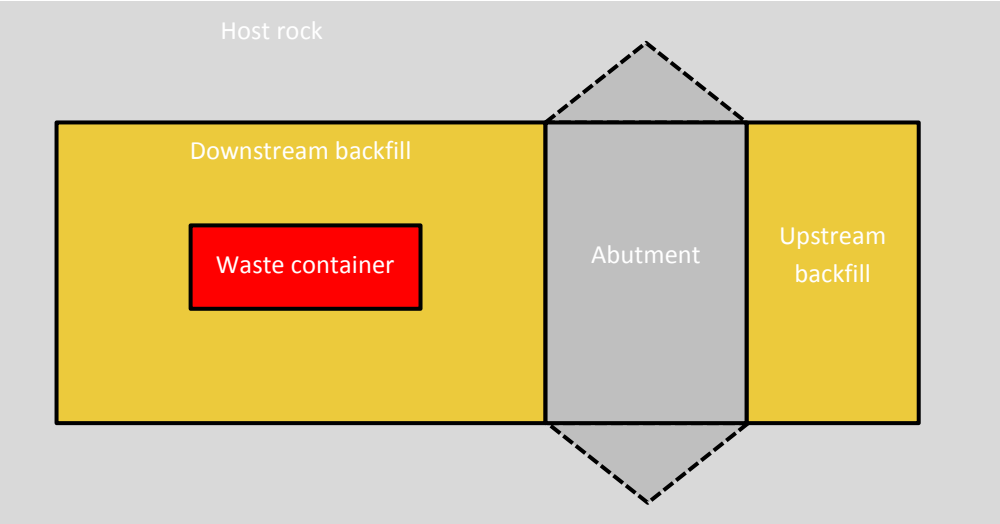

Fig. 11.2: Simplified functional abstraction

In many cases, an additional, often watertight sealing element is added, resulting in the need of an additional abutment. Here, one or two concrete blocks and a sealing element are the main structural elements of a plug/seal (see Fig. 11.3). Auxiliary components such as concrete walls or filters are mainly used to facilitate the construction of the plug. The functional period of the plugs designed for repositories in granitic rock are shorter (~100 years) than the plugs designed for geological disposal in argillaceous formations and salt rock (~1000s of years).

The host rock has a significant impact on the design of the plugs and seals:

– The main function of the deposition tunnel plugs for repositories in *crystalline rock* is a mechanical one - to keep the backfill in place. The backfill on its turn ensures that no advective transport of water and/or contaminated solutions takes place. The sealing element of the plug in this case has mainly the function to seal any cracks present in the concrete block and the space between the concrete block and the host rock, ensuring a low permeability of the overall plug construction until full saturation of the backfill is reached.
– The plugs developed for repositories in *argillaceous host rocks* have as main function to restrict water flow within the repository structure. The concrete blocks have the function of keeping the sealing element in place. The seal of the plug ensures low hydraulic conductivity and by this solute transport within the repository structure by diffusion only, until the host rock and the backfill are (re)saturated and reached their full hydraulic performance.

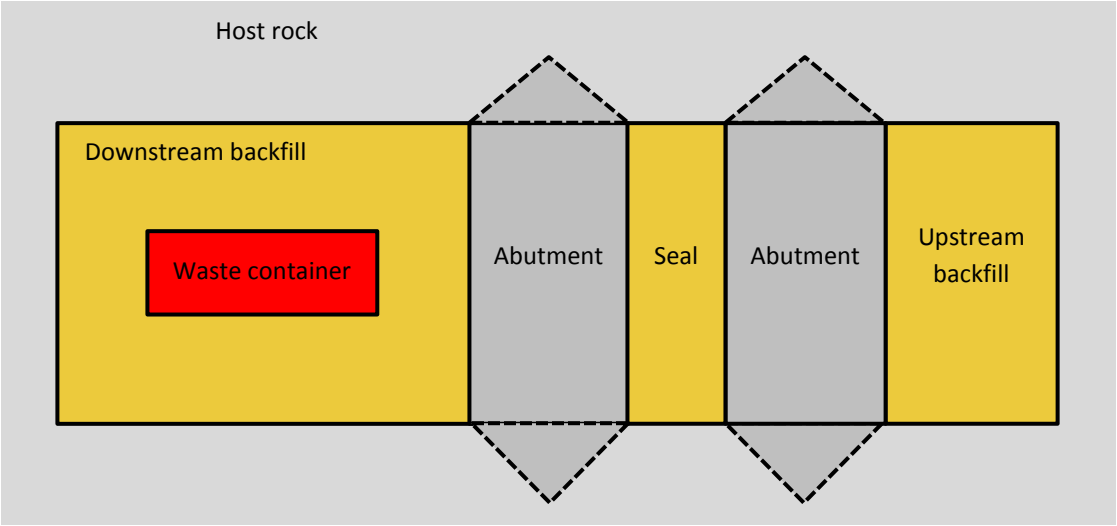

Fig. 11.3: Generic design of a horizontal plug/seal (based on DOMPLU, POPLU, FSC and EPSP plug designs)

11.3 Definition of additional PA-related indicators

11.3.1 Relevance of monitored processes for the long-term safety

The DOPAS demonstrators can be subdivided in sub-components: concrete block(s), sealing element, filter, backfill, back wall, test box, near-field. Components used for the purpose of the demonstrator, but which are not part of the actual disposal design, (e.g. the FSS test box or the DOMPLU tunnel back wall) or components having no relevance for the long-term safety (e.g. concrete abutment) were not considered in the analysis.

The demonstrator components relevant for the long-term safety are either the *backfill ("backfill end zone")* in the case of DOMPLU or the *sealing element* made of swelling clay situated between two concrete abutments in the case of FSS, ELSA and EPSP. The POPLU demonstrator contains no component with an explicit defined long-term safety function.

11.3.2 Key process for PA

The main function of the sealing element and/or backfill material is to restrict the water flow within the repository structure to avoid a transfer that bypasses the host formation during permanent, post-closure conditions. This is achieved when a *sufficiently low hydraulic conductivity* of the material is reached and diffusion is the dominant transport mechanism. In case of swelling clay, sealing will be achieved after (re)saturation of the clay, ensuring self-sealing (and self-healing). In case of rock salt, the creep of salt grit by convergence will ensure sealing. In both cases, pressure will build up in the sealing or backfill material.

There are two critical processes that may affect the long-term performance of the engineered barriers made of swelling clays:

– Loss of clay material from the engineered barriers by piping and erosion;

– Chemical alteration of the swelling clay material.

Both these effects are driven by groundwater flow and -chemistry, which are dependent on the characteristics of the site and on climate evolution.

The effect of the mass loss on the performance of the barrier made of swelling clay depends on the amount of mass lost, how local the mass loss is, and how the mass loss from the engineered barriers will be redistributed within the repository structure.

Elevated temperatures, pore water chemistry and microbial processes may cause alteration of montmorillonite and impact the performance of the seal and the buffer.

11.3.3 Indicators related to radionuclide migration through repository structure

Based on the discussion in the previous section, additional requirements can be established for an indicator assessing the long-term safety:

– The indicator considers the radionuclide migration through the repository structure;
– The indicators make a distinction between advective and diffusive transport within the repository structure (thus also the plug and/or seal) allowing the assessment of the dominant transport mechanism;
– The indicator permits the visualization of the influence of the performance of the EBS on the PA results.

The performance indicators satisfying the requirements above as well as the initial requirements (see Section 11.1) were identified and are listed and shortly described below. The relevance of these indicators for the long-term safety will be qualified in Section 11.3.4.

Hydraulic conductivity
The principal parameter identified as relevant for the long-term safety is the hydraulic conductivity, either of the sealing elements of the plug and/or of the backfill. If the hydraulic conductivity is sufficiently low, the system develops according to the (favourable) normal evolution scenario. If however the hydraulic conductivity is too high a less favourable altered evolution may occur:

– advective transport may in the long term lead to alteration of the chemical environment,
– erosion may occur,
– which may lead to increased corrosion rates of the waste package,
– and faster migration of nuclides that are released from the waste packages.

The hydraulic conductivity can be related to the swelling pressure and the density in case of a swelling clay material, or to the salt compaction and backfill pressure in case of salt grit. The threshold for the hydraulic conductivity is design- and site specific. Examples of quantitative criteria defined for the DOMPLU demonstrator are:

– $p_{swell\ backfill} > 0.1$ MPa
– $k_{backfill} < 10^{-10}$ m/s

Péclet number

The *Péclet number* reflects the ratio between the rate of advective and diffusion driven transport and provides a good indication of the hydraulic regime (Fig. 11.4). This indicator allows the formulation of a generic threshold value:

– if the Péclet number is <1, the bentonite or clay system develops in accordance with the normal evolution scenario (diffusion dominated transport),
– if the Péclet number is >1, a potential for development into a less a less favourable altered evolution scenario emerges (advective transport).

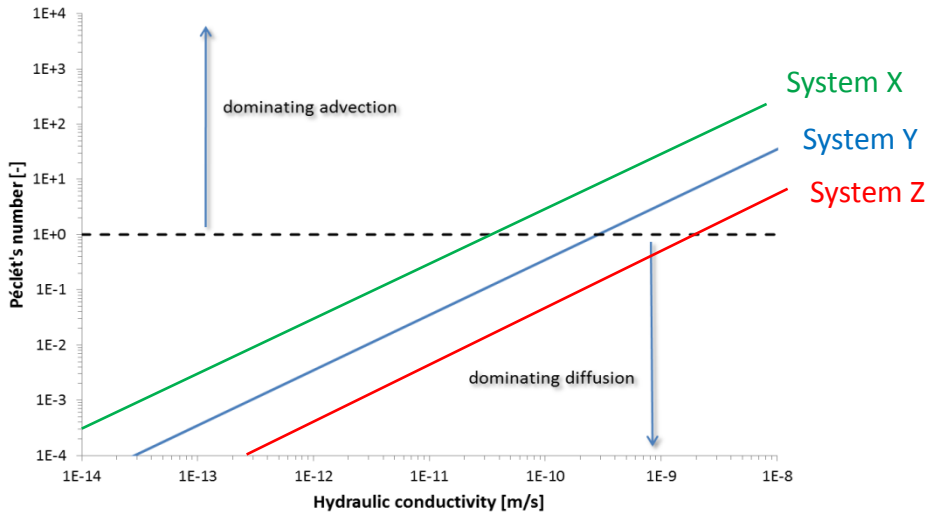

Fig. 11.4: Péclet number as function of the hydraulic conductivity

The Péclet number for a natural or engineered barrier gives an indication of its performance, however, a Péclet number large than one does not necessarily imply increased risks. The Péclet number is used by Andra (2005) and SKB (2006b) to determine the transport regime in the repository and host rock. This indicator includes system-specific information, i.e. is more 'universally' applicable than the hydraulic conductivity.

The Péclet number could be related to the scenarios used in PA, by establishing the conditions under which long-term safety cannot be guaranteed ('*scenario B*' in Fig. 11.5):

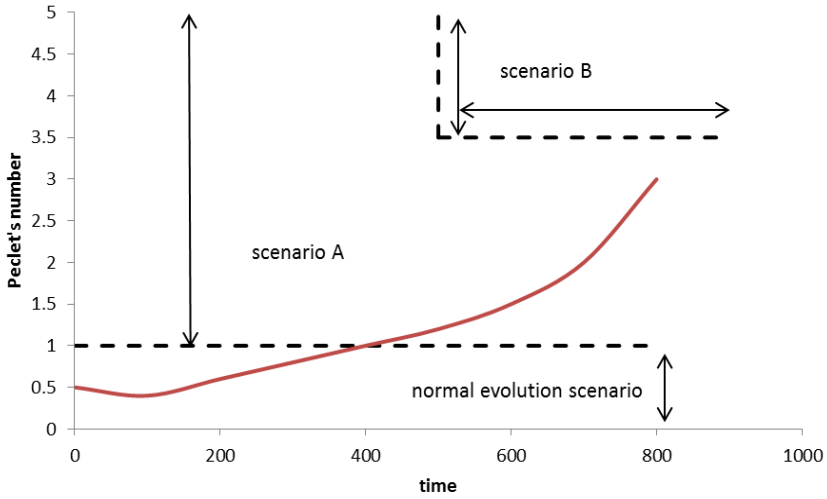

Fig. 11.5: Performance indicator *Péclet number* showing the ratio between characteristic times of advection and diffusion

Advective and diffusive flow indicators

Two other indicators making a distinction between the advective and diffusive transport are used by Andra:

- The *advective and diffusive flow indicator* provides a comparison of the advective and diffusive flows exiting the clay enclosing the repository (Marivoet et al., 2008, p. 362),
- The *distribution of radionuclide mass through different calculation compartments* permits the quantitative assessment of radionuclide distribution between unaltered host formation and the repository structures (Marivoet et al., 2008, p.366).

However, these and other concentration- and flux-based performance indicators are not measurable, and can only be linked indirectly to monitoring, e.g. via the hydraulic conductivity.

Travel-time based indicator

A *travel-time based indicator* was developed by NRG as part of *PAMINA* (Schröder et al., 2009a). This indicator supports the understanding of the system by visualizing the evolution of the repository and depicting in one graph the most relevant variables influencing the breakthrough of the radionuclides.

This indicator can be linked to several safety functions and can be either flow- or concentration-related (e.g. '*dose rate in the biosphere'*, '*radiotoxicity concentration in groundwater*', '*radiotoxicity flow to biosphere'*). It also allows to decompose the problem into several elements: breakthrough curves can be computed without knowledge of waste inventory, and do not need to account for radionuclide decay (chains). Other parameters of interest can be varied (e.g. hydraulic conductivity, porosity), or different scenarios could be combined in one graph. The indicator can be calculated for different scenarios and is expected to be applicable on different disposal designs and host rocks.

11.3.4 Indicators of relevance for the long-term safety

The potential weight (or relevance) of a barrier-related indicator for the overall safety can be assessed by a '*relevance related indicator'*. *Performance indicator related to safety functions* were used in *PAMINA* to quantify the contribution of a safety function to the overall safety (Becker et al. 2009). By specifying the indicators on barrier level rather than on safety function level, the relevance of each component of a multi-barrier system could be evaluated.

In PA, next to a central, most likely evolution of the disposal system, several altered scenarios are analysed (e.g. subrosion, earthquake, abandonment, human intrusion, early failure). Alternative to the screening of FEPs, analysis of potential failures modes of EBS components can serve for the identification of additional scenarios, e.g. by analysing the influence of a poor performance of a plug on:

– displacement, permeability, porosity & density of backfill & buffer,
– (local) erosion of backfill & buffer,
– effects on canister corrosion.

If necessary, additional synthetic '*what-if*'-scenarios can be defined or 'Design-Based-Accident' type of analysis could be performed, assuming systematic (fictional) failures or inadequate performance of barriers components.

Next to the analyses of *performance indicator related to safety functions* on barrier- and component level, sensitivity- and uncertainty analyses allows to analyse barrier functions on process- and parameter level, hence allowing the link to monitorable entities.

Such an approach would allow a systematic quantification of the relevance of barriers or barrier components and their related processes and parameters to the overall safety for a variety of scenarios and assumptions (Fig. 11.6):

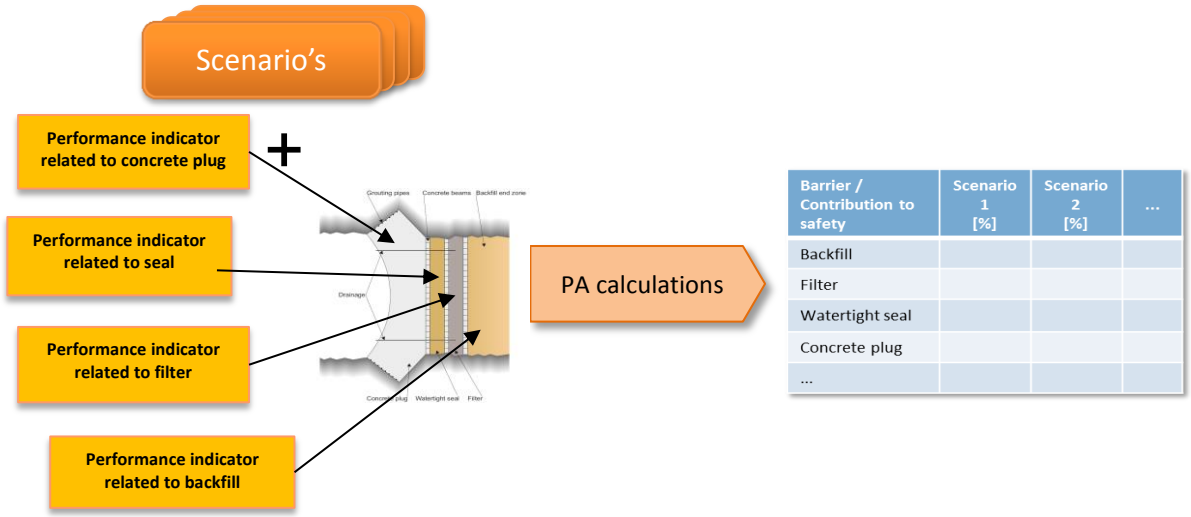

Fig. 11.6: General approach to access the relevance of individual barrier elements on the long-term safety

11.4 Establishment of a generic demonstrator case

For assessing potential evolutions in time of indicators relevant for the performance of plug and seals, a generic demonstrator case was established. The PA model developed by GRS as part of the DOPAS project to assess the performance of the ELSA shaft sealing concept utilizing the LOPOS computer tool (Rübel et al., 2016) forms the basis of this demonstrator. The main objective of the LOPOS simulations was to assess the amount of brine inflow, given the situation of a brine presence on top of the shaft, through the different shaft layers into the model repository. In the LOPOS simulation, properties of the shaft and repository (e.g. porosity, permeability) were assumed constant.

A sketch of the model segment structure for the ELSA shaft sealing concept (GRS, left) and the generic demonstrator case (NRG, right) are depicted in Fig. 11.7. Details of the LOPOS model developed by GRS (Rübel et al. , 2016) and NRG's generic demonstrator case (Schröder & Rosca-Bocancea, 2016) are described in the indicated references.

NRG adopted the following assumptions for the demonstrator case:

- The shaft has been modelled as a single porous medium with properties averaged from the LOPOS data.
- On top of the shaft a layer of brine with constant properties models a flooding scenario; as a result of the hydraulic gradient over the shaft, brine percolates through the shaft into the repository (1).
- The infrastructure area of the repository is modelled as a single segment containing salt grit backfill, enabling the repository volume to converge as a result of pressure exerted by the overburden (2). The development of the convergence rate in dry (initially) and wet (after start of the brine inflow) is simulated according to the models describing the compaction behaviour of salt grit in (Schröder et al., 2009b).
- As soon as the volume of the brine inside the infrastructure area of the repository equals the pore volume of the compacting repository, the inflow of brine is terminated and is subsequently reversed (3) due to the ongoing compaction of the repository volume. This effect has not been taken into account in the LOPOS simulations.

The main difference between GRS's LOPOS model and NRG's demonstrator case relates to the assumptions made for the backfill of the infrastructure area of the repository: in the LOPOS model the infrastructure volume is backfilled with non-compacting gravel, whereas in NRG's demonstrator case compacting salt grit is assumed as backfill.

The purpose of backfilling the infrastructure areas with non-compacting gravel is to allow potential brines and gases to accumulate there. Additionally, the gravel impedes the convergence of this volume due to pressure exerted by the overburden, and therefore also any outflow of brine trapped inside the repository.

Assuming a compactible salt grit backfill (NRG) enables the repository volume to converge, and squeezing out of trapped brine and, if present, any dissolved radionuclides.

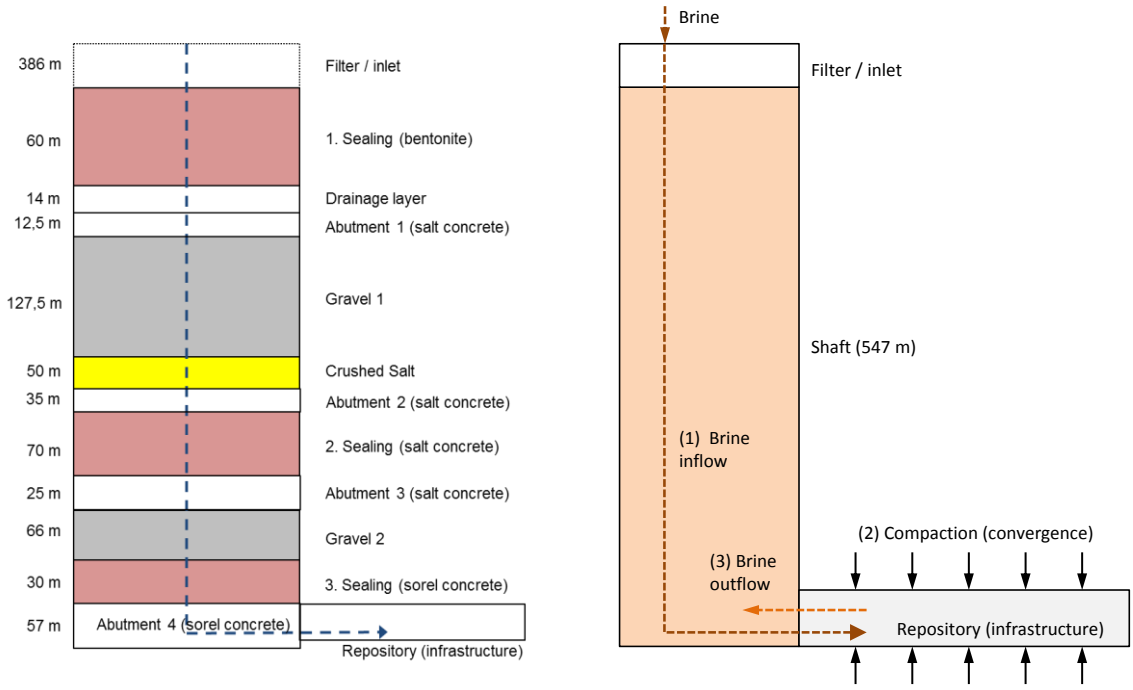

Fig. 11.7: Set-up of NRG's generic demonstrator case (right) based on GRS's PA LOPOS model (left)

The overall system behaviour of the modelled repository is shown in Fig. 11.8. By imposing an initial convergence rate ($1 \cdot 10^{-4}$/a), the repository pore volume decreases in time (green curve). Starting from 700 years, brine slowly percolates into the repository (red curve), until the volume of the infiltrated brine equals the decreasing repository pore volume, at approximately 41'000 years. From that time on brine present inside the repository is squeezed out due to the ongoing convergence of the repository (red and blue curves). It is noted that the outflow of brine is restricted in the time interval 41'000 to 58'000 years due to the hydraulic resistance of the vertical shaft.

As a result of the ongoing convergence of the repository, the salt grit backfill experiences stress from the surrounding host rock and will therefore be compacted as time progresses. Consequently the porosity and therefore also the permeability of the plug will decrease. At a certain point in time (here: about 80'000 a) the repository' effective pressure equals the backfill stress, and the ongoing convergence rate is slowed down significantly, as is the outflow of brine.

At the end of the simulation a total amount of approximately 4300 m^3 of brine is squeezed out of the repository into the vertical shaft. This amount of brine would fill up the shaft from below up to the "Gravel 1"-layer (cf. Fig. 11.7).

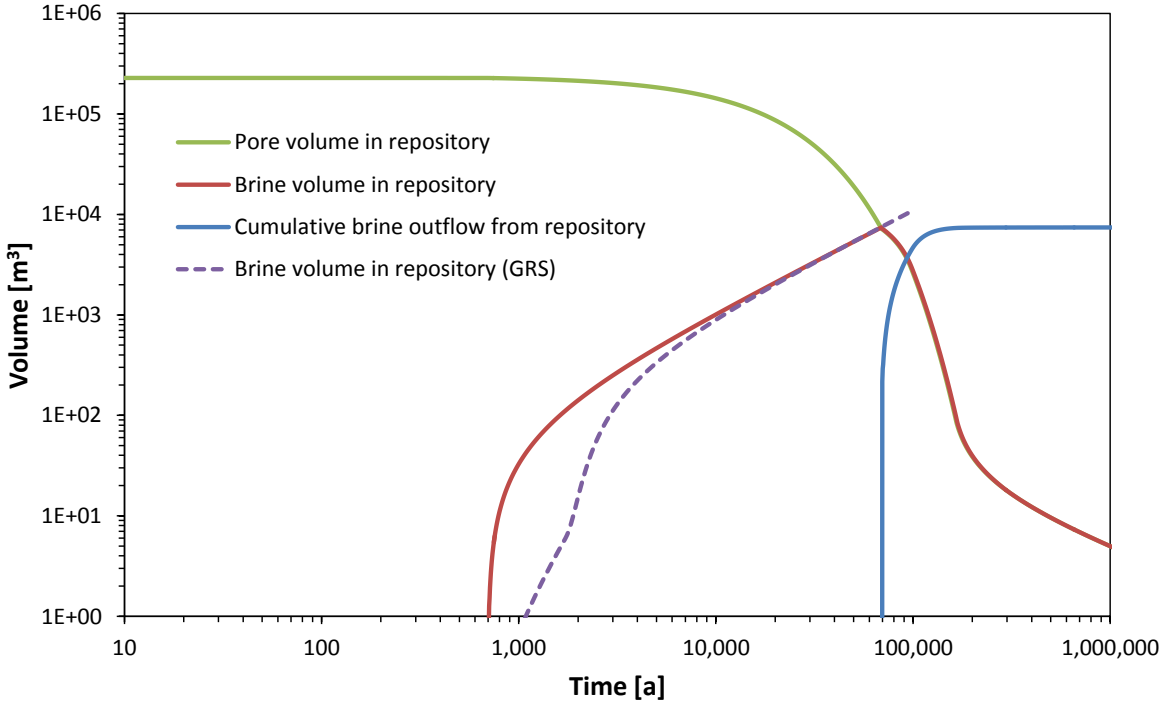

Fig. 11.8: Evolution of repository and brine volumes

Combining the system behaviour described above with the travel-time based indicator described in Section 11.3.3 provides insight about the breakthrough of radionuclides in the repository. In the present generic demonstrator case the following assumptions have been applied:

- Three different initial convergence rates for the repository pore have been considered, viz $0.5 \cdot 10^{-4}$/a, $1.0 \cdot 10^{-4}$/a, and $2.0 \cdot 10^{-4}$/a;
- For the safety indicator *radiotoxicity flux to the geosphere*, a reference value (criterion) of 0,1 Sv/a at the exit of the repository has been assumed (Becker et al., 2009; Table 5.8).
- Given the long time period until the outflow of brine (several ten thousands of years), it is conservatively assumed that all brine from the disposal will be directly enter the geosphere, rather than entering the shaft (i.e. the reference value is applied to the interface repository/shaft).
- Conservatively, a perfect mixing of the brine in the infrastructure area is assumed.

The travel time indicator can be calculated by dividing the reference value by the outflow of brine from the repository, and is depicted in Fig. 11.9 (red, black, and green curves). It shows the maximum concentration of radiotoxicity that can be present in the infrastructure area of the repository without exceeding the given reference value for the case considered.

For comparison, the evolution of the total radiotoxicity of the inventory of a single CSD-V container of vitrified high-level waste (HLW) has been indicated in Fig. 10.9 (blue dotted solid line), including parameter uncertainties of the used process model parameters (blue dotted lines). The blue curves are based on an assessment of the generic Dutch disposal concept

in rock salt (Schröder et al., 2009b), quite comparable to the German concept, with a borehole plug from salt grit compacting due to convergence processes. The inventory of the borehole consists of 300 CSD-V containers with vitrified high-level waste (HLW). A synthetic assumption of a flooding scenario was made, combined with an immediate failure of all canisters. The figure shows - even for the very conservative and unlikely scenario assumptions - that the radiotoxicity in the repository remains below the indicator value at all times and for all assumed repository convergence rates that in the time interval 20'000 to 200'000 years, the indicator falls below the radiotoxicity of the container. Consequently, existing downstream barriers (i.e. sealing dams, plugs of the disposal galleries, and disposal gallery backfill) need to reduce the radiotoxicity concentrations in the infrastructure area by a factor of 16 for each container in order to meet the reference value.

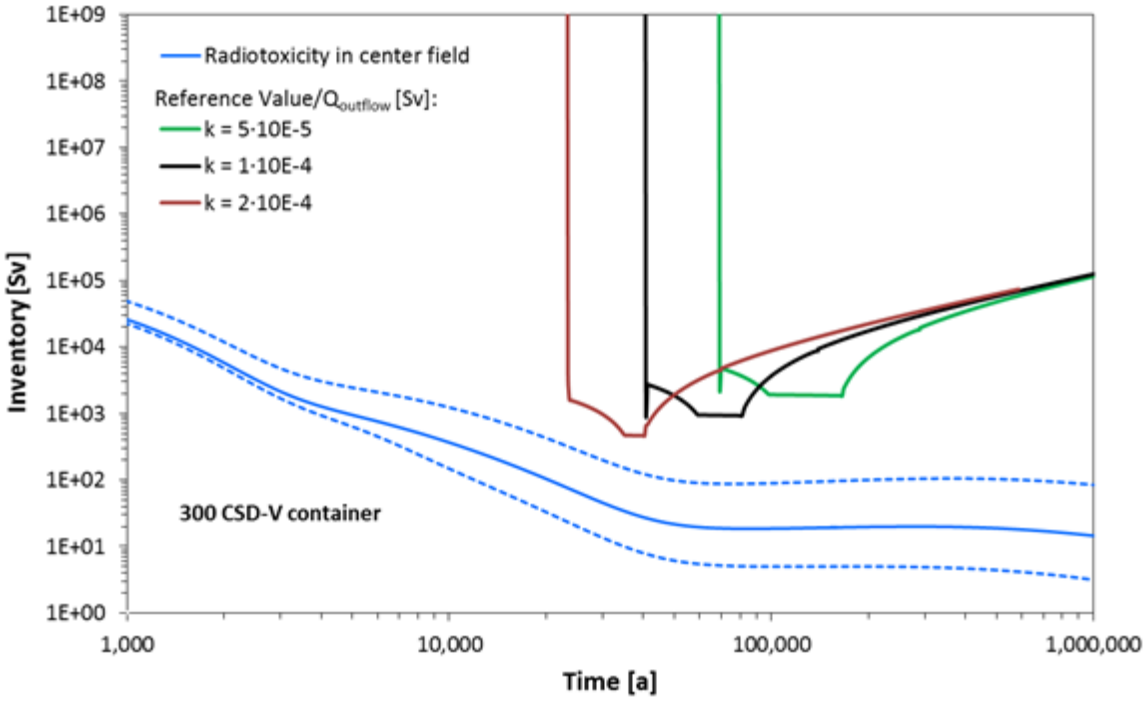

Fig. 11.9: Evolution of indicator and radiotoxicity in repository for three initial convergence rates *k* and an inventory of 300 CSD-V containers

The following observations apply on the results of the present generic demonstrator case:

- Although the results are not shown here, the temperature has a minor effect on the convergence rate of the repository, and therefore the outflow of contaminated brine from the repository. Consequently, measurement of the temperature is less relevant for providing information about the long-term safety of the repository.
- The absence / presence of brine (humidity) is crucial in relation to the long-term safety of the repository. Determination of the presence of brine by monitoring can be easily achieved, e.g. by measurement of the electrical conductivity. However, due to the long time scales involved - percolation of brine is expected only after several hundred years - currently no mature technology is available to monitor this.

– The presence of brine at various locations inside the shaft can in principle be detected in time frames shorter than several hundred years. If brine would be detected inside the shaft this information may help to analyse in detail the consequences of repository flooding.
– A parameter that is relatively straightforward to measure and that provides relevant information about the development of the repository system, including the shaft, is the pressure (pore pressure, total pressure). Although not analysed in the present generic demonstrator case, the pressure inside the shaft can provide information about the convergence of (parts of) the shaft, and therefore the further reduction of the permeability and resistance to brine intrusion.

Additional simulations and consideration on the generic demonstrator case are reported in (Schröder & Rosca-Bocancea, 2016).

11.5 Synthesis & conclusions

– *Monitoring* of demonstrators can provide relevant evidence for safety, and knows less technical limitations than repository monitoring. However, operation time is a critical aspect in demonstrator monitoring, because relevant processes, e.g. the resaturation of swelling clay (bentonite), are rather slow and may exceed the operational life time of the demonstrator.
– *Safety functions* are useful abstractions of the safety concept on a barrier level. Generally, two safety functions of plugs and seals can be distinguished:

  - *isolation and containment*, sometimes taken over by other EBS-components at later phases, and
  - *retardation* of radionuclide migration, of interest from the moment of container failure.

– *Indicators* are important tools in communicating safety. For "monitorable" indicators, only performance indicators are of relevance. From these, the *safety function indicators* and *performance indicators related to safety functions* are of most interest:

  - *Safety function indicators* and their related *criteria* are useful tools in providing evidence for safety. However, they do not provide direct information on the long-term safety in case criteria are not met: due to the multi-barrier principle and the complex interactions of repository components, non-compliance with a criterion not necessarily implies an unsafe repository, and relevantly increased risks might be limited to few scenarios with limited likelihood. Currently provided SFI criteria have limited value for PA, because these are based on identifying what 'guarantees' safety rather than evaluating under which unfavourable circumstance references values still can be met.
  - *Performance indicators related to safety functions* allow to quantify the contribution of each safety function or EBS-(sub)component to the long-term safety, eventually broken down to process- and parameter level by the use of uncertainty- and sensitivity analysis. Such analyses can be performed for each considered scenario, and for better

system understanding, "*what-if*"-scenarios can be defined in order to challenge each barrier component within a multi-barrier approach.

- *Scenario definition* and *-analysis* are useful tools, they allow identifying conditions under which the performance of an individual barrier can be of relevance for the overall safety. Furthermore, the full set of scenarios considered in a programme defines for each parameter a value range in which monitoring data should fall. However, a deviation of parameters from their expected evolution does not necessarily imply an unsafe repository.
- The constructional components of plugs and seals made of cementitious materials as considered in DOPAS have no relevance for safety on the long term, i.e. the period after container failure. The EBS components relevant for the long-term safety in DOPAS are either the backfill or the sealing element made of swelling clay located between two concrete abutments.
- Identification of monitorable parameters relevant for PA should focus on hydraulic aspects, related to permeability, pressure, porosity, compaction, and convergence etc. For disposal systems in rock salt, the presence of brine is an important factor, which is monitorable by e.g. measurement of the electrical conductivity.
- A simplified approach for analysis of plugs and seals is provided, based on the DOPAS input, distinguishing between two functions: (1) *isolation and containment* of the waste, and (2) *retardation* of radionuclide migration. The latter is of relevance for PA, and hydraulic abstraction of the sealing system together with known source terms and/or reference values allows the assessment of the long-term safety.
- One of the primary goals in geological disposal is to prevent or otherwise minimize the transport of radionuclides and other potentially hazardous substances within the repository and through the host rock. Most of the parameters characterising the mass transfer cannot be monitored neither in demonstrators or *in-situ*, but can be determined through indirect measurements or laboratory experiments only. The derivation of these parameters involves process assumptions as a rule.
- None of the indicators relevant for the long-term safety and analysed in this work is directly measurable in the DOPAS demonstrators. Indicators providing information about the long-term safety are based on indirect measured parameters in combination with a set of assumptions related to the rest of (not monitored) compartments of the system. Only on the longer term, i.e. after several decades, in the case of resaturation of clay or compaction of rock salt grit, these indicators may provide relevant information about the evolution of the seals and plugs in geological disposal.
- The principal parameter identified as relevant for the long-term safety is the *hydraulic conductivity* within the repository system. The hydraulic conductivity can be related to the swelling pressure and the density in case of a swelling clay material, or to the salt compaction and backfill pressure in case of salt grit. It varies strongly with the degree of saturation or compaction and reaches a constant value when equilibrium within the system is established: saturation in case of swelling clay or far-reaching compaction in case of salt grit. Only the value of the hydraulic conductivity at equilibrium is relevant for the long-term safety.

12 Conclusions

Geological disposal of radioactive waste involves isolation and containment of the waste from the biosphere. Containment and isolation can be provided through a series of complementary barriers, e.g. the waste form itself, waste containers, buffer and backfill materials, and the host geology, each of which will be effective over different timescales. As part of the backfilling and closure of a repository, specific parts will have to be closed and sealed. The purpose of plugs and seals will depend on the disposal concept, the nature of the geological environment and the inventory to be disposed. Plugs and seals e.g. may be required to

- isolate emplaced waste from the rest of the underground excavations during the operating phase to limit radiological exposure to the workers,
- support other EBS components until the repository has evolved to its desired state,
- limit groundwater flow and radionuclide migration,
- prevent inadvertent or unauthorized human access.

Five different plugs and seals were the subject of the DOPAS project. The function of these plugs and seal were mainly related to the two requirements given above to support other EBS components until the repository has evolved to its desired state and to limit groundwater flow and radionuclide migration. Those plugs and seals that limit water and radionuclide flow have a much longer requested functional life than those that support other EBS components.

The DOPAS Project aimed to improve the industrial feasibility of full-scale plugs and seals, the measurement of their characteristics and the control of their behaviour in repository conditions. The role of WP5 within the DOPAS project was mainly twofold: to support the planning, construction and experimental work of the large-scale demonstrators by predictive process modelling and to understand the implications of the plugs and seal performance on the overall safety for the whole reference period of a final waste repository. A variety of modelling tasks has been performed within the Work package 5 of the DOPAS project to fulfil this role with the following objectives:

- simulation of processes and their evolution within individual sealing components,
- predictive modelling to support the design and the construction of the large-scale seals,
- modelling of small and mid-scale experiments performed in WP3 to gain process understanding,
- identification of the main processes that are relevant and thus to be considered for predicting the short and long-term behaviour of the plug and sealing systems,
- identification of remaining uncertainties and their influence on performance assessment,
- development and justification of conceptual models of plugs and seals for the different disposal concepts and geological environments and
- development and application of the PA methodology and integrated PA models to analyse the system behaviour.

The work has been reported in various WP5 and WP3 deliverables. This report shortly summarises this work and provide links to all the underlying reports that give more detailed information.

The high-level design basis of a sealing system (reported in the DOPAS WP2 deliverables) describes the principal safety functions that plugs and seals have to fulfil as part of the overall safety objective of a repository system, typically in a qualitative fashion. The safety functions and performance requirements of the seal which are tested in the DOPAS modelling work of Work package 5 are:

- the mechanical stability and
- the hydraulic conductivity, i.e. water tightness of the seal.

The latter is investigated regarding two aspects, either the initial hydraulic conductivity at the time of construction, or its long-term development.

The large part of the modelling work was predictive modelling performed prior to or in parallel to the experiments and only a small part was to evaluate obtained results after the experiments. The main use of the predictive WP5 process modelling was to

- design the seals,
- to support construction,
- to predict experiment evolution,
- to predict material behaviour and
- to test models.

The input data which was used in this type of modelling was derived only to a minor part from experiments from WP3 of DOPAS, but mainly from existing data obtained in laboratory experiments of the participating organisations prior to the DOPAS project, and from existing literature. The experiment related models did use the planned or similar material specifications and structural designs what was implemented at DOPAS. The validation of the work based on the monitoring results was not done. The reason for this is that the main results from the larger scale experiments were not available within the project duration of DOPAS. Even for the mid- or small-scale laboratory experiments, only a minor part of the modelling work was performed to evaluate results of experiments. A large amount of experiments that have been started in DOPAS will be continued beyond the end of the DOPAS project. Therefore, more modelling work is expected to be performed in the future to interpret the results. Additionally, it has to be recognised that the work is only a small part of the large context of a repository system subject to many processes with or without interaction with each other/s. The implications to the safety case will be evaluated at the next stages of the individual waste management programmes as part of the forthcoming integrated performance assessments and safety cases.

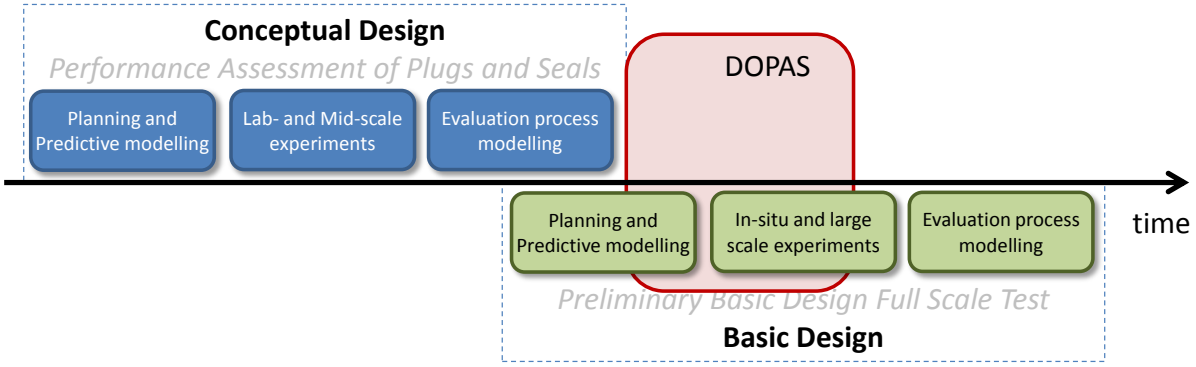

Fig. 12.1: DOPAS in the life-time of the experimental program to investigate plug and seal behaviour

The aspect of DOPAS in the life-time of the experimental program to investigate plug and seal behaviour is further illustrated in figure 12.1. Even for DOPAS, with 48 months of duration being a long running EU project, this project can only represent a short section of the long time-span for the iterative process of preparative laboratory work, planning of a large-scale experiment, executing the experiment and finally investigating the results by process modelling. For example even for the metric scale experiment (REM) by ANDRA, which only acts as a small scale model for the full scale experiment, the full resaturation time was estimated to be about 30 years. Due to the different stages the different experiments were in at the beginning of DOPAS, mostly all parts of the experimental cycle were covered by DOPAS, except the evaluation process modelling of a large-scale experiment. While on the one hand, the ELSA experiment still was in an early stage of laboratory and mid-scale experiments, on the other hand the installation of the DOMPLU experiment was already ongoing. Due to this temporal shift, different stages of the experimental process were investigated in DOPAS.

As a consequence of what has been said before, the process modelling tasks related to the EPSP, FSS and ELSA were not regarding the full-scale experiments, but smaller analogues. Only the process modelling related to the POPLU experiment regarded the full-scale experiment, but as predictive modelling. Some modelling tasks addressed questions of integrated modelling for safety assessment and the integration of the results in the safety case. The integrated performance assessment model to represent the near-field of the repository in salt was updated to better represent the experimental findings on material behaviour (GRS, chapter 8) and to investigate the use of indicators in total system performance assessment to test the performance of sealing systems (NRG, chapter 11).

The aim of the modelling work in DOPAS can be concluded in general as being clearly related to the behaviour of the individual experiments, but not to predict the long-term behaviour of the full plug in the repository system and can be summarised for the individual experiments as follows:

– **FSS**: The modelling related to the FSS experiment does not address the behaviour of the full-scale sealing system, but the complementary metric-scale REM experiment which in-

vestigates the saturation of the bentonite. The timescale regarded in this experiment and the modelling is some decades of years.

- **EPSP:** The modelling related to the EPSP plug does not address the behaviour of the full-scale seal itself. Modelling includes the investigation of the bentonite during resaturation in a complementary laboratory experiment. The time-scale of the modelling is some years.
- **DOMPLU:** Modelling of the DOMPLU experiment was not part of the DOPAS Project since it was done prior to DOPAS, but monitoring within DOPAS WP4 gave feedback to the model validation and design iterations.
- **POPLU:** The modelling related to the POPLU plug includes water tightness and mechanical stability of the plug related to the plug performance during the experiment. The POPLU experiment is the only experiment where modelling of the behaviour of the full plug system has been performed in WP5. This timescale regarded in the modelling is the intended lifetime of the experiment.
- **ELSA:** The modelling related to the ELSA experiment includes the mechanical and chemical performance of the reference shaft materials. There has been an integrated modelling of the full system and lifetime of the ELSA sealing system, but that of course lacks a detailed description of the actual long-term development on the process-level, but is only an abstracted one. The timescale regarded in the process modelling is the timescale of the individual experiments.

All types of processes were modelled in DOPAS including thermal (T), mechanical (M), hydraulic (H) and chemical (C) processes. However, coupling of those processes was addressed only to a very minor degree in WP5. Table 12.1 shows which process have been regarded in the modelling of the different experiments. The processes regarded comprise the following hydraulic and geomechanical evolution of the seals and sealing materials:

- Hydraulic state evolution of the seal
  - Flow rates of fluid through the seal with time
  - Temporal evolution saturation state of the sealing pore space
  - Temporal evolution of the pore pressure of fluids in the seal
- Mechanical state evolution of the seal
  - Temporal evolution of the mechanical stress and load of the seal
- Hydraulic and mechanical coupled evolution of the seal
  - Temporal evolution of seal permeability
  - Temporal evolution of the sealing porosity
  - Temporal evolution of the total pressure in the seal
- Chemical evolution of the sealing and the sealing material
  - Mineral phase changes in sealing material

These processes present a large variety of the different processes which can be expected in the lifetime of an experiment. However, no fully coupled model was used in DOPAS.

Tab. 12.1: Information on the processes modelled in DOPAS: thermal (T), hydraulic (H), mechanical (M), chemical (C)

	T	H	M	C
DOMPLU [1]		x	x	
POPLU		x	x	
EPSP		x		
FSS		x		
ELSA	x	x	x	x

[1] Work was not performed as part of the DOPAS project

Different computer codes were used to perform the modelling work reported in DOPAS. With two exceptions of integrated level codes, all other are process level codes. Most of the codes are either free available within the nuclear waste research community or are commercial codes. The use of codes which are available to the research community clearly has the advantage that the results presented in DOPAS can be exploited by other organisations outside of DOPAS by serving as test case library for model comparison or by adopting the models to their own boundary conditions together with source of information on the internet. An overview of the computer codes used is given in table 12.2.

Tab. 12.2: Information on the codes used in DOPAS for modelling. Processes modelled: thermal (T), hydraulic (H), mechanical (M), chemical (C)

	Capabilities used				
Code Name	T	H	M	C	Internet address for information
Commercial codes					
Particle Flow Code (PFC™)	x		x		http://www.itascacg.com/software/pfc
3DEC™			x		http://www.itascacg.com/software/3dec
ALGOR			x		http://www.algor.com
FEFLOW		x			http://www.mikepoweredbydhi.com/products/feflow
Goldsim		x	x	x	http://www.goldsim.com
Free available codes					
EQ3/6	x			x	https://missions.llnl.gov/energy/technologies/geochemistry
PHREEQC	x			x	http://wwwbrr.cr.usgs.gov/projects/ GWC_coupled/phreeqc
Code_Bright	x	x	x		https://www.etcg.upc.edu/recerca/webs/code_bright
OpenGeoSys		x			http://www.opengeosys.org
Company owned codes					
CLOE		x	x		-
LOPOS		x			-

The DOPAS project and Work package 5 contribute significantly to the further development of the safety cases for radioactive waste repositories by bringing forward the plug and sealing concepts in three main host rock types considered in Europe: crystalline rock, clay rock and salt rock. The role of the Work package 5 in this contribution is shown in figure 12.2 and results from predictive and evaluation process modelling of laboratory (blue boxes) as well as in-situ and large-scale experiments (green boxes). The different aspects of the achievements are (white boxes):

- **Gain in process understanding and improvement of models for safety assessment by evaluation process modelling of laboratory experiments:** Process modelling performed of laboratory experiments (GRS, chapter 8 & UJV, chapter 10) in Work package 5 was able to predict and interpret the results from laboratory experiments enhancing the confidence in the suitability of the used models to describe the observed processes. The process models were party converted to abstract models that could be included in integrated safety assessment models to achieve a better process representation in future total system performance assessments. Future comparison of the performed predictive modelling on mid-scale experiments (ANDRA, chapter 6) with experimental results will contribute in the confidence of the validity of the up-scaling of process modelling results from small scale to metric scale.
- **Advancement of the sealing concept:** The process modelling of laboratory and mid-scale in-situ experiments (GRS, chapter 8 & DBETEC, chapter 7) contributed update of the sealing concept and the choice of sealing materials. The predictive process modelling of the in-situ experiment (Posiva, chapter 5) directly supported and influenced the layout and construction of the experiment.
- **Confidence in concept and models:** Future comparison of the predictive modelling with experimental results will contribute in the confidence of the validity of the up-scaling of process modelling results from small scale to large scale.
- **Proof of constructability:** All aspects given before jointly contribute to the confidence in the fact that the plugging and sealing systems will develop as planned and will be able to meet their designed function in the overall repository concept.

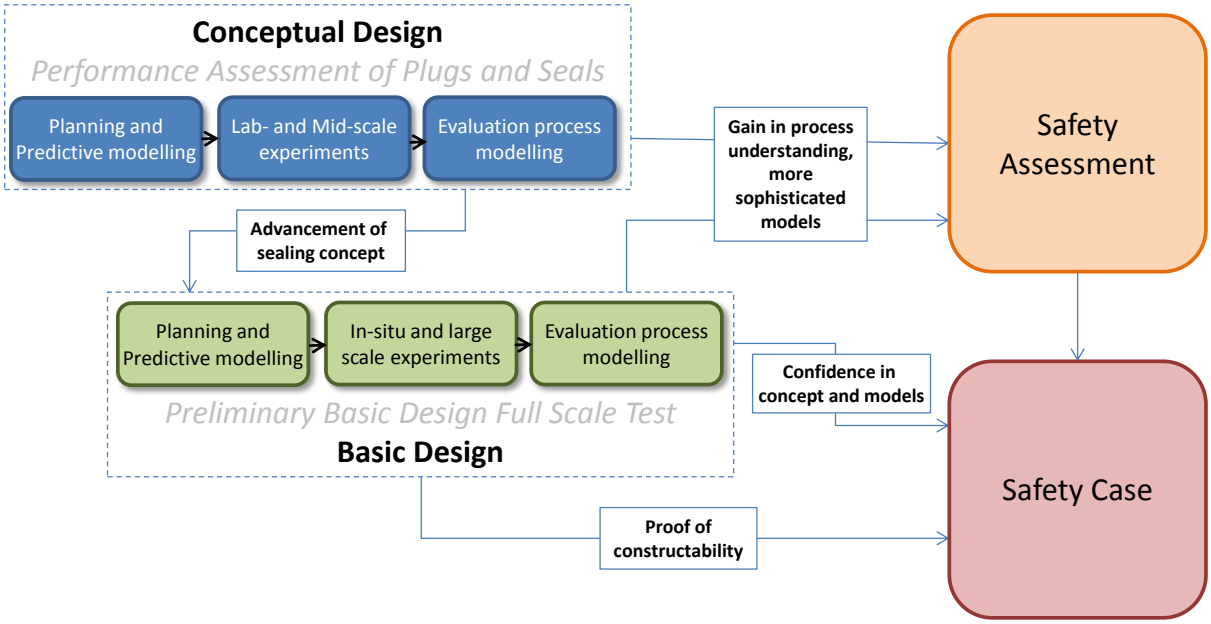

Fig. 12.2: Contribution of Work package 5 to safety assessment and the development of the safety case

Finally it can be concluded that the process modelling work performed in Work package 5 of DOPAS has significantly contributed to the preparation and execution of the experiments and has helped to interpret the obtained results of some of the experiments. Since many of the experiments are not finished at the date of reporting more updated process modelling is expected in the future to investigate the experimental results and to confirm predictive modelling. This also is true for the full analyses of the in-situ large scale experimental data for integrated performance assessment which will mostly be feasible in following programme stage. This work consequently will be reported in company reports of the organisations which performed the work presented in this report.

13 References

Åkesson, M. and Andersson, L. (2013). BRIE Water-uptake test. Clay Technology AB, Lund, Sweden, April / September 2013.

Åkesson, M., Börgesson, B., Kristensson, O. (2010a). Sr-Site Data report. SKB Technical Report TR-10-44.

Åkesson, M., Börgesson, B., Kristensson, O., Dueck, A., Hernelind, J. (2010b). THM modelling of buffer, backfill and other system components. Critical processes and scenarios. SKB Technical report TR-10-11.

Alkan, H. (2009). Percolation model for dilatancy-induced permeability of the excavation damaged zone in rock salt. International Journal of Rock Mechanics & Mining Sciences 46, 716–724

ANDRA (2005). Andra research on the geological disposal of high-level long-lived radioactive waste. Results and perspectives. English Translation - Dossier 2005. Paris, France.

ANDRA (2005a). Safety evaluation of a geological repository. English Translation - Evaluation de Sûreté du Stockage Géologique, Dossier 2005 Argile. Paris, France.

Bailey L., Becker D.-A., T. Beuth, M. Capouet, J.L. Cormenzana, M. Cuñado, L. Griffault, J. Marivoet, C. Serres (2011). PAMINA - Performance Assessment Methodologies in Application to Guide the Development of the Safety Case. European Handbook of the state-of-the-art of safety assessments of geological repositories – Part 1. PAMINA Deliverable D1.1.4.

Becker, D.-A., D. Buhmann, R. Storck, J. Alonso, J.-L. Cormenzana, M. Hugi, F. van Gemert, P. O'Sullivan, A. Laciok, J. Marivoet, X. Sillen, H. Nordman, T. Vieno, M. Niemeyer, (2002). Testing of Safety and Performance Indicators (SPIN). European Commission Report EUR 19965 EN, Brussels, Belgium.

Becker, D.-A., J.-L. Cormenzana, A. Delos, L. Duro, J. Grupa, J. Hart, J., Landa, J., Marivoet, J., Orzechowski, L., Schröder, T.J., Vokal, A., Weber, E. Weetjens, J. Wolf (2009). Safety and Performance Indicators. PAMINA Deliverable D3.4.2.

BMU (2010). Safety requirements governing the final disposal of heat-generating radioactive waste. Bundesministerium für Umwelt, Naturschutz und Reaktorsicherheit, Berlin, Germany.

Bollingerfehr, W., D. Buhmann, W. Filbert, S. Keller, J. Krone, A. Lommerzheim, J. Mönig, S. Mrugalla, N. Müller-Hoeppe, J.R. Weber, J Wolf (2013). Status of the safety concept and safety demonstration for an HLW repository in salt - Summary report. TEC-15-2013-AB, FKZ 02 E 10719 and 02 E10729, Peine.

Bonen, D. (1992). Composition and appearance of magnesium silicate hydrate and its relation to deterioration of cement-based materials. J. Am. Ceram. Soc. (75), p 2904-2906.

Börgesson L, Sandén T, Andersson L, Johannesson L-E, Goudarzi R, Åkesson M, (2015). System design of Dome Plug. Preparatory modelling and tests of the sealing and draining components. Clay Technology. SKB R-14-25, Svensk Kärnbränslehantering AB.

Chapman N., Hooper A. (2011). The disposal of radioactive wastes underground. Proceedings of the Geologists' Association, Elsevier.

Conil N., Talandier J., Noiret A., Armand G., Bosgiraud J.M. (2015). Report on Bentonite Saturation Test (REM). DOPAS Work package 4, Deliverable D4.2.

Cundall, P.A. & Strack, O.D.L. (1979). A discrete numerical model for granular assemblies. Géotechnique, vol. 29, p. 47-65.

Czaikowski, O., Dittrich, J., Hertes, U., Jantschik, K., Wieczorek, K., Zehle, B. (2016). ELSA related testing on mechanical-hydraulical behaviour - LASA, Final Report. DOPAS Work package 3, Deliverable D3.31, Bericht GRS-A-3851, Gesellschaft für Anlagen- und Reaktorsicherheit (GRS) gGmbH, Braunschweig.

de La Vaissiere, R., Conil, N; Leveau, F., Armand, G. (2015). Large-Scale Sealing Experiment in the Meuse/Haute Marne Underground Research Laboratory. The 6th International Clay conference – Clays in Natural & Engineered Barriers for Radioactive Waste Confinement, March 23-26, 2015, Brussels.

DOPAS (2016a). WP2 Final Report: Design Basis for DOPAS Plugs and Seals. DOPAS Work package 2, Deliverable D2.4.

DOPAS (2016b). WP3 Final Summary Report: Summary of, and Lessons Learned from, Design and Construction of the DOPAS Experiments. DOPAS Work package 3, Deliverable D3.30.

DOPAS (2016c). WP4 Integrated Report: Summary of Progress on, and Performance Evaluation of, Design, Construction and Monitoring of Plugs and Seals. DOPAS Work package 4, Deliverable 4.4.

EN 1990:2002, Eurocode - Basis of structural design. December 2005.

EN 1992-1-1: 2004: Eurocode 2: Design of concrete structures - Part 1-1: General rules and rules for buildings. December 2004.

European Commission. Directorate-General for Research & Innovation, Grant agreement number 662177 — Modern2020. ANNEX 1 (part A) Research and Innovation action, Ref. Ares(2015)1992647, 2015.

Foin R. et al. (2015). FSS (Full Scale Seal) Experiment summary report. DOPAS Work package 4, Deliverable D4.8.

Gens, A. A., Olivella, S. (2006). Coupled Thermo-Hydro-Mechanical Analysis of Engineered Barriers for High-Level Radioactive Waste. Chinese Journal of Rock Mechanics and Engineering, 2006, 25(4), 670 -680.

Gens, A., Garcia-Molina, A.J., Olivella, S., Alonso, E.E., Huertas, F. (1998). Analysis of a Full Scale in-situ Test Simulating Repository Conditions. Int. J. Numer. Anal. Meth. Geomech., 22, 515-548, 1998.

Glaubach, U., Hofmann, M., Königer, F., Emmerich, K., Schuhmann, R., Viertel, T. & Wilsnack, T. (2016). Teilbericht zum Arbeitspaket 3: Laborversuche zu den Arbeitsschritten 2.1 bis 2.6 Im Rahmen des Vorhabens „Schachtverschlüsse für Endlager für hochradioaktive Abfälle“ ELSA-Phase 2: Konzeptentwicklung für Schachtverschlüsse und Test von Funktionselementen von Schachtverschlüssen. Technische Universität Bergakademie Freiberg, Institut für Bergbau und Spezialtiefbau (in German)

Haaramo, M., Lehtonen, A. (2009). Principle plug design for Deposition Tunnels. Posiva Working Report 2009-38.

Hagemann, S. & Meyer Th, (2003). Unsicherheits- und Sensitivitätsanalyse zur Korrosion von Salzbeton durch salinare Lösungen. GRS-A-3458, Project Morsleben, PSP Element 9M 232 200 11, 114 p.

Hansen, J. et al. (2016). DOPAS Final Project Summary Report. DOPAS Work package 6, Deliverable D6.4.

Herold, P. and Müller-Hoeppe, N. (2013). Safety Demonstration and Verification Concept – Principle and Application Examples. Technical Report (Extraction from Kudla et al. 2013), DBE TECHNOLOGY, Peine.

Hirsekorn, R.-P.; Boese, B.; Buhmann, D. (1999). LOPOS: Programm zur Berechnung der Schadstofffreisetzung aus netzwerkartigen Grubengebäuden. Gesellschaft für Anlagen- und Reaktorsicherheit (GRS) mbH, GRS-157, Braunschweig.

Holt, E., Dunder, J. (2014). Detailed design of POPLU deposition tunnel end plug. DOPAS Work package 3, Deliverable D3.24

Holt, E., Koho, P. (2016). POPLU Experimental Summary Report. Work package 4 Deliverable D 4.5.

Hudson, J. A., Cosgrove, J. W. & Johansson, E. (2008). Estimating the Mechanical Properties of the Brittle Deformation Zones at Olkiluoto. Posiva Working Report 2008-67.

IAEA (2001). International Atomic Energy Agency (IAEA). Monitoring of Geological Repositories for High Level Radioactive Waste. IAEA TECDOC 1208, IAEA, Vienna, 2001.

IAEA (2003). International Atomic Energy Agency (IAEA), Safety Indicators for the Safety Assessment of Radioactive Waste Disposal, Sixth report of the INWAC Subgroup on Principles and Criteria for Radioactive Waste Disposal. IAEA-TECDOC-1372. IAEA, Vienna, Austria, 2003.

IAEA (2007). International Atomic Energy Agency (IAEA), IAEA Safety Terminology used in nuclear safety and radiation protection. 2007 Edition, IAEA, Vienna, Austria.

IAEA (2012). International Atomic Energy Agency (IAEA), The Safety Case and Safety Assessment for the Disposal of Radioactive Waste, Specific Safety Guide No. SSG-23. STI/PUB/1553, Vienna, September 2012.

Itasca (2008). PFC2D, Version 4.0 Online Manual.

Itasca Consulting Group, Inc. (2012). FLAC3D – Fast Lagrangian Analysis of Continua in Three-Dimensions, Ver. 5.0. Minneapolis, Itasca.

Jantschik, K.; Herbert, H.-J.; Hertes, U.;Meyer, T.; Moog, H.C. (2016). ELSA related testing on chemical-hydraulical behaviour - LAVA, Final Report. DOPAS Work package 3, Deliverable D3.29, Bericht GRS-A-3850, Gesellschaft für Anlagen- und Reaktorsicherheit (GRS) gGmbH, Braunschweig.

Johannesson, L.-E., Sandén, T., Dueck, A. (2008). Deep repository – engineered barrier system. Wetting and homogenization processes in backfill materials. Laboratory tests for evaluating modeling parameters. SKB R-08-136.

Kudla, W., Schreiter, F., Gruner, M., Jobmann, M., Bollingerfehr, W., Müller-Hoeppe, N., Herold, P., Freyer, D., Wilsnack, T., Grafe, F. (2013). Schachtverschlüsse für Endlager für hochradioaktive Abfälle – ELSA Teil 1. TU Bergakademie Freiberg und DBE TECHNOLOGY, Freiberg, Peine (in German).

Larue, J., Baltes, B., Fischer, H., Frieling, G., Kock, I., Navarro, M., Seher, H. (2013). Radiologische Konsequenzenanalyse. Bericht zum Arbeitspaket 10. Vorläufige Sicherheitsanalyse für den Standort Gorleben. GRS-289, Gesellschaft für Anlagen- und Reaktorsicherheit, Köln.

Marivoet J., E. Weetjens, F. Raeymaekers, S. Seetharam (2009). PAMINA. Testing Safety and Performance Indicators for a Geological Repository in Clay: SCK•CEN's Results. PAMINA Milestone report M3.4.10.

Marivoet J., E. Weetjens, F. Raeymaekers, S. Seetharam (2010). Testing Safety and Performance Indicators for a Geological Repository in Clay. SCK•CEN Report ER-125, Mol, Belgium.

Marivoet J., T. Beuth, J. Alonso, D.-A Becker (2008). Task reports for the first group of topics: Safety Functions Definition and Assessment of Scenarios Uncertainty Management and Uncertainty Analysis Safety Indicators and Performance/Function Indicators. PAMINA Deliverable D1.1.1.

Meyer Th. (2004). Corrosion of cementitious materials under geological disposal conditions. CSNI/RILEM Workshop, Madrid, 15-16 March 2004, 10p.

Meyer Th. and Herbert H.-J. (2003). The long-term performance of cementitious materials in underground repositories for nuclear waste. International Congress on the Chemistry of Cements, Durban, South Africa, 2003, 10p.

Meyer Th., Herbert, H.-J, Schmidt-Döhl, F. (2003). Endlager Morsleben – Korrosion von Salzbeton durch salinaren Lösungen. GRS Report, GRS-A-3170, PSP-Element 9M 212 200 11/12, 210 S.

Meyer Th., Herbert, H.-J, Schmidt-Döhl, F. (2003a). Endlager Morsleben – Korrosion zementhaltiger Materialien bei Mehrfachdurchströmung mit salinaren Lösungen. GRS Report, GRS-A-3150, PSP-Element 9M 212 200 11/12, 205 S.

Meyer Th., Herbert, H.-J, Schmidt-Döhl, F., Dettmer F. (2002). Endlager Morsleben – Zementkorrosion. GRS Report, GRS-A-3034, PSP-Element 9M 212 200 11/12, 221 S.

Meyer, Th. und Herbert, H.-J. (1999). Geochemische Modellierung der Betonkorrosion - International Symposium Environment 2000, Halle, Sept. 22.-25th. 1999.

MoDeRn (2011). AITEMIN, Technical requirements report, MoDeRn Deliverable D2.2.1.

MoDeRn (2012). Bergmans, A., M. Elam, P. Simmons, G. Sundqvist, MoDeRn. Monitoring the Safe Disposal of Radioactive Waste: a Combined Technical and Socio-Political Activity, MoDeRn Deliverable D1.3.1.

MoDeRn (2013a). AITEMIN, NDA, Andra, NRG, NAGRA, ENRESA, EURIDICE, ETH ZURICH, NRG, RWMC, DBE Technology, Posiva, SKB, RAWRA & GSL, State of Art Report on Monitoring Technology, MoDeRn Deliverable D2.2.2.

MoDeRn (2013b). Jobmann, M. (ed.), Case Studies. Final Report, MoDeRn Deliverable D4.1, October 2013.

MoDeRn (2013c). NDA, Nagra, NRG (eds.), MoDeRn Monitoring Reference Framework report. MoDeRn Deliverable D1.2, November 2013.

Müller-Hoeppe, N.; Engelhardt, H.-J.; Lerch, C.; Linkamp, M.; Buhmann, D.; Czaikowski, O.; Herbert, H.-J.; Wieczorek, K.; Xie, M. (2012). Integrität geotechnischer Barrieren Teil 1: Vorbemessung. Bericht zum Arbeitspaket 9, Vorläufige Sicherheitsanalyse für den Standort Gorleben, GRS-287, Gesellschaft für Anlagen- und Reaktorsicherheit, Köln.

NAGRA (2002). Project Opalinus Clay: Safety Report, Demonstration of the Disposal Feasibility for Spent Fuel, Vitrified HLW and Long-lived ILW. Nationale Genossenschaft für die Lagerung radioaktiver Abfälle (Nagra), Nagra Technical Report 02-05. Wettingen, Switzerland.

NEA (2008). Nuclear Energy Agency (NEA), Safety Cases for Deep Geological Disposal of Radioactive Waste: Where Do We Stand? Symposium Proceedings, Paris, France, 23-25 January 2007, OECD/NEA report No. 6319, Paris, 2008.

NEA (2012). Nuclear Energy Agency (NEA), Indicators in the Safety Case, A report of the Integrated Group on Safety Case (IGSC), NEA/RWM/R(2012)/7, NEA, Paris, 2012.

NWMO (2011). OPG's Deep Geologic Repository for Low and Intermediate Level Waste – Postclosure Safety Assessment. NWMO Document DGR-TR-2011-25 R001. Toronto, Canada.

Olivella, S., Alonso, E. E. (2008). Gas flow through clay barriers. Geotechnique, 58, 157-176.

Olivella, S., Carrera, J., Gens, A., Alonso, E.E. (1994). Non-isothermal multiphase flow of brine and gas thorough saline media. Transport Porous Media, 15: 271–293.

Olivella, S., Carrera, J., Gens, A., Alonso, E.E. (1994). Nonisothermal Multiphase Flow of Brine and Gas Through Saline Media. Transport in Porous Media, 15, 271-293.

Olivella, S., Gens, A., Carrera, J., Alonso, E.E. (1996). Numerical formulation for a simulator (CODE-BRIGHT) for the coupled analysis of saline media. Eng. Comput., 1: 87–112.

ONDRAF/NIRAS (2001). SAFIR 2: Safety Assessment and Feasibility Interim Report 2. ONDRAF/NIRAS Report NIROND 2001-06 E.

Parkhurst, D. L., Appelo, C. A. J. (1999). User's guide to PHREEQC (Version 2): A computer program for speciation, batch-reaction, one-dimensional transport, and inverse geochemical calculations.

Pastina, B. & Hellä, P. (eds.) (2010). Models and data report 2010. Eurajoki, Finland: Posiva Oy. Posiva 2010-01. 478 p. ISBN 978-951-652-172-8.

Poller, A., Smith, P., Mayer, G. & Hayek, M. (2014). Modelling of Radionuclide Transport along the Underground Access Structures of Deep Geological Repositories. Nagra Tech. Ber. NTB 14-10.

Posiva (2012a). Safety Case for the Disposal of Spent Fuel at Olkiluoto – Performance Assessment 2012. Posiva 2012-04.

Posiva (2012b). Safety Case for the Disposal of Spent Nuclear Fuel at Olkiluoto - Assessment of Radionuclide Release Scenarios for the Repository System 2012. Posiva 2012-09.

Posiva (2013a). Backfill design 2012. Posiva 2012-15.

Posiva (2013b) Backfill production line. Posiva 2012-18.

Röhlig K.-J., A. Van Luik, J. Schneider, L. Griffault, P. Gierszewski, U. Noseck, J. Mönig, M. Navarro (2012). Methods for Safety Assessment of Geological Disposal Facilities - for Radioactive Waste - Outcomes of the NEA MeSA Initiative, NEA Report No. 6923, ISBN 978-92-64-99190-3, OECD/NEA, Paris.

Rosca-Bocancea E., T.J. Schröder (2013). Development of Safety and Performance Indicators, OPERA Milestone report OPERA-CF-NRG010.

Rübel, A., Buhmann, D. and Kindlein, J. (2014). Status report on conceptual and integrated modelling activities. DOPAS Work package 5, Deliverable 5.6.

Rübel, A.; Becker, D.-A.; Fein, E.; Ionescu, A.; Noseck, U.; Lauke, T.; Mönig, J.; Schneider, A.; Spießl, S.; Wolf, J. (2010). Development of Performance Assessment Methodologies. GRS-259, Gesellschaft für Anlagen und Reaktorsicherheit (GRS) mbH, Braunschweig.

Rübel, A.; Buhmann, D.; Kindlein, J.; Lauke, T. (2016). Performance Assessment of Sealing Systems - Conceptual and integrated modelling of plugs and seals. GRS-415, Gesellschaft für Anlagen- und Reaktorsicherheit (GRS) mbH, Braunschweig.

Schatz, T. & Martikainen, J. (2012). Laboratory tests and analyses on potential Olkiluoto backfill materials. Posiva Oy, Eurajoki, Finland. Working Report 2012-74.

Schröder T.J, J. Hart, A. Costescu-Badea, R. Bolado Lavin (2009b). PAMINA Task 2.1.D, Techniques for Sensitivity and Uncertainty Analysis, Analysis of a repository design in a rock salt formation. PAMINA Milestone Report M2.1D.7, NRG-21952/09.95945, Petten, The Netherlands.

Schröder T.J., E. Rosca-Bocancea (2013). Safety and performance indicator calculation methodology. OPERA Milestone report OPERA-PU-NRG7312.

Schröder, T.J., E. Rosca-Bocancea, J. Hart (2009a). PAMINA Task WP3.4, Other methodological advancements: Safety Indicators and Performance Indicators Calculation results of a repository design in argillaceous rock. PAMINA Milestone Report M3.4.15, NRG report NRG-21952/09.95482, Petten, The Netherlands.

Skalny, J., Marchand, J., Odler, I. (2002). Sulphate attack on concrete. Spon Press, London.

SKB (2006a). Svensk Kärnbränslehantering AB (SKB), Long-Term Safety for KBS-3 Repositories at Forsmark and Laxemar. A First Evaluation: Main Report of the SR-Can Project. SKB Report TR-06-09, Stockholm, Sweden.

SKB (2006b). Svensk Kärnbränslehantering AB (SKB), Buffer and backfill process report for the safety assessment SR-Can, SKB Report TR-06-18, Stockholm, Sweden.

SKB (2015). Svensk Kärnbränslehantering AB, Long-term safety for the final repository for spent nuclear fuel at Forsmark, Main report of the SR-Site Project. TR-11-01, 2011, Updated 2015.

T.J. Schröder, E. Rosca-Bocancea, J. Hart (2016). Integration of demonstrator activities in performance assessment: analysis of processes and indicators. DOPAS Work package 5, Deliverable D5.9.

UPC – Universitat Plitecnica de Catalunya (2015). User's Guide of CODE-BRIGHT - A 3-D Program for Thermo-Hydro-Mechanical Analysis in Geological Media, Department of Geotechnical Engineering and Geosciences of Technical University of Catalonia (UPC), Barcelona, Spain. https://www.etcg.upc.edu/recerca/webs/code_bright/downloads/manual-users-guide-v4/view

UPC – Universitat Plitecnica de Catalunya (2015a). Code_Bright Tutorial Manual. Barcelona, Spain. https://www.etcg.upc.edu/recerca/webs/code_bright/downloads/tutorials/view

USDOE (1996). Title 40 CFR Part 191, Compliance Certification Application for the Waste Isolation Pilot Plant. US Department of Energy (DOE) Document DOE/CAO 1996 2184. Carlsbad, NM: Carlsbad Field Office.

USDOE (2009). Title 40 CFR Part 191 Compliance Recertification Application for the Waste Isolation Pilot Plant (March). 10 vols. DOE/WIPP-09-3424. Carlsbad, NM: Carlsbad Field Office.

Vašíček, R., Hausmannová, L., Šťástka, J., Svoboda, J., Nádherná, D., Pacovská, D., Hubálovská, J., Večerník, P., Trpkošová, D., Gondolli, J., Dvořáková, D., Hanusová, I., Bělíčková, L. (2016). Final results of EPSP laboratory testing. DOPAS Work package 3, Deliverable D3.21, CTU in Prague, 67 p.

Weetjens E., J. Marivoet, S. Seetharam (2010). Performance indicators Quantifying the Contribution of Safety Functions to the Confinement of Radionuclides in a Geological Repository System. Scientific Basis for Nuclear Waste Management XXXIV, Symposium Proceedings, San Francisco, United States, 5-9 April 2010 / Materials Research Society (MRS), Warrendale, United States.

Wendling J., Calsyn L., Bosgiraud J.M. (2015). Report on Andra's PA Methodology for Sealing Systems. DOPAS Work package 5, Deliverable D5.2

Wendling J., Pepin G.., Bosgiraud J.M. (2015a). Report on Andra's Understanding of Processes involved in Time and Space. DOPAS Work package 5, Deliverable D5.3

Wendling J., Pepin G.., Bosgiraud J.M. (2015b), Report on Andra's PA approach concerning uncertainties. DOPAS Work package 5, Deliverable D5.4

White M., Doudou, S., Neall, F. (2014). Design Bases and Criteria. DOPAS Work package 2, Deliverable D2.1.

White, M.J. and Doudou, S. (2014). Design of Reference Concepts and DOPAS Experiments. DOPAS Work package 2, Deliverable D2.2.

White, M.J. and Doudou, S. (2015). Strategies for Demonstrating Compliance of the Reference Designs with the Design Basis. DOPAS Work package 2, Deliverable D2.3.

Wieczorek, K., Förster, B., Rothfuchs, T., Zhang, C.-L., Olivella, S., Kamlot, P., Günther, R.-M., Lerch, C. (2010). THERESA Subproject MOLDAU, Coupled Thermal-Hydrological-Mechanical-Chemical Process in Repository Safety Assesment. Deutsche Gesellschaft zum Bau und Betrieb von Endlagern Technology (DBE Tec), Gesellschaft für Anlagen- und Reaktorsicherheit (GRS), Institut für Gebirgsmechanik (IfG), GRS-262, ISBN: 978-3-939355-37-3, Deutschland.

Zhang, C.L. (2016). Sealing behaviour of fractured clystone and seal materials, Final Report, DOPAS Work package 3, Deliverable D3.32. Bericht GRS-A-3852, Gesellschaft für Anlagen- und Reaktorsicherheit (GRS) gGmbH, Braunschweig.